eman ta zabal zazu

Universidad del País Vasco

Euskal Herriko Unibertsitatea

# DOCTORAL THESIS

# INVOLVEMENT OF NITRIC OXIDE SIGNALING MECHANISMS UNDERLYING OPIOID TOLERANCE

**Doctoral thesis presented by Patricia Pablos Laría**

**Leioa, 2015**

This Doctoral Thesis has been carried out thanks to a predoctoral fellowship (Formación de Personal Investigador, 2011-2014) from the Basque Government.

# AGRADECIMIENTOS / ACKNOWLEDGEMENTS

En primer lugar me gustaría agradecer a mis directores de tesis, el Dr. Joseba Pineda y la Dra. Aitziber Mendiguren por haberme dado la oportunidad de llevar a cabo este proyecto, por haberme guiado durante todos estos años y por todo lo que he aprendido de vosotros. Gracias Mari, me recibiste con los brazos abiertos y me enseñaste con paciencia cuando la palabra electrofisiología me sonaba a otro idioma. Contigo todo fue fácil, mil gracias por tu apoyo y tus buenos consejos. Gracias a Amaia, Irati, Iranzu, Txetxu, Julia y demás compañeros que he tenido en el laboratorio, todos me habéis aportado buenos momentos a lo largo de esta etapa.

Vorrei anche ringraziare la Proff.sa Carla Ghelardini e il Prof. Lorenzo Di Cesare Mannelli dell´Università di Firenze per avermi dato l'opportunità di lavorare nel vostro gruppo di ricerca e imparare tanto sui meccanismi responsabili del dolore. Grazie anche a Laura, Matteo, Francesca, Mario, Barbara, Antonio, Cristina. Grazie per tutti i momenti divertenti passati in laboratorio. È stato un piacere conoscervi. Mi avete fatto sentire come a casa.

Quiero dar las gracias a mis amigos de toda la vida: Iraide, Yaiza, Imanol, Diego, Ana, Andrea, Paul... Os conozco prácticamente desde que tengo uso de razón y hemos compartido muchos momentos. Todos os habéis interesado por mi tesis, me habéis dado ánimos, me habéis hecho reír y desconectar de todo. Sois para mí esos amigos de referencia, con los que siempre podré contar a pesar del paso de los años. Gracias a Esther y Naiara, que conocéis de primera mano lo que supone hacer una tesis. Unas prácticas y un máster hicieron que os conociese más a fondo y que se forjase una amistad de las que van para largo. Gracias también a Janire, Matxalen, María y Enara, con quienes he pasado cinco años codo con codo en la facultad. Cuando nos juntamos vuelvo a 2006 otra vez, recordando aquellos tiempos con una sonrisa.

Por supuesto, muchísimas gracias a toda mi familia. A mis padres, Inés y Jose, realmente los mejores padres que pudiera pedir. A mi abuela Lucía, mucho más que una abuela. Impagable la dedicación y el cariño que me has dado y me sigues dando día tras día. A mis abuelos Isidro y Catali, sé lo orgullosos y felices que estáis también. A Yrama y Paula, oficialmente primas pero también hermanas y amigas, hemos crecido juntas y no os puedo querer más. A Juanmi, insuperable como “compi” pero aún mejor persona. No puedo olvidarme de Woody, fuente de cariño incondicional, me llena de felicidad. A Marta, los viajes y buenos momentos contigo son irrepetibles. Gracias a “los del octavo”

Gloria, Jesus, Miriam y Nara, que me tiene robado el corazón, sois muy importantes para mí. Quiero mencionar también a Asun, una persona inolvidable, siempre será para mí la mejor tía del mundo.

Por último, millones de gracias Izei, has vivido este proyecto conmigo desde el minuto cero y sé que para ti tampoco ha sido fácil. Has sigo testigo directo de las alegrías, pero también de los momentos complicados. Siempre al pie del cañón. Gracias por ser uno de mis grandes apoyos, por tu cariño, tu simpatía y sentido del humor, por tu empatía y lealtad, en definitiva, por ser tal y como eres.

“Nothing in life is to be feared,

it is only to be understood”

Marie Curie

A mi familia

# SUMMARY

## SUMMARY

This work focuses on the study of neuropharmacological mechanisms underlying opioid tolerance, in particular, the involvement of NO signalling pathways. Opioids are potent drugs used for pain relief. However, their therapeutic potential is limited as their long-term use leads to the development of tolerance to their analgesic effects. Opioid tolerance is a complex phenomenon and the underlying mechanisms have not been fully elucidated. Understanding the ways in which tolerance can be attenuated would be a significant advantage in the therapeutic use of these agents. The noradrenergic nucleus locus coeruleus (LC) contains a high-density of MORs and it has been extensively used as a model to explore the cellular and molecular mechanisms underlying opioid tolerance. In this regard, there is substantial evidence showing the involvement of mu-opioid receptor (MOR) desensitization in the development of tolerance.

The signaling messenger nitric oxide (NO) has been widely recognized to play pivotal roles in the regulation of multiple physiologic and pathophysiological processes. It is produced from L-arginine by the enzymatic action of NO synthase (NOS). The main target of NO is the enzyme soluble guanylyl cyclase (sGC), which catalyzes the formation of 3'5'-cyclic guanosine monophosphate (cGMP). This second messenger activates a number of effectors, such as the cGMP-dependent protein kinase (PKG). NO also reacts with oxygen derivatives to produce reactive oxygen and nitrogen species (ROS), such as the powerful oxidant molecule peroxynitrite. NO modulates opioid actions, as it was found to be involved in $Met^5$-enkephalin (ME)-induced MOR desensitization *in vitro* and in the neuronal adaptations occurring *in vivo* during morphine tolerance. We carried out four studies to explore the role of NO and its downstream signaling pathways (sGC/cGMP and ROS) in the adaptations triggered by different opioid agonists both *in vitro* and *in vivo*.

### STUDY 1

In the first study, we investigated by single-unit extracellular recordings *in vitro* the involvement of NO-activated pathways in MOR desensitization induced by ME (3 or 10 μM) in the rat LC. For this purpose, we tested the effect of different modulators of the sGC/PKG pathway and antioxidants on ME-induced desensitization in LC neurons from

rat brain slices. Perfusion with ME (3 and 10 μM) reduced ME (0.8 μM) effect in a concentration-related manner, indicative of MOR desensitization. ME (3 μM)-induced desensitization was enhanced by the NO donor DEA/NO (100 μM) and the soluble guanylate cyclase (sGC) activators A 350619 (30 μM) or BAY 418543 (1 μM). DEA/NO-induced enhancement was blocked by the sGC inhibitor NS 2028 (10 μM). Paradoxically, ME (10 μM)-induced desensitization was not modified by the sGC inhibitor NS 2028 (10 and 30 μM), the PKG inhibitor Rp-8-Br-PET-cGMP (1 μM) or the antioxidants Trolox (200 μM), U-74389G (10 μM) or melatonin (100 μM). However, it was attenuated by a combination of a sGC inhibitor (NS 2028 10 μM) and an antioxidant (Trolox 200 μM). Our results suggest that MOR desensitization in the LC may be mediated or regulated by NO through sGC and reactive oxygen species signaling pathways.

**STUDY 2**

The ability of morphine to induce rapid MOR desensitization in native LC neurons has been questioned. In the second study, we characterized by single-unit extracellular recordings *in vitro* the desensitization of MOR induced by morphine in KCl-excited LC neurons from rat brain slices. ME-induced desensitization was tested as a reference for morphine. This KCl-protocol allowed us to monitor continuously the effect of supramaximal concentrations of opioid agonists. Since the contribution of NO to MOR desensitization induced by non-peptide opioid agonists is unknown, we further explored the involvement of the neuronal NOS isoform in acute MOR desensitization. As expected, ME (10 μM) induced substantial desensitization of MOR, since the inhibitory effect of ME (0.8 or 25.6 μM) was diminished after or during application of ME (10 μM). Our results show that morphine (30 μM) also causes significant desensitization of MOR in the LC, so that the inhibitory effect of a supramaximal test concentration of ME (25.6 μM), applied before-after or during the desensitization period, was markedly reduced. In contrast, the inhibitory effect of gamma-aminobutyric acid (GABA; 1 mM) was unaltered after application of ME (10 μM) or morphine (30 μM). Perfusion with a combination of the nNOS inhibitors 7-nitroindazole (7-NI, 100 μM) and S-methyl-L-thiocitrulline (SMTC, 10 μM) attenuated the induction of MOR desensitization induced by ME, but it failed to alter the desensitization induced by morphine. These results demonstrate the

ability of morphine to induce acute MOR desensitization *in vitro* and highlight the agonist-selective regulation of MOR desensitization by neuronal NOS.

**STUDY 3**

In this study, we examined by electrophysiological techniques in LC neurons the effect of chronic treatments with 7-nitroindazole (7-NI; 30 mg/kg/12 h, i.p.), a selective neuronal nitric oxide synthase (nNOS) inhibitor, and the antioxidants Trolox + ascorbic acid (TX+AA; 40 and 100 mg/kg/day, respectively, i.p.) and U-74389G (10 mg/kg/day, i.p.), on the development of cellular tolerance induced by three different opioid agonists (morphine, methadone and fentanyl). For induction of morphine tolerance, rats were treated subcutaneously (s.c.) with a slow release emulsion containing free base morphine (200 mg/kg) for 72 h. For methadone (60 mg/kg/day, 6 days) and fentanyl (0.2 mg/kg/day, 7 days), tolerance was induced by s.c. implantation of osmotic pumps. Concentration-effect curves for the inhibitory effect of the opioid agonist ME on the cell firing rate was evaluated by single-unit extracellular recordings of LC neurons from brain slices. Morphine, methadone and fentanyl treatments caused different degrees of rightward shifts of concentration-effect curves for ME and they increased the $EC_{50}$ by 4, 2 and 3 folds, respectively, as compared to those in sham-treated animals. This suggests that opioids induce agonist-dependent cellular tolerance in LC neurons. Co-administration of TX+AA or U-74389G attenuated tolerance to ME effect in morphine-treated animals when compared to the control (morphine/vehicle group). In contrast, co-treatment with either U-74389G or 7-NI failed to alter the tolerance to the inhibitory effect of ME in methadone- or fentanyl-treated animals. Administration of TX+AA, U-74389G or 7-NI in sham-treated rats failed to change the effects induced by ME as compared to vehicle groups. Taken together, our results suggest that NO/ROS pathways modulate the development of cellular tolerance induced by morphine treatments, but not by treatments with other opioid agonists that have different pharmacodynamic profiles.

**STUDY 4**

In the fourth study, we used the tail-flick technique in rats to examine the effect of 7-nitroindazole (7-NI; 30 mg/kg/12 h, i.p.), a selective nNOS inhibitor, and the antioxidant

agent U-74389G (10 mg/kg/day, i.p.) on the development of opioid antinociceptive tolerance induced by prolonged treatments with morphine, methadone and fentanyl. For induction of morphine tolerance, rats were treated subcutaneously with a slow release emulsion containing free base morphine (200 mg/kg) for 72 h. For methadone (60 mg/kg/day, 6 days) and fentanyl (0.2 mg/kg/day, 7 days), tolerance was induced by s.c. implantation of osmotic pumps. Thus, morphine treatments induced a strong degree of tolerance to the antinociceptive effect of a challenge dose of morphine. Methadone treatments induced weaker a degree of antinociceptive tolerance. On the contrary, no tolerance to morphine challenge effects was observed in fentanyl-treated animals. Co-treatment with the antioxidant U-74389G partially blocked morphine-induced analgesic tolerance. On the contrary, 7-NI or U-74389G administration failed to affect the development of antinociceptive tolerance induced by methadone. Our results suggest that NO/ROS pathways are involved in the development of opioid antinociceptive tolerance induced by morphine treatments, but not by treatments with other opioids that have different pharmacodynamic profiles.

**A 350619:**3-[2-[(4-chlorophenyl)thiophenyl]-*N*-[4-(diμethylamino)butyl]-2-propenamide hydrochloride

**aCSF:** artificial cerebrospinal fluid

**cAMP:** cyclic adenosine monophosphate

**ANOVA:** analysis of variance

**ANCOVA:** analysis of covariance

**BAY 418543:** 2-[1-[(2-fluorophenyl)methyl]-1H-pyrazolo[3,4-b]pyridin-3-yl]-5-(4-morpholinyl)-4,6 pyrimidinediamine

**CaM:** calmodulin

**CaMKII:** calcium/calmodulin-dependent protein kinase II

**cGMP:** cyclic guanosine monophosphate

**CNQX:** 6-cyano-7-nitroquinoxalline-2,3-dione disodium salt

**CNS:** central nervous system

**DAMGO:** [D-Ala2,N-Me-Phe4,Gly5-ol]-enkephalin

**D-AP5:** D-(-)-2-amino-5-phosponopentanoic acid

**DEA/NO:** diethylamine NONOate

**DMSO:** dimethylsulphoxide

**DOR** δ receptor

**eNOS:** endothelial nitric oxide synthase

**ERK:** extracellular-signal-regulated kinases

**Fig.:** figure

**GABA:** gamma-aminobutyric acid

**GDP:** guanosine diphosphate

**GIRK:** G protein-coupled inward rectifier potassium

**GPCR:** G protein-coupled receptors

**GTP:** guanosine triphosphate

**5-HT:** serotonin

**iNOS:** inducible nitric oxide synthase

**i.p.:** intraperitoneal

**KCl:** potassium chloride

**KOR** κ receptor

**LC:** locus coeruleus

**MAPK:** mitogen-activated protein kinase

**ME:** $Met^5$-enkephalin

**MOR:** μ opioid receptor

**M6G:** morphine-6β-glucuronide

**NA:** noradrenaline

**7-NI:** 7-nitroindazole

**NMDA:** N-methyl-D-aspartate

**N/OFQ:** nociceptin/orphanin FQ

**NO:** nitric oxide

**NOS:** nitric oxide synthase

**nNOS:** neuronal nitric oxide synthase

**NS 2028:** 8-Bromo-1H,4H-[1,2,4]oxadiazolo[3,4-*c*][1,4]benzoxazin-1-one

**NOX:** NADPH-oxidase

**$^{\bullet}O_2^-$**: superoxide radical

**$OONO^-$**: peroxynitrite

**PD** Parkinson disease

**PGi:** nucleus paragigantocellularis

**PKA:** cAMP-dependent protein kinase

**PKC:** protein kinase C

**PKG:** cGMP-dependent protein kinase

**PrH:** nucleus prepositus hypoglossi

**RGS:** regulator of G-protein signaling

**ROS:** reactive oxygen species

**Rp-8-Br-PET-cGMP:** Rp-β-Phenyl-1,$N^2$-etheno-8-bromoguanosine 3′,5′-cyclic monophosphorothioate

**s.c.:** subcutaneous

**S.E.M:** standard error of the mean

**sGC:** soluble guanylate cyclase

**SMTC:** S-Methyl-L-thiocitrulline

**Trolox:** 6-hydroxy-2,5,7,8-tetramethylchroman-2-carboxylic acid

**TX+AA:** Trolox and ascorbic acid

**U-74389G:** 21-[4-(2,6-di-1-pyrrolidinyl-4-pyrrimidinyl)-1-piperazinyl]-pregna-1,4,9(11)-triene-3,20-dione(Z)-2-butenedioate

# 1. INTRODUCTION

## 1.1 OPIOID RECEPTORS

The existence of opioid-binding sites was first proposed by Beckett and Casy in 1954 and in 1973 they were found in mammalian brain tissue (Pert and Snyder, 1973; Simon et al., 1973; Terenius, 1973). The confirmed presence of opioid receptors led to a search for endogenous ligands, resulting in the discovery of the enkephalins (Hughes et al., 1975), β-endorphin (Cox et al., 1976) and dynorphins (Goldstein et al., 1979). However, it was not until 1976 when Martin and colleagues presented the first evidence of the existence of different types of opioid receptors.

To date, four opioid receptors have been cloned, μ receptor (MOR), δ receptor (DOR), κ receptor (KOR) and the nociceptin receptor (NOP), also known as the opioid receptor like-1 (ORL-1), or nociceptin/orphanin FQ (N/OFQ) receptor. Despite high sequence similarity of the NOP receptor to opioid receptor subtypes (63–65%), endogenous opioid peptides have very low affinity for the NOP receptor (for review, see Donica et al., 2013). Moreover, NOP receptor-mediated actions oppose many antinociceptive actions of classic opioid agonists. Although both hyperalgesic and analgesic actions of supraspinally administered N/OFQ have been reported, spinally administered N/OFQ predominantly produces analgesia (Mogil and Pasternak, 2001). On the other hand, other receptors such as σ or ζ were initially proposed as opioid receptors. However, the σ receptor was cloned and classified as a single transmembrane-spanning protein and it is no longer considered a member of the opioid receptor family (Monassier and Bousquet, 2002). The ζ receptor is an opioid growth factor receptor with no homology with classical opioid receptors (Zagon et al., 2000). In addition, a λ receptor and a β-endorphin-sensitive ε receptor were described (Wüster et al., 1979). However, these receptors are poorly characterized, and verification for their existence through identification of their respective genes is still lacking.

The nomenclature for the opioid receptors remains controversial. In molecular biology, δ, κ and μ opioid receptors are DOR, KOR and MOR, respectively (Dhawan et al., 1996). However, the International Union of Pharmacology Committee on Receptor Nomenclature and Drug Classification (NC-IUPHAR) considers that the well-established greek letter names (μ, δ and κ) are most appropriate, but when Greek symbols are not permitted or impractical, the use of mu, delta or kappa, or MOP, DOP or KOP is permissible (Cox et al., 2015) (Table 1.1). The terms “μ opioid receptor” or “MOR” have

been used throughout this thesis because this terminology is the most commonly used in our field.

**Table 1.1. Classification of opioid receptors. The International Union of Pharmacology Committee on Receptor Nomenclature and Drug Classification (NC-IUPHAR)-approved nomenclature for opioid receptors (IUPHAR Review 9) (Cox et al., 2015).**

| Current NC-IUPHAR-approved nomenclature[a] | Other (non-approved) nomenclature | Presumed endogenous ligand(s) |
|---|---|---|
| μ, mu or MOP | MOR, $OP_3$ | β-Endorphin (not selective[c])<br>Enkephalins (not selective[c])<br>Endomorphin-1[b]<br>Endomorphin-2[b] |
| δ, delta or DOP | DOR, $OP_1$ | Enkephalins (not selective[c])<br>β-Endorphin (not selective[c]) |
| κ, kappa or KOP | KOR, $OP_2$ | Dynorphin A<br>Dynorphin B<br>α-Neoendorphin |
| NOP | ORL1, $OP_4$ | Nociceptin/orphanin FQ (N/OFQ) |

### 1.1.1 Molecular and structural aspects of MOR

Among all the opioid receptors, MORs have been the most extensively studied due to their role in mediating the actions of morphine and other clinically relevant analgesic agents, as well as drugs of abuse. Thus, opioid agonists such as morphine, fentanyl or methadone show a considerably higher affinity for MOR than for DOR and KOR (Raynor et al., 1994).

Opioid receptors belong to the large superfamily of seven transmembrane-spanning G protein-coupled receptors (GPCRs), which produce their cellular effects via coupling with $G_i/G_o$ transduction cascades. Genetic knock-out studies have established that MORs are encoded by a single structural gene (OPRM1), which was isolated and its sequence was defined in the 90s (Chen et al., 1993; Liang et al., 1995; Wendel and Hoehe, 1998). Pharmacological studies have long suggested that this gene generates a wide diversity of MOR spliced variants (Wolozin and Pasternak, 1981; Pasternak, 2014). There are three major classes of MOR splice variants in mice, rats and humans. The first class comprises full length 7 transmembrane domain variants. The second set lacks exon 1, which generates truncated 6 transmembrane domain variants. The third set involves a single

transmembrane protein encoded by exon 1. All three classes are functionally relevant (Pasternak, 2014) (Fig. 1.1). Disruption of exons 1, 2 or 3 eliminates morphine actions, indicating that morphine responses depend upon the full-length, 7 transmembrane variants. However, knock-out animals targeting exon 1 retain morphine-6β-glucuronide (M6G) analgesia, suggesting that its analgesic mechanisms are distinct from those of morphine (Schuller et al., 1999). On the other hand, when targeting the exon 11, morphine and methadone analgesia is mantained, but the analgesic actions of heroin, M6G and fentanyl are markedly diminished (Pan et al., 2009).

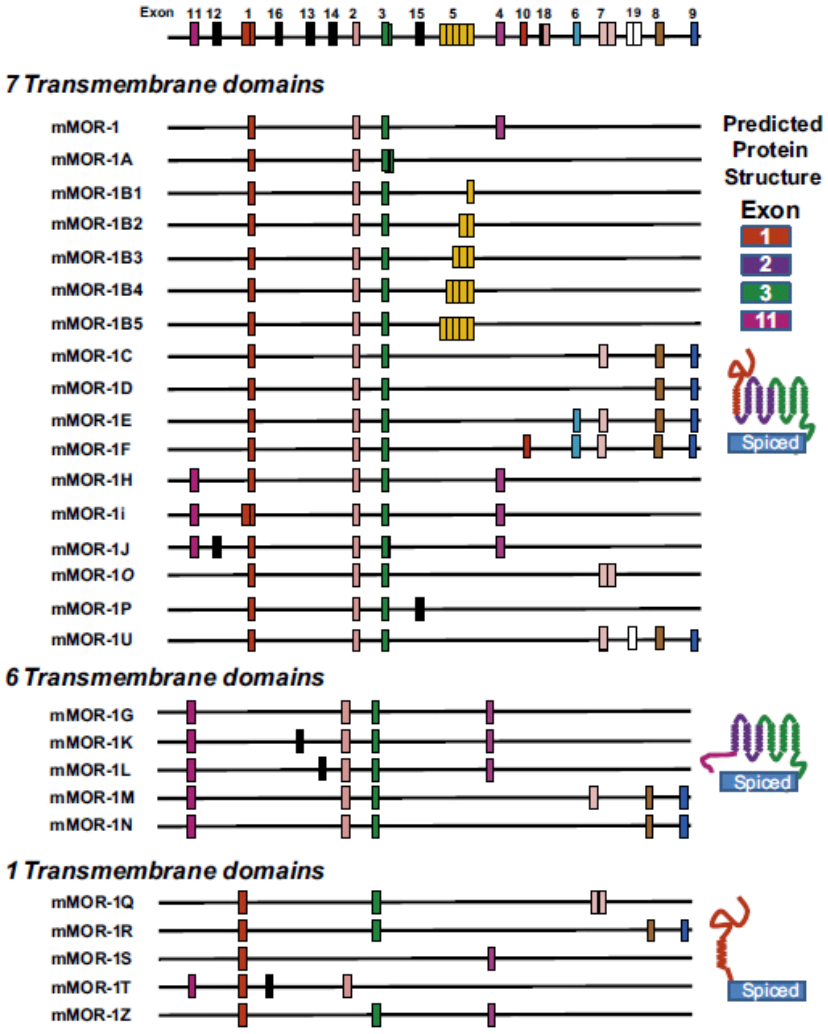


**Figure 1.1.** The mouse Oprm1 gene and the MOR splice variants (Pasternak, 2014).

X-ray crystallography has revealed the atomic structures of the mouse MOR (Manglik et al., 2012) (Fig. 1.2) and DOR (Granier et al., 2012). Recently, the crystal structures of the human KOR (Wu et al., 2012), DOR (Fenalti et al., 2014) and NOP

(Thompson et al., 2012) have been also unveiled. As in other GPCRs, the structure of the MOR consists of seven transmembrane alpha-helices that are connected by three extracellular loops and three intracellular loops. In most available GPCR structures, the ligand is partially buried within the helical bundle. In contrast, the binding pocket of the MOR has been found to be large and accessible (Manglik et al., 2012). The openness of the binding site may explain why opioids display their actions so quickly and why their effects can be also rapidly reversed. Endomorphin 1 and 2 are small peptides with the highest affinity and selectivity profile for MOR (Zadina et al., 1997). However, it is not clear whether they function as endogenous opioids in the mammalian CNS, since no precursor protein has been identified yet (Corbett et al., 2006).

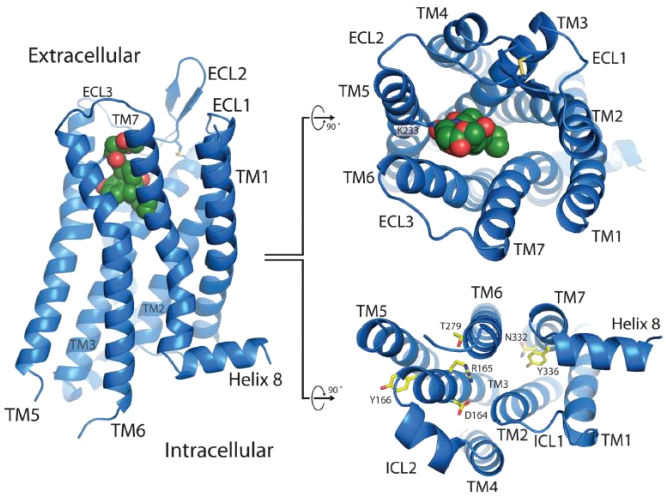


**Figure 1.2.** Overall view of MOR receptor structure. Views from within the membrane plane (left), extracellular side (top, center panel) and intracellular side (bottom, center panel) show the typical seven-pass transmembrane GPCR architecture of MOR. The ligand is shown in green spheres (Manglik et al., 2012).

Over the last decade, an increasing number of studies have explored the ability of GPCRs, including opioid receptors, to heteromerize. It has been suggested that MOR exists primarily as a dimer that may oligomerize with DOR into tetramers (Golebiewska et al., 2011). In agreement, Manglik et al. (2012) observed that MOR crystallizes in tightly linked pairs, through a four-helix bundle pattern that is formed by transmembrane segments 5 and 6 (Fig. 1.3).

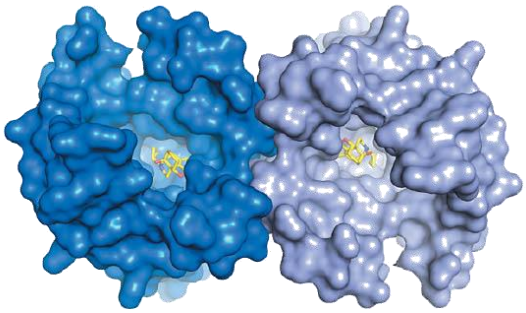

**Figure 1.3.** MORs crystallized with a ligand (yellow), forming an intimate pair (Buchen, 2012)

Interestingly, opioid receptor heteromers are becoming novel therapeutic targets (for review, see Fujita et al., 2014). The MOR/DOR heteromer has been the most extensively studied. Both receptors exist in close proximity to form interacting complexes in living cells (Gomes et al., 2004). While MOR or DOR homomers are coupled to a $G_{i/o}$-protein, MOR/DOR heteromer could signal via $G_z$ proteins (Hasbi et al., 2007) and/or through β-arrestin 2 (Rozenfeld et al., 2007). An anti-analgesic role for the DOR/MOR heteromer has been reported (Milan-Lobo et al., 2013) and it might be a novel therapeutic target in the treatment of pain. Furthermore, MOR/KOR heteromers may also be viable targets for pain management. Thus, administration of a MOR/KOR heteromer selective ligand exhibits 50-times greater antinociceptive potency than morphine, it does not lead to physical dependence and it promotes low antinociceptive tolerance upon chronic intracerebroventricular administration (Yekkirala et al., 2011).

### 1.1.2 Anatomical location and functions of MOR

MORs are widely distributed throughout the CNS. High densities of MOR are found in regions such as the cortex, caudate-putamen, habenula and interpeduncular nuclei, hippocampus, hypothalamic nuclei, raphe medianus, inferior colliculus, parabrachial nuclei, locus coeruleus, ambiguus nucleus, sensory trigeminal complex, nucleus of the solitary tract and the dorsal horn of the spinal cord. MORs are also present on dorsal root ganglion cells and on peripheral nerves (Mansour et al., 1994; Arvidsson et al., 1995; Truong et al., 2003).

MOR activation by endogenous and exogenous ligands results in a multitude of effects, which include analgesia, sedation, respiratory depression, euphoria, dependence and reward, hormone release, inhibition of gastrointestinal transit or cell proliferation (Waldhoer et al., 2004; Feng et al., 2012) (Fig. 1.4). In general, agonists selective for MOR or DOR are analgesic and rewarding, whereas KOR-mediated actions have been reported to be psychotomimetic and dysphoric (Pfeiffer et al., 1986). Pain modulation by MOR takes place at the periphery (Stein, 1991) and the spinal and supraspinal levels of the CNS (Yaksh, 1987; Dickenson, 1991). Dissociating pain control from side effects such as respiratory depression has long been a goal in opioid drug development. Unfortunately, to date, opiate drugs showing good analgesic profile with lack of respiratory depression have not been identified. On the other hand, it has been proposed that an endogenous antiopioid system exists to regulate and compensate the opioid system and maintain the homeostasis (Harrison et al, 1998). The most studied endogenous antiopioid peptides are the Tyr-Pro-Leu-Gly-NH2 (Tyr-MIF-1) family of peptides and nociceptin/orphanin FQ (Ciccocioppo et al., 2000; Pan and Kastin, 2007).

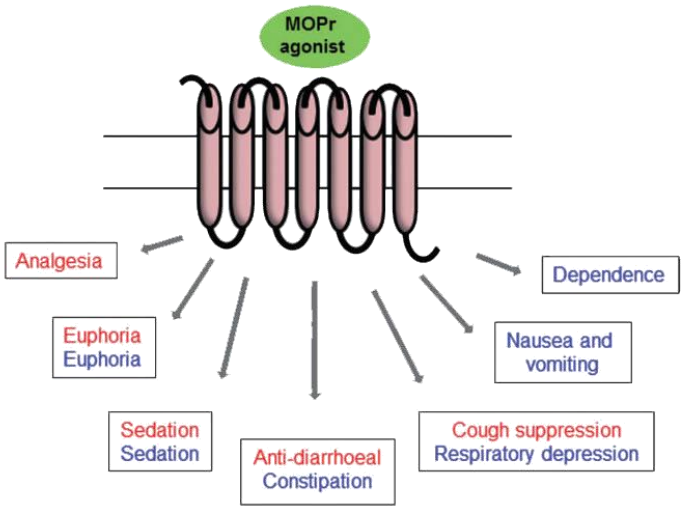


**Figure 1.4.** Most relevant functions mediated by MOR. Effects in red are desirable effects, whereas those in blue are adverse effects. Some, such as sedation or euphoria, can be therapeutic or adverse depending upon the context (Kelly, 2013).

### 1.1.3 Molecular aspects of acute activation of MOR

As previously mentioned, MORs are coupled to pertussis toxin-sensitive $G_i/G_o$ proteins. In the resting state, G proteins are heterotrimers consisting of a GDP-bound α subunit and a βγ dimer. Upon activation of the receptor, there is a conformational change that permits G protein binding to the receptor and the release of GDP from the Gα subunit. Next, the Gα subunit binds a new molecule of GTP. This exchange destabilizes the complex and triggers the dissociation of the Gα subunit from the Gβγ dimer and the receptor. Then, both Gα-GTP and Gβγ can activate different signaling cascades.

Both Gα and Gβγ interact with multiple cellular effector systems, which lead to inhibition of adenylyl cyclases and voltage-gated $Ca^{2+}$ channels and stimulation of G protein-activated inwardly rectifying $K^+$ channels (GIRKs) (for review, see Law et al., 2000; Nagi and Pineyro, 2014). These actions hyperpolarize the neuron, reducing its electrical activity and therefore, decreasing the ability to release neurotransmitters. Furthermore, MOR-coupled G proteins can activate other effectors, including G protein-coupled receptor kinases (GRKs) or β-arrestins. Additionally, MORs have been reported to interact with phospholipase Cβ (PLCβ), which mobilizes intracellular $Ca^{2+}$, and also with mitogen-activated protein kinase (MAPK) cascades, such as extracellular-signal-regulated kinases (ERKs) and the Jun N-terminal kinases (JNKs) (Law et al., 2000).

Although opioid receptors are predominantly coupled to $G_i/G_o$ proteins, coupling to pertussis toxin-insensitive $G_s$ or $G_z$ proteins has been also reported (Crain et al., 1996; Garzón et al., 1998). In fact, it has been suggested that chronic morphine treatment induces a change in the coupling of MOR from $G_{i/o}$ to $G_s$ and this switch in the Gα subunit coupling is associated with a stimulation of adenylyl cyclases (Wang et al., 2005; Wang and Burns, 2006). In addition, it has been hypothesized that GPCRs exist in different states regarding the association with G proteins. Thus, GPCRs that are preassociated with G proteins (pre-coupled receptors) are thought to signal more rapidly than receptors that are dependent on collision coupling (Lohse et al., 2008).

On the other hand, over the past decades, numerous studies have shown that not all agonists activate the same intracellular signaling pathways, even though they act at the same receptor (Kenakin, 1995; Raehal et al., 2011; Kelly, 2013). Indeed, the term "functional selectivity" or "biased agonism" has emerged to describe these different

efficacies of ligands to activate diverse signaling pathways. Functional selectivity has been demonstrated at the MOR (Fig. 1.5). Thus, there are agonist-dependent differences in MOR responses with respect to key signaling events, including phosphorylation, endocytosis and trafficking (Raehal et al., 2011; Kelly, 2013). These differences between agonists may be related to the differential development of analgesic tolerance after prolonged use of various opioids *in vivo*. However, the precise nature of this diversity remains to be elucidated.

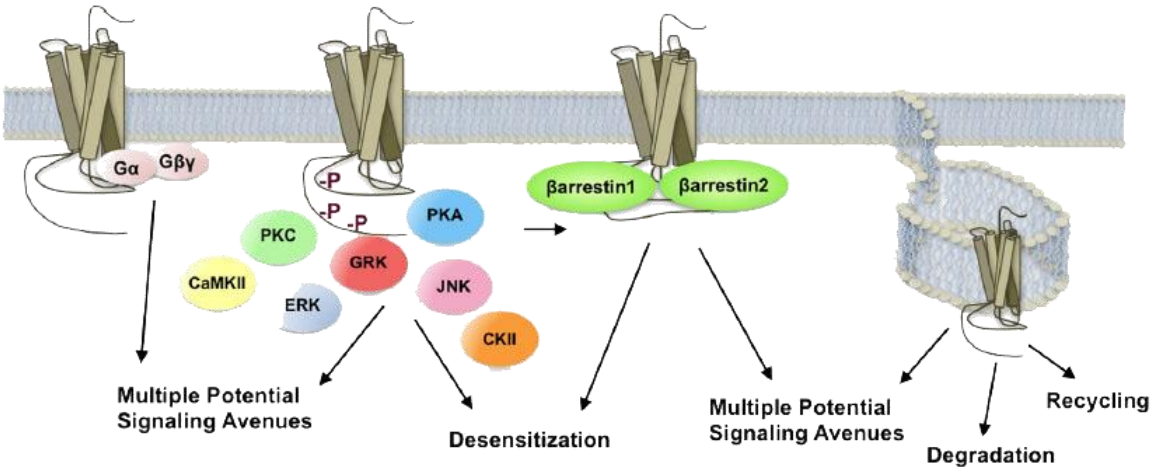


**Figure 1.5.** Scheme representing functional selectivity at the MOR. The specific Gαi subunits to which MORs couple are dictated by the agonist and the cellular system. Moreover, MORs can be phosphorylated in response to agonist occupation by multiple kinases. Phosphorylation by a particular kinase influences secondary cascade interactions. Receptor interaction with β-arrestins can be dependent or independent of receptor phosphorylation. In addition, the MOR can be internalized in response to an agonist. Endocytosis may involve clathrin- or caveolin-dependent processes and may result in the activation of subsequent signaling pathways, receptor recycling or degradation. Image modified from Raehal et al. (2011).

### 1.1.4 MOR regulation: desensitization and tolerance

One major limitation of opioids used in clinical practice is the development of tolerance after long-term administration. Therefore, it is relevant to study the cellular and molecular mechanisms underlying this process. Tolerance is a complex physiological adaptation that involves, at the very least, receptor, cellular, synaptic and behavioral changes. There is good evidence that desensitization is a key process that contributes to the development of tolerance. In fact, both terms tolerance and desensitization are

referred to a loss of responsiveness to an opioid agonist. However, desensitization is linked to molecular changes at the level of receptor signaling that occurs within seconds or minutes during agonist application, whereas opioid tolerance applies to the loss of responsiveness after long-term exposure (days to weeks) (Dang and Christie, 2012; Williams et al., 2013). Both desensitization and tolerance may be associated with a reduction of functional receptors. Desensitization can be homologous if the reduced effects are restricted to the activated receptor, or it can be heterologous if desensitization generalizes to other receptors (Lefkowitz et al., 1983).

As it happens with other GPCRs, MORs can undergo rapid desensitization. The classic model of GPCR desensitization has been described to begin with phosphorylation of activated receptors by kinases followed by β-arrestin binding. After phosphorylation and β-arrestin binding, receptors are presumably uncoupled from their effectors and at this point, the receptor is in a desensitized state. Then, β-arrestin-bound receptors can be internalized via a clathrin-dependent pathway. Finally, after endocytosis, receptors can be recycled back to the membrane or they can suffer lysosomal degradation (for review, Connor et al., 2004; Williams et al., 2013) (Fig. 1.6). To add more complexity to the process, opioid agonists differ in their ability to promote MOR regulation (Borgland et al., 2003; von Zastrow, 2010). These differences among opioid agonists to cause MOR regulation may lead to differential abilities to induce tolerance (Dang and Christie, 2012).

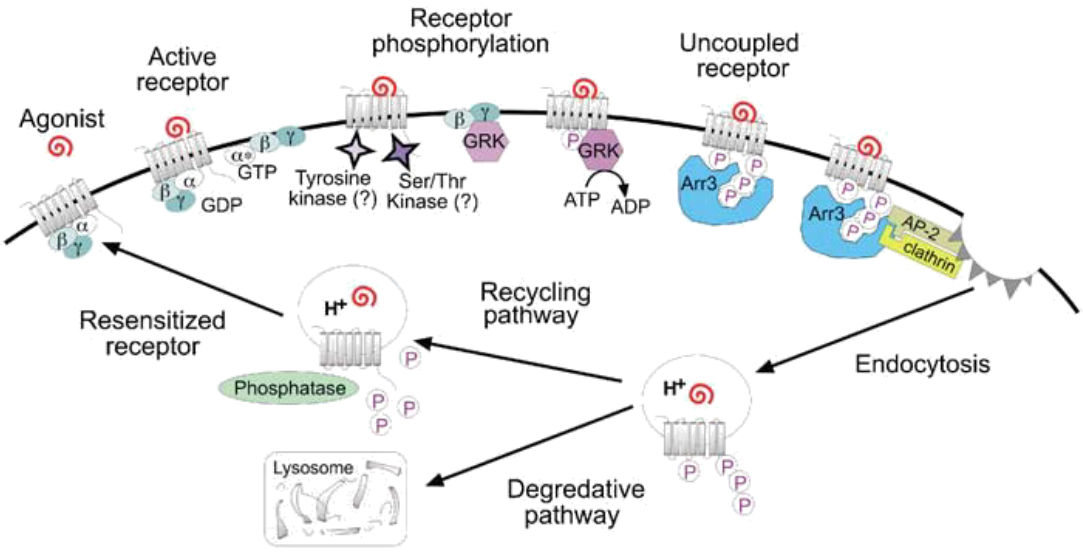


**Figure 1.6.** The generally accepted pathway for acute MOR regulation. Modified from Connor et al. (2004).

Opioid agonists elicit distinctive agonist-selective patterns of phosphorylation, which account for the agonist-selective ability to promote MOR internalization (Doll et al., 2011; Illing et al., 2014). Different types of kinases have been reported to phosphorylate MOR, depending on the agonist used to activate the receptor. For example, the full agonist [D-Ala$^2$, N-MePhe$^4$, Gly-ol]-enkephalin (DAMGO) induces desensitization by a G protein-coupled receptor kinase (GRK)-dependent mechanism (Johnson et al., 2006). GRKs selectively recognize ligand-activated receptors (Freedman and Lefkowitz, 1996). For that reason, phosphorylation by GRKs is associated with homologous desensitization (Gainetdinov et al., 2004). Both GRK2 and GRK3 have been implicated in MOR desensitization *in vitro* (Kovoor et al., 1998; Zhang et al., 1998). In addition, cyclic AMP dependent protein kinase A (PKA), protein kinase C (PKC), calcium/calmodulin-dependent protein kinase (CaMKII) (Mestek et al., 1995), tyrosine kinases (Pak et al., 1999) or MAPK (Polakiewicz et al., 1998) have all been described to phosphorylate MOR and promote desensitization. In contrast to DAMGO, morphine-induced desensitization has been described to be PKC-dependent (Bailey et al., 2004; Johnson et al., 2006; Bailey et al., 2009b; Levitt and Williams, 2012). Unlike GRK-dependent phosphorylation, PKA- or PKC-mediated phosphorylation is not necessarily followed by rapid endocytosis. Moreover, second messenger-dependent protein kinases not only phosphorylate agonist-activated receptors, but they can phosphorylate indiscriminately other receptors that have not been activated by the agonist, which can lead to heterologous desensitization (Gainetdinov et al., 2004).

Phosphorylation of a GPCR appears to increase the affinity of the receptor for β-arrestin binding (Lohse et al., 1993). In the CNS, β-arrestin 1 and β-arrestin 2 are concentrated especially at postsynaptic sites (Attramadal et al., 1992). Arrestin-dependent internalization promotes sequester of MORs in receptor-containing endosomes. Internalization of MOR is also an agonist-dependent phenomenon. Thus, enkephalins, DAMGO, fentanyl and methadone induce significant internalization of MOR, whereas morphine fails to promote internalization in different systems (Arden et al., 1995; Keith et al., 1996; Sternini et al 1996; Trapaidze et al., 2000; Alvarez et al., 2002; Bailey et al., 2003; Minnis et al., 2003). It has been suggested that agonists that induce substantial MOR internalization have less potential to cause tolerance (Finn and Whistler, 2001), because they would allow for receptor reinsertion in the membrane. On the contrary, some studies have established that internalization is not necessary for recovery of MOR-

mediated effects (Arttamangkul et al., 2006; Dang et al., 2011). In addition, there is no clear evidence that strongly internalizing agonists produce differential tolerance compared with weakly internalizing opioids in humans. Thus, continuous administration of transdermal fentanyl in pain patients (high efficacy, moderate endocytosis) was found to produce greater tolerance in comparison with buprenorphine (low efficacy, non-internalizing) (Sittl et al., 2006).

Regarding the time-course of these pathways involved in MOR regulation, phosphorylation of MOR at putative GRK sites is rapid, apparently saturating within 1–2 minutes when receptors are stimulated by highly efficacious peptide agonists. Internalization seems to be slower with time constants generally in the order of ≥5 minutes and reaching steady state in less than 30 minutes. Recovery from rapid desensitization is thought to occur in approximately 1 hour (Williams et al., 2013) (Fig. 1.7). On the other hand, down-regulation refers to a reduced number of receptors present in cells, as a result of enhanced degradation and/or reduced biosynthesis of receptors (Tsao and von Zastrow, 2000). It can be distinguished from the process of internalization, which is characterized by a physical redistribution of receptors between the membrane and intracellular compartments without a detectable change in total receptor number. Down-regulation is also a much slower process, typically induced over a period of hours to days after prolonged or repeated exposure to an agonist (Law et al., 1982).

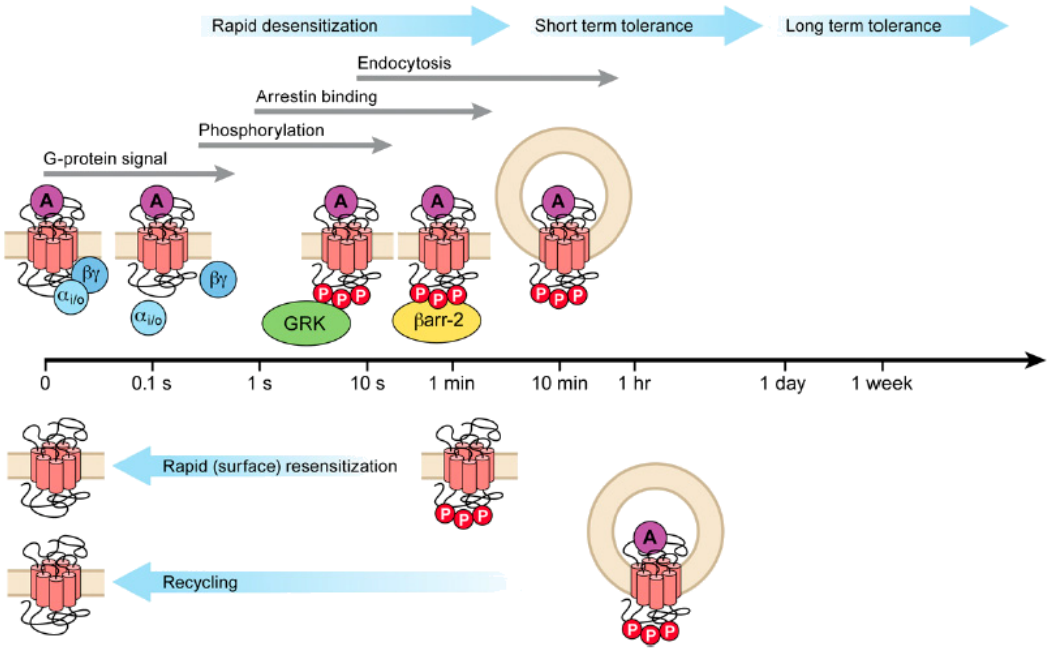


**Figure 1.7.** Time-course of the mechanisms that lead to MOR desensitization (Williams et al., 2013).

On the other hand, other mechanisms have also been suggested to participate in MOR desensitization. These mechanisms include regulators of Gβγ dimers such as the phosducin-like proteins (Garzón et al., 2002) or the regulators of G protein signaling (RGS) (Potenza et al., 1999; Garzón et al., 2001, 2005). RGS proteins accelerate the hydrolysis of GTP by the Gα subunit, thereby limiting the duration of GPCR signaling (for review, see Jean-Baptiste et al., 2006). Moreover, RGSs have been reported to favor MOR desensitization by binding and sequestering agonist-activated Gα subunits (Garzón et al., 2001, 2005). On the other hand, Raveh et al. (2010) have suggested that GRKs enable rapid GIRK desensitization through a mechanism that, surprisingly, does not involve their kinase activity, but rather depends on their ability to bind the Gβγ subunits required for downstream signaling.

As previously mentioned, desensitization of MOR is thought to contribute to opioid tolerance. However, other multiple mechanisms participate in the development of tolerance at both spinal and supraspinal levels *in vivo*. Thus, opioid tolerance is associated with impaired receptor resensitization and with receptor down-regulation (Dang and Christie, 2012; Williams et al., 2013). Studies that have explored fast components of desensitization and recovery in neurons from chronically treated animals are of particular interest. Thus, MOR desensitization is facilitated in rats treated with morphine, whereas recovery from desensitization is inhibited when compared to untreated animals (Dang and Williams, 2004). Hence, a desensitizing stimulus applied to neurons following chronic morphine treatment causes subsequent MOR uncoupling to a much greater extent than those from untreated animals.

On the other hand, a large list of molecules acting on different pathways have been reported to block opioid tolerance, including N-methyl-D aspartate receptor (NMDAR) antagonists (Elliott et al., 1994), nNOS inhibitors (Santamarta et al., 2005), PKC inhibitors (Hull et al., 2010), substance P antagonists (Foran et al., 2000), serotonin reuptake inhibitors (Nayebi et al., 2009), calcium channel blockers (Dogrul et al., 2005) or calcitonin gene-related peptide receptor antagonists (Powell et al., 2000). Spinal glia activation and neuronal apoptosis also appear to contribute to opioid tolerance (Song and Zhao, 2001; Mao et al., 2002; Watkins et al., 2005; Zhou et al., 2010). Unfortunately, despite decades of study, the mechanisms underlying opioid tolerance remain far from clear.

### 1.1.5 Morphine, methadone and fentanyl: three different opioids

The six most common clinically used opioids are morphine, oxycodone, hydromorphone, fentanyl, buprenorphine and methadone (Pergolizzi et al., 2008). Although these drugs differ in their chemical structure, the primary target for their actions is the MOR (Eddy and May, 1973; Raynor et al., 1994). Methadone is a synthetic opioid with potent analgesic effects that has been widely used for the treatment of opioid dependence (Dole et al., 1966), but its use has extended to pain management as well. Thus, it has been studied as a therapy for cancer pain and other chronic pain states (De Conno et al., 1996; Gardner-Nix, 1996; Ripamonti et al., 1997). However, the clinical use of methadone as an analgesic is complex because of its prolonged and variable half-life (typically ≈ 24 hours). Methadone has no active metabolites or prodrug forms and it is administered clinically as a racemic mixture. The R-isomer possesses analgesic activity whereas the S-isomer is inactive or weak as an opioid (Scott et al., 1948; Ingoglia and Dole, 1970). It has been reported that R-methadone has a 10-fold higher affinity for MOR than S-methadone and both isomers have a low affinity for DOR and KOR (Kristensen et al., 1995). In addition, methadone has non-opioid pharmacologic actions including inhibition of the reuptake of monoamines (Codd et al., 1995), blockade of NMDARs (Gorman et al., 1997; Ebert et al., 1998; Matsui and Williams, 2010) and blockade of GIRK channels (Rodríguez-Martín et al., 2008; Matsui and Williams, 2010). The blockade of NMDARs by methadone might be considered as one of its potentially relevant therapeutic actions because the NMDAR antagonist, MK801, reduces hyperalgesia (Mao et al., 1992), enhances opioid analgesia (Ebert et al., 1998) and attenuates morphine tolerance and dependence (Trujillo and Akil, 1991; Bilsky et al., 1996). Moreover, it has been shown that opioid analgesics that inhibit monoamine reuptake, such as methadone, induce antidepressant-like effects that may account for their analgesic effects by regulating the affective dimension of pain (Rojas-Corrales et al., 2002). However, this observation seems to disagree with the clinical reports about methadone-treated patients showing more risk to suffer depression (Brienza et al., 2000; Peles et al., 2007).

Fentanyl is a synthetic opioid which was first synthesized by Janssen in the 1960s, in an effort to produce opioid analgesics with stronger analgesic activity and better safety profile than morphine. Fentanyl and analogues are among the most potent opioid

analgesics known, estimated to be up to 100 times more potent than morphine (Vardanyan and Hruby, 2014). It has short-acting analgesic activity after intravenous or subcutaneous administration. However, the low molecular weight, high potency and lipid solubility of fentanyl make it suitable for transdermal delivery. Transdermal fentanyl is effective and well tolerated for the treatment of chronic pain caused by malignancy and non-malignant conditions (Kornick et al., 2003). Concerning future prospects, there are still many possibilities for development of novel fentanyl-related multivalent ligands. Of particular interest would be ligands with mixed and/or balanced μ and δ opioid receptor activities (Vardanyan and Hruby, 2014).

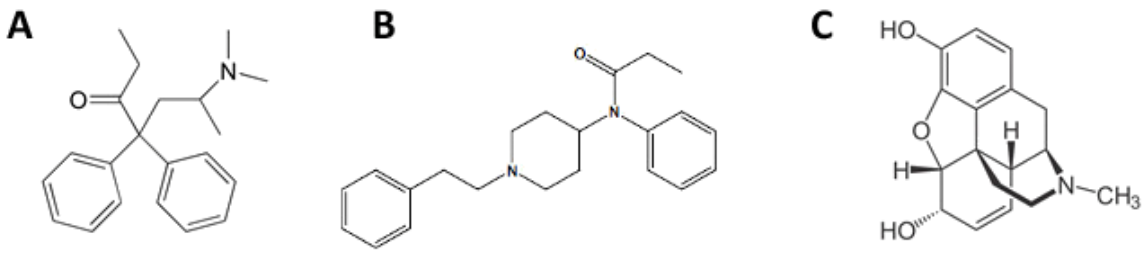


**Figure 1.8.** Molecular structures of methadone (A), fentanyl (B) and morphine (C).

The pharmacological actions of methadone and fentanyl differ in many ways from morphine. Morphine is the prototypical opioid drug used clinically for severe pain control and its potent antinociceptive effects have been shown to be mediated by the MOR (Matthes et al., 1996). It has been reported that fentanyl and morphine are full agonists for inhibiting cAMP accumulation and partial agonists for stimulating GTPγS binding (Zaki et al., 2000). Methadone has been described to be a full agonist in GTPγS binding studies (Rodríguez-Martín et al., 2008). Other studies measuring GIRK currents have reported that morphine and methadone are partial agonist at the MOR (Bailey et al., 2003; Johnson et al., 2006), but this may be because methadone blocks GIRK channel-mediated potassium conductance (Rodríguez-Martín et al., 2008; Matsui and Williams, 2010).

At the molecular level, morphine, methadone and fentanyl display different regulatory events at the MOR. Studies examining morphine-induced desensitization have yielded inconsistent and often contradictory results. While some authors have reported that morphine is a very poor desensitizing agent (Blake et al., 1997; Alvarez et al., 2002; Bailey et al., 2003), others have observed a more significant MOR desensitization by morphine (Dang and Williams, 2005; Arttamangkul et al., 2008). Accordingly, there is

considerable evidence that ongoing PKC activity is required for morphine-induced desensitization and tolerance (Bailey et al., 2004, 2009a; 2009b; Hull et al., 2010; Levitt and Williams, 2012; Sánchez-Blázquez et al., 2013). On the other hand, methadone- and fentanyl-induced analgesic tolerances have been reported to be GRK3-dependent (Terman et al., 2004; Melief et al., 2010). Moreover, as explained in section 1.1.4, morphine differs from most opiates in its poor ability to internalize MORs (Arden et al., 1995; Keith et al., 1996; Sternini et al 1996; Trapaidze et al., 2000; Alvarez et al., 2002; Bailey et al., 2003; Minnis et al., 2003). On the contrary, methadone and fentanyl have been found to induce rapid desensitization and efficacious internalization in different systems (Whistler et al., 1999; Zaki et al., 2000; Alvarez et al., 2002; Minnis et al., 2003; Koch et al., 2005; Arttamangkul et al., 2008; Virk and Williams, 2008; Anselmi et al., 2013). On the other hand, systemic administration of fentanyl has been reported to have the greatest relative efficacy, followed by methadone and morphine (Sirohi et al., 2008; Madia et al., 2009).

## 1.2 NITRIC OXIDE

In 1980, Furchgott and Zawadzki reported that the relaxation of the smooth muscle of *in vitro* preparations of rabbit aorta in response to acetylcholine was dependent on the presence of endothelial cells in the preparation. They established that acetylcholine-treated endothelium was releasing a diffusible factor that would relax blood vessels by activating guanylate cyclase (Furchgott and Zawadzki, 1980). The diffusible factor was then termed the endothelium-derived relaxing factor (EDRF), although it was later identified as nitric oxide (NO) (Ignarro et al., 1987; Palmer et al., 1987). Soon after, its presence in the CNS was detected (Garthwaite et al., 1988).

### 1.2.1 Synthesis of NO

NO is produced when L-arginine is transformed to L-citrulline through catalysis by the NO synthase (NOS) (Tayfun-Uzbay and Oglesby, 2001). Three isoforms of NOS have been identified, products of different genes, with different localization, regulation and catalytic properties (for review see Marletta, 1994; Alderton et al., 2001). Neuronal NOS (nNOS) (also known as NOS-1) was the first synthase to be cloned and it is found in the

brain, peripheral nerves and some non-neuronal tissues. The second NOS to be cloned was isolated from macrophages and it is known as inducible NOS (iNOS or NOS-2) because it is readily induced in many tissues by proinflammatory cytokines. Finally, endothelial NOS (eNOS or NOS-3) was the last to be cloned. eNOS can be bound to plasma membranes and is typically expressed in vascular endothelium, airway epithelium and endocardial cells. Both nNOS and eNOS, are grouped together as constitutive NOS (cNOS), because they are usually constitutively expressed in the cell. Unlike iNOS, $Ca^{2+}$-calmodulin (CaM) is required for the activation of nNOS and eNOS (Toda et al., 2009). Furthermore, a mitochondrial NOS (mtNOS) has been described (Bates et al., 1995, 1996). Its existence is questioned (Lacza et al., 2006), but the presence and the relevance of heart mitochondrial NOS has been recently reviewed (Zaobornyj and Ghafourifar, 2012).

### 1.2.2 nNOS: structure, localization and regulation

The nNOS consists of 1434 amino acids with a predicted molecular weight of 160.8 kDa (Boissel et al., 1998). The active form of the nNOS is the dimer. Each monomer contains an oxygenase domain (N-terminal) and a reductase domain (C-terminal), which can be separated by a regulatory CaM binding motif (for review, see Zhou and Zhu, 2009). The oxygenase domain binds the substrate L-arginine and contains a tetrahydrobiopterin (BH4) binding site and a heme active site. The reductase domain binds the substrate nicotinamide adenine dinucleotide phosphate (NADPH) and it contains a binding site for flavin mononucleotide (FMN) and flavin adenine dinucleotide (FAD). Electrons ($e^-$) donated by NADPH flow from the reductase domain to the oxygenase domain via FMN and FAD, a process that is regulated by CaM binding (Roman et al., 2006) (Fig. 1.9).

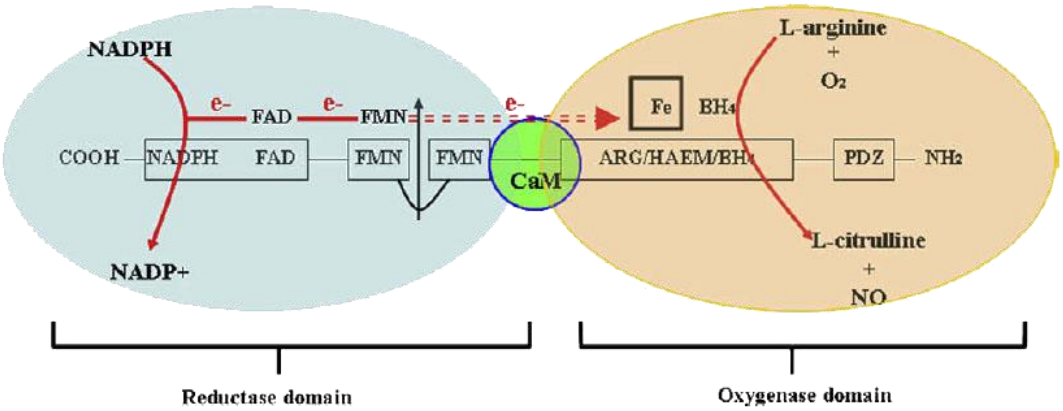


**Figure 1.9.** Schematic representation of the nNOS structure. nNOS catalyzes the oxidation of L-arginine to form L-citrulline and NO. The enzyme contains an oxygenase domain and a reductase domain, separated by a calmodulin binding motif. Electrons are donated by NADPH and transfer from the reductase domain to the oxygenase domain via FMN and FAD (Zhou and Zhu 2009).

In the CNS, nNOS-containing neurons are present in many areas, with the highest densities occurring in the accessory olfactory bulb and granule cells of the cerebellum. nNOS can be located either pre- or post-synaptically. Although neurons that express nNOS represent only roughly 1% of cell bodies in the cerebral cortex, virtually every neuron in the cortex is exposed to nNOS nerve terminals (for review, see Esplugues, 2002).

As NO is a highly diffusible molecule that cannot be stored in the cells, new synthesis is required to exert its actions. Fractionation studies have demonstrated that brain nNOS exists in particulate and soluble forms (Hecker et al., 1994). Rothe et al (1998) showed that nNOS immunoreactivity of brain neurons was mainly distributed in cytosol far from membranes. A nuclear localization of nNOS in cultured astrocytes of rats has also been reported (Yuan et al., 2004). Differential subcellular localization of nNOS in the cell may contribute to its diverse functions.

It has been shown that phosphorylation of nNOS regulates its activity. Several kinases have been reported to phosphorylate the nNOS, such as PKA, calmodulin-dependent kinases or PKC. Phosphorylation by CaMKII results in a decrease in enzyme activity, whereas a moderate increase in enzyme activity is observed after phosphorylation by protein kinase C (Nakane et al., 1991; Rameau et al., 2004).

However, the most important regulator of nNOS activity seems to be free $Ca^{2+}$, which stimulates nNOS through interaction with CaM. It has been reported that electron flow from FAD to FMN slows down when CaM and $Ca^{2+}$ are absent (Matsuda and Iyanagi, 1999). When $Ca^{2+}$ levels increase, CaM binds to nNOS, activating nNOS. On the contrary, when $Ca^{2+}$ concentration decreases to basal levels, CaM dissociates from nNOS, and it becomes inactive again (For review, Zhou and Zhu, 2009). Availability of calcium ions to stimulate NOS may originate from the extracellular space through voltage-dependent $Ca^{2+}$ channels (Alagarsamy et al., 1994) or glutamate ionotropic NMDARs (Bredt and Snyder, 1989; East and Garthwaite, 1991). NO has been also reported to mediate the release of $Ca^{2+}$ from neuronal intracellular $Ca^{2+}$ stores via ryanodine receptors (Kakizawa et al., 2012).

### 1.2.3 Targets for NO

The potential reactions of NO are numerous and dependent on many different factors. NO can readily diffuse through cell membranes and reacts with cellular components, exerting both direct and indirect effects (Davis et al., 2001). The direct effects are mediated by the reaction of NO with metal complexes, whereas indirect effects are mediated by the formation of reactive nitrogen species (RNS) and reactive oxygen species (ROS) (shortening, from now on, we will name them indistinctly ROS). The source, the site and the concentration of NO are the major factors determining whether NO will elicit direct or indirect effects (Wink and Mitchell, 1998). Thus, direct effects occur at low NO concentrations (< 1 μM), far from the site of NO production, whereas indirect effects of NO become significant at higher local concentrations of NO (> 1 μM).

#### 1.2.3.1 The NO/cGMP signal transduction pathway

The first characterized and probably the most physiologically relevant direct effect of NO involves the interaction of NO with the soluble hemeprotein guanylate cyclase (sGC) (Arnold et al., 1977; Ignarro, 1999). However, NO has been described to react also with a variety of other $Fe^{II}$-systems including the heme centres of haemoglobin, myoglobin, NOS and cytochrome P450 (Heinrich et al., 2013).

The enzyme sGC catalyzes the formation of 3'-5'-cyclic-guanosine-monophosphate (cGMP) from guanosine 5'-triphosphate (GTP), which acts as an intracellular messenger. This enzyme is typically found as a heterodimer, consisting of a larger α-subunit and a smaller heme-binding β-subunit, although homodimers of these subunits can also form (Zabel et al., 1999). Mammals express four sGC subunits ($\alpha_1$, $\alpha_2$, $\beta_1$ and $\beta_2$) and two existing isoforms of the heterodimeric guanylyl cyclase are known: $\alpha_1\beta_1$ and $\alpha_2\beta_1$, which are functionally indistinguishable (Russwurm and Koesling, 2002). The $\beta_2$ subunit does not yield a catalytically active GC upon coexpression with the other subunits (Russwurm et al., 2013). Studies on the expression revealed a ubiquitous distribution of the $\alpha_1\beta_1$ isoform and a more limited occurrence of $\alpha_2\beta_1$ (Mergia et al., 2003). The highest expression of $\alpha_2\beta_1$ is found in brain where both isoforms are present in similar amounts. On the other hand, there are seven transmembrane forms of GCs, known as particulate GCs (pGCs). In contrast to sGC, pGCs are activated by natriuretic peptides (Leitman et al., 1994).

Although sGC possesses basal activity, it is activated many fold by NO. The activation of sGC by NO *in vitro* and *in vivo* occurs in milliseconds. The generally accepted mechanism for sGC activation is the nitrosylation of the regulatory ferrous heme, producing a pentacoordinate ferrous-nitrosyl ($Fe^{2+}$-NO) complex (Stone and Marletta, 1996; Derbyshire and Marletta, 2012; Heinrich et al., 2013). One major prerequisite for the NO-induced activation of sGC is the presence of the reduced $Fe^{2+}$ heme moiety; its removal abolishes any NO-induced enzyme activation (Ignarro et al., 1986). It should be noted that the sGC response decreases upon repeated exposure to NO and a single pretreatment of cells with NO can significantly reduce cGMP stimulation upon the second exposure (Schroder et al., 1988; Bellamy et al., 2000).

cGMP acts on different targets, such as specific protein kinases, cyclic nucleotide-degrading phosphodiesterases (PDEs) and cyclic nucleotide-gated ion channels (Lucas et al., 2000) (Fig. 1.10). The cGMP-dependent protein kinases (PKGs) are attractive candidates as mediators of cGMP signaling. The PKGs belong to the serine/threonine kinase family. Molecular cloning has identified two genes that encode PKGI and PKGII. The N terminus of PKGI is encoded by two alternatively spliced exons that produce the isoforms PKGIα and PKGIβ. PKGs exist as homodimers and share common structural features. They are composed of three functional domains: an N-terminal domain, a

regulatory domain and a catalytic domain (Feil et al., 2003). PKGI family is more commonly involved when cGMP signaling is mediated by NO (Potter et al., 2011).

PKGI is majorly expressed in all types of smooth muscle, platelets and specific neuronal areas such as cerebellar Purkinje cells, hippocampal neurons and the lateral amygdala. PKGII is prominent in most brain regions, intestinal mucosa and kidney (Lohmann et al., 1997; Hofmann and Wegener, 2013). The Iα and Iβ PKGs are soluble enzymes and interact with different proteins through their distinct N termini. On the contrary, the PKGII is anchored at the plasma membrane. PKGs have been reported to phosphorylate a large amount of target proteins including the PKA type I regulatory subunit (Geahlen and Krebs, 1980), PDE5 (Thomas et al., 1990) or the ryanodine receptor (Takasago et al., 1991).

PDEs are enzymes that regulate the cellular levels of the second messengers cAMP and cGMP, by controlling their rates of degradation. In mammals, PDEs are encoded by 21 genes, producing 11 distinct PDE families and splice variants. They are classified as cAMP specific (PDEs 4, 7, 8), cGMP specific (PDEs 5, 6, 9) and dual specificity PDEs (PDE 1, 2, 3, 10, 11) (Bender and Beavo, 2006). On the other hand, cyclic nucleotide-regulated cation channels are ion channels which are also activated by the binding of cGMP or cAMP. These channels pass $Na^+$, $K^+$ and $Ca^{2+}$. They have been originally identified in photoreceptors and olfactory receptor neurons, where they play a fundamental role in sensory transduction, buy they have been also reported to exist in several other cell types and tissues including brain, kidney or endocrine tissues (Kaupp and Seifert, 2002; Biel, 2009).

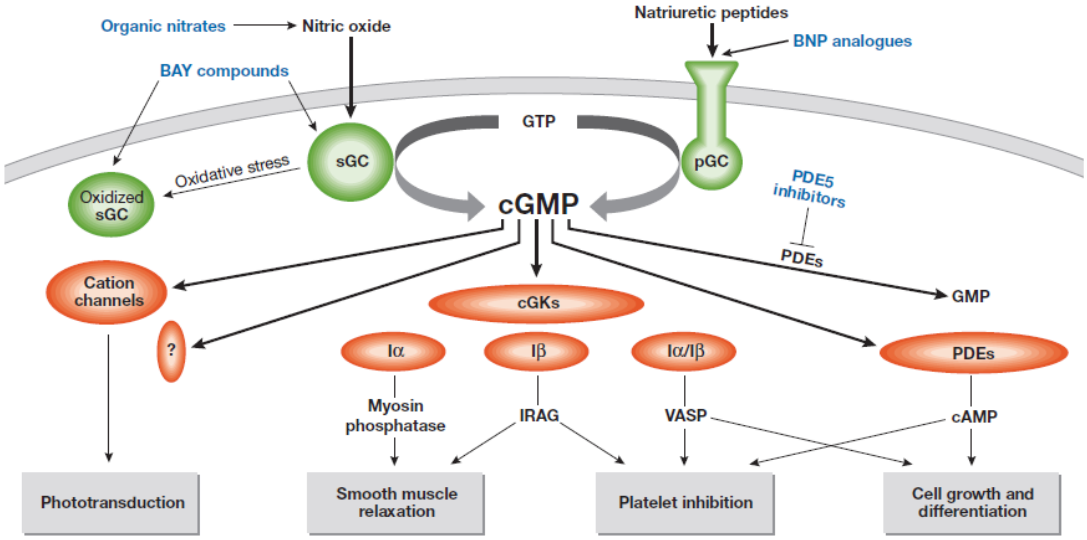


**Figure 1.10.** cGMP signaling pathways: cGMP generators (green) and effectors (red), as well as some downstream pathways and cellular functions (grey boxes) that are involved in the effects of endogenous cGMP and/or cGMP-elevating drugs (blue) (modified from Feil and Kemp-Harper, 2006).

### 1.2.3.2 ROS generation

NO can react with either $O_2$ or $O_2^{\cdot-}$ to produce ROS, through reactions of nitrosation, oxidation or nitration (Huie and Padmaja, 1993; Wink and Mitchell, 1998). NO can also react with $NO_2$ to produce $N_2O_3$. More importantly, reaction of NO with $O_2^{\cdot-}$ involves the generation of the powerful oxidant peroxynitrite ($ONOO^-$), a key mediator of NO toxicity (for review see Radi, 2013).

Mitochondria is a central intracellular source of $O_2^{\cdot-}$, and peroxynitrite formation is favored by the easy diffusion of NO from the cytosol (Poderoso et al., 1996). $O_2^{\cdot-}$ is continuously forming during normal cellular metabolism as a product of cellular oxidases such as NADPH oxidase (NOX) and xanthine oxidase. Its production is tightly controlled by manganese superoxide dismutase (MnSOD) as well as other antioxidant enzymes such as catalase or glutathione peroxidase (GPx). However, superoxide production rates increase several fold during the disruption of cellular redox homeostasis and with inflammatory stimuli. Under these conditions of nitroxidative stress, increased $O_2^{\cdot-}$ production overwhelms the cellular antioxidant defenses and allows the generation of peroxynitrite (Salvemini and Neumann, 2010) (Fig. 1.11). Peroxynitrite is a potent oxidant and pro-inflammatory molecule. It mediates the oxidation of both non-protein and

protein sulfhydryls (Radi et al., 1991a), lipid peroxidation (Radi et al., 1991b) and protein tyrosine nitration (Beckman, 1996).

Another remarkable target for ROS is DNA. Chemical alteration of DNA may provide important consequences in a variety of pathological mechanisms. There are three potential chemical mechanisms by which NO can damage DNA. The first is direct reaction of ROS with the DNA structure. The second is through inhibition of repair processes and the third is increasing genotoxic species production, such as alkylating agents (Wink and Mitchell, 1998). NO/ROS are involved in many pathological processes, as discussed below.

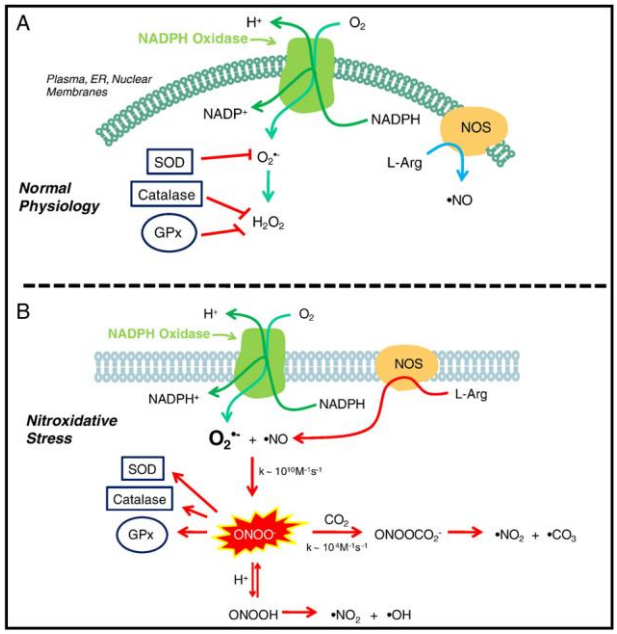


**Figure 1.11.** ROS are generated under tightly controlled antioxidant conditions during normal physiology (A). However, under nitroxidative stress conditions antioxidant defenses are not sufficient and peroxynitrite production is significantly increased (B) (Salvemini and Neumann, 2010).

### 1.2.4 Physiological and pathophysiological role of NO signaling pathways

NO has an array of functions (for review, see Pacher et al., 2007) (Fig. 1.12). In the CNS, it is involved in neuronal plasticity, facilitating long-term potentiation, which is a long-lasting enhancement in signal transmission between two neurons (Malen and Champman, 1997). NO has complex influences on memory formation through regulation of synaptic plasticity. Thus, NO regulates fear memory consolidation (Ota et al., 2008). Inhibition of NO synthesis produces amnesia (Holscher and Rose, 1992) and disrupts spatial learning and olfactory memory (Bohme et al., 1993; Kendrick et al., 1997). NO

has also been implicated in visual processing, discriminative learning, food and drinking behavior, thermoregulation and circadian rhythms, among other central functions (Esplugues, 2002).

Physiological amounts of NO have been found to be neuroprotective, whereas higher concentrations are clearly neurotoxic (Calabrese et al., 2007). NO has been shown to mediate the neurotoxicity of glutamate (Dawson et al., 1991). Thus, in a situation where there is an excessive release of glutamate, such as during cerebral ischemia, this neurotransmitter exerts its actions via NMDARs, which promotes the entry of $Ca^{2+}$ into the cell and triggers the activation of nNOS and the overproduction of NO. Peroxynitrite seems to be the major cytotoxic mediator in glutamate-induced damage (Lafon-Cazal et al., 1993; Tanaka et al., 1997; Fukuyama et al., 1998). The damage caused to DNA by NO and peroxynitrite appears to be a remarkable neurotoxic mechanism. NO is also involved in the etiology of neurologic conditions, including autoimmune and chronic neurodegenerative diseases. Thus, NO has been reported to contribute to the progression of Alzheimer's disease (Fernandez et al., 2010), Parkinson's disease (Del-Bel et al., 2011), Huntington's disease (Butterfield et al., 2001) or amyotrophic lateral sclerosis (Urushitani and Shimohama, 2001).

NO-signaling pathways also modulate cell proliferation, cell cycle arrest and apoptosis. Thus, low concentrations of NO seem to favor cell proliferation and antiapoptotic responses whereas higher levels of NO favor apoptosis (Napoli et al., 2013). Similarly, high levels of NOS expression appear to be cytostatic or cytotoxic for tumor cells, whereas low levels can have the opposite effect and promote tumour growth (Xu et al., 2002). The mitochondria is emerging as a key feature of peroxynitrite-mediated apoptosis. Permeability pore opening in response to peroxynitrite has been documented in isolated mitochondria (Scarlett et al., 1996; Brookes et al., 2004). Moreover, peroxynitrite-induced nitration of mitochondrial proteins has been reported to inactivate mitochondrial respiratory chain, reduce ATP production and promote cell death (Yamamoto et al., 2002). In addition to directly targeting the mitochondria, peroxynitrite can also activate cell death mechanisms through the modulation of various signal transduction processes, such as MAPKs (Shacka et al., 2006). Finally, exposure of cells to higher concentrations of the peroxynitrite has been associated with necrosis (Bonfoco et al., 1995, Virág et al., 2003), which is a complex process involving DNA damage and activation of the DNA repair enzyme poly(ADP-ribose) polymerase (PARP) (Szabo et al.,

1996). On the other hand, NO plays several roles in immunity: as a toxic agent towards infectious organisms, an inducer or suppressor of apoptosis or an immunoregulator (for review see Coleman, 2001).

NO/cGMP has long been known to be involved in smooth muscle relaxation and platelet aggregation. Thus, an impaired NO signaling represents a crucial pathogenic mechanism in cardiovascular diseases. Accumulating evidence suggests that alterations in NO synthesis and NO/sGC/cGMP signaling are key contributors to the pathogenesis of hypertension, one of the most common worldwide diseases (Escobales and Crespo, 2005; Wolin, 2005; Paravicini and Touyz, 2006). However, a role for NO and peroxynitrite in other cardiovascular conditions, such as stroke, myocardial infarction, chronic heart failure, diabetes or circulatory shock has also been reported (for review, Pacher et al., 2007). Since NO enhances vascular smooth muscle relaxation, sGC stimulators could have unique clinical utility in the treatment of essential hypertension, pulmonary hypertension and associated cardiac and renal complications. Riociguat (BAY 63-2521) is the first sGC stimulator that has been clinically developed. Clinical trials have shown that it significantly improves pulmonary vascular hemodynamics and increases exercise ability in patients with pulmonary arterial hypertension (Ghofrani et al., 2013).

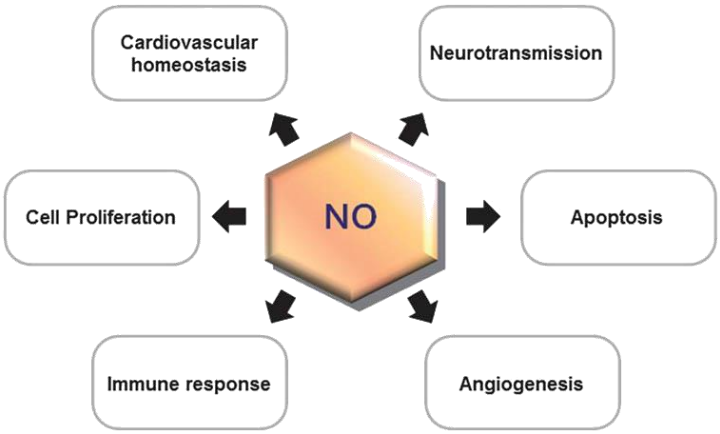


**Figure 1.12.** Some of the functions mediated by NO *in vivo* (Kim et al., 2014).

## 1.3 LOCUS COERULEUS (LC)

### 1.3.1 Anatomy of the LC

The LC is a compact cell group located in the brainstem. It consists of almost exclusively noradrenaline (NA)-containing neurons and represents the main noradrenergic nucleus in the central nervous system (CNS) (Foote et al., 1983). The first description of the LC was published by Reil in 1809, but the actual term "locus coeruleus" was proposed by the anatomists Wenzel and Wenzel in 1812 (reviewed by Russell, 1955). This Latin term means "blue spot" due to the melanin granules inside LC neurons, which provide a bluish shade to the nucleus.

The noradrenergic nuclei in the brain include mainly the LC (A6 cell group) and several other less studied clusters of noradrenergic neurons (A1, A2, A5, A7) that primarily target subcortical regions (Dahlstrom and Fuxe, 1964; Bruinstroop et al., 2012). The LC is a dorsal pontine region placed bilaterally on the floor of the fourth ventricle and it is surrounded by the medial parabrachial nucleus, the mesencephalic trigeminal nucleus and the Barrington's nucleus (Figure 1.13). The rat LC is composed by small number of neurons: approximately 1,500. Although it is generally accepted that NA is the main transmitter of LC neurons, the cell bodies also secret several neuropeptides, such as galanin, vasopressin, neuropeptide Y or somatostatin (for review, see Berridge and Waterhouse, 2003).

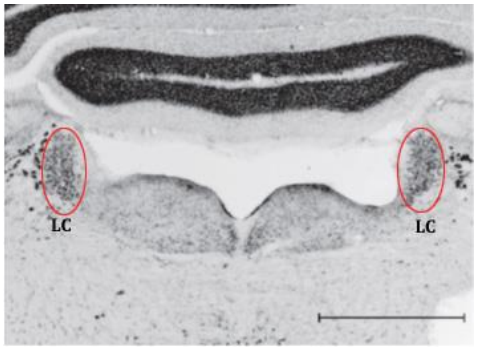


**Figure 1.13.** Photomicrograph of Nissl-stained coronal section of the brainstem region containing the LC (Scale bar, 1 mm). Image modified from Bernuci et al. (2008).

#### 1.3.1.1 Afferent projections to the LC

The LC receives direct excitatory and inhibitory inputs. The major afferents to the LC arise from two structures: the lateral paragigantocellularis nucleus (PGi) and the nucleus prepositus hypoglossi (PrH) (Aston-Jones et al., 1986), both located in the rostral medulla. The PGi provides a potent excitatory amino acid input to the LC, whilst the PrH potently inhibits LC neurons by a GABAergic input (Aston-Jones et al., 1991). Both PrH and PGi endow the LC with enkephalinergic projections (Drolet et al., 1992). Moreover, the LC receives additional gabaergic afferents from the periaqueductal gray (PAG) and the ventrolateral preoptic hypothalamic area (Steininger et al., 2001), serotonergic afferents from the dorsal raphe nucleus (DRN) (Kim et al., 2004), dopaminergic inputs from the ventral tegmental area (VTA) (Maeda et al., 1994) and noradrenergic afferents from the bulbar/pontine nuclei and the contralateral LC (Singewald and Philippu, 1998). Corticotropin-releasing hormone (CRH) innervation is also present in the LC which comes from the Barrington's nucleus (Valentino et al., 1996) and orexin/hypocretin and histaminergic inputs that originate in the hypothalamus (Pollard et al., 1978; Horvath et al., 1999; de Lecea, 2010).

On the other hand, a dense dendritic plexus has been reported to extend beyond the borders of the nucleus (Shipley et al., 1996). This pericoerulear region is the target for a large number of presynaptic fibers from several brain regions such as the prefrontal cortex, amygdala, hypothalamus or the DRN (Berridge and Waterhouse, 2003). GABAergic interneurons have been shown to be present in this pericoerulear region (Aston-Jones et al., 2004).

#### 1.3.1.2 Efferent projections from the LC

LC gives rise to a broad, noradrenergic efferent network that innervates most of the major areas of the brain including the cerebral cortex, cerebellum, thalamus, hypothalamus, hippocampus, brainstem and dorsal and ventral horns of the spinal cord (Samuels and Szabadi, 2008, part I) (Fig. 1.14). The LC has long been considered a homogeneous assembly of NE-containing cells with broad and uniform actions throughout the cerebral cortex (Fallon and Loughlin, 1982; Berridge and Waterhouse,

2003). However, recent studies have challenged this notion and postulate that LC neurons exhibit a more heterogeneous and complex organization than previously thought (Chandler et al., 2014a, 2014b). According to this research, populations of LC neurons that communicate with the prefrontal cortex show different molecular phenotypes and electrophysiological properties in comparison with those LC neurons that project to the motor cortex. Thus, this heterogeneity might result in a differential noradrenergic modulation of these areas. Moreover, recent findings by Robertson et al. (2013) have shown that the insular cortex is innervated by non-LC derived NE terminals, challenging the longstanding notion that LC is the sole source of NA-containing fibers to the forebrain.

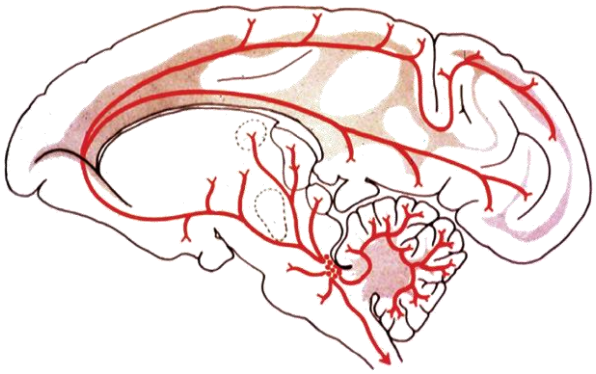

**Figure 1.14.** Sagittal view of a monkey brain showing major efferent projections of the LC throughout the CNS (Aston-Jones and Cohen, 2005).

### 1.3.2 Physiology of the LC: intrinsic properties and physiological regulation

In both anesthetized and unanesthetized animals LC neurons show some distinctive and representative electrophysiological properties, such as broad action potential spikes (2-4 ms) and a spontaneous, tonic activity characterized by relatively slow and regular firing rates (0.5-5 Hz). LC neurons respond to afferent stimuli by a phasic activity distinguished by burst discharges followed by a prolonged period of decreased firing (Cedarbaum and Aghajanian, 1976; Andrade et al., 1983; Andrade and Aghajanian, 1984; Berridge and Waterhouse, 2003). These two patterns of discharge, tonic and phasic, promote different modes of signal processing and behaviors (Aston-Jones and Cohen, 2005). Moreover, both characteristics of LC discharge, the frequency and the pattern, are

determinants for NA release; bursts are more effective in increasing NA terminal release (Florin- Lechner et al., 1996).

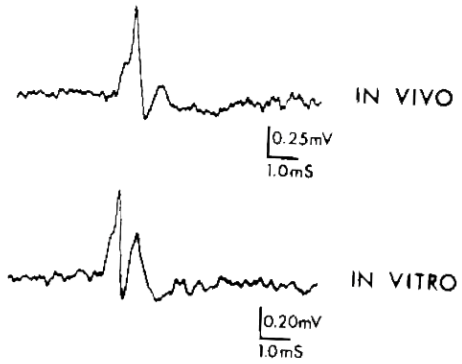


**Figure 1.15.** Characteristic extracellular waveforms of LC neurons recorded *in vivo* and *in vitro*, which consist of an initial positive component followed by a negative and a second positive deflection (Andrade et al., 1983).

Probably, one of the most remarkable physiological characteristic of the LC is that its neurons fire action potentials spontaneously *in vitro* in the absence of any stimulation. This pacemaker activity depends on intrinsic membrane currents. One is an inward $Na^+$ current that is active near the threshold for action potential generation. The second is a $K^+$ current that is activated following the entry of calcium during the action potential and it is responsible for hyperpolarization (Williams et al., 1984, 1991).

Multiple mechanisms modulate the spontaneous firing activity of LC cells. Firing rate of LC neurons is increased by activation of cAMP pathway (Wang and Aghajanian, 1987). In addition, NA exerts its action through postsynaptic α2-adrenoceptors, which are coupled to $G_{i/o}$ proteins and reduce the electrical activity of LC neurons by acting on GIRK channels (Egan et al., 1983; Arima et al., 1998). Likewise, activation of MOR inhibits the firing rate of LC cells by acting on GIRK channels (North et al., 1987) and inhibiting adenylyl cyclase activity and cAMP signaling (Duman et al., 1988). A role for 5-HT receptors in LC cell activity has been reported. Thus, 5-$HT_{1A}$ receptors may mediate an inhibitory response on the LC (Bobker and Williams, 1989), although other authors have observed an excitatory regulation of LC neurons by 5-$HT_{1A}$ receptors (Szabo and Blier, 2001). Recent work has described that 5-$HT_3$ promotes a decrease in the firing rate of LC neurons, by stimulating NA release (Ortega et al., 2012). Moreover, cannabinoids increase the spontaneous firing activity in the rat LC through CB1 receptors, apparently by an indirect mechanism located at the peripheral level (Mendiguren and Pineda, 2006). Furthermore, activation of CB1 receptors enhances postsynaptic excitatory responses to NMDA in LC neurons (Mendiguren and Pineda,

2004). $I_1$ and non-$I_1$/$I_2$-types imidazoline receptors have been described to stimulate NA cells (Pineda et al., 1993; Ugedo et al., 1998). $CO_2$ has also been shown to maintain the tonic activity of LC neurons by decreasing intracellular pH, which closes inward rectifier potassium channels (Pineda and Aghajanian, 1997).

Spontaneous activity is altered by both glutamatergic and gabaergic synaptic inputs (Williams et al., 1991). It has been described that LC neurons are only weakly excited by glutamatergic afferents during tonic activity (Kawahara et al., 1999). However, during the phasic mode periods concurrent with peripheral stimuli glutamatergic afferents turn physiologically active in LC neurons (Ennis et al., 1992). The excitatory response is mediated by glutamate receptors of both NMDA and non-NMDA type, but several studies indicate that, under control conditions, non-NMDA (AMPA) receptors exert a stronger influence on LC cells (Cherubini et al., 1988, Ennis et al., 1992). The inhibitory activity is triggered among others by GABA, acting mainly on $GABA_A$ receptors (Osmanovic and Shefner, 1990; Williams et al., 1991).

A further remarkable electrical characteristic of LC neurons is the cell-to-cell coupling via gap junctions (Ishimatsu and Williams, 1996). This type of intercellular connection facilitates a fast communication between cells and it allows for coordination of the firing of LC neurons, since the entire nucleus fires simultaneously in response to sensory inputs (Christie et al., 1989; Nestler et al., 1999). Additionally, it has been reported that neurons and glia are electrically coupled in the LC (Álvarez-Maubecin et al., 2000).

### 1.3.3 Physiological and pathophysiological aspects of LC-NA system

#### 1.3.3.1 Involvement of the LC in physiological activities

Given the fact that the LC receives and projects multiple inputs and outputs, this nucleus is involved in a wide variety of functions, controlling different physiological processes:

- Sleep cycle and awakening: The LC is recognized as a major wakefulness-promoting nucleus. The firing activity of LC neurons varies with stages of the sleep-

waking cycle. Thus, LC neurons display the highest firing rates during wakefulness, they fire more slowly during slow-wave sleep and cease firing during rapid eye movement (REM) sleep (Aston-Jones and Bloom, 1981). Sleep process has been described to start with deactivation of waking-promoting neurons from the forebrain and brainstem (Takahashi et al., 2010). The wakefulness-promoting action of the LC is the consequence of its projections to most areas of the cerebral cortex and to alertness-modulating nuclei (Samuels and Szabadi, 2008, part II). A recent study has reported that the orexinergic hypothalamic neurons contacting with the LC are implicated in the stage succession during sleep-wakefulness cycle (Tortorella et al., 2013).

- Learning and memory*:* NA release in different parts of the brain is essential for the modulation of memory. Stimulation of LC neurons has been shown to increase NA release in terminal regions and also within the LC itself, enhancing memory formation and consolidation (Clayton and Williams, 2000; Gibbs et al., 2010)**.**

- Attention: Studies examining the activity of LC neurons in monkeys during performance of a task that required focused attention have indicated that LC cells exhibit phasic or tonic patterns of discharge, in a close correlation with good or poor performance on that task respectively (for review, see Aston-Jones et al., 1999). It has been reported that phasic mode facilitates behavioral responses to specific tasks. Thus, phasic mode is associated with focused attention. Conversely, a tonic activity mode is associated with disconnection with the current task and a search for alternative behaviors (Aston-Jones and Cohen, 2005).

- Pain regulation: The LC and the A5 and A7 cell groups in the pons have been implicated as a key component in the descending control of pain (Jones, 1991; Millan, 2002; Pertovaara, 2006). Thus, electrical or chemical stimulation of the LC has been shown to be analgesic in a number of acute pain models (Jones and Gebhart, 1986; Miller and Proudfit, 1990; West et al., 1993). However, the potential of the descending noradrenergic system to suppress pain has not been successfully approached therapeutically. Thus, the use of systemic α2-adrenergic agonists is limited by side effects including sedation and hypotension (Pertovaara, 2006). Similarly, NA reuptake inhibitors, although moderately efficacious for

neuropathic pain (Finnerup et al., 2010), are also restricted by side effects. However, in a recent study, a novel acute pronociceptive effect of LC activation has been described (Hickey et al., 2014). They propose that distinct subpopulations of neurons in the LC drive opposing antinociceptive/pronociceptive actions.

- Autonomic functions*:* The activation of the LC results in a well-defined pattern of autonomic changes: in tissues receiving a predominantly sympathetic innervation, there is an increase in activity, whereas in those receiving predominantly parasympathetic innervation, there is a decrease in activity (for review, Samuels and Szabadi, 2008, part II). Thus, activation of LC increases pupil diameter (Phillips et al., 2000), increases heart rate and blood pressure (Gurtu et al., 1984) and reduces salivation (Szabadi and Tavernor, 1999) among other functions. On the contrary, fall of blood pressure increases the firing rate of LC neurons (Curtis et al., 1993) and enhances the *in vivo* release of NA in the LC (Singewald et al., 1999). The LC is also implicated in the control of ventilation (for review, see de Carvalho et al., 2014). It is considered a central $CO_2$/pH chemoreceptor site in amphibians and mammals (Gargaglioni et al., 2010; Santin and Hartzler, 2013) and more than 80% of its neurons are chemosensitive, responding to hypercapnia with an increased firing rate (Pineda and Aghajanian, 1997).

#### 1.3.3.2 Involvement of the LC in pathophysiological activities

- Anxiety and stress: NA is involved in neural mechanisms underlying fear and stress. Stress exposure is associated with an increase in firing of LC cells and with an increased release of NA in brain regions which receive innervation from the LC (Bremner et al., 1996; Tanaka et al., 2000). Increased firing of LC neurons has also been associated with behavioral manifestations of fear (Bremner et al., 1996). A recent study *in vivo* using a validated rat model of post-traumatic stress shows persistent changes in LC function, such as lower spontaneous LC activity, elevated phasic responses to a noxious event, decreased recovery from post-

stimulus inhibition and increased tyrosine hydroxylase mRNA expression in the LC (George et al., 2013).

- Sleep/arousal disorders: noradrenergic neurotransmission can initiate and maintain prolonged periods of alert waking (Berridge and Foote, 1996). Therefore, NA system can be considered as an appropriate target in the treatment of sleep and arousal disorders (insomnia and narcolepsy). A recent study has shown that the firing pattern of LC neurons was markedly altered in narcoleptic mice, and this change might be due to a functional change of GABAergic input to these cells (Tsujino et al., 2013).

- Depression: An animal model that identifies the LC activity as a biological mediator of depression has been proposed (Weiss et al, 2005). It was developed after observing that many behavioral symptoms of depression appear in conjunction with an increased firing activity of LC neurons (Simson and Weiss, 1988). In addition, long-term but not acute administration of certain selective serotonin reuptake inhibitors **(**SSRIs) antidepressants significantly decreases spontaneous LC cell activity (Szabo et al., 1999). Moreover, depression is associated with altered concentrations of several noradrenergic proteins in the LC. Thus, elevated levels of tyrosine hydroxylase (TH) (Zhu et al., 1999), increased agonist binding to $\alpha_2$-adrenergic receptors (Ordway et al., 2003) and reduced levels of norepinephrine transporters (Klimek et al., 1997) have been reported in major depressive subjects and in suicide victims. Moreover, long-term antidepressant treatment induces a significant desensitization of $\alpha_2$-adrenoceptors in the LC (Mateo et al., 2001).

- Neurodegenerative diseases*:* The LC is impaired in Parkinson disease (PD), as revealed by the extensive cell loss occurring in PD patients (Forno, 1996). The LC has also been implicated in L-DOPA-induced dyskinesias, the main side effect of the dopaminergic treatment of PD (Miguelez et al., 2011). Finally, dysfunction of the LC/NA system has been associated with PD-related dementia (Del Tredici and Braak, 2013). However, LC loss is not only a feature of PD. It has been published that in both Parkinson and Alzheimer diseases the most severe neuronal loss is found in the LC in post-mortem human brain (Zarow et al., 2003).

- Opioid withdrawal: The NA system has been proposed to play an important role in the expression of some signs of opiate withdrawal. It has been suggested that the LC is the structure mediating the expression of the somatic syndrome of opioid withdrawal. Thus, there is an overactivation of LC neurons during morphine withdrawal that is associated with an elevated release of glutamate from excitatory afferent projections (Rasmussen, 1991; Maldonado, 1997). Moreover, chronic opioid administration upregulates the adenosine-5´-monophosphate (cAMP) pathway in the LC and this adaptation is also involved in the increase in electrical excitability of LC neurons (Nestler and Aghajanian, 1997; Lane-Ladd et al., 1997; Valverde et al., 2004; Parlato et al., 2010). This increased firing activity has also been associated with specific opioid withdrawal behaviors (Punch et al., 1997).

### 1.3.4 MOR in the LC

The LC has long been used as a model to explore the cellular mechanisms underlying opioid tolerance and withdrawal (Nestler et al., 1994). The three classes of opioid receptors, MOR, DOR and KOR are present within the LC, but with distinct distribution. Thus, MORs are prominently localized at extrasynaptic sites on noradrenergic dendrites (Van Bockstaele et al., 1996). On the contrary, DORs are primarily located in the plasma membranes of presynaptic axon terminals (Van Bockstaele et al., 1997) and KORs are also presynaptically found to modulate diverse afferent signaling in the LC (Kreibich et al., 2008; Reyes et al., 2009).

In the LC, acute binding of opioid agonists to the MOR leads to decreased adenylyl cyclase activity and cAMP signaling (Duman et al., 1988). Opioids also inhibit the spontaneous discharge of LC neurons by activating GIRK channels (Pepper and Henderson, 1980; Williams et al., 1982); specifically, these GIRK channels contain GIRK2 and GIRK3 subunits (Torrecilla et al., 2002). During chronic opioid exposure there is an up-regulation of the cAMP signaling pathway (adenylyl cyclase, PKA…). This increase becomes functionally evident during withdrawal (Nestler and Tallman, 1988; Kogan et al., 1992; Lane-Ladd et al., 1997; Mazei-Robison and Nestler, 2012), when the firing rate of LC neurons is significantly increased (Rasmussen et al., 1990).

As in other systems, sustained opioid exposure induces MOR desensitization in LC neurons (Harris and Williams, 1991). The degree of MOR desensitization and the differential involvement of regulatory events (phosphorylation, internalization, recycling…) depend on the opioid agonist used (see section 1.1.4). The opioid agonist ME induces a concentration-related desensitization of MOR responses in the LC (Harris and Williams, 1991; Santamarta et al., 2014). Inhibition of GRK2 activity in LC neurons has no effect on the acute desensitization induced by ME (Quillinan et al., 2011), but concurrent blockade of GRK2 and ERK 1 and 2 reduces ME-induced desensitization (Dang et al., 2009). In contrast, Arttamangkul et al. (2012) have reported that protein kinase inhibition by the nonselective inhibitor staurosporine does not reduce the extent of ME-induced desensitization, although it increases the rate of recovery from desensitization (resensitization, see section 1.1.4).

Other opioid agonists such as methadone, fentanyl, oxymorphone, normorphine or etorphine have been reported to induce significant MOR desensitization in the LC (Alvarez et al., 2002; Virk and Williams, 2008). Morphine induces significantly less receptor desensitization than other MOR agonists in LC neurons (Alvarez et al., 2002; Bailey et al., 2003; Blanchet et al., 2003; Virk and Williams, 2008). Morphine leads to MOR desensitization in LC neurons under enhanced PKC activity (Bailey et al., 2004; 2009a, 2009b). Furthermore, chronic administration of morphine induces tolerance to the inhibitory effect of ME in the LC (Santamarta et al., 2005). Levitt and Williams (2012) have reported that both desensitization and cellular tolerance are present in LC neurons from morphine-treated animals and that these processes can be distinguished by the time course of recovery and mechanism. Moreover, after chronic treatment with morphine, but not with methadone, there is a diminished recovery from acute ME-induced desensitization in LC neurons (Quillinan et al., 2011).

# 2. HYPOTHESIS AND OBJECTIVES

Opioids are effective for the treatment of pain. Unfortunately, their long-term utility is limited by the development of tolerance and dependence. The mechanisms underlying opioid tolerance are multifaceted and, despite extensive research, they have not been fully identified. Opioid receptors undergo several adaptations following sustained agonist exposure, including desensitization, internalization, recycling or down-regulation (see Introduction, section 1.1.4). Desensitization of MOR is thought to be an important initial step underlying tolerance and it depends on agonist identity (Williams et al., 2013). The LC, the main noradrenergic nucleus in the CNS, contains a high-density of MORs (van Bockstaele et al., 1996). Chronic administration of opioid agonists produces adaptive changes in this nucleus. Thus, the LC has long been used as a model to study the molecular mechanisms underlying opioid tolerance and dependence (Nestler et al., 1994; Mazei-Robison and Nestler, 2012).

The signaling messenger NO modulates nociceptive processing and it is implicated in different pain states (Luo and Cizkova, 2000). In the LC, NO regulates the neuronal firing activity (Pineda et al., 1996; Torrecilla et al., 2007) and it is a key mediator in the mechanisms underlying MOR regulation following agonist exposure (Pineda et al., 1998). Previous results from our group have shown that *in vitro* administration of nNOS inhibitors attenuates ME-induced MOR desensitization in the LC (Torrecilla et al., 2001; Santamarta et al., 2014), whereas perfusion with NO donors enhances it (Llorente et al., 2012). The NO system has been also implicated in neuronal adaptations occurring *in vivo* during opioid tolerance. NOS expression in the CNS is increased following morphine treatment (Machelska et al., 1997; Cuéllar et al., 2000; Wong et al., 2000). Co-treatment with the selective nNOS inhibitor 7-NI attenuates the development of tolerance to the electrophysiological effect of opioids on LC neurons and to the antinociceptive effect of morphine challenge in morphine-treated rats (Santamarta et al., 2005). In agreement, mice deficient in nNOS exhibit less analgesic tolerance after prolonged morphine exposure than control animals (Heinzen and Pollack, 2004).

NO interacts with the enzyme sGC to form cGMP, which in turn, targets different effectors, such as PKGs (Francis et al., 2010). The LC has been shown to express sGC (Matsuoka et al., 1992; Furuyama et al., 1993), PKG (El-Husseini et al., 1995), as well as detectable concentrations of cGMP (Xu et al, 1998a; Vulliemoz et al., 1999). Previous studies performed in our laboratory have shown that perfusion with the PKG activator 8-Br-cGMP completely restores ME-induced MOR desensitization from the blockade

elicited by the nNOS inhibitor 7-NI in LC neurons (M.T. Santamarta, Doctoral Thesis). Moreover, modulators of the enzyme sGC regulate the development and expression of morphine tolerance (Ozdemir et al., 2011; Durmus et al., 2014).

On the other hand, NO reacts with oxygen derivatives to produce ROS, such as the powerful oxidant molecule peroxynitrite (Hughes, 2008). NO enhances MOR desensitization in the LC, in part, through a ROS-involving mechanism (Llorente et al., 2012). ROS are also involved in the development of pain of several etiologies *in vivo*, including that associated with opiate-induced hyperalgesia and antinociceptive tolerance (Salvemini et al., 2011; Janes et al., 2012). Previous results from our group have shown that co-administration of the antioxidant Trolox together with ascorbic acid attenuates the development of antinociceptive tolerance in morphine-treated rats (Llorente J. Doctoral Thesis, unpublished data). Likewise, peroxynitrite decomposition catalysts reduce morphine-induced analgesic tolerance in mice (Muscoli et al., 2007; Batinić-Haberle et al., 2009).

Taken together, these evidences establish a link between NO and opioid desensitization and tolerance. However, a detailed study of NO-dependent downstream signaling pathways (sGC/PKG and ROS) involved in MOR desensitization in LC neurons remains to be performed *in vitro*. In addition, it has to be further studied whether ROS are involved in the development of cellular tolerance induced by morphine in LC neurons. Although morphine causes significant behavioral tolerance *in vivo*, there is controversy about its ability to induce acute MOR desensitization *in vitro*. Some studies performed in LC neurons using intracellular recording techniques have reported that morphine is a very poor desensitizing agent (Alvarez et al., 2002; Bailey et al., 2003). However, others have observed a significant desensitization of MOR induced by morphine under activation of PKC (Bailey et al., 2004; 2009b; Arttamangkul et al., 2015). To date, morphine-induced MOR desensitization has not been characterized by extracellular recordings *in vitro*. In addition, the involvement of nNOS in morphine-induced acute MOR desensitization remains to be further studied in the LC. Finally, morphine is the prototypical MOR agonist used in tolerance studies, but we also hypothesize that nNOS and ROS may modulate the development of both cellular and antinociceptive tolerance induced by other opioid agonists (methadone and fentanyl).

The global aim of this study was to elucidate the involvement of NO-dependent pathways in the development of MOR desensitization in LC neurons *in vitro* and in the induction of cellular and analgesic tolerance *in vivo* induced by different opioid agonists. The specific objectives of the present study were:

1. To characterize *in vitro* the NO-dependent downstream signaling pathways (i.e. cGMP and ROS) involved in ME-induced and NO-enhanced MOR desensitization in rat LC neurons by single-unit extracellular recordings. For this purpose, we tested the effect of different modulators of the sGC/PKG pathway and antioxidants.

2. To investigate *in vitro* the involvement of nNOS in morphine-induced MOR desensitization in LC cells by single-unit extracellular recordings. For this purpose, we evoked an excitation of LC neurons with KCl to study the desensitization of MOR induced by morphine and we tested the effect of selective nNOS inhibitors.

3. To investigate *in vitro* the involvement of nNOS and ROS in the induction of cellular tolerance induced by prolonged treatments with different opioids (morphine, methadone and fentanyl) in LC neurons. For this purpose, we studied by single-unit extracellular recordings the development of tolerance to the electrophysiological effects of an opioid agonist following prolonged treatments with different opioids (morphine, methadone and fentanyl) and we evaluated its regulation by a selective nNOS inhibitor and antioxidant agents.

4. To explore *in vivo* the involvement of nNOS and ROS in the development of opioid analgesic tolerance. We examined by the tail-flick test the development of analgesic tolerance following prolonged treatments with different opioids (morphine, methadone and fentanyl) and we evaluated its regulation by a selective nNOS inhibitor and antioxidant agents.

# 3. MATERIALS AND METHODS

## 3.1 MATERIALS

### 3.1.1 Animals

Male Sprague-Dawley rats (200-300 g) obtained from the animal house of the University of the Basque Country were used for the electrophysiological and behavioral assays. The animals were kept under controlled environmental conditions (22º C, 12-h light/dark cycle, humidity of 65-70%) and free access to food and water. All experimental procedures were conducted in accordance with the European Communities Council Directive on "Protection of Animals Used in Experimental and Other Scientific Purposes" of 24 November 1986 (86/609/EEC) and with institutional guidelines for animals used in research (Animal Care and Use Committee of the University of the Basque Country). All the efforts were made to minimize animal suffering and to reduce the number of animals used.

### 3.1.2 Treatments

#### a) Opioids

For induction of morphine tolerance, rats were treated subcutaneously (s.c.) with a slow release emulsion containing free base morphine (200 mg/kg) for 72 h, as described by Santamarta et al. (2005) (see section 3.1.3b for preparation details). The emulsion was injected subcutaneously on the back of the rat under light anesthesia with chloral hydrate (200 mg/kg, intraperitoneally (i.p.)). Sham animals were implanted with the same vehicle emulsion without morphine. Behavioral or electrophysiological experiments were conducted 72h after administration of morphine or sham emulsions.

Tolerance to fentanyl (0.2 mg/kg/day, 7 days) and methadone (60 mg/kg/day, 6 days) was induced by s.c. implantation of Alzet® 2ML1 osmotic pumps (Fig. 3.1), as described by Trujillo et al. (2004) and Quillinan et al. (2011), respectively. These pumps have a 2 ml reservoir and deliver the drug at the rate of 10 µl/h. The required amount of the drug was dissolved in saline and introduced into the pump with a needle provided by the manufacturer. Rats were anaesthetized with isoflurane and a little incision was made in the mid-scapular region to place the minipump in the subcutaneous space. Sham animals were also implanted with a minipump filled with saline under the same experimental

conditions. As methadone requires high doses to induce tolerance, rats were given i.p. injections of methadone before minipump implantation as follows: the day before, rats received 5 mg/kg at 09:00 h and 7 mg/kg at 18:00 h. Next day, rats where administered 7 mg/kg at 09:00 h and the minipump was finally inserted at 18:00 h. Behavioral or electrophysiological **e**xperiments were carried out on day 7 in methadone-treated rats (6 days after minipump implantation) and on day 8 in fentanyl-treated rats (7 days after minipump implantation).

**b) Antioxidants and nNOS inhibitors**

Sham and morphine-treated animals were daily injected with the antioxidant U-74389G (10 mg/kg, i.p.), Trolox (40 mg/kg, i.p.) or their vehichles (saline). Every time Trolox was administered, rats also received ascorbic acid (100 mg/kg, i.p.) (TX+AA) to prevent the oxidation of Trolox. Sham-, methadone- and fentanyl-receiving rats were intraperitoneally injected every day with U-74389G (10 mg/kg) or its vehicle (saline).

In another set of experiments, sham-, methadone- and fentanyl-treated animals were intraperitoneally injected every 12 h with the nNOS inhibitor 7-NI (30 mg/kg) or its vehicle (peanut oil).

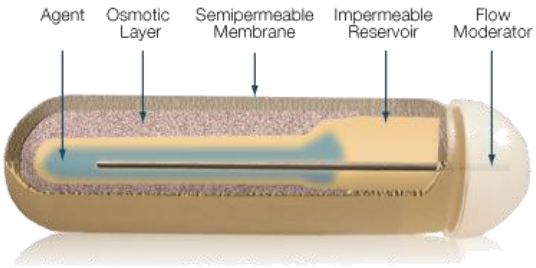


**Figure 3.1.** Schematic illustration of an Alzet® minipump. The content is released because of the osmotic pressure difference between the compartment within the pump and the tissue environment in which the pump is implanted. Obtained from www.alzet.com.

### 3.1.3 Drugs and reagents

**a) Drug sources**

***Opioids.*** Met$^5$-enkephalin (ME) was purchased from Bachem (Bodendorf, Germany). The following drugs were obtained from Sigma-Aldrich Quimica S.A. (Madrid, Spain):

fentanyl citrate salt, methadone hydrochloride and naloxone hydrochloride. Morphine base and morphine hydrochloride were purchased from Alcaliber (Madrid, Spain).

***Modulators of NO-dependent pathways.*** 8-Bromo-1H,4H-[1,2,4]oxadiazolo[3,4-*c*][1,4]benzoxazin-1-one (NS 2028) and 3-[2-[(4-chlorophenyl)thiophenyl]-*N*-[4-(dimethylamino)butyl]-2-propenamide hydrochloride (A 350619) were purchased from Tocris Bioscience (Bristol, UK). Ascorbic acid (AA), diethylamine NONOate diethylammonium salt (DEA/NO), 7-nitroindazole (7-NI), Rp-8-bromo-β-phenyl-1,$N^2$-ethenoguanosine 3′,5′-cyclic monophosphorothioate sodium salt (Rp-8-Br-PET-cGMPS) and S-methyl-L-thiocitrulline acetate salt (SMTC) were obtained from Sigma-Aldrich Quimica S.A. (Madrid, Spain). 21-[4- (2,6-di-1-pyrrolidinyl-4-pyrrimidinyl)-1-piperazinyl]-pregna-1,4,9(11)-triene-3,20-dione (Z)-2-butenedioate (U-74389G), melatonin and Trolox were purchased from Enzo Life Sciences, Inc. (New York, USA). 2-[1-[(2-fluorophenyl)methyl]-1H-pyrazolo[3,4-b]pyridin-3-yl]-5-(4-morpholinyl)-4,6 pyrimidinediamine (BAY 418543) was obtained from Biotrend Chemikalien GmbH (Köln, Germany).

***Other drugs and chemicals.*** Chloral hydrate and γ-aminobutyric acid (GABA) were obtained from Sigma-Aldrich Quimica S.A. (Madrid, Spain). D-(-)-2-Amino-5-phosphonopentanoic acid (D-AP5) and 6-Cyano-7-nitroquinoxaline-2,3-dione disodium salt (CNQX) were purchased from Tocris (Bristol, UK). Isoflurane was purchased from Esteve (Barcelona, Spain).

## b) Drug preparations

### *In vitro*

For electrophysiological studies, DEA/NO was first dissolved in NaOH (25 mM; pH = 12) to prevent the spontaneous release of NO. Then, just before the assay, it was neutralized with HCl (1 M) and diluted in aCSF up to its final concentration. Trolox and 7-NI were directly dissolved in aCSF before the experiment. 7- NI required prolonged sonication to facilitate homogeneity. The rest of the drugs used for *in vitro* perfusions, were prepared first as stock solutions in milliQ water (A 350619, CNQX, D-AP5, GABA, ME, morphine hydrocloride, naloxone, Rp-8-Br-PET-cGMP, SMTC), etanol (melatonin) or DMSO (NS 2028, U-74389G, BAY 418543), stored at –25 ºC and diluted in aCSF to

their final volume before the experiment. The maximum concentration of DMSO or etanol in the perfusion fluid was 0.1%, which was found not to affect the firing responses of LC neurons.

The composition of the aCSF used was (in mM): NaCl 130, KCl 3, $NaH_2PO_4$ 1.25, glucose 10, $NaHCO_3$ 21, $CaCl_2$ 2 and $MgSO_4$ 2. The aCSF was saturated with 95% $O_2$/ 5% $CO_2$ for a final pH of ~7.34. In some assays, KCl (14 mM) was used. In those cases, the osmolarity of KCl was compensated with a lower concentration of NaCl (119 mM).

***In vivo***

For chronic treatments, a slow-release emulsion containing morphine base was prepared. The emulsion contained, appart from morphine, the following vehicle: mannide mono-oleate (Arlacel A), liquid paraffin and 0.9% NaCl (saline) (0.08:0.42:0.5, v/v/v). Morphine was mixed with the oils using a magnetic stirrer and then saline was added gradually to create an oil/water emulsion.

Methadone, fentanyl and ascorbic acid were dissolved in saline. 7-NI was dissolved in peanut oil. For chronic treatments, Trolox was dissolved in NaOH (1 M), neutralized with HCl (1 M) and diluted to the last volume with saline. U-74389G was dissolved in 0.01 M HCl. The final pH prior to i.p administration was in all cases 6-7.

## 3.2 METHODS

### 3.2.1 Electrophysiological procedures

#### *a) Brain slice preparation*

Rats were anaesthetized with chloral hydrate (400 mg/kg, i.p.) and decapitated. The brain was rapidly removed and placed in an ice-cold aCSF (4 °C), where NaCl was replaced with sucrose to improve neuronal viability (Aghajanian and Rasmussen, 1989). Coronal brainstem sections of 600 μm thickness containing the LC were cut using a vibratome (FHC Inc., Bowdoin, ME, USA) and a Valet blade (World Precision Instruments, Inc., Sarasota, FL, USA). Then, the slice was allowed to recover for 90 min in a glass containing oxygenated aCSF (95% $O_2$ and 5% $CO_2$). Next, the slice was carefully transferred to a modified Hass-type interface chamber and placed on an elevated polypropylene mesh covered with cellulose paper (Sigma-Aldrich Química, Madrid, Spain) and lens paper (Olympus Iberia, Barcelona, Spain). The slice was incubated at 33ºC and continuously perfused with oxygenated aCSF through a system of threads and tubes at a flow rate of 1.5 ml/min (Fig. 3.2). Drugs were perfused in the bathing medium by switching to a drug-containing solution using a system of manually controlled three-way valves. This system offered an excellent exchange of aCSF and drugs in the slice.

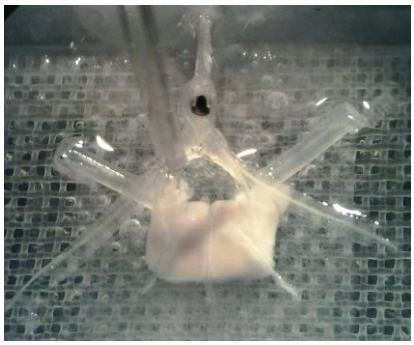

**Figure 3.2.** The assembly of threads and tubes provides continuous perfusion to the slice containing the LC.

#### *b) Uni-extracellular recording of LC neurons*

Single-unit extracellular recordings of LC neurons were made as described previously (Mendiguren and Pineda, 2004). The recording electrode, an Omegadot glass

micropipette, was made with a horizontal pipette puller (Sutter Instruments Co., Novato, CA, USA). This instrument allows us to shape the micropipette tip by adjusting the parameters of heat or speed. The electrode was filled with 50 mM sodium chloride by a Yale spinal needle (0.5 x 90 mm, 25 G, Beckton Dickinson, Madrid, Spain), which was coupled to a Sartorius cellulose filter (0.20 μm, Filtros Anoia S.A., Barcelona, Spain). Once filled, the tip was broken back to a diameter of 2-5 μm for a final resistance of 3-5 MΩ. Finally, the electrode was positioned on the LC by means of a binocular microscope (model C011, Olympus Iberia, Barcelona, Spain). This nucleus was visually identified in the rostral pons as a dark oval area on the lateral borders of the central gray and the 4th ventricle, just anterior to the genu of the facial nerve.

Then, the electrode was lowered at 4 μm intervals by a piezoelectric micropositioner (model 6000-ULN, Burleigh Instruments, Quebec, Canada), until the signal from one neuron was recognized from the background noise. Noradrenergic LC cells were identified by their spontaneous discharge activity, the regular, slow firing rate and the long-lasting biphasic positive-negative waveforms (Andrade and Aghajanian, 1984). As summarized in Figure 3.3, the extracellular signal from the electrode was passed through a high-input impedance headstage (HS- 2A, Axon Instruments, Foster City, CA, U.S.A.) that acted as a signal filter and, together with the amplifier (Axoclamp-2A, Axon Instruments, Foster City, CA, U.S.A.), amplified the signal (x 10). Next, the signal passed through a post-amplifier (Cibertec S.A., Spain), which further filtered and amplified the signal (x 1-500). The signal was then monitored by an oscilloscope (Hameg Instruments, Germany) and an audio-analyzer (Cibertec S.A., Spain). Individual (single-unit) neuronal spikes were isolated from the background noise with a window discriminator (Cibertec S.A., Madrid, Spain) and the firing rate was analyzed by a PC-based custom-made software (HFCP®, Cibertec S.A., Spain), which generated histogram bars representing the cumulative number of spikes in consecutive 10 s bins. To maintain the slice at a physiological temperature (33-34 ºC) a thermoregulatory system was used (Cibertec S.A., Madrid, Spain). All the extracellular-recording equipment was connected to a ground wire to prevent electrical interference.

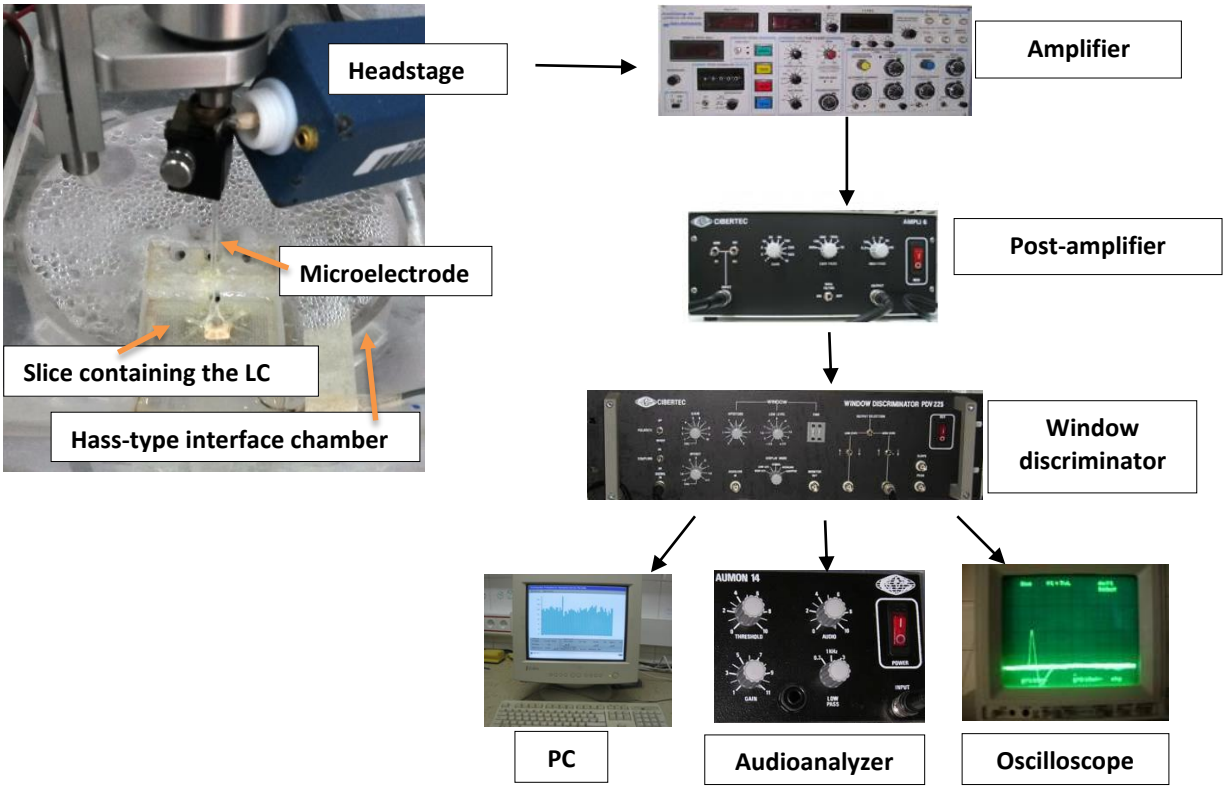


**Figure 3.3.** Schematic illustration of extracellular electrophysiological procedures

### 3.2.2 Measurement of analgesic tolerance to opioids: tail-flick technique

The antinociceptive effect of morphine hydrocloride was measured by the tail-flick test (Le Bars et al., 2001), which evaluates the response of the animal to a thermal nociceptive stimulus (Fig. 3.4). First, the rat was placed in a Plexiglas trap covered with a cloth for 20 min to allow the animal to some degree of habituation and to minimize the stress due to manipulation. Then, a beam of light was focused on the middle third of the tail. When the animal removed the tail with an energetic movement, the time (latency) was recorded. Three basal measures were taken from each animal at three different points of the tail, with a 15 s interval between measures. The mean of these three values was used as the result. The light intensity was initially adjusted with naive animals so that the basal latency ($t_{basal}$) was close to 3 s. Next, the rat was injected with a challenge dose of morphine hydrocloride (10 mg/kg, i.p.) and the latency ($t_{reaction}$) was tested again 30 min later to measure the effect of the opioid. This dose of morphine was selected based on previous experiments that observed a near maximal effect. This strong effect of morphine was appropriate to achieve a measurable tolerance after chronic opioid treatments. To

minimize tail skin damage, a cut-off latency time ($t_{max}$) was set at 10 s. Antinociception was expressed as a percentage of the maximal possible effect (M.P.E) according to the following formula (see section 3.2.4 for details):

$$\text{M. P. E (\%)} = \frac{t_{reaction} - t_{basal}}{t_{max} - t_{basal}} \cdot 100$$

**Figure 3.4**. The antinociceptive effect of morphine was measured by the tail-flick test, which evaluates the response of the animal to a thermal nociceptive stimulus.

### 3.2.3 Pharmacological procedures

***a) Characterization of the NO-dependent signaling pathways involved in ME-induced MOR desensitization in spontaneously active LC neurons in vitro***

Acute MOR desensitization in LC neurons was studied by measuring the inhibitory effect of a short application of a test concentration of ME (0.8 μM, 1 min) before (basal effect) and 5 min after perfusion with a high concentration of ME (3 or 10 μM, 10 min), according to the following scheme:

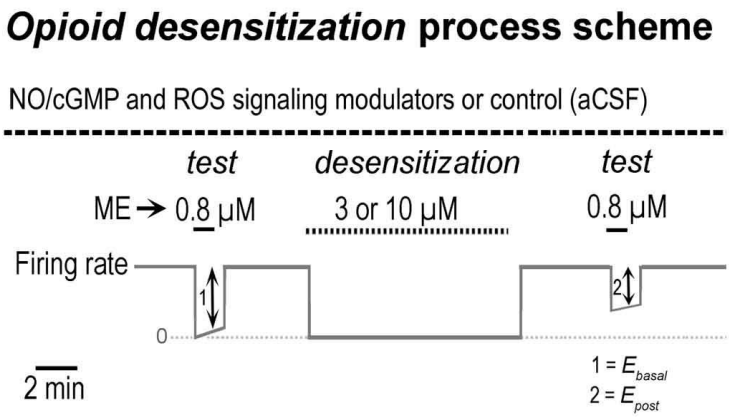


**Figure 3.5.** Scheme of the protocol used to evaluate the degree of opioid desensitization induced by ME in spontaneously firing LC neurons. The acute effect of ME (0.8 µM, 1 min) was tested before ($E_{basal}$) and 5 min after ($E_{post}$) inducing desensitization with ME (3 or 10 µM, 10 min). The decrease in ME (0.8 µM, 1 min) effect was taken as a measure of the degree of desensitization (Modified from Santamarta et al., 2014).

ME concentrations were chosen on the basis of previous studies (Harris and Williams, 1991; Torrecilla et al., 2001; Santamarta et al., 2014). To avoid variability between groups, we only recorded cells that showed slow spontaneous firing rates between 0.4 and 1.5 Hz, as well as strong inhibitory effects induced by ME (0.8 µM, 1 min) (higher than 80%).

To characterize the involvement of NO-dependent pathways (sGC/PKG and ROS) in ME-induced desensitization, the following drugs were perfused for at least 20-30 min before inducing desensitization with ME (3 or 10 µM) and then during the whole desensitization assay:

- sGC activators: A-350619 (30 µM) and BAY 418543 (1 µM)
- sGC inhibitor: NS 2028 (10 µM and 30 µM)
- PKG inhibitor: Rp-8-Br-PET-cGMP (1 µM)
- Antioxidants: melatonin (100 µM), Trolox (200 µM), U-74389G (10 µM)

In some assays, the NO donor DEA/NO (100 µM) was previously perfused to explore whether the sGC inhibitor NS 2028 (10 µM) regulated ME-induced desensitization. Finally, in one series of experiments, Trolox (200 µM) was administered together with NS 2028 (10 µM) to further evaluate the involvement of both sGC/cGMP and ROS pathways in MOR desensitization.

The desensitization induced by ME (3 μM) was used to investigate the effect of sGC activators, since we have previously demonstrated that this model is sensitive to the potentiation induced by NO (Llorente et al., 2012). Moreover, we induced desensitization with a higher concentration of ME (10 μM) to study the effect of sGC/PKG inhibitors or antioxidants, because this protocol is sensitive to the blockade of MOR desensitization induced by the NOS inhibitor 7-NI (Torrecilla et al., 2001; Santamarta et al., 2014).

***b) Involvement of nNOS in morphine- and ME-induced MOR desensitization in KCl-excited LC neurons in vitro***

The desensitization model that we have previously used in spontaneously firing neurons (see Fig. 3.5) was particularly suitable to study the desensitization induced by ME because it rapidly washes out from the preparation, so that the effect of a test concentration of ME (0.8 μM, 1 min) can be evaluated several times in the same neuron within few minutes. However, that protocol is not suitable to evaluate morphine effects repeatedly in the same neuron, since it does not quickly wash out from slices (Levitt and Williams, 2012). For those reasons, we quantified the extent of receptor desensitization induced by morphine by evoking a positive DC shift (a shift in the resting potential/ equilibrium potential in the positive direction) with KCl (14 mM)-containing aCSF, so that LC cells were excited to 2.0 – 7.3 Hz and morphine effects could be continously monitored. In these assays, NaCl was equiosmotically replaced with KCl. All the experiments were performed in the presence of CNQX (a non-NMDA glutamate receptor antagonist, 30 μM) and D-AP5 (a NMDA receptor antagonist, 100 μM) to avoid the interference of KCl-induced glutamate release on MOR desensitization. In each of the experiments, GABA (1 mM) was tested as an internal control before and after the desensitization with ME (10 μM, 10 min) or morphine (30 μM, 10 min).

ME and morphine effects on KCl-excited LC neurons were characterized by performing concentration-effect curves for the inhibitory effects of ME (0.1-25.6 μM, 2x, 1 min) and morphine (0.1-30 μM, 3x, 5 min) on the firing rate of LC neurons from rat brain slices.

To characterize the acute desensitization of MOR induced by ME or morphine under these experimental conditions, two possible designs were used:

- First, we compared the inhibitory effect of a supramaximal concentration of ME (25.6 μM, 1 min) before and 3-5 min after inducing desensitization with ME (10 μM, 10 min) or morphine (30 μM, 10 min). Once the last test concentration of ME (25.6 μM, 1 min) was applied, naloxone (1 μM) was perfused to reverse the morphine-induced hyperpolarization and to return the firing rate to control conditions. The decrease in the ME (25.6 μM, 1 min) effect after ME (10 μM) or morphine (30 μM) was taken as a measure of the degree of desensitization (see Fig. 3.6). With the purpose of comparisons, in some experiments, we used ME (0.8 μM, 1 min) as a test concentration before and after inducing desensitization with ME (10 μM, 10 min). These assays were similar to those described in section 3.2.3a (see Fig. 3.5), but in the presence of KCl (14 mM).

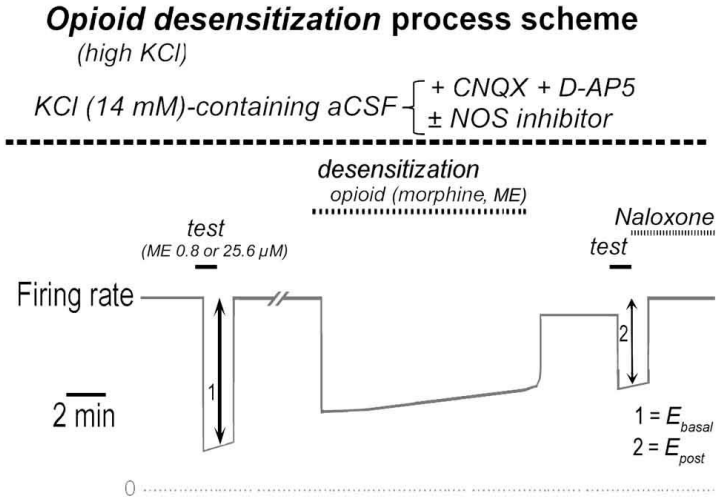


**Figure 3.6.** Scheme of one of the experimental designs used to evaluate the degree of opioid desensitization induced by ME or morphine in LC neurons under KCl-evoked excitation. The acute effect of ME (0.8 or 25.6 μM) was tested before and after inducing desensitization with ME (10 μM, 10 min) or morphine (30 μM, 10 min). The inhibitory effect induced by morphine was reversed by naloxone (1 μM). The decrease in the effect of ME (25.6 μM, 1 min) was taken as a measure of the degree of desensitization. All the experiments were performed in the presence of CNQX (non-NMDA glutamate receptor antagonist, 30 μM) and D-AP5 (NMDA receptor antagonist, 100 μM) to avoid the interference of KCl-induced glutamate release on MOR desensitization.

- Second, we measured the maximal response to ME (25.6 μM) at two times during a prolonged application of ME (10 μM, 10 min) or morphine (30 μM, 10 min): (1)

40-60 s after initiating the 10 min ME (10 µM) or morphine (30 µM) perfusion and (2) just after finishing it (see Fig. 3.7). Finally, naloxone (1 µM) was applied to reverse morphine-induced effects. The decrease in the ME (25.6 µM, 1 min) effect after ME (10 µM) or morphine (30 µM) was taken as a measure of the degree of desensitization.

In all cases, the application of the supramaximal test concentration of ME (25.6 µM) was limited to 1 min and a washout period of approximately 10 min was set between applications in order to reduce the induction of desensitization by test ME applications alone.

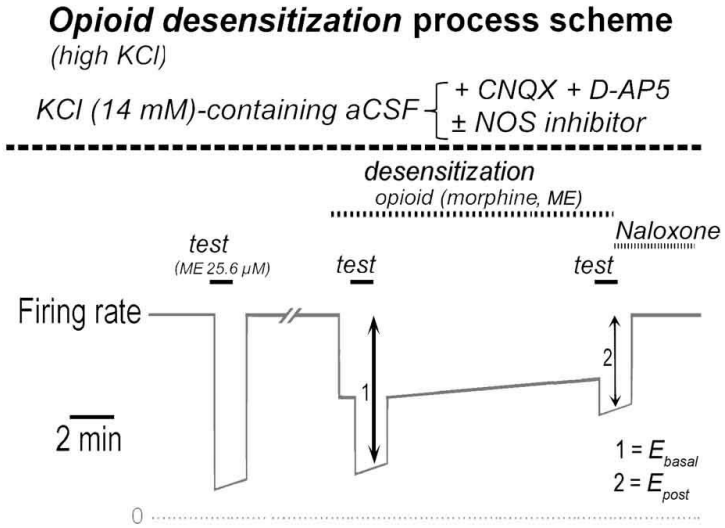


**Figure 3.7.** Scheme of one of the experimental designs used to evaluate the degree of opioid desensitization induced by ME or morphine in LC neurons under KCl-evoked excitation. The maximal effect induced by ME (25.6 µM) was tested during the continuous perfusion with ME (10 µM, 10 min) or morphine (30 µM, 10 min). The inhibitory effect induced by morphine was reversed by naloxone (1 µM). The decrease in the effect of ME (25.6 µM, 1 min) was taken as a measure of the degree of desensitization. All the experiments were performed in the presence of CNQX (non-NMDA glutamate receptor antagonist, 30 µM) and D-AP5 (NMDA receptor antagonist, 100 µM) to avoid the effects of KCl-induced glutamate release on MOR desensitization.

On the other hand, previous experiments have shown that administration of nNOS inhibitors attenuate the development of ME-induced MOR desensitization in spontaneously firing LC neurons *in vitro* (Santamarta et al., 2014). Here, we evaluated the effect of nNOS inhibitors on ME- and morphine-induced acute desensitization of MOR under KCl-induced activation. Thus, SMTC (10 µM) was perfused together with 7-NI (100 µM) for 20 min before starting the experiment and during the entire desensitization

assay with ME (10 μM, 10 min) or morphine (30 μM, 10 min). MOR desensitization in the presence of nNOS inhibitors was explored under the two experimental designs of MOR desensitization.

***c) Involvement of nNOS and ROS generation in the development of tolerance to the inhibitory effect of ME on LC cells after chronic treatment with morphine, methadone and fentanyl***

It has been previously shown that co-treatment with the nNOS inhibitor 7-NI attenuates the development of cellular tolerance in LC neurons from morphine-treated rats (Santamarta et al., 2005). To examine whether nNOS is involved in the development of tolerance by chronic treatments with other opioid agonists, such as methadone or fentanyl, rats treated with the opioid (methadone or fentanyl) or the sham were also co-treated with 7-NI or its vehicle. To further investigate the involvement of ROS in the development of cellular tolerance, sham- and opioid-treated rats were co-treated with the antioxidants TX+AA, U-74389G or their vehicles (see section 3.1.2 for treatment details).

To evaluate the development of tolerance, concentration-effect curves for the inhibitory effect of ME were performed as described by Santamarta et al. (2005) in LC neurons from sham- and opioid-treated rats, co-treated with 7-NI or the antioxidants. Thus, increasing concentrations of ME (0.05-12.8 μM, 2x, 1 min) were perfused at 5-min intervals until a maximal effect was reached. To avoid variability between groups, we only recorded cells that showed slow spontaneous firing rates between 0.4 and 1.5 Hz.

***d) Involvement of nNOS and ROS generation in the development of tolerance to the analgesic effects of morphine after chronic treatments with morphine, methadone and fentanyl***

Previous experiments have shown that *in vivo* administration of the nNOS inhibitor 7-NI attenuates the development of analgesic tolerance in morphine-treated rats (Santamarta et al., 2005). Moreover, co-treatment with TX+AA also attenuates the development of analgesic tolerance normally induced by morphine treatment (Llorente J., Doctoral Thesis, unpublished data). To study whether the nNOS is involved in the development of antinociceptive tolerance by chronic treatments with other opioid agonists, such as methadone and fentanyl, rats treated with the opioid (methadone or fentanyl) were co-treated with the nNOS inhibitor 7-NI or with its vehicle. To further

explore the involvement of ROS, sham and opioid-treated rats were co-treated with the antioxidant U-74389G or its vehicle (see section 3.1.2 for treatment details). Then, the antinociceptive response was measured by the tail-flick test (Le Bars et al., 2001), as explained in the section 3.2.2.

### 3.2.4 Data analysis and statistics

In electrophysiological experiments neuronal firing rate (FR) was collected in 10 s bin frequency histograms, where each bar represents the accumulated neuronal discharges in 10 seconds (spikes/10 s). The firing rate of LC cells was recorded before (baseline) and after the test application of the agonist (ME 0.8 – 12.8 μM, 1 min). Thus, the inhibitory effect (E) induced by ME (0.8 μM, 1 min) (Fig. 3.8) was calculated as the percentage of reduction of firing rate from baseline, according to the following formula:

$$E\ (\%) = \frac{FR_{pre} - FR_{post}}{FR_{basal}} \cdot 100$$

Where:

- E is the inhibitory effect of (ME 0.8 – 12.8 μM, 1 min) in percentages.
- $FR_{basal}$ is the average firing rate for 60 at the beginning of the recording.
- $FR_{pre}$ is the average firing rate for 60 s before each ME application.
- $FR_{post}$ is the average firing rate for 90 s after ME application, ruling out the 30-40 s that approximately take the drugs to reach the slice through the perfusion system.

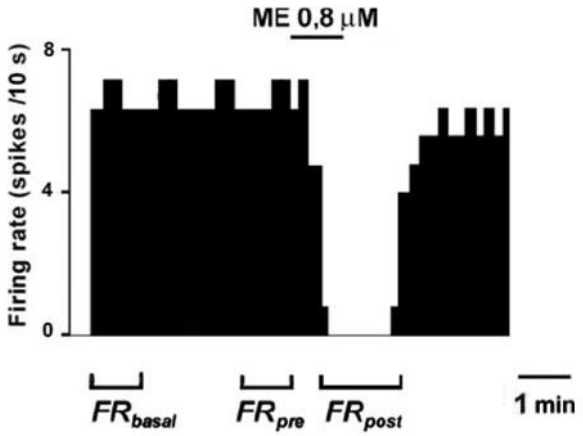


**Figure 3.8.** Representative example of a firing-rate recording from a LC neuron showing the inhibitory effect of a test concentration of ME (0.8 μM, 1 min). The vertical line refers to the neuronal firing rate and the horizontal line represents the period of ME application. The time scale corresponds to 1 min.

In those experiments in which the effect of opioids was tested under KCl (14 mM)-evoked excitation of LC neurons (Fig. 3.9) the inhibitory effect (E) induced by the test concentrations of ME (0.8 µM or 25.6 µM, 1 min) or GABA (1 mM, 1 min) was calculated by the same equation with the parameters being defined as follows:

- E is the inhibitory effect of ME (0.8 µM or 25.6 µM, 1 min) or GABA (1 mM, 1 min) in percentages.
- $FR_{basal}$ is the average firing rate for 60 s at the beginning of the recording.
- $FR_{pre}$ is the average firing rate for 60 s before each ME or GABA test application.
- $FR_{post}$ is the average firing rate for 30 s at the peak time after ME or GABA test application.

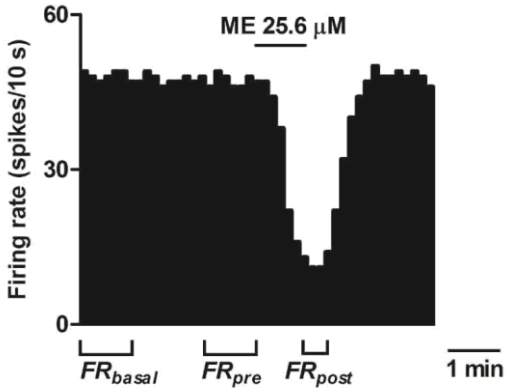


**Figure 3.9.** Representative example of a firing-rate recording from a LC neuron. The recording shows the inhibitory effect of a test concentration of ME (25.6 µM, 1 min). The vertical line refers to the KCl-excited firing rate and the horizontal line represents the period of ME application. The time scale corresponds to 1 min.

When naloxone (1 µM) was perfused to reverse morphine-induced effects (Fig. 3.10) the inhibitory effect (E) induced by the test concentration of ME (25.6 µM, 1 min) was calculated as follows:

$$E\ (\%) = \frac{FR_{nalox.} - FR_{post}}{FR_{basal}} \cdot 100$$

Where:

- E is the inhibitory effect of ME (25.6 µM, 1 min) in percentages.
- $FR_{basal}$ is the average firing rate for 60 s at the beginning of the recording.
- $FR_{post}$ is the average firing rate for 30 s at the peak time after ME (25.6 µM, 1 min) application, just before naloxone.
- $FR_{nalox}$ is the average firing rate for 60 s after naloxone (1 µM) application, once the firing rate returned to a plateau.

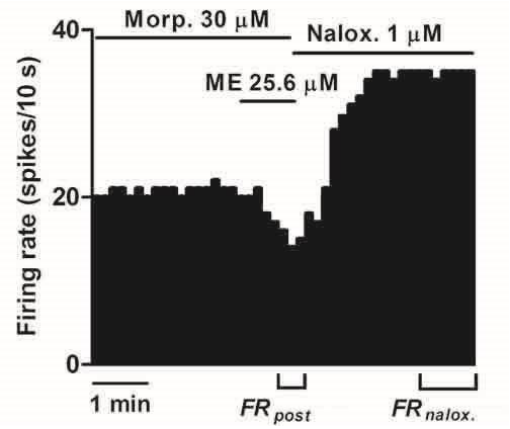


**Figure 3.10.** Representative example of a firing-rate recording from a LC neuron. The recording shows the inhibitory effect of a test concentration of ME (25.6 µM, 1 min) and the naloxone (1 µM)-induced reversal of the inhibitory effect. The vertical line refers to the KCl-evoked firing rate and the horizontal line represents the period of ME application. The time scale corresponds to 1 min.

In both *in vitro* models of acute MOR desensitization (the spontaneous firing rate model and the KCl-evoked firing excitation model), the degree of agonist-induced desensitization was calculated as follows:

$$degree\ of\ desensitization\ (\%) = \left[1 - \frac{E_{post}}{E_{basal}}\right] \cdot 100$$

Where:

- $E_{basal}$ is the inhibitory effect of the test concentration of the agonist (ME 0.8 µM, 25.6 µM or GABA 1 mM, 1 min) before perfusing the desensitizing concentrations of the opioid agonists (ME 3 and 10 µM; morphine 30 µM; 10 min) (Figures 3.5 and 3.6). In those experiments in which ME (25.6 µM, 1 min) was applied during a continuous opioid perfusion, $E_{basal}$ is the initial inhibitory effect of ME (25.6 µM, 1 min) applied 40-60 s after starting the perfusion with ME (10 µM) or morphine (30 µM) (Figure 3.7).

- $E_{post}$ is the inhibitory effect of the test concentration of the agonist (ME 0.8 µM, 25.6 µM or GABA 1 mM, 1 min) 3-5 min after finishing the desensitization with ME (3 µM or 10 µM, 10 min) or morphine (30 µM, 10 min) ) (Figures 3.5 and 3.6). In those experiments in which ME (25.6 µM, 1 min) was applied during a continuous opioid perfusion, $E_{post}$ is the final inhibitory effect of ME (25.6 µM, 1 min) applied immediately at the end of the 10 min perfusion with ME (10 µM) or

morphine (30 μM) and calculated with respect to the naloxone reversal (Figure 3.7).

To construct concentration-effect curves, we perfused increasing concentrations of ME until a maximal effect was reached. Curve fitting analysis was performed to obtain the best simple nonlinear fit to the following three-parameter logistic equation:

$$E\ (\%) = \frac{E_{max}}{1 + \left(\frac{EC_{50}}{A}\right)^{n}} \cdot 100$$

Where:

- E is the effect induced by each concentration of the agonist.
- A is the concentration of the agonist (μM).
- $E_{max}$ is the maximal effect achieved.
- $EC_{50}$ is the concentration of the agonist needed to elicit a 50% of the maximal effect (μM).
- n is the slope factor of the concentration-effect curve.

These parameters were determined by nonlinear analysis. Then, $EC_{50}$ values were transformed to the corresponding logarithmic data to convert them to a Gaussian distribution (Carpenter, 1986) and the corresponding statistical test was applied to the converted log units.

In behavioral experiments, analgesia was calculated as a percentage of the maximal possible effect (M.P.E.) (as explained in section 3.2.2)

$$\text{M. P. E}\ (\%) = \frac{t_{reaction} - t_{basal}}{t_{max} - t_{basal}} \cdot 100$$

Where:

- $t_{basal}$ is the time at which the animal withdrew the tail, before the morphine challenge.
- $t_{reaction}$ is the time at which the animal withdrew the tail after the morphine challenge.
- $t_{max}$ is the cut-off time, which was set at 10 s.

Analyses were performed by the software GraphPad Prism (version 5.0 for Windows), SPSS statistics (version 22.0 for Windows) and Microsoft Excel 2013. Data are expressed as mean ± S.E.M. For statistical evaluation, the following analyses were applied:

- Paired Student's t test: when the values were compared within the same cell or the same animal, before and after a pharmacological intervention.
- Two-sample Student's t test: when the values were compared between two independent groups.
- One-way analysis of variance (ANOVA) was used when values were compared between more than two groups. In case of significative results, the differences between two specific groups were further evaluated by a Tukey's post-hoc test. In some cases, analysis of covariance (ANCOVA) was performed to statistically control an external variable which might affect the results, followed by a Tukey's test.

A probability level of 0.05 was accepted as significantly different.

# 4. RESULTS

## 4.1 STUDY 1: CONTRIBUTION OF NITRIC OXIDE-DEPENDENT GUANYLATE CYCLASE AND REACTIVE OXYGEN SPECIES SIGNALING PATHWAYS TO DESENSITIZATION OF μ-OPIOID RECEPTORS IN THE RAT LOCUS COERULEUS

### Involvement of soluble guanylate cyclase/cyclic GMP in opioid-induced MOR desensitization in the LC

We have previously reported that different NO donors enhance ME (3 μM)-induced MOR desensitization (Llorente et al., 2012). It is well known that NO targets the heme group of the sGC, elevating cGMP concentrations (Ignarro et al., 1991). To study the involvement of sGC/cGMP pathway in the effect of NO donors on MOR desensitization, we tested the effect of DEA/NO, a nucleophile complex that spontaneously releases NO in aqueous solution, in the presence of the sGC inhibitor NS 2028. As expected, perfusion with ME (3 μM, 10 min) desensitized the inhibitory effect of ME (0.8 μM) by 30 ± 6% ($n$ = 5, $p$ < 0.05), whereas DEA/NO (100 μM) enhanced ME (3 μM)-induced MOR desensitization by 65 ± 18% ($n$ = 5, $p$ < 0.05 *vs* control) (Figs. 4.1A, B and D). The firing activity of LC cells was also elevated by DEA/NO (100 μM) perfusion (firing rate increase: 101 ± 14%, $n$ = 5, $p$ < 0.05; compare baselines in Figs. 4.1A and B), which is in agreement with previous studies showing a neuronal hyperactivity induced by NO donors (Llorente et al., 2012; Pineda et al., 1996). More importantly, administration of NS 2028 (10 μM) fully prevented both DEA/NO (100 μM)-induced enhancement of MOR desensitization ($n$ = 5, $p$ < 0.05, DEA/NO + NS 2028 *vs* DEA/NO) (Figs. 4.1C and D) and DEA/NO (100 μM)-elicited hyperactivity of LC neurons (firing rate changed by DEA/NO, with NS 2028: -9 ± 5%, $n$ = 5, $p$ < 0.005 *vs* without NS 2028, see above). NS 2028 (10 μM) itself did not modify MOR desensitization ($n$ = 3) (Fig. 4.1D). Finally, no changes were found in the acute effect of ME (0.8 μM) between the different groups (ME effect, control: 86 ± 3%, $n$ = 5; NS 2028: 90 ± 2%, $n$ = 3; DEA/NO: 87 ± 5%, $n$ = 5; and DEA/NO + NS 2028: 92 ± 2%, $n$ = 5). These data suggest the contribution of sGC in the enhancement of MOR desensitization and hyperactivity of LC cells induced by NO donors.

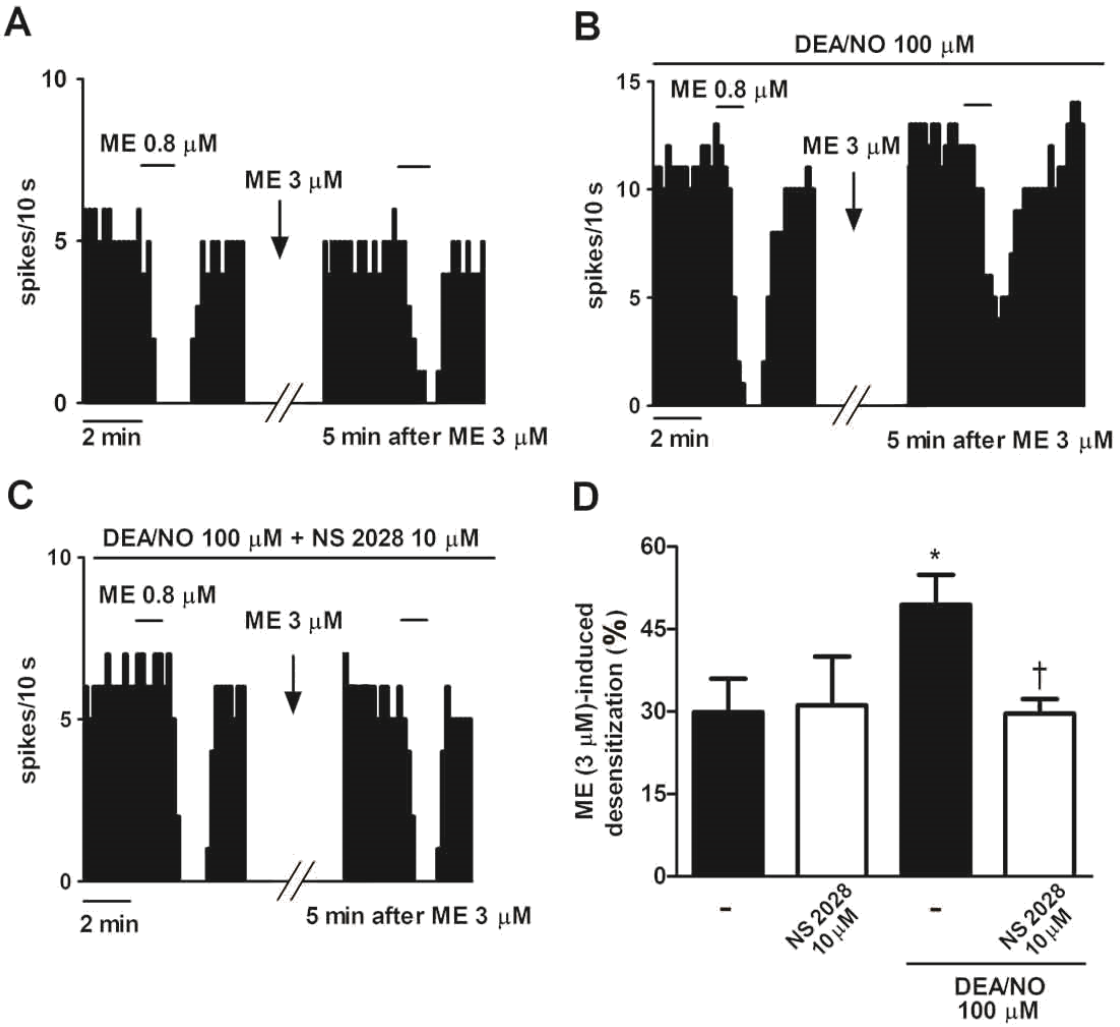


**Figure 4.1.** Effect of DEA/NO and DEA/NO + NS 2028 on ME (3 μM, 10 min)-induced MOR desensitization. **A, B, C.** Representative examples of firing-rate recordings of LC cells showing the effect of ME (0.8 μM, 1 min) before and 5 min after application of ME (3 μM, 10 min) in control slices (**A**), in slices perfused with DEA/NO (100 μM (**B**) or DEA/NO (100 μM) + NS 2028 (10 μM) (**C**). The horizontal bars indicate the period of drug applications and the vertical lines show the number of spikes recorded every 10 s. **D.** Bar histograms show the mean ± S.E.M of ME (3 μM, 10 min)-induced desensitization in the absence ($n$ = 5) or the presence of NS 2028 (10 μM, $n$ = 3), DEA/NO (100 μM, $n$ = 5) or NS 2028 (10 μM) + DEA/NO (100 μM) ($n$ = 5). Desensitization degrees were calculated as percentage values (see *Data analysis and statistics*). Note that DEA/NO markedly enhanced MOR desensitization and NS 2028 fully prevented the enhancement of MOR desensitization induced by DEA/NO. *$p$ < 0.05 when compared with the control group (two-sample Student's $t$ test), and † $p$ < 0.05 when compared with the DEA/NO group (two-sample Student's $t$ test).

To further explore the involvement of sGC/cGMP pathway in MOR desensitization, we evaluated the direct effect of different sGC modulators on ME (3 and 10 μM)-induced desensitization. Perfusion with the sGC activators A 350619 (30 μM) and BAY 418543 (1 μM) enhanced by 93 ± 15% and 90 ± 6%, respectively, ME (3 μM)-induced MOR desensitization ($n$ = 5, $p < 0.01$ *vs* control; and $n$ = 5, $p < 0.005$ *vs* control; respectively) (Figs. 4.2A, B and C). BAY 418543 (1 μM) also elevated the firing activity of LC neurons by a 51 ± 16% ($n$ = 5, $p < 0.05$). There was no change in the acute effect of ME (0.8 μM) between the different groups (ME effect, A 350619: 88 ± 3%, $n$ = 5; BAY 418543: 94 ± 2%, $n$ = 5). On the other hand, perfusion with a higher concentration of ME (10 μM, 10 min) caused a greater degree of MOR desensitization, with a strong decrease in ME (0.8 μM) effect (desensitization: 61 ± 3%, $n$ = 8, $p < 0.005$) (Figs. 4.3A and C). Unexpectedly, administration of two different concentrations of the sGC inhibitor NS 2028 (10 and 30 μM) failed to modify ME (10 μM)-induced MOR desensitization, so that desensitization remained significant ($n$ = 6, $p < 0.005$; and $n$ = 3, $p < 0.005$) (Figs. 4.3B and C).

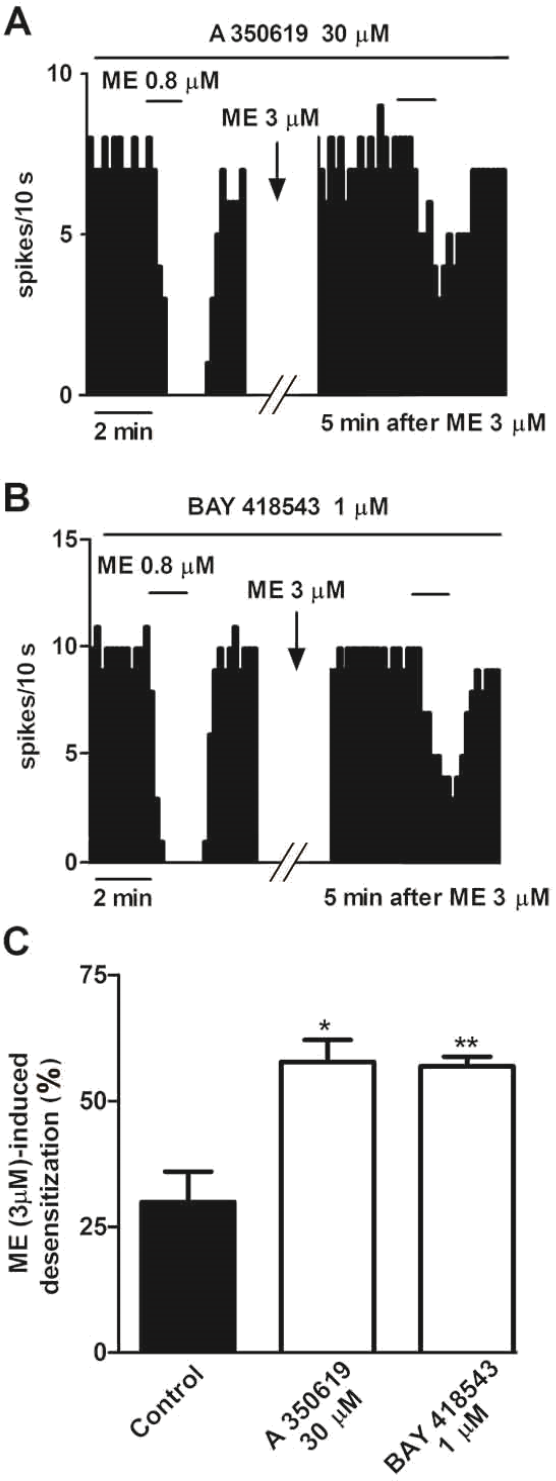
A
A 350619 30 μM
ME 0.8 μM
ME 3 μM
spikes/10 s
10
5
0
2 min
5 min after ME 3 μM
B
BAY 418543 1 μM
ME 0.8 μM
ME 3 μM
spikes/10 s
15
10
5
0
2 min
5 min after ME 3 μM
C
ME (3μM)-induced desensitization (%)
75
50
25
0
*
**
Control
A 350619 30 μM
BAY 418543 1 μM

**Figure 4.2.** Effect of A 350619 and BAY 418543 on ME (3 μM, 10 min)-induced desensitization. **A, B.** Representative examples of firing-rate recordings of LC cells showing the effect of ME (0.8 μM, 1 min) before and 5 min after application of ME (3 μM, 10 min) in slices perfused with A 350619 (30 μM) (**A**) or BAY 418543 (1 μM) (**B**). The horizontal bars indicate the period of drug applications and the vertical lines show the number of spikes recorded every 10 s. **C.** Bar histograms show the mean ± S.E.M of ME (3 μM, 10 min)-induced desensitization in the presence of A 350619 (30 μM, $n = 5$) or BAY 418543 (1 μM, $n = 5$). Desensitization degrees were calculated as percentage values (see *Data analysis and statistics*). Note that A 350619 and BAY 418543 markedly enhanced MOR desensitization. *$p < 0.01$ and **$p < 0.005$ when compared with the control group (two-sample Student's *t* test).

## Involvement of cGMP-dependent protein kinase in opioid-induced MOR desensitization in the LC

Previous studies from our group have reported that perfusion with the PKG activator 8-Br-cGMP completely restores ME-induced MOR desensitization from the blockade elicited by the nNOS inhibitor 7-NI in LC neurons (M.T. Santamarta, Doctoral Thesis). To further explore the involvement of PKG in acute desensitization of MOR, we tested the highly selective PKG inhibitor Rp-8-Br-PET-cGMP (1 μM). Unexpectedly, administration of the PKG inhibitor Rp-8-Br-PET-cGMP (1 μM) failed to modify the degree of ME (10 μM)-induced desensitization. Thus, desensitization induced by ME (10 μM) in the presence of or Rp-8-Br-PET-cGMP (1 μM) was significant ($n = 4$, $p < 0.005$) (Fig. 4.3C).

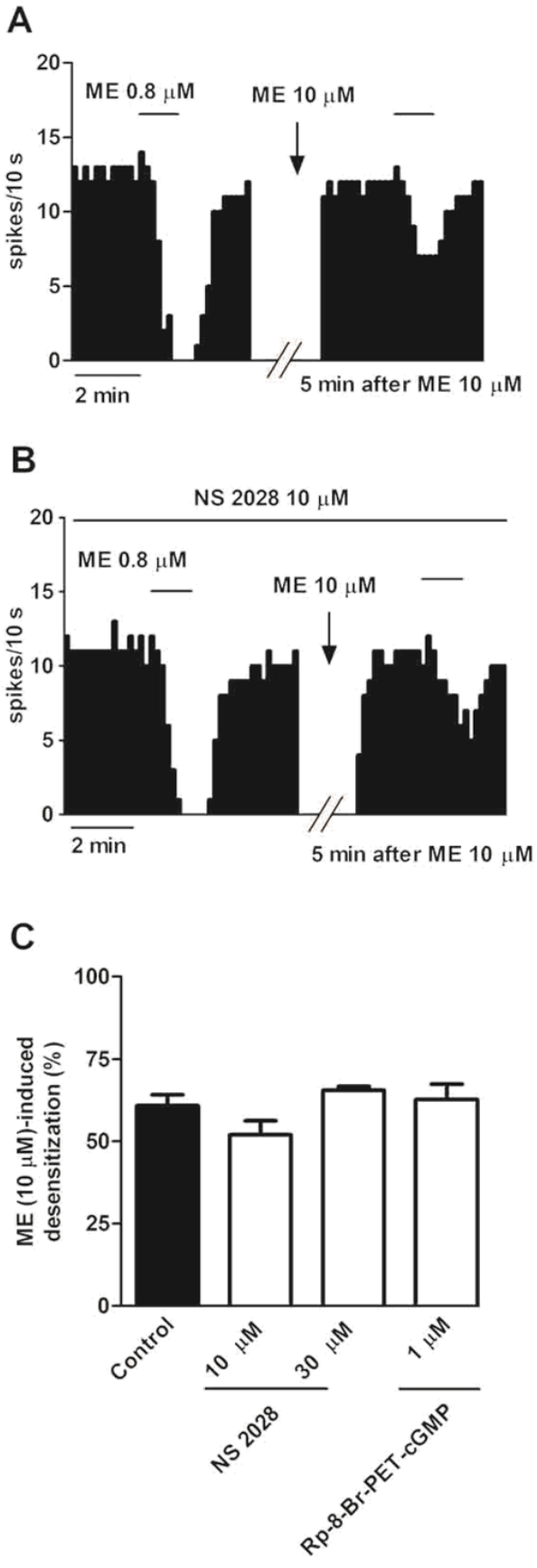
A
ME 0.8 μM
ME 10 μM
spikes/10 s
20
15
10
5
0
2 min
5 min after ME 10 μM
B
NS 2028 10 μM
ME 0.8 μM
ME 10 μM
spikes/10 s
20
15
10
5
0
2 min
5 min after ME 10 μM
C
ME (10 μM)-induced desensitization (%)
100
75
50
25
0
Control
10 μM
30 μM
1 μM
NS 2028
Rp-8-Br-PET-cGMP

**Figure 4.3.** Effect of NS 2028 and Rp-8-Br-PET-cGMP on ME (10 µM, 10 min)-induced desensitization. **A, B.** Examples of firing-rate recordings of LC cells showing the effect of ME (0.8 µM, 1 min) before and 5 min after application of ME (10 µM, 10 min) in control slices (**A**) and in slices perfused with NS 2028 (10 µM) (**B**). The horizontal bars indicate the period of drug applications and the vertical lines show the number of spikes recorded every 10 s. **C.** Effect of NS 2028 and Rp-8-Br-PET-cGMP on MOR desensitization induced by ME (10 µM, 10 min). Bars represent the mean ± S.E.M. of *n* experiments. Desensitization degrees were calculated as percentage values (see *Data analysis and statistics*). Note that ME (10 µM)-induced desensitization was not changed in the presence of NS 2028 (10 µM or 30 µM, $n = 6$ and $n = 3$, respectively) or Rp-8-Br-PET-cGMP (1 µM, $n = 4$).

## Involvement of reactive oxygen species in opioid-induced MOR desensitization in the LC

NO reacts with oxygen derivatives to produce reactive nitrogen species and ROS (Davis et al., 2001), which have been shown to contribute to NO-induced enhancement of MOR desensitization in the LC (Llorente et al., 2012). We further explored whether ROS would itself mediate ME (10 µM)-induced desensitization by administration of three structurally unrelated antioxidants. Perfusion of either of the antioxidants U-74389G (10 µM), melatonin (100 µM) or Trolox (200 µM) failed to modify the degree of ME (10 µM)-induced desensitization ($n = 4$, $n = 4$ and $n = 4$, respectively) when compared to the corresponding control group (Figs. 4.4A and C). However, perfusion of the antioxidant Trolox (200 µM) together with the sGC inhibitor NS 2028 (10 µM) attenuated by 37 ± 6% ($n = 5$, $p < 0.005$ *vs* control) ME (10 µM)-induced desensitization (Figs. 4.4B and C). This combination (Trolox 200 µM + NS 2028 10 µM) slightly reduced the firing rate of LC neurons (firing rate change: -22 ± 4%, $n = 5$, $p < 0.005$), although the basal firing rate after the combination was not different from that in control (basal firing rate before desensitization, control: 0.72 ± 0.09, n = 8; Trolox + NS 2028: 0.67 ± 0.13, $n = 5$). Finally, no changes were found in the acute ME (0.8 µM) effect between the two groups (ME effect, control: 93 ± 1%, $n = 8$; Trolox + NS 2028: 91 ± 3%, $n = 5$). This indicates that ROS and sGC/cGMP signaling cascades may be required for induction of MOR desensitization, but either of these pathways independently may be enough to mediate it.

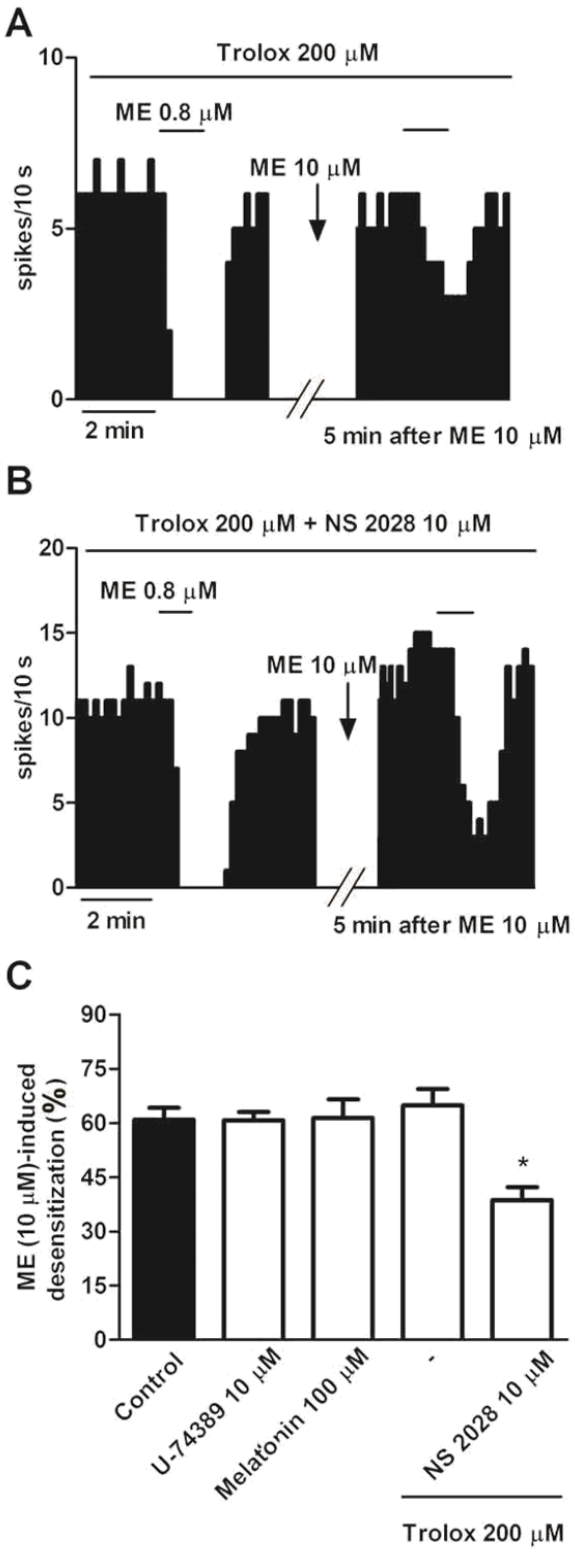
A
Trolox 200 μM
ME 0.8 μM
ME 10 μM
spikes/10 s
10
5
0
2 min
5 min after ME 10 μM
B
Trolox 200 μM + NS 2028 10 μM
ME 0.8 μM
ME 10 μM
spikes/10 s
20
15
10
5
0
2 min
5 min after ME 10 μM
C
ME (10 μM)-induced desensitization (%)
90
75
60
45
30
15
0
*
Control
U-74389 10 μM
Melatonin 100 μM
-
NS 2028 10 μM
Trolox 200 μM

**Figure 4.4.** Effect of Trolox, Trolox + NS 2028, U-74389G and melatonin on ME (10 μM, 10 min)-induced desensitization. **A, B.** Representative examples of firing-rate recordings of LC cells showing the effect of ME (0.8 μM, 1 min) before and 5 min after application of ME (10 μM, 10 min) in slices perfused with Trolox (200 μM) (**A**) or Trolox (200 μM) + NS 2028 (10 μM) (**B**). Drugs were bath applied for the time indicated by the horizontal bars. Vertical lines represent the number of spikes recorded every 10 s. **C**. Bar histograms show the mean ± S.E.M of ME (10 μM)-induced desensitization in the absence ($n$ = 8, control) or the presence of U-74389G (10 μM, $n$ = 4), melatonin (100 μM, $n$ = 4), Trolox (200 μM, $n$ = 4) or Trolox (200 μM) + NS 2028 (10 μM) ($n$ = 5). Desensitization degrees were calculated as percentage values (see *Data analysis and statistics*). Note that in the presence of Trolox + NS 2028 MOR desensitization was markedly attenuated. *$p$ < 0.005 compared with the control group (two-sample Student's $t$ test).

## 4.2 STUDY 2: STUDY OF THE INVOLVEMENT OF NEURONAL NITRIC OXIDE SYNTHASE IN MORPHINE-INDUCED DESENSITIZATION OF μ-OPIOID RECEPTORS IN THE RAT LOCUS COERULEUS

### Characterization of acute inhibitory effects of ME and morphine on KCl-excited LC neurons *in vitro*

A sustained perfusion with KCl (14 mM) increased by 6 fold the firing rate of LC neurons (firing rate before KCl: 0.80 ± 0.04 Hz; after KCl: 4.29 ± 0.16 Hz, $n = 52$, $p < 0.005$). In order to characterize the acute inhibitory effects of ME and morphine, increasing concentrations of ME (0.1-25.6 μM, 2x, 1 min) or morphine (0.1-30 μM, 3x, 5 min) were perfused in the slice (Figs. 4.5A and B). No differences were found in the KCl-excited basal firing rate between groups (basal firing rate, before ME: 3.08 ± 0.44 Hz, $n = 5$; before morphine: 3.27 ± 0.56 Hz, $n = 5$). The $pEC_{50}$ value for ME effect obtained by nonlinear analysis was 6.12 ± 0.02 ($EC_{50}$ = 0.75 μM, $n = 5$), whereas the $pEC_{50}$ for morphine effect was 6.41 ± 0.09 ($EC_{50}$ = 0.39 μM, $n = 5$). The maximum inhibitory effects ($E_{max}$) induced by ME and morphine were 81 ± 8% and 55 ± 5% from the KCl-excited basal firing rate, respectively (Figs. 4.5C and D). GABA promoted a 100% inhibition from baseline in all cases. These results indicate that morphine behaves as partial agonist at the MOR in LC neurons.

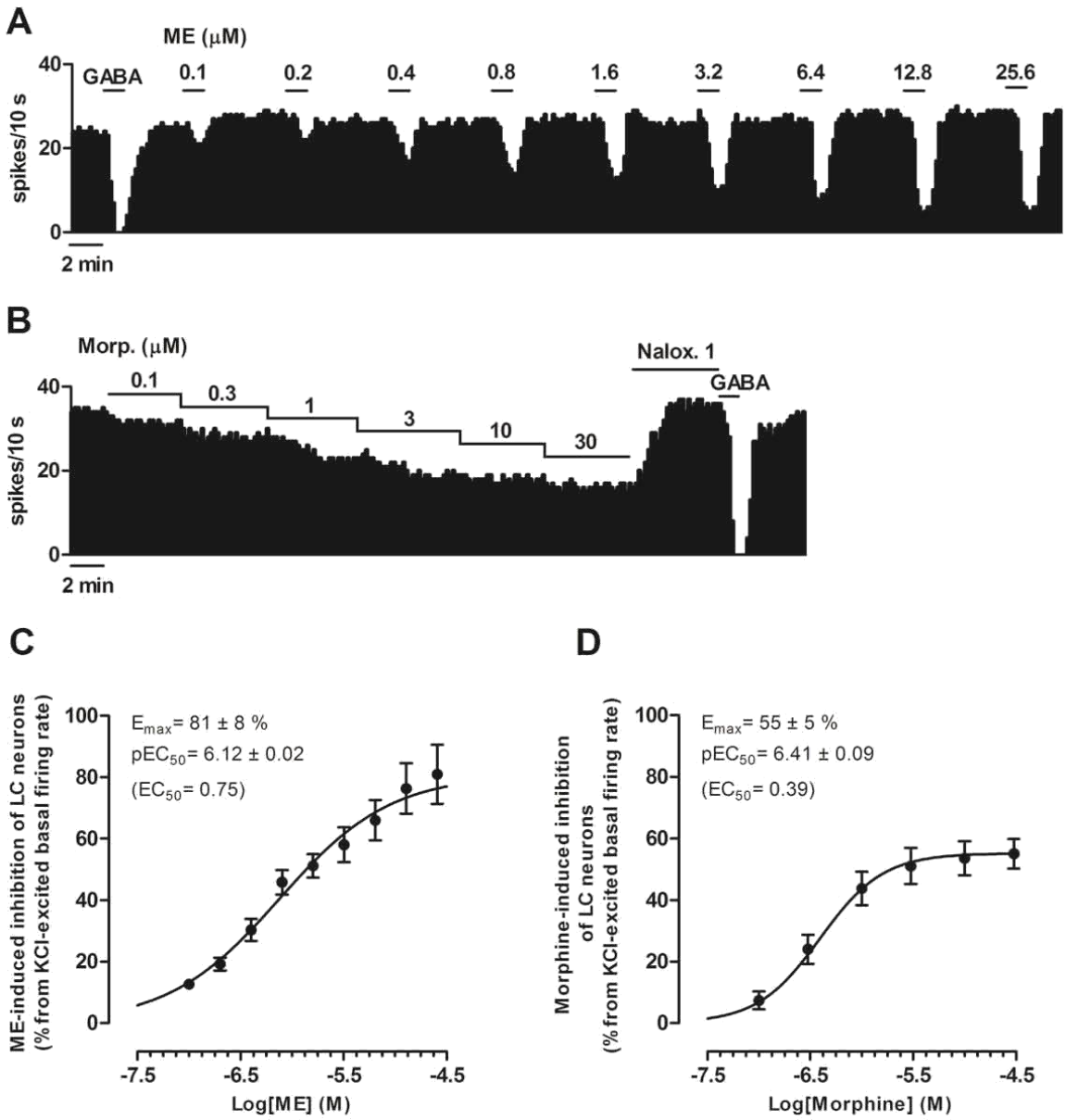


**Figure 4.5.** Characterization of acute ME and morphine effects under KCl-evoked activation of LC neurons *in vitro*. **A, B.** Examples of firing-rate recordings of LC cells showing the inhibitory effect of ME (**A**) and morphine (**B**). Each horizontal bar represents the period of application of each ME (0.1 - 25.6 μM, 2x) or morphine concentration (0.1 - 30 μM, 3x) and the vertical lines show the number of spikes recorded every 10 s. **C, D.** Concentration-effect curves for the inhibitory effect of ME (**C**) and morphine (**D**) in KCl-excited LC neurons. The horizontal axis represents the logarithms of ME and morphine concentrations in linear scale. The vertical axis expresses the reduction in the firing rate of LC neurons as a percentage from the KCl-induced basal firing rate. Symbols are the mean ± SEM of ME or morphine effects at each concentration obtained from *n* animals. The lines through the data are the theoretical curves constructed from the mean of the individual concentration-effect curve parameters, as estimated by nonlinear regression (see Materials and Methods for details).

**Characterization of acute MOR desensitization induced by ME and morphine in LC neurons**

First, we evaluated the effect of short applications of two test concentrations of ME (0.8 μM or 25.6 μM, 1 min) before and after perfusing with a high, desensitizing concentration of ME (10 μM, 10 min) or morphine (30 μM, 10 min). ME (0.8 μM) is a concentration that is close to the $EC_{50}$ in this KCl model and ME (25.6 μM) allows us to see changes in the maximum response. Thus, after finishing the ME (10 μM, 10 min) administration, the inhibitory effect of ME (0.8 μM) was desensitized by 55 ± 3% ($n$ = 5, $p$ < 0.005), whereas the effect of ME (25.6 μM) was reduced by 26 ± 3% ($n$ = 5, $p$ < 0.005) (Figs. 4.6A, C and G). On the other hand, after finishing the morphine (30 μM, 10 min) perfusion, the inhibitory effect of (25.6 μM) was desensitized by 39 ± 4% ($n$ = 5, $p$ < 0.005) (Figs. 4.6D and G). This degree of desensitization was higher than that induced by ME (10 μM) ($p$ < 0.05, Fig. 4.6G). As morphine (30 μM) produces a near maximal receptor occupancy and does not quickly wash out from the slice, we had to use the supramaximal test concentration of ME (25.6 μM) to measure maximal activity of MOR. For that reason, ME (0.8 μM) was not tested in morphine experiments. After inducing desensitization with morphine, naloxone was applied to return to control firing rate values in the absence of MOR activation. In fact, the firing rate after naloxone (1 μM) was not different when compared to the firing rate before desensitization (firing rate, before desensitization: 4.1 ± 0.5 Hz, $n$ = 5; after naloxone (1 μM): 4.0 ± 0.5 Hz, $n$ = 5).

Second, we compared the maximal response to ME (25.6 μM) applied at two times during a continuous application of ME (10 μM, 10 min) or morphine (30 μM, 10 min). By this approach the inhibitory effect of ME (25.6 μM, 1 min) was desensitized by 36 ± 4% ($n$ = 5, $p$ < 0.05) following ME (10 μM, 10 min) perfusion and by 32 ± 5% ($n$ = 5, $p$ < 0.01) after morphine (30 μM, 10 min) (Figs. 4.6E, F and G). The firing rate after naloxone (1 μM) did not differ from the firing rate before desensitization (firing rate, before desensitization: 4.7 ± 0.4 Hz, $n$ = 5; after naloxone (1 μM): 4.5 ± 0.4 Hz, $n$ = 5).

In each desensitization experiment, GABA (1 mM) was tested as an internal control. The inhibitory effect of GABA (1 mM, 1 min) was close to 100% from baseline (>95%) both before and after perfusion with ME (10 μM, 10 min) ($n$ = 15) (Figs. 4.6B and G) or morphine (30 μM, 10 min) ($n$ = 9) (Fig. 4.6G).

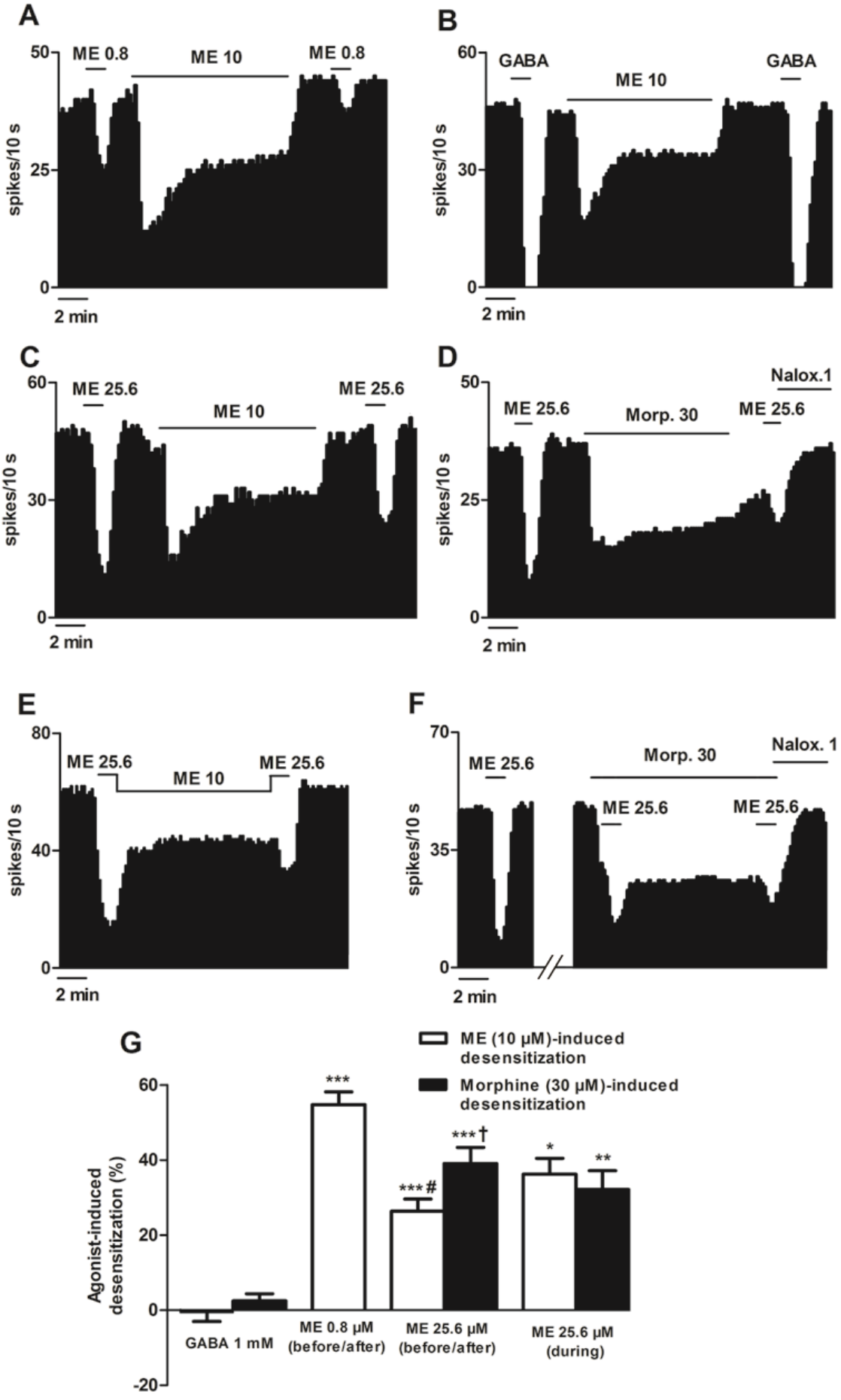
A
ME 0.8
ME 10
ME 0.8
spikes/10 s
50
25
0
2 min
B
GABA
ME 10
GABA
spikes/10 s
60
30
0
2 min
C
ME 25.6
ME 10
ME 25.6
spikes/10 s
60
30
0
2 min
D
Nalox.1
ME 25.6
Morp. 30
ME 25.6
spikes/10 s
50
25
0
2 min
E
ME 25.6
ME 10
ME 25.6
spikes/10 s
80
40
0
2 min
F
ME 25.6
Morp. 30
Nalox. 1
ME 25.6
ME 25.6
spikes/10 s
70
35
0
2 min
G
ME (10 µM)-induced desensitization
Morphine (30 µM)-induced desensitization
Agonist-induced desensitization (%)
60
40
20
0
-20
***
***#
***†
*
**
GABA 1 mM
ME 0.8 µM (before/after)
ME 25.6 µM (before/after)
ME 25.6 µM (during)

**Figure 4.6** Characterization of acute desensitization of MOR induced by ME and morphine in KCl-excited LC neurons *in vitro*. **A, B, C.** Examples of firing-rate recordings of LC cells showing the effect of ME (0.8 μM, 1 min) (**A**), GABA (1 mM, 1 min) (**B**) or ME (25.6 μM, 1 min) (**C**) before and after inducing desensitization with ME (10 μM, 10 min). **D,** Example of firing-rate recording of a LC neuron showing the effect of ME (25.6 μM, 1 min) before and after inducing desensitization with morphine (30 μM, 10 min). **E, F.** Examples of firing-rate recordings of LC cells showing the effect of ME (25.6 μM, 1 min) applied at two times during a sustained perfusion with ME (10 μM, 10 min) (**E**) or morphine (30 μM, 10 min) (**F**). The horizontal bars indicate the period of drug applications and the vertical lines show the number of spikes recorded every 10 s. **G.** Bar histograms show the mean ± S.E.M of ME (10 μM)-, or morphine (30 μM)-induced desensitization. Different test concentrations and experimental designs were used (see *Pharmacological procedures*). GABA was used as an internal control. All the experiments were performed in the presence of the glutamate receptor antagonists CNQX (30 μM) and D-AP5 (100 μM). Desensitization degrees were calculated as percentage values (see *Data analysis and statistics*). Note that significant reductions in the effect of ME (0.8 μM, 1 min) or ME (25.6 μM, 1 min) were observed when applied before and after or during ME (10 μM, 10 min) ($n$ = 5, in all cases), but the degree of desensitization was greater when it was quantified by ME (0.8 μM). Likewise, substantial reduction in ME (25.6 μM) effect was observed when applied before and after ($n$ = 5) or during ($n$ = 5) morphine (30 μM, 10 min). The desensitization induced by morphine (30 μM) was greater than that induced by ME (10 μM) when the test concentration was applied before and after. The effect of GABA (1 mM) was unaltered after perfusion with either ME (10 μM) or morphine (30 μM) ($n$ = 15 and $n$ = 9, respectively). *$p$ < 0.05, **$p$ < 0.01 and **$p$ < 0.005 when the effect of the test concentration of ME after desensitization was compared to the basal effect by a paired Student's t test**.** $^{\#}p$ < 0.005 when compared to the ME (0.8 μM) group by a two-sample Student's t test; $^{\dagger}p$ < 0.05 when compared to the corresponding ME (10 μM) group by a two-sample Student's t test.

**Effect of neuronal NOS inhibitors on acute MOR desensitization induced by ME and morphine**

It has been shown that nNOS contributes to ME-induced MOR desensitization in spontaneously active LC neurons (Santamarta et al., 2014). To further study the involvement of nNOS on morphine (30 μM)-induced desensitization, we perfused a combination of two nNOS inhibitors 7-NI (100 μM) and SMTC (10 μM). Perfusion with the nNOS inhibitors did not alter the firing rate of LC neurons (firing rate change: 2 ± 1%, $n = 17$). Moreover, acute effects of both test concentrations of ME (0.8 and 25.6 μM) in the presence of nNOS inhibitors were not different from those in the control group (change in acute effect, ME (0.8 μM): 15 ± 7%, $n = 5$; ME (25.6 μM): 5 ± 7%, $n = 15$).

As in spontaneously firing neurons, administration of nNOS inhibitors in KCl-excited LC neurons reduced by 27 ± 6% ($n = 5$, $p < 0.05$ *vs* control) the desensitization induced by ME (10 μM) when ME (0.8 μM) was applied before and after inducing desensitization (Figs. 4.7A and E). In addition, nNOS inhibitors blocked the desensitization by 58 ± 8% ($n = 5$, $p < 0.005$ *vs* control) when ME (25.6 μM) was applied before and after ME (10 μM), (Figs. 4.7B and E). Finally, nNOS inhibitors reduced by 43 ± 8% ($n = 5$, $p < 0.05$ *vs* control) the desensitization when ME (25.6 μM) was applied during ME (10 μM), (Figs. 4.7D and E). The basal firing rate in the presence of nNOS inhibitors was not significantly different when compared to the control group (basal firing rate, control: 4.35 ± 0.26 Hz, $n = 15$; in the presence of nNOS inhibitors: 4.92 ± 0.32 Hz, $n = 15$). GABA (1 mM, 1 min) caused a 100% reduction from baseline before and after inducing desensitization ($n = 14$) (Figs. 4.7C and E). These results reaffirm that nNOS contributes to ME-induced MOR desensitization in rat LC neurons.

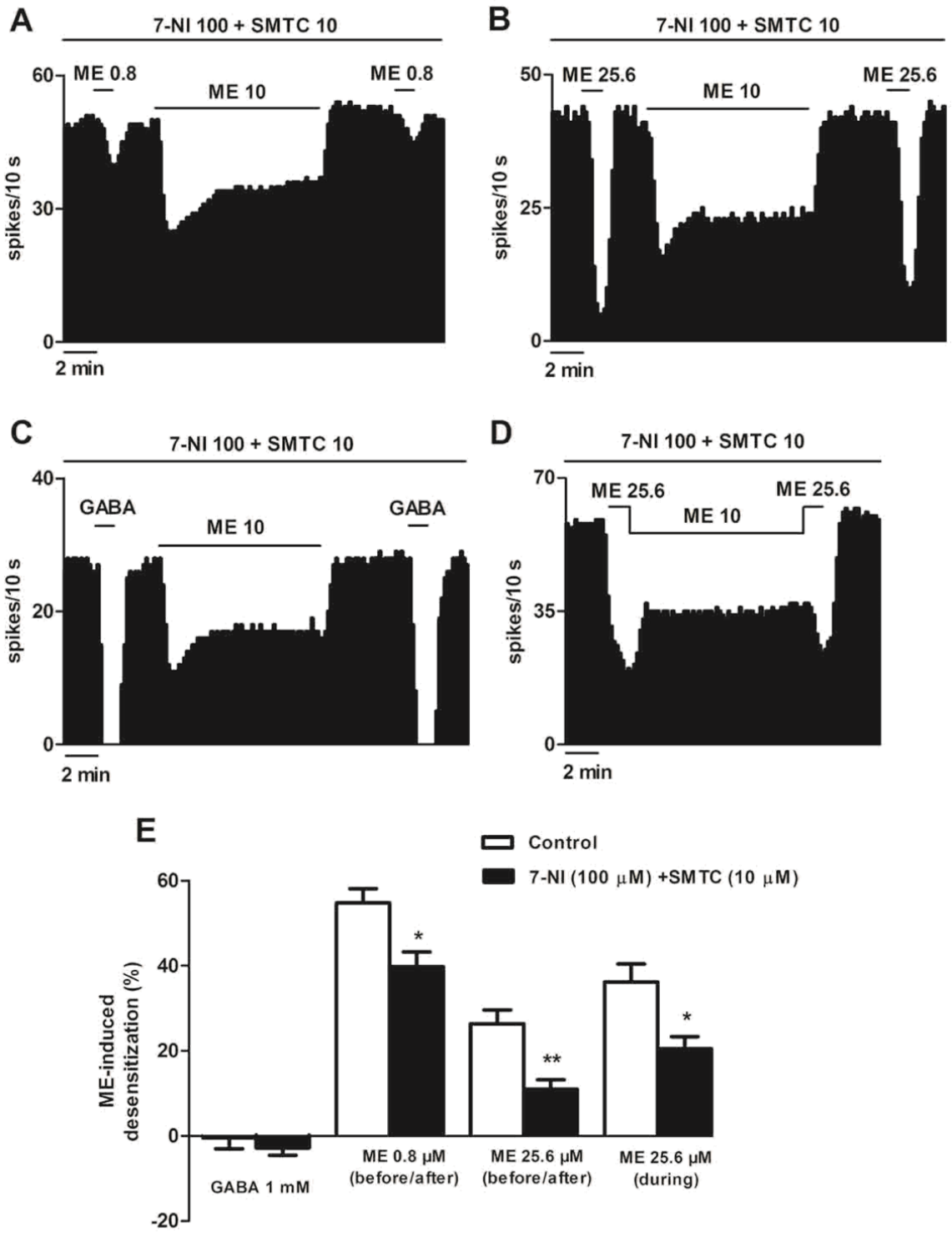
A
7-NI 100 + SMTC 10
ME 0.8
ME 10
ME 0.8
spikes/10 s
60
30
0
2 min
B
7-NI 100 + SMTC 10
ME 25.6
ME 10
ME 25.6
spikes/10 s
50
25
0
2 min
C
7-NI 100 + SMTC 10
GABA
ME 10
GABA
spikes/10 s
40
20
0
2 min
D
7-NI 100 + SMTC 10
ME 25.6
ME 10
ME 25.6
spikes/10 s
70
35
0
2 min
E
Control
7-NI (100 μM) +SMTC (10 μM)
ME-induced desensitization (%)
60
40
20
0
-20
*
**
*
GABA 1 mM
ME 0.8 μM (before/after)
ME 25.6 μM (before/after)
ME 25.6 μM (during)

**Figure 4.7.** Effect of nNOS inhibitors on acute MOR desensitization induced by ME in KCl-excited LC neurons *in vitro*. **A, B, C.** Representative examples of firing-rate recordings of LC cells showing the effect of ME (0.8 μM, 1 min) (**A**), ME (25.6 μM, 1 min) (**B**) or GABA (1 mM, 1 min) (**C**) applied before and after inducing desensitization with ME (10 μM, 10 min) in the presence of 7-NI (100 μM) and SMTC (10 μM). **D.** Example of firing-rate recording of LC cell showing the effect of ME (25.6 μM, 1 min) applied at two times during a sustained perfusion with ME (10 μM, 10 min) in the presence of 7-NI (100 μM) and SMTC (10 μM). The horizontal bars indicate the period of drug applications and the vertical lines show the number of spikes recorded every 10 s. **E.** Bar histograms show the mean ± S.E.M of ME (10 μM)-induced desensitization in the absence and in the presence of nNOS inhibitors. Different test concentrations and experimental designs were used (see *Pharmacological procedures*). GABA was used as an internal control. All the experiments were performed in the presence of the glutamate receptor antagonists CNQX (30 μM) and D-AP5 (100 μM). Desensitization degrees were calculated as percentage values (see *Data analysis and statistics*). Note that nNOS inhibitors attenuated ME (10 μM)-induced desensitization when it was quantified by ME (0.8 μM, $n = 5$), or ME (25.6 μM) applied before and after ($n = 5$) or during ME 10 μM ($n = 5$). In contrast, GABA (1 mM) effect was not affected ($n = 14$). *$p < 0.05$ and **$p < 0.005$ when compared to the corresponding control group by two-sample Student's t test.

On the contrary, perfusion with 7-NI (100 μM) together with SMTC (10 μM) failed to alter morphine (30 μM)-induced desensitization. Thus, desensitization induced by morphine (30 μM) in the presence of nNOS inhibitors was significant ($n$ = 5, $p$ < 0.005) (Figs. 4.8A and B). No differences were found between the firing rate before morphine (30 μM) and after naloxone (1 μM) (firing rate before morphine (30 μM): 5.0 ± 0.2 Hz, $n$ = 5; firing rate after naloxone (1 μM): 4.8 ± 0.3 Hz, $n$ = 5). GABA (1 mM) promoted a 100% inhibition from baseline before and after inducing desensitization ($n$ = 5) (Figs. 4.8A and B). These results suggest that nNOS is not involved in acute MOR desensitization induced by morphine in LC neurons.

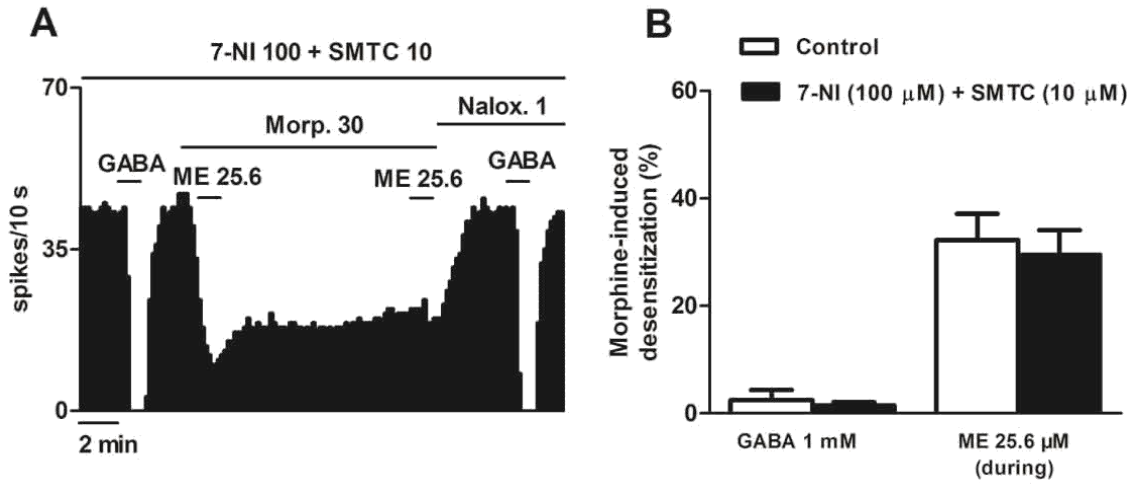


**Figure 4.8.** Effect of nNOS inhibitors on acute MOR desensitization induced by morphine in KCl-excited LC neurons *in vitro*. **A.** Representative example of a firing-rate recording of LC cell showing the effect of ME (25.6 μM, 1 min) applied at two times during a sustained perfusion with morphine (30 μM, 10 min) in the presence of 7-NI (100 μM) and SMTC (10 μM). The horizontal bars indicate the period of drug applications and the vertical lines show the number of spikes recorded every 10 s. **B.** Bar histograms show the mean ± S.E.M of morphine (30 μM)-induced desensitization in the absence and in the presence of nNOS inhibitors. GABA was used as an internal control. All the experiments were performed in the presence of the glutamate receptor antagonists CNQX (30 μM) and D-AP5 (100 μM). Desensitization degrees were calculated as percentage values (see *Data analysis and statistics*). Note that nNOS inhibitors failed to block morphine (30 μM)-induced desensitization ($n$ = 5). The effect of GABA (1 mM) was not affected by morphine perfusion ($n$ = 5).

## 4.3 STUDY 3: EFFECT OF NEURONAL NITRIC OXIDE SYNTHASE INHIBITION AND ANTIOXIDANTS ON THE DEVELOPMENT OF TOLERANCE BY DIFFERENT OPIOID AGONISTS IN THE RAT LOCUS COERULEUS.

### Effect of chronic treatments with morphine, methadone and fentanyl on concentration-effect curves for ME in rat LC neurons

To evaluate the development of tolerance, concentration-effect curves for the inhibitory effect of ME were performed. It has been reported that the firing rate of LC neurons is elevated in brain slices from opioid-treated rats (Kogan et al., 1992). In this study we attempted to minimize the differences in firing rates among groups by performing concentration-effect curves only in cells that displayed standard spontaneous firing rates in the range of 0.4-1.5 Hz (mean ± SEM: 0.80 ± 0.02 Hz, $n$ = 95). This procedure attempted to avoid the possibility that a change in the spontaneous activity of LC cells could influence the quantification of opioid effects. Thus, the firing rate of LC neurons from morphine-, methadone- and fentanyl-treated animals was not different when compared to the corresponding sham groups (Tables 4.1 and 4.2). Morphine treatment (200 mg/kg, s.c., 72 h) induced a strong degree of tolerance in the LC, which was revealed by a substantial rightward shift in the concentration-effect curves for ME and an increase in the $EC_{50}$ of about 4 fold, as compared to the corresponding sham group ($p$ < 0.005) (Figs. 4.9A and 4.10A; Table 4.2). Similarly, chronic treatment with methadone (60 mg/kg/day, s.c., 6 days) induced a rightward shift in the concentration-effect curves for ME and increased by about 2 fold the $EC_{50}$ value when compared to the corresponding sham group ($p$ < 0.005) (Figs. 4.9B and 4.10B; Table 4.2). Finally, chronic treatment with fentanyl (0.2 mg/kg/day, s.c., 7 days) also caused a rightward shift in the concentration-effect curves for ME with an increase of the $EC_{50}$ of about 3 fold, as compared to the corresponding sham group ($p$ < 0.005) (Figs. 4.9B and 4.10C; Table 4.2). These results indicate that morphine, methadone and fentanyl induce different degrees of tolerance to the inhibitory effect of ME in LC neurons. In all groups, the maximal effect of ME was 100% of baseline, which corresponded with an absolute inhibition from the basal firing rate.

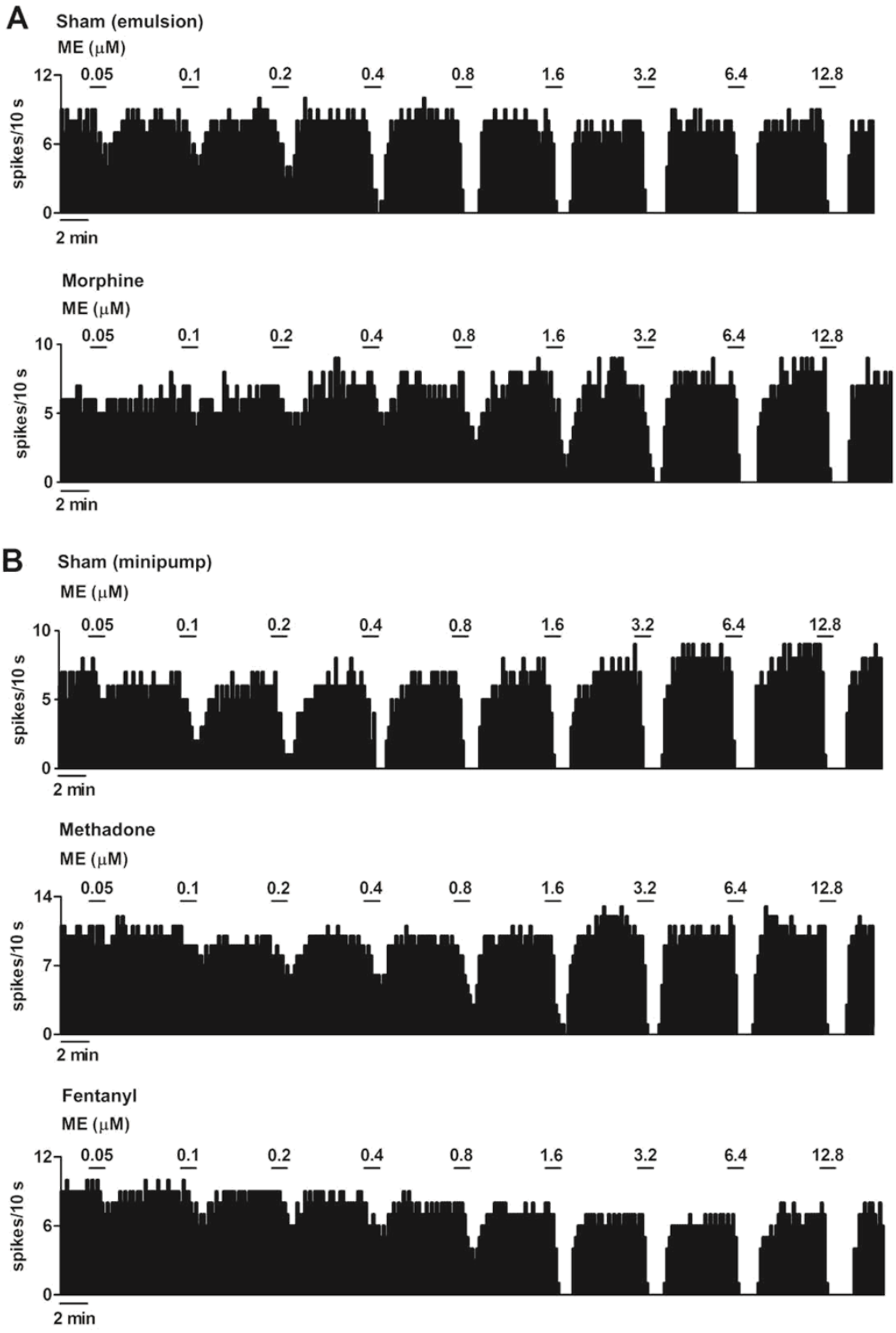
A
Sham (emulsion)
ME (μM)
0.05
0.1
0.2
0.4
0.8
1.6
3.2
6.4
12.8
spikes/10 s
12
6
0
2 min
Morphine
ME (μM)
0.05
0.1
0.2
0.4
0.8
1.6
3.2
6.4
12.8
spikes/10 s
10
5
0
2 min
B
Sham (minipump)
ME (μM)
0.05
0.1
0.2
0.4
0.8
1.6
3.2
6.4
12.8
spikes/10 s
10
5
0
2 min
Methadone
ME (μM)
0.05
0.1
0.2
0.4
0.8
1.6
3.2
6.4
12.8
spikes/10 s
14
7
0
2 min
Fentanyl
ME (μM)
0.05
0.1
0.2
0.4
0.8
1.6
3.2
6.4
12.8
spikes/10 s
12
6
0
2 min

**Figure 4.9.** Effect of chronic treatments with morphine, methadone or fentanyl on the acute ME effect in rat LC neurons. Rats were treated for 72 h with a morphine ($n$ = 5) or sham emulsion ($n$ = 5). Another group of animals were treated for 6 days with methadone ($n$ = 7), 7 days with fentanyl ($n$ = 5) or sham ($n$ = 5) minipumps. **A, B**. Representative examples of firing-rate recording of LC cells from rats receiving the following treatments: sham (emulsion) or morphine (**A**), sham (minipump), methadone or fentanyl (**B**). Each horizontal bar represents the period of application of each ME concentration (0.05 - 12.8 μM, 2x) and the vertical lines show the number of spikes recorded every 10 s. The inhibitory effect induced by each application was calculated as a percentage from the basal firing rate. Note that greater concentrations of ME are needed to inhibit the neuron activity in rats treated with morphine, methadone and fentanyl, compared with sham animals, indicative of tolerance.

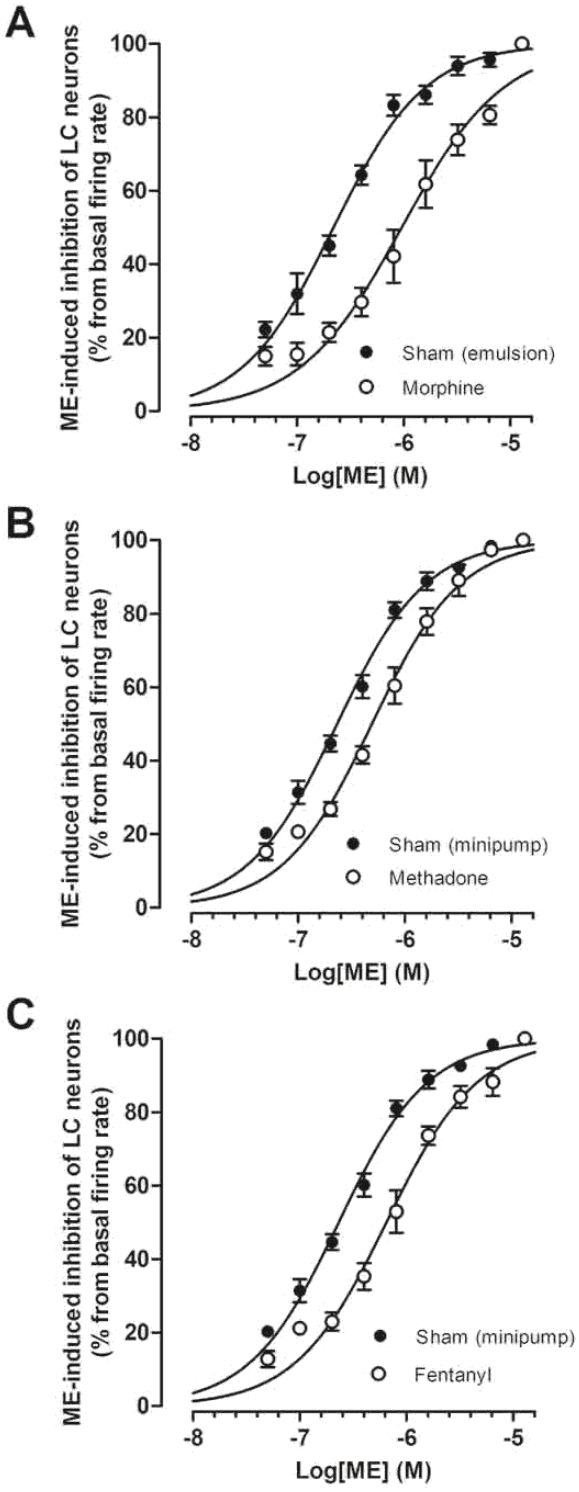
A
ME-induced inhibition of LC neurons
(% from basal firing rate)
100
80
60
40
20
0
-8
-7
-6
-5
Log[ME] (M)
Sham (emulsion)
Morphine
B
ME-induced inhibition of LC neurons
(% from basal firing rate)
Log[ME] (M)
Sham (minipump)
Methadone
C
ME-induced inhibition of LC neurons
(% from basal firing rate)
Log[ME] (M)
Sham (minipump)
Fentanyl

**Figure 4.10.** Concentration-effect curves for the inhibitory effect of ME in LC neurons from rats treated chronically with morphine, methadone or fentanyl. Rats were treated for 72 h with a morphine ($n$ = 5) or sham emulsion ($n$ = 5). Another group of animals were treated for 6 days with methadone ($n$ = 7), 7 days with fentanyl ($n$ = 5) or sham ($n$ = 5) minipumps. **A, B, C**. Concentration-effect curves for the inhibitory effect of ME in LC neurons from rats receiving morphine (**A**), methadone (**B**), fentanyl (**C**) or sham treatment. The horizontal axis represents the logarithms of ME concentrations (0.05 - 12.8 μM, 2x) in linear scale. The vertical axis expresses the reduction in the firing rate of LC neurons as a percentage from the basal firing rate. Symbols are the mean ± SEM of ME effect at each concentration obtained from *n* animals. The lines through the data are the theoretical curves in each group constructed from the mean of the individual concentration-effect curve parameters, as estimated by nonlinear regressions (see Materials and Methods for details and Table 4.2 for mean values). Note that administration of morphine, methadone or fentanyl induces a shift to the right of the ME curves, representative of tolerance. In all groups, the maximal effect of ME was 100% of baseline, which corresponded with an absolute inhibition from the basal firing rate.

## Effect of the nNOS inhibitor 7-NI on opioid tolerance in rat LC neurons

*In vivo* administration of the nNOS inhibitor 7-NI has been shown to attenueate the development of cellular tolerance in LC neurons from morphine-treated rats (Santamarta et al., 2005). Herein, we tested the effect of 7-NI on the tolerance induced by chronic treatments with other opioid agonists such as methadone and fentanyl. Co-administration of 7-NI in methadone- and fentanyl-treated rats (methadone/7-NI group and fentanyl/7-NI group) failed to prevent the development of tolerance. Thus, the $pEC_{50}$ values of concentration-effect curves for ME in the methadone/7-NI or fentanyl/7-NI group were statistically lower than those in the corresponding sham group ($p < 0.005$ *vs* sham/7-NI; in both cases), but they were not different from the corresponding vehicle groups (i.e., *vs* methadone/vehicle and fentanyl/vehicle) (Fig. 4.11; Table 4.1). 7-NI administration in sham-treated animals (sham/7-NI group) did not modify the concentration-effect curves for ME in the LC as compared to the sham-vehicle group (Fig. 4.11; Table 4.1). No differences were found in the basal firing rate among groups (Table 4.1). Therefore, unlike morphine (Santamarta et al., 2005), the neuronal NOS inhibitor 7-NI fails to affect the development of opioid tolerance after methadone or fentanyl treatments.

**Table 4.1. Effect of 7-nitroindazole (7-NI) on the basal firing rate and the inhibition induced by ME in the LC of sham- and opioid-treated rats.**

| | | Concentration-effect curves[2] | | | |
|---|---|---|---|---|---|
| **Treatment groups[1]** | **Basal firing rate (Hz)** | **$pEC_{50}$ (M)** | **($EC_{50}$, µM)** | **Slope factor** | **n** |
| Sham (minipump) | | | | | |
| Vehicle (peanut oil) | 0.74 ± 0.03 | 6.66 ± 0.03 | (0.22) | 1.15 ± 0.07 | 5 |
| 7-NI | 0.69 ± 0.06 | 6.84 ± 0.04 | (0.15) | 0.93 ± 0.07 | 5 |
| Methadone | | | | | |
| Vehicle (peanut oil) | 0.75 ± 0.06 | 6.29 ± 0.09* | (0.52) | 0.96 ± 0.03 | 5 |
| 7-NI | 0.57 ± 0.02 | 6.43 ± 0.04* | (0.37) | 1.02 ± 0.13 | 5 |
| Fentanyl | | | | | |
| Vehicle (peanut oil) | 0.96 ± 0.08 | 6.23 ± 0.05* | (0.58) | 1.03 ± 0.09 | 6 |
| 7-NI | 0.82 ± 0.10 | 6.38 ± 0.05* | (0.42) | 0.97 ± 0.04 | 5 |

[1]Animals were co-treated for 6 days with methadone or 7 days with fentanyl by an osmotic minipump and 7-NI injections (methadone/7-NI group, fentanyl/7-NI group), or with their vehicles (sham/vehicle group, sham/7-NI group, methadone/vehicle group, and fentanyl/vehicle group).

[2]Parameters of concentration-effect curves for ME were estimated in each experiment by nonlinear regression. $pEC_{50}$ values (negative logarithm of the concentration needed to elicit a 50% of maximal effect) and slope factors are shown as mean ± SEM of *n* experiments. Maximal effect values were 100% in all cases. $*p < 0.005$ when compared to the corresponding sham group (one-way ANOVA followed by a post-hoc Tukey's test).

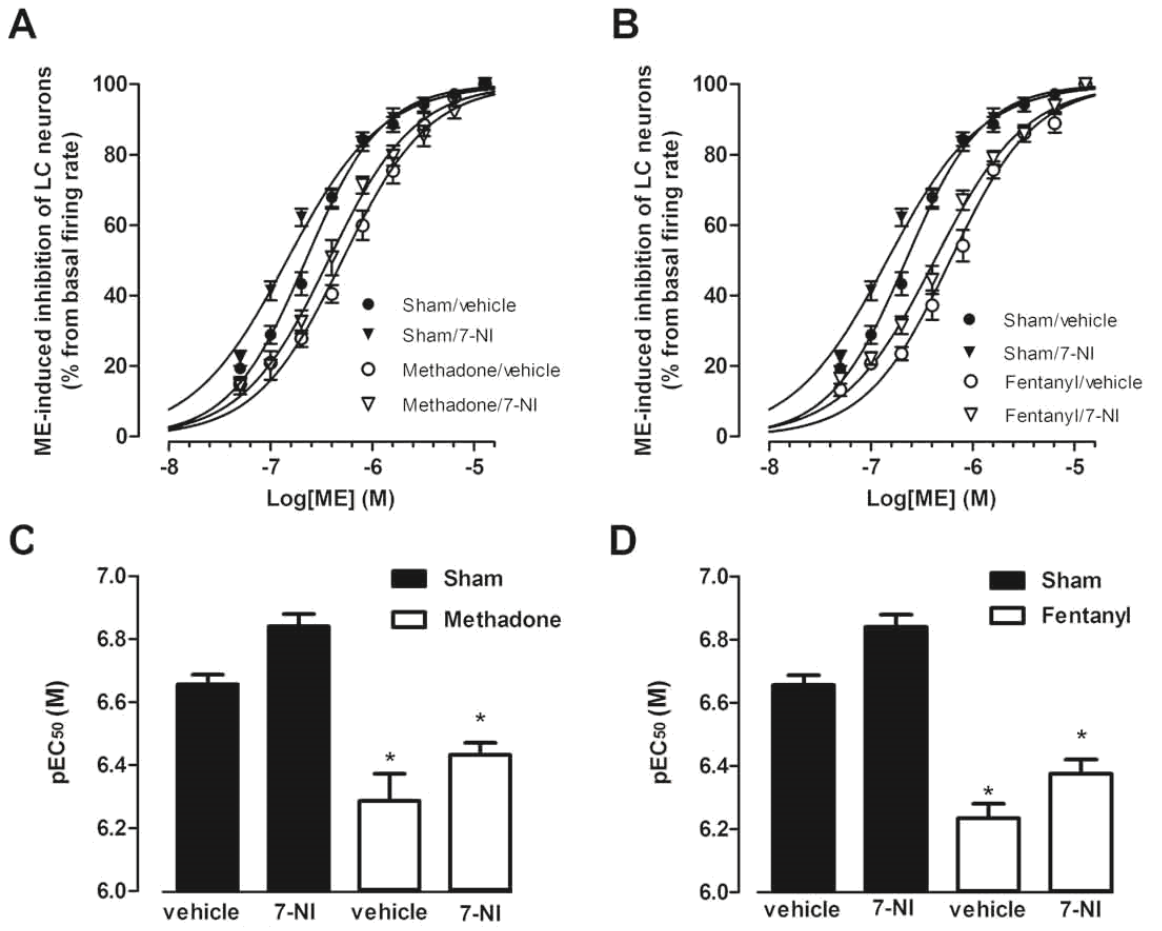


**Figure 4.11.** Effect of 7-nitroindazole (7-NI) on the concentration-effect curves for the inhibitory effect of ME and $pEC_{50}$ values for ME in LC neurons from methadone- and fentanyl-treated rats. Animals were co-treated with methadone or fentanyl minipumps and 7-NI injections for 6 and 7 days, respectively (methadone/7-NI group, $n$ = 5; fentanyl/7-NI group, $n$ = 5) or with their vehicles (sham/vehicle group, $n$ = 5; sham/7-NI group, $n$ = 5; methadone/vehicle group, $n$ = 5 and fentanyl/vehicle group, $n$ = 6). **A, B**. Concentration-effect curves for the inhibitory effect of ME in LC neurons from rats receiving 7-NI together with methadone (**A**), fentanyl (**B**) or sham treatment. The horizontal axis represents the logarithms of ME concentration (0.05 - 12.8 μM, 2x) in linear scale. The vertical axis expresses the reduction in the firing rate of LC neurons as a percentage from the basal firing rate. Symbols are the mean ± SEM at each ME concentration obtained from $n$ rats. The lines through the data are the theoretical curves in each group constructed from the mean of the individual concentration-effect curve parameters, as estimated by nonlinear regressions (see Materials and Methods for details and Table 4.1 for mean values). **C, D**. Ordinate represents $pEC_{50}$ values for ME effect in sham-, methadone- or fentanyl-treated rats. Bars are mean ± S.E.M. of $n$ rats. Note that administration of methadone and fentanyl induces a rightward shift to the right of the ME curves, but co-administration of the nNOS inhibitor 7-NI does not prevent this change. In all groups, the maximal effect of ME was 100% of baseline, which corresponded with an absolute inhibition from the basal firing rate. *$p < 0.005$ when compared to the corresponding sham group (one-way ANOVA followed by a post-hoc Tukey's test).

**Effect of antioxidants on opioid tolerance in rat LC neurons**

Previous results from our group have shown that the co-administration of the free radical scavenger Trolox together with ascorbic acid (TX+AA) blocked partially the development of analgesic tolerance in morphine-treated rats (J. Llorente, Doctoral Thesis, unpublished data). To verify these results with other antioxidants and other opioid agonists, we evaluated the effect of co-administration of TX+AA or U-74389 on the development of tolerance in morphine-, methadone- and fentanyl-treated animals. In agreement with previous results, co-administration of the vitamin E analogue Trolox, together with ascorbic acid in morphine-treated rats (morphine/TX+AA group) attenuated the development of cellular tolerance, which was shown by a blockade of the rightward shift of the concentration-effect curve in this group. Thus, the $pEC_{50}$ value for ME effect in the morphine/TX+AA group did not differ statistically from the value in the sham/TX+AA group, but it was significantly less than that in the morphine/vehicle group ($p < 0.05$), indicating that the blockade of morphine tolerance by TX+AA was complete (Figs. 4.12A and C; Table 4.2). In contrast, TX+AA administration in sham-treated animals (sham/TX+AA) did not modify the concentration-effect curves for ME in the LC, as compared to the sham/vehicle group (Figs. 4.12A and C; Table 4.2). Likewise, co-treatment with U-74389G, a structurally unrelated antioxidant in morphine-treated rats (morphine/U-74389G group), attenuated the development of morphine tolerance, revealed by a blockade of the rightward shift of the concentration-effect curves in this group and an overlap with sham curves, indicating that the blockade was also complete. Hence, the $pEC_{50}$ for ME effect in the morphine/U-74389G group was not different from that in the sham/U-74389G group, but was significantly less than that in the morphine/vehicle group ($p < 0.01$) (Figs. 4.12B and C; Table 4.2). Administration of U-74389G in sham animals (sham/U-74389G) failed to modify the concentration-effect curves for ME when compared to the sham/vehicle group (Figs. 4.12B and C; Table 4.2). Moreover, no differences were found in the basal firing rate among groups (Table 4.2).

**Table 4.2. Effect of antioxidants (Trolox + ascorbic acid and U-74389G) on the basal firing rate and the inhibition induced by ME in the LC of sham- and opioid-treated rats.**

| | | Concentration-effect curves[2] | | | |
|---|---|---|---|---|---|
| **Treatment groups[1]** | **Basal firing rate (Hz)** | **$pEC_{50}$ (M)** | **($EC_{50}$, µM)** | **Slope factor** | **n** |
| Sham (emulsion) | | | | | |
| Vehicle (saline) | 0.87 ± 0.05 | 6.66 ± 0.05 | (0.22) | 1.01 ± 0.05 | 5 |
| TX+AA | 0.71 ± 0.04 | 6.58 ± 0.10 | (0.26) | 1.06 ± 0.06 | 5 |
| U-74389G | 0.72 ± 0.05 | 6.52 ± 0.01 | (0.30) | 1.14 ± 0.05 | 5 |
| Morphine | | | | | |
| Vehicle (saline) | 1.05 ± 0.14 | 6.02 ± 0.10*** | (0.95) | 0.91 ± 0.04 | 5 |
| TX+AA | 0.89 ± 0.09 | 6.41 ± 0.11$^{\dagger}$ | (0.39) | 0.92 ± 0.06 | 5 |
| U-74389G | 0.85 ± 0.06 | 6.42 ± 0.08$^{\dagger\dagger}$ | (0.38) | 1.03 ± 0.09 | 5 |
| Sham (minipump) | | | | | |
| Vehicle (saline) | 0.78 ± 0.04 | 6.64 ± 0.03 | (0.23) | 1.05 ± 0.08 | 5 |
| U-74389G | 0.78 ± 0.03 | 6.58 ± 0.06 | (0.27) | 1.06 ± 0.05 | 5 |
| Methadone | | | | | |
| Vehicle (saline) | 0.81 ± 0.06 | 6.31 ± 0.05*** | (0.49) | 1.05 ± 0.04 | 7 |
| U-74389G | 0.68 ± 0.09 | 6.34 ± 0.04* | (0.45) | 1.16 ± 0.10 | 7 |
| Fentanyl | | | | | |
| Vehicle (saline) | 0.93 ± 0.09 | 6.19 ± 0.03*** | (0.64) | 1.02 ± 0.11 | 5 |
| U-74389G | 0.81 ± 0.09 | 6.19 ± 0.09** | (0.65) | 1.04 ± 0.11 | 5 |

[1]Animals were co-treated for 72 h with a morphine emulsion, for 6 days with methadone and 7 days with fentanyl by an osmotic minipump and Trolox + ascorbic acid or U-74389G injections (morphine/TX+AA group, morphine/U-74389G group, methadone/U-74389G group, fentanyl/U-74389G group), or with their vehicles (sham/vehicle group, sham/TX+AA group, sham/U-74389G group, morphine/vehicle group, methadone/vehicle group and fentanyl/vehicle group).

[2]Parameters of concentration-effect curves for ME were estimated in each experiment by nonlinear regression. $pEC_{50}$ values (negative logarithm of the concentration needed to elicit a 50% of maximal effect) and slope factors are shown as mean ± SEM of *n* experiments. Maximal effect values were 100% in all cases. *$p < 0.05$, **$p < 0.01$ and ***$p < 0.005$ when compared to the corresponding sham group. $^{\dagger}p < 0.05$ and $^{\dagger\dagger}p < 0.01$ when compared to the corresponding vehicle group (one-way ANOVA followed by a post-hoc Tukey's test).

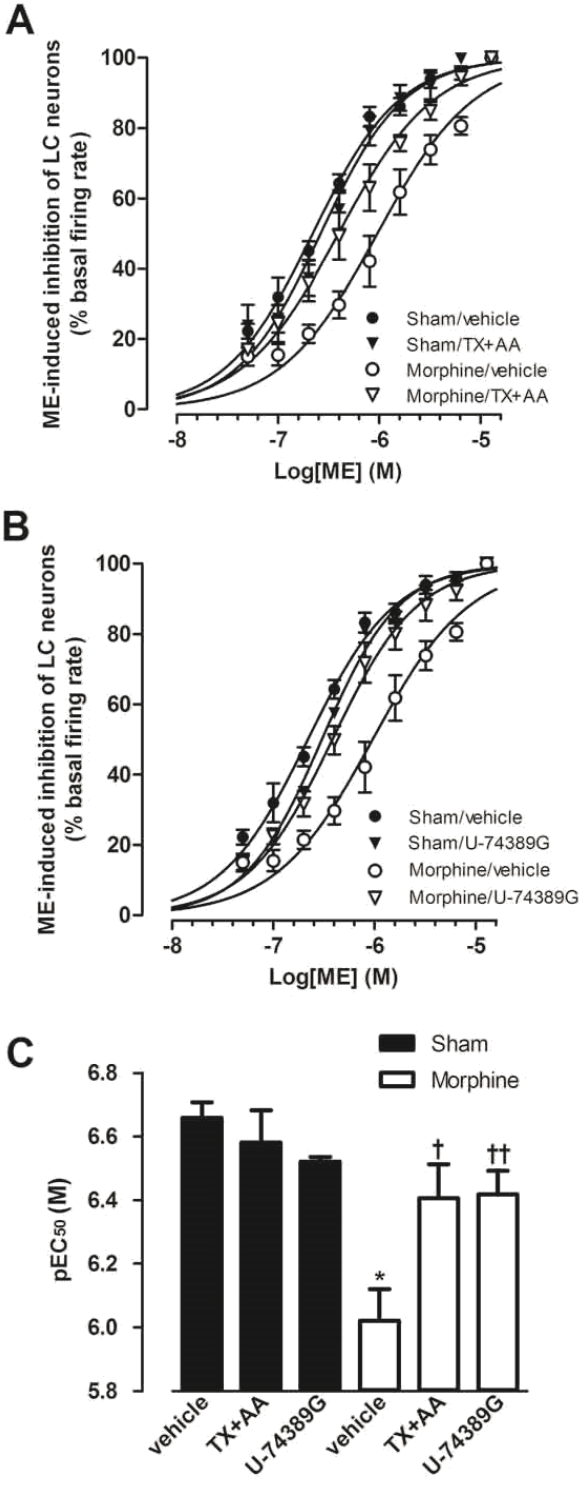
A
ME-induced inhibition of LC neurons
(% basal firing rate)
100
80
60
40
20
0
-8
-7
-6
-5
Log[ME] (M)
Sham/vehicle
Sham/TX+AA
Morphine/vehicle
Morphine/TX+AA
B
ME-induced inhibition of LC neurons
(% basal firing rate)
Log[ME] (M)
Sham/vehicle
Sham/U-74389G
Morphine/vehicle
Morphine/U-74389G
C
Sham
Morphine
pEC50 (M)
6.8
6.6
6.4
6.2
6.0
5.8
*
†
††
vehicle
TX+AA
U-74389G
vehicle
TX+AA
U-74389G

**Figure 4.12**. Effect of Trolox + ascorbic acid (TX+AA) and U-74389G on the concentration-effect curves for the inhibitory effect of ME and $pEC_{50}$ values for ME in LC neurons from morphine-treated rats. Animals were co-treated for 72 h with a morphine emulsion and TX+AA or U-74389G injections (morphine/TX+AA group, $n$ = 5; morphine/U-74389G group, $n$ = 5) or with their vehicles (sham/vehicle group, $n$ = 5; morphine/vehicle group, $n$ = 5; sham/TX+AA group, $n$ = 5; sham/U-74389G group, $n$ = 5). **A, B**. Concentration-effect curves for the inhibitory effect of ME in LC neurons from morphine-treated rats receiving TX+AA (**A**) or U-74389G (**B**). The horizontal axis represents the logarithms of ME concentration (0.05 - 12.8 μM, 2x) in linear scale. The vertical axis expresses the reduction in the firing rate of LC neurons as a percentage from the basal firing rate. Data points are the mean ± SEM at each ME concentration obtained from $n$ animals. The lines through the data are the theoretical curves in each group constructed from the mean of the individual concentration-effect curve parameters, as estimated by nonlinear regressions (see Materials and Methods for details and Table 4.2 for mean values). **C**. Ordinate represents pEC50 values for ME effect in sham- and morphine-treated animals. Bars are mean ± S.E.M. of $n$ rats. Note that administration of morphine induces a strong shift to the right of the ME curves, and co-administration of antioxidants TX+AA and U-74389G blocks this rightward displacement. In all groups, the maximal effect of ME was 100% of baseline, which corresponded with an absolute inhibition from the basal firing rate. $^{*}p < 0.005$, when compared to the corresponding sham group, $^{\dagger}p < 0.05$ and $^{\dagger\dagger}p < 0.01$, when compared to the vehicle group (one-way ANOVA followed by a post-hoc Tukey's test).

On the contrary, co-treatment with U-74389G in rats treated chronically with methadone or fentanyl (methadone/U-74389G and fentanyl/U-74389G group) did not prevent the development of cellular tolerance induced by these opioids, so that the concentration-effect curves from either methadone/U-74389G or fentanyl/U-74389G group were overlapped with those from their respective vehicle groups (methadone/vehicle and fentanylvehicle, respectively). Thus, the $pEC_{50}$ values for ME effect in the methadone/U-74389G or fentanyl/U-74389G groups were statistically different from the corresponding sham group (sham/ U-74389G; $p < 0.05$ and $p < 0.01$, respectively), but they were not different from the corresponding vehicle groups (methadone/vehicle and fentanyl/vehicle, respectively) (Fig. 4.13; Table 4.2). U-74389G administration in sham animals (sham/U-74389G) failed to modify the concentration-effect curves for ME when compared to the sham/vehicle group (Fig. 4.13; Table 4.2). No differences were found in the basal firing rate among groups (Table 4.2).

Taken together, these data indicate that antioxidants reduce the development of cellular tolerance after morphine, but not methadone or fentanyl, and therefore, ROS seem to be differentially involved in opioid-induced cellular tolerance in the LC.

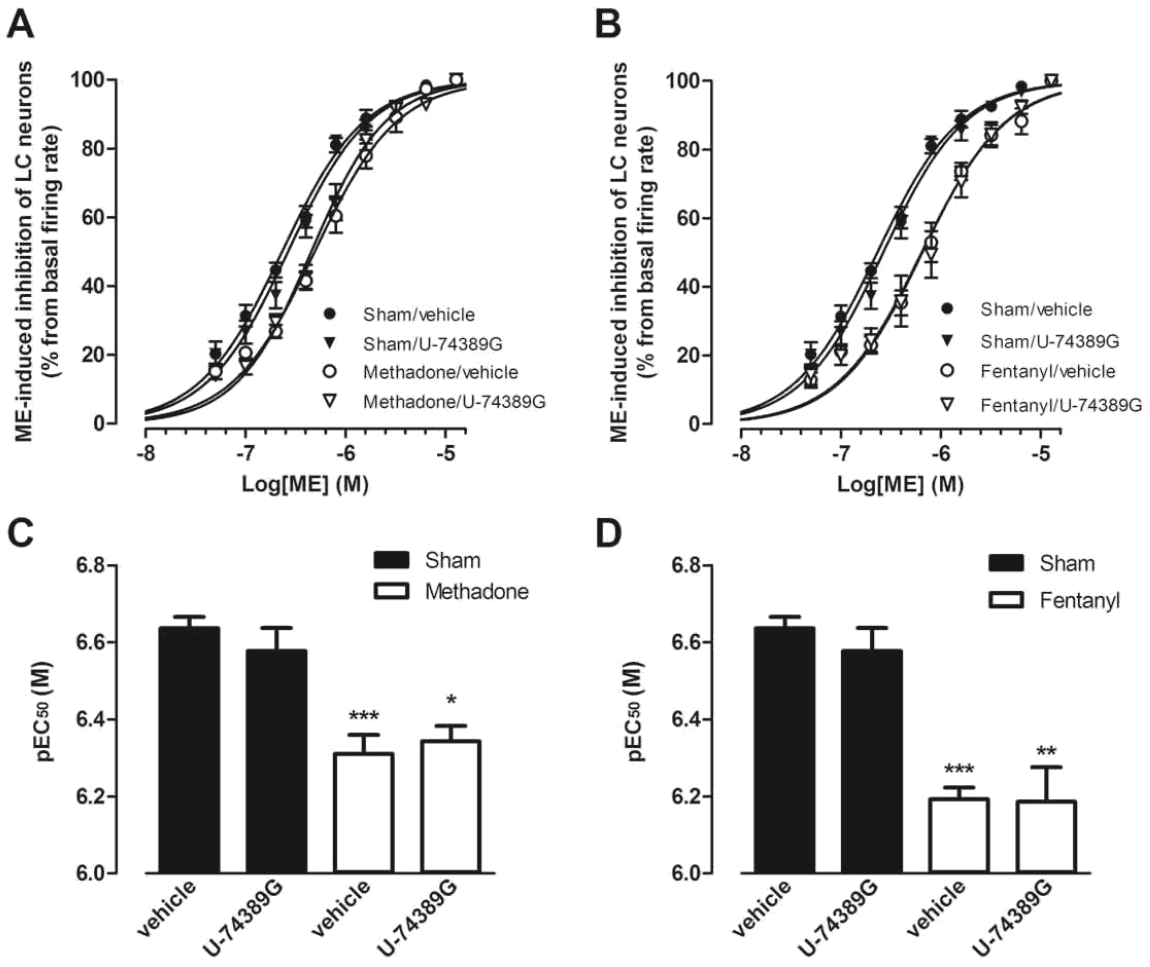


**Figure 4.13.** Effect of U-74389G on the concentration-effect curves for the inhibitory effect of ME and $pEC_{50}$ values for ME in LC neurons from methadone- or fentanyl-treated rats. Animals were co-treated with methadone or fentanyl minipumps for 6 and 7 days, respectively, and U-74389G injections (methadone/U-74389G group, $n$ = 7; fentanyl/U-74389G group, $n$ = 5) or with their vehicles (sham/vehicle group, $n$ = 5; sham/U-74389G group, $n$ = 5; methadone/vehicle group, $n$ = 7 and fentanyl/vehicle group, $n$ = 5). **A, B.** Concentration-effect curves for the inhibitory effect of ME in LC neurons from rats receiving U-74389G together with methadone (**A**), fentanyl (**B**) or sham treatment The horizontal axis represents the logarithms of ME concentration (0.05 - 12.8 μM, 2x) in linear scale. The vertical axis expresses the reduction in the firing rate of LC neurons as a percentage from the basal firing rate. Symbols are the mean ± SEM at each ME concentration obtained from $n$ rats. The lines through the data are the theoretical curves in each group constructed from the mean of the individual concentration-effect curve parameters, as estimated by nonlinear regressions (see Materials and Methods for details and Table 4.2 for mean values). **C, D.** Ordinate represents $pEC_{50}$ values for ME effect in sham-, methadone- and fentanyl-treated rats. Bars are mean ± S.E.M. of $n$ rats. Note that administration of methadone of fentanyl induces a rightward shift to the right of the ME curves, but co-administration of the antioxidant U-74389G does not block this change. In all groups, the maximal effect of ME was 100% of baseline, which corresponded with an absolute inhibition from the basal firing rate. *$p < 0.05$, **$p < 0.01$ and ***$p < 0.005$ when compared to the corresponding sham group (one-way ANOVA followed by a post-hoc Tukey's test).

## 4.4 STUDY 4: ROLE OF NEURONAL NITRIC OXIDE SYNTHASE AND REACTIVE OXYGEN SPECIES IN THE DEVELOPMENT OF ANTINOCICEPTIVE TOLERANCE INDUCED BY DIFFERENT OPIOID AGONISTS

### Development of tolerance for morphine-induced antinociception in morphine-, methadone- and fentanyl-treated animals

In nontreated animals, morphine challenge (10 mg/ kg, i.p.) increased by more than three times the tail-flick latency, which corresponded with an average antinociceptive effect of 98 ± 1% (M.P.E.; basal latency = 2.99 ± 0.05 s; $n$ = 104). To explore the development of opioid analgesic tolerance, the tail-flick test was performed in animals treated with different opioids (morphine, methadone and fentanyl). As expected, before opioid treatments the basal latencies and the antinociceptive effects induced by a challenge dose of morphine were not significantly different between groups.

After morphine treatment, basal latencies were not different between sham (emulsion) and morphine-treated animals (Fig. 4.14A; Table 4.3). Morphine challenge increased by four times the latency in sham animals when compared to the basal latency ($p < 0.005$). In contrast, it failed to change the latency in morphine-treated animals (Fig. 4.14A; Table 4.3). Thus, the analgesic effects induced by morphine challenge were statistically different between sham and morphine-treated animals, so that post-hoc analysis showed that morphine challenge induced a less pronounced analgesic effect in the morphine/vehicle group than it did in the sham/vehicle group ($p < 0.005$) (Fig. 4.14C; Table 4.3), which indicated the development of tolerance.

On the other hand, basal latencies were found to be significantly different between sham (minipump) and methadone-treated rats ($p < 0.005$) (Table 4.4; compare methadone/vehicle *vs* sham/vehicle group). In sham animals, morphine challenge increased by four times the latency ($p < 0.005$ *vs* basal latency) and in methadone-treated rats it increased the latency by two times ($p < 0.005$ *vs* basal latency) (Fig. 4.14B; Table 4.4). The analgesic effects induced by a challenge dose of morphine were significantly different between sham and methadone-treated rats even when the basal latency values were used as a covariate by ANCOVA. Thus, morphine challenge caused a less

antinociceptive effect in the methadone/vehicle group than in the sham/vehicle group, representative of tolerance ($p < 0.005$) (Fig. 4.14C; Table 4.4).

Finally, basal latencies were not significantly different between sham (minipump) and fentanyl-treated rats. The challenge dose of morphine in fentanyl-treated rats increased more than three times the latency when compared to the basal latency ($p < 0.005$). This increase was not different when compared to that in the sham group (Fig. 4.14B; Table 4.4). Hence, the antinociceptive effect of morphine challenge in the fentanyl/vehicle group did not differ from that in the sham/vehicle group (ig. 4.14C; Table 4.4). Therefore, unlike morphine and methadone, this protocol of fentanyl infusion did not induce significant tolerance.

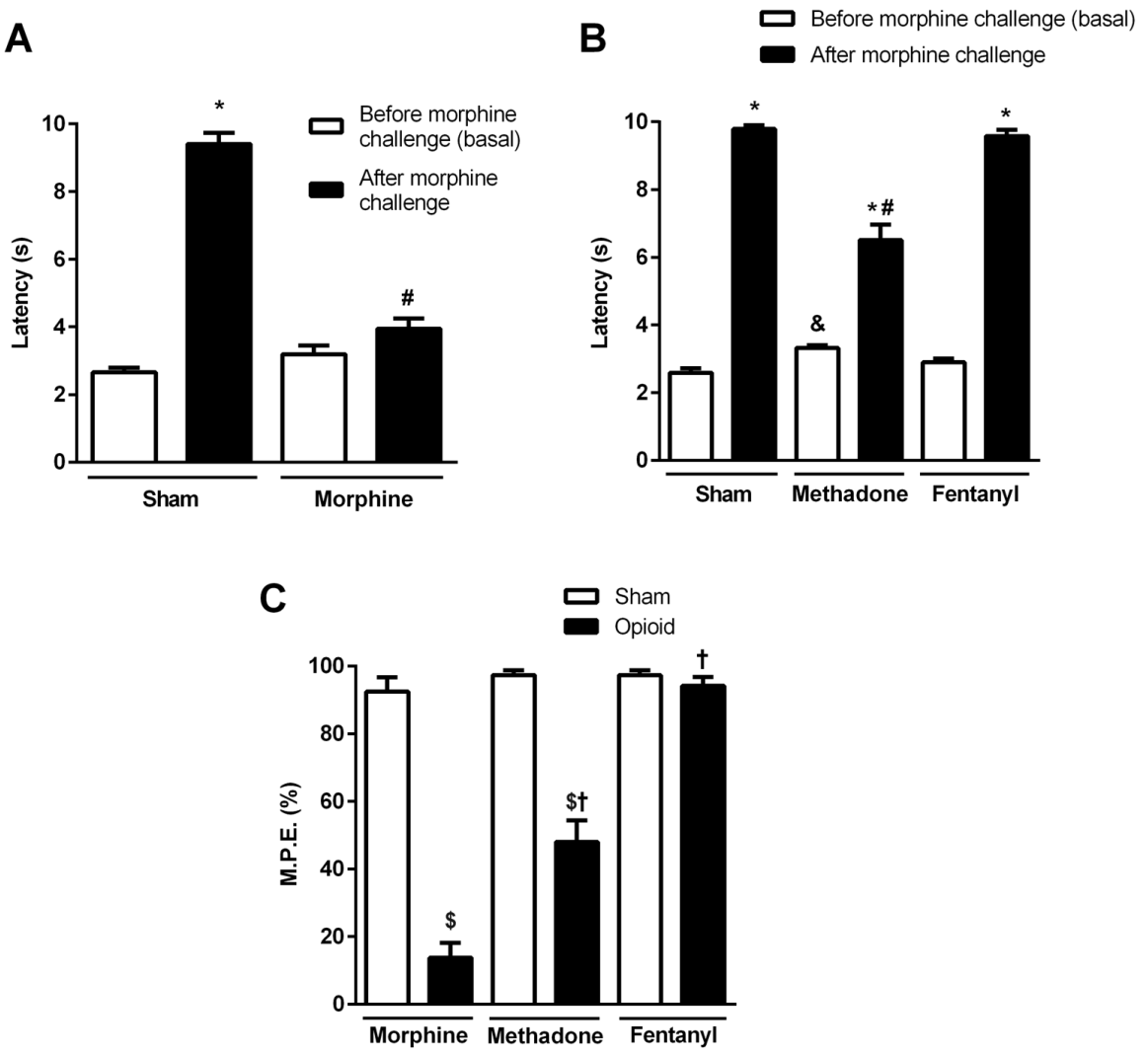


**Figure 4.14.** Development of tolerance for morphine-induced antinociception in morphine-, methadone- and fentanyl-treated animals. **A, B.** Bar histograms show the mean ± S.E.M of the latency before (basal) and after a challenge dose of morphine in sham (emulsion) ($n$ = 10), sham (minipump) ($n$ = 10), morphine- ($n$ = 9), methadone- ($n$ = 9) and fentanyl-treated animals ($n$ = 6). Basal latencies were statistically different between methadone and sham groups $^{\&}p < 0.005$ when compared to the corresponding sham/vehicle group. Note that morphine challenge significantly increased the latency in sham-, methadone- and fentanyl-treated rats, but not in morphine-treated animals. $^{*}p < 0.005$ when compared to the corresponding basal latency by a paired Student's t test, and $^{\#}p < 0.005$, when compared to the corresponding sham group by two-sample Student's t test. **C.** Bar histograms represent the mean ± S.E.M of the maximum possible effect (M.P.E.) in sham (emulsion) ($n$ = 10), sham (minipump) ($n$ = 10) morphine- ($n$ = 9), methadone- ($n$ = 9) and fentanyl-treated animals ($n$ = 6). Note that morphine and methadone treatments reduce the analgesic effect of morphine challenge, indicative of tolerance. $^{\$}p < 0.005$ when compared to the corresponding sham group by two-sample Student's t test. $^{\dagger}p < 0.005$ when compared to the morphine group by two-sample Student's t test.

**Effect of the antioxidant U-74389G on morphine-induced analgesic tolerance**

We have previously shown that the co-administration of the selective nNOS inhibitor 7-NI prevents the antinociceptive tolerance induced by a subchronic morphine treatment (3 days) in rats (Santamarta et al., 2005). Moreover, previous experiments have shown that co-administration of the vitamin E analogue Trolox and ascorbic acid (TX+AA) partially prevents the development of morphine analgesic tolerance (J. Llorente Doctoral Thesis, unpublished results). Likewise, in our work, co-treatment with U-74389G (10 mg/kg/day), a structurally unrelated antioxidant, partially prevented the development of tolerance in morphine-treated rats. Hence, the antinociceptive response of the challenge dose of morphine in the morphine/U-74389G group was significantly greater than that in the morphine/vehicle group ($p < 0.005$), but smaller than that in the corresponding sham group (Fig. 4.15; Table 4.3). On the other hand, subchronic administration of U-74389G in sham-treated animals (sham/U-74389G group) failed to affect the morphine-induced analgesic effect, as compared to the sham/vehicle group (Fig. 4.15; Table 4.3).

**Table 4.3. Effect of U-74389G on the tail-flick latencies and the analgesic response of sham- and morphine-treated rats.**

| Treatment groups[1] | Basal latency (s)[2] | Latency (s)[3] | M.P.E (%)[4] | n |
|---|---|---|---|---|
| Sham (emulsion) | | | | |
| Vehicle (saline) | 2.66 ± 0.14 | 9.41 ± 0.33* | 92.41 ± 4.23 | 10 |
| U-74389G | 2.57 ± 0.14 | 9.93 ± 0.06* | 99.08 ± 0.73 | 7 |
| Morphine | | | | |
| Vehicle (saline) | 3.19 ± 0.26 | 3.94 ± 0.30 | 13.77 ± 4.38$^{\$}$ | 9 |
| U-74389G | 2.80 ± 0.14 | 7.20 ± 0.65* | 61.74 ± 8.85$^{\$\dagger}$ | 8 |

[1]Animals were co-treated for 72 h with a morphine emulsion and U-74389G injections (morphine/U-74389G group), or with their vehicles (sham/vehicle group, sham/U-74389G group and morphine/vehicle group).

[2]Basal latency values refer to the time until tail removal before administration of the morphine challenge. Data are shown as mean ± SEM of n experiments. After chronic treatments, basal latencies were not statistically different between groups.

[3]Latency values refer to the time until tail removal after administration of the morphine challenge. Data are shown as mean ± SEM of n experiments. Latencies were statistically different when compared to basal latencies in all groups except in morphine/vehicle group. $^{*}p < 0.005$ (paired Student's t test).

[4]M.P.E is the percentage of the maximal possible effect (see Materials and Methods). Data are shown as mean ± SEM of n experiments. Note that morphine treatment attenuates the analgesic effect of morphine challenge and co-administration of U-74389G partially blocks this change. $^{\$}p < 0.005$, when compared to the corresponding sham group (ANOVA followed by a post-hoc Tukey's test), $^{\dagger}p < 0.005$ when compared to the corresponding vehicle group (ANOVA followed by a post-hoc Tukey's test).

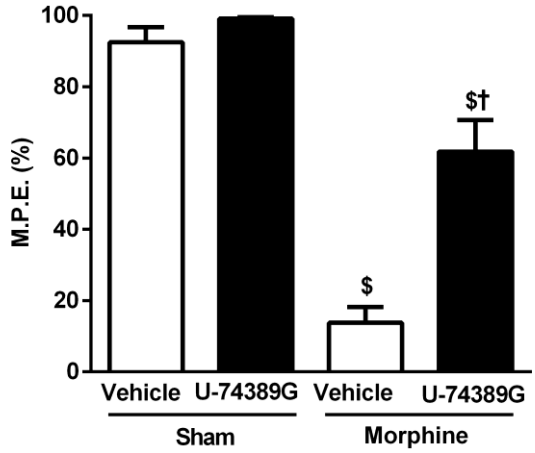


**Figure 4.15.** Effect of U-74389G on the on the antinociception induced by a challenge dose of morphine in sham-, and morphine-treated rats. Bar histograms show the mean ± S.E.M of the maximum possible effect (M.P.E.) in rats co-treated with the morphine emulsion and U-74389G (morphine/U-74389G group, $n$ = 8) or with their vehicles (sham-vehicle group, $n$ = 10; morphine-vehicle group, $n$ = 9; sham/U-74389G group, $n$ = 7). Note that morphine treatment reduces the analgesic effect of morphine challenge and co-administration of U-74389G partially blocks this change. $^{\$}p < 0.005$, as compared to the corresponding sham group; $^{\dagger}p < 0.005$, as compared to the corresponding vehicle group (ANOVA followed by a post-hoc Tukey's test).

## Effect of the neuronal nitric oxide synthase inhibitor 7-NI and the antioxidant U-74389G on methadone-induced analgesic tolerance

To study the role of neuronal NOS in the antinociceptive tolerance induced by other opioid agonists, we tested the effect of 7-NI in the group of rats receiving methadone. As noted above, basal latencies were found to be significantly higher ($p < 0.05$) in methadone/vehicle than in sham/vehicle groups (Table 4.4). However, in animals cotreated with 7-NI, basal latencies were not different between methadone and sham broups. Co-administration of the nNOS inhibitor 7-NI (30 mg/kg/12 h) in rats treated chronically with methadone failed to modify the development of analgesic tolerance, even when the basal latency values were used as a covariate by ANCOVA. Thus, the analgesic effect induced by morphine challenge in the methadone/7-NI group did not differ from that in the methadone/7-NI vehicle group, but it was lower than that in sham/7-NI group (Fig. 4.16A; Table 4.4). Chronic treatment with 7-NI failed to change the morphine challenge-induced effect, as compared the sham/7-NI group with the sham/7-NI vehicle group (Fig. 4.16A; Table 4.4).

To further explore the involvement of ROS, methadone-treated animals were co-treated with the antioxidant U-74389G (10 mg/kg/day). As mentioned, basal latencies were significantly higher in methadone/vehicle than in sham/vehicle groups, but this difference was not significant between methadone and sham animals after co-treatment with U-74389G. Co-treatment with U-74389G in methadone-treated rats failed to modify the development of analgesic tolerance, even when the basal latency values were used as a covariate by ANCOVA. Thus, the analgesic response after a challenge dose of morphine in the methadone/U-74389G group was not different from that in the methadone/U-74389G vehicle group, but it was lower than that in sham/U-74389G group (Fig. 4.16B; Table 4.4). Chronic treatment with U-74389G failed to affect the morphine challenge-induced analgesic effect, as compared the sham/ U-74389G group with the sham/ U-74389G vehicle group (Fig. 4.16B; Table 4.4).

Taken together, these data indicate that NO/ROS pathways play a key role in the development of morphine-, but not methadone-induced analgesic tolerance and therefore, these pathways seem to be differentially involved in opioid-induced analgesic tolerance *in vivo*.

**Table 4.4. Effect of 7-nitroindazole (7-NI) and U-74389G on the tail-flick latencies and the analgesic response of sham and methadone-treated rats.**

| Treatment groups[1] | Basal latency (s)[2] | Latency (s)[3] | M.P.E (%)[4] | n |
|---|---|---|---|---|
| Sham (minipump) | | | | |
| 7-NI vehicle (peanut oil) | 2.64 ± 0.14 | 9.87 ± 0.10* | 98.29 ± 1.29 | 7 |
| 7-NI | 2.93 ± 0.14 | 9.74 ± 0.14* | 96.43 ± 2.00 | 7 |
| U-74389G vehicle (saline) | 2.59 ± 0.14 | 9.79 ± 0.11* | 97.31 ± 1.43 | 10 |
| U-74389G | 2.66 ± 0.17 | 9.90 ± 0.06* | 98.75 ± 0.73 | 7 |
| Methadone | | | | |
| 7-NI vehicle (peanut oil) | 3.24 ± 0.07$^{\&}$ | 6.61 ± 0.41* | 49.48 ± 6.40$^{\$}$ | 9 |
| 7-NI | 2.86 ± 0.16 | 5.51 ± 0.61* | 37.77 ± 8.12$^{\$}$ | 8 |
| U-74389G vehicle (saline) | 3.32 ± 0.09$^{\&\&}$ | 6.51 ± 0.45* | 47.98 ± 6.40$^{\$}$ | 9 |
| U-74389G | 3.01 ± 0.07 | 5.99 ± 0.52* | 42.45 ± 7.41$^{\$}$ | 7 |
| Fentanyl | | | | |
| Vehicle (saline) | 2.90 ± 0.11 | 9.58 ± 0.18* | 94.14 ± 2.66 | 6 |

[1]Animals were co-treated for 6 days with methadone by an osmotic minipump and 7-NI or U-74389G injections (methadone/7-NI group, methadone/U-74389G group) or with their vehicles (sham/7-NI vehicle group, sham/U-74389G vehicle group, sham/7-NI group, sham/U-74389G group, methadone/7-NI vehicle group and methadone/U-74389G group). Another group of animals were co-treated for 7 days with fentanyl by an osmotic minipump.

[2]Basal latency values refer to the time until tail removal before administration of the morphine challenge. Data are shown as mean ± SEM of n experiments. After chronic treatments, basal latencies were statistically different between groups. $^{\&}p < 0.05$ and $^{\&\&}p < 0.005$ when compared to the corresponding sham/vehicle group (one-way ANOVA followed by a post-hoc Tukey's test).

[3]Latency values refer to the time until tail removal after administration of the morphine challenge. Data are shown as mean ± SEM of n experiments. Latencies were statistically different when compared to basal latencies in all groups. $^{*}p < 0.005$ (paired Student's t test).

[4]M.P.E is the percentage of the maximal possible effect (see Materials and Methods). Data are shown as mean ± SEM of n experiments. Note that chronic methadone treatment attenuates the analgesic effect of morphine challenge, but co-administration of either 7-NI or U-74389G failed to block this effect, even when the basal latency values were used as a covariate. $^{\$}p < 0.005$ when compared to the corresponding sham group (ANCOVA followed by a post-hoc Tukey's test). Chronic treatment with fentanyl does not alter the analgesic effect of morphine challenge.

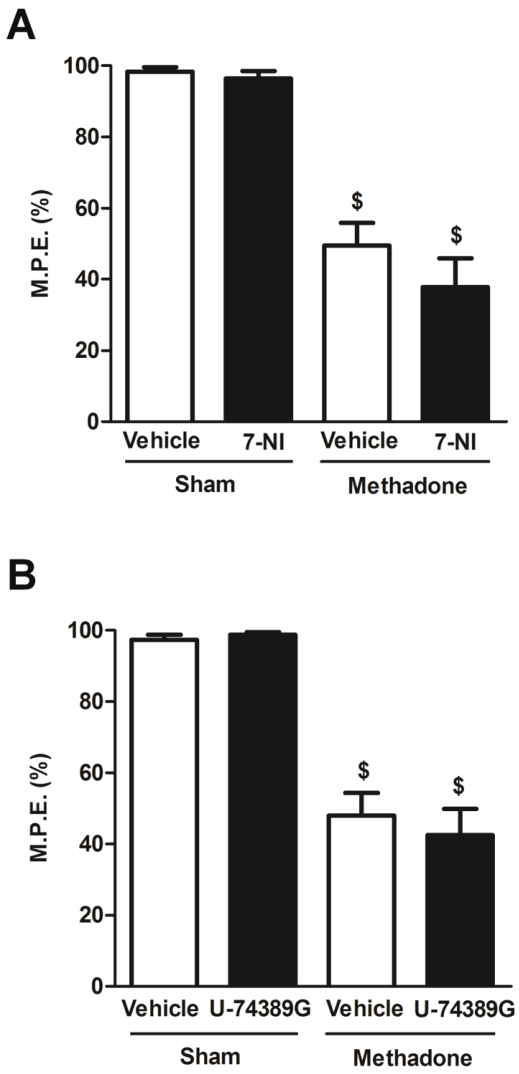


**Figure 4.16.** Effect of 7-NI and U-74389G on the on the antinociception induced by a challenge dose of morphine in sham-, and methadone-treated rats. **A.** Bar histograms show the mean ± S.E.M of the maximum possible effect (M.P.E.) in rats co-treated with methadone and 7-NI (methadone/7-NI group, $n$ = 8) or with their vehicles (sham/vehicle group, $n$ = 7; methadone/vehicle group, $n$ = 9; sham/7-NI group, $n$ = 7). **B.** Bar histograms show the mean ± S.E.M of the maximum possible effect (M.P.E.) in rats co-treated with methadone minipumps and U-74389G (methadone/U-74389G group, $n$ = 7) or with their vehicles (sham/vehicle group, $n$ = 10; methadone/vehicle group, $n$ = 9; sham/U-74389G group, $n$ = 7). Note that chronic methadone treatment reduces the analgesic effect of morphine challenge, but co-administration of either 7-NI or U-74389G fails to block this change. $^{\$}p < 0.005$, as compared to the corresponding sham group (ANCOVA followed by a post-hoc Tukey's test).

# 5. DISCUSSION

## 5.1 STUDY 1: CONTRIBUTION OF NITRIC OXIDE-DEPENDENT GUANYLATE CYCLASE AND REACTIVE OXYGEN SPECIES SIGNALING PATHWAYS TO DESENSITIZATION OF μ-OPIOID RECEPTORS IN THE RAT LOCUS COERULEUS

Previous electrophysiological experiments have shown that NO regulates MOR desensitization in the LC (Torrecilla et al., 2001; Llorente et al., 2012; Santamarta et al., 2014). We have used single-unit extracellular recording techniques in brain slices to characterize the NO-dependent pathways (i.e., sGC and ROS) involved in MOR desensitization in the LC *in vitro*. Our results confirm that ME (3–10 μM) causes a concentration-related desensitization of MOR in the LC, so that the inhibitory effect of ME (0.8 μM) was markedly reduced. ME (3 μM)-induced MOR desensitization was enhanced by perfusion with the NO donor DEA/NO, whereas this enhancement was blocked by the sGC inhibitor NS 2028. Accordingly, ME (3 μM)-induced MOR desensitization was enhanced by two activators of sGC, A 350619 and BAY 418543. In contrast, ME (10 μM)-induced desensitization was not modified by inhibition of sGC with NS 2028 or PKG with Rp-8-Br-PET-cGMP. Perfusion with the antioxidants Trolox, melatonin or U-74389G failed to change ME (10 μM)-induced desensitization, but a combination of an antioxidant (Trolox) with a sGC inhibitor (NS 2028) was able to attenuate ME (10 μM)-induced desensitization.

To study MOR desensitization in the LC, we measured the inhibitory effect of a test concentration of the opioid agonist ME (0.8 μM). ME was used as an indicator of MOR function, because it exerts a full inhibition of the firing activity of LC neurons almost exclusively through MOR (Williams and North, 1984; McPherson et al., 2010). Moreover, ME effect can be tested several times in the same cell, since it rapidly washes out from the tissue after bath perfusion. Therefore, MOR desensitization can be readily measured by extracellular recordings after recovery of the firing from ME-induced inhibition. Our results confirm that sustained application of ME (3 and 10 μM) causes MOR desensitization in the LC, expressed as a concentration-related decline in the test ME effect (30% and 61%, respectively). This protocol including variable desensitization degrees (i.e., by ME 3 and 10 μM) allowed us to investigate possible regulation of this phenomenon by activators or inhibitors of sGC pathway. Similar degrees of MOR desensitization by ME (3 and 10 μM) have been described by both intracellular electrodes

measuring ion currents (Harris and Williams, 1991) and extracellular electrodes recording cell firing rates (Llorente et al., 2012; Santamarta et al., 2014). The firing activity recorded by extracellular techniques may be considered as a closer physiological end-point of MOR desensitization at the synaptic level of the neuron.

ME (3 μM)-induced MOR desensitization was enhanced by 65% in the presence of the NO donor DEA/NO. Likewise, previous electrophysiological experiments *in vitro* have shown that the NO donor sodium nitroprusside also enhances MOR desensitization in the LC (Llorente et al., 2012). The main direct target of NO is the sGC, which catalyzes the production of cGMP from GTP (Kots et al., 2009; Hoffmann and Chen, 2014). The LC has been reported to express the $\alpha_1$ and ß$_1$ subunits of the sGC (Matsuoka et al., 1992; Furuyama et al., 1993; Pifarré et al., 2007) and, accordingly, detectable concentrations of cGMP are measured in the LC (Xu et al., 1998a; Vulliemoz et al., 1999). Herein, ME (3 μM)-induced MOR desensitization in LC neurons was enhanced by ~90% after perfusion with two structurally unrelated sGC activators, A 350619 or BAY 418543. Both activators enhance the catalytic function of sGC in an NO-independent manner, although they can also act synergically with NO (Mayer and Koesling, 2001; Stasch et al. 2002). BAY 418543 lacks any effect on phosphodiesterase activity (Stasch et al., 2002). Accordingly, we found that DEA/NO-induced enhancement of MOR desensitization was prevented by NS 2028, an irreversible inhibitor of NO-dependent sGC activation in homogenates and slice preparations of the brain (Olesen et al., 1998). A high concentration of NO in the LC as that reached during DEA/NO administration could be obtained when nNOS expression is elevated in this nucleus, as described by chronic morphine treatments (Cuéllar et al., 2000). None of the drugs targeting the NO/sGC pathway in the present work (DEA/NO, NS 2028, A 350619 or BAY 418543) altered the acute effects of ME (0.8 μM) (before desensitization). Therefore, our data indicate that activation of sGC signaling can enhance MOR desensitization and also mediate the enhancement of MOR desensitization induced by raising the NO concentration in the LC. Other authors have reported *in vivo* that treatment with sGC activators enhances the development and expression of analgesic tolerance to morphine (Ozdemir et al., 2011) and administration of sGC inhibitors prevents the development of analgesic tolerance to morphine (Xu et al., 1998b; Durmus et al., 2014).

As discussed above, perfusion with high concentrations of ME (10 μM) induce a near-maximal degree of MOR desensitization in the absence of NO enhancers ("high MOR desensitization") (Harris and Williams, 1991; Santamarta et al., 2014). Previous *in vitro* reports have described that lowering the endogenous production of NO by different neuronal-selective NOS inhibitors also attenuates the development of high MOR desensitization in the LC (Torrecilla et al., 2001; Santamarta et al., 2014). Likewise, inhibition of nNOS *in vivo* has been described to reduce the induction of morphine tolerance (Highfield and Grant, 1998; Santamarta et al., 2005) and morphine withdrawal (Pineda et al., 1998) in the LC. A high amount of type II PKG mRNA, one of the main cGMP targets (Kots et al., 2009), has been detected in the LC (El-Husseini et al., 1995). We have previously observed that high MOR desensitization is restored from 7-NI-induced blockade by addition of 8-Br-cGMP (M.T. Santamarta, Doctoral Thesis), a cell permeable cGMP analogue with high potency for type II PKG activation (Pöhler et al., 1995). This suggests that downstream regulation of cGMP/PKG pathway by NO may account for the effect of nNOS inhibitors on high MOR desensitization in the LC. Interestingly, sGC activity and type II PKG expression are up-regulated by morphine treatments in mice (Muraki et al., 1982; Liang and Clarck, 2004) and, therefore, the contribution of cGMP to MOR desensitization mediated by endogenous NO could be functionally relevant *in vivo*. Paradoxically, we did not detect any change in the extent of high MOR desensitization after independent administrations of high concentrations of the sGC inhibitor NS 2028 (10–30 μM) or the PKG inhibitor Rp-8-Br-PET-cGMP (1 μM). These drugs have been previously used as effective inhibitors of cGMP/PKG signaling. Thus, NS 2028 inhibits brain sGC activity *in vitro* with higher potency than ODQ (Garthwaite et al., 1995; Olesen et al., 1998). Rp-8-Br-PET-cGMP is a cell-permeable, potent inhibitor of PKG that shows 300-fold higher selectivities for PKG than for PKA (Smolenski et al., 1998). Similarly, intracerebroventricular administration of the PKG inhibitor KT-5823 fails to alter morphine tolerance *in vivo* (Bernstein and Welch, 1997).

On the other hand, ROS have been reported to regulate MOR desensitization in the LC (Llorente et al., 2012). We found no change in the degree of high MOR desensitization (ME 10 μM) after separate administrations of antioxidant agents (U-74389G, melatonin or Trolox). U-74389G and melatonin are two lipid-soluble antioxidants that protect against the effects induced by ROS (Khalil et al., 1998; Noda et al., 1999; Taherzadeh et al., 2006), whereas Trolox is a cell-permeable vitamin E

derivative that prevents oxidative stress in rat models (Balogh et al., 2005). In contrast, combined administrations of a sGC inhibitor (NS 2028) and an antioxidant agent (Trolox) significantly attenuated the development of high MOR desensitization, whereas they did not affect the acute effect of ME. Therefore, these results indicate that endogenous production of NO from nNOS purportedly caused by high ME concentrations would induce MOR desensitization by independent activation of sGC/PKG and ROS signaling pathways. Either of these cascades would be enough by itself to trigger the induction of high MOR desensitization by endogenous NO, so that both pathways should be simultaneously blocked to observe a reduced desensitization. The mechanism by which NO is generated and the exact NO-dependent events regulated by sGC/PKG and ROS remain as yet to be elucidated. Thus, NO-dependent activation of PKG has been speculated to mediate MOR desensitization by phosphorylating a substrate that affects MOR/G protein interaction or by counteracting the opioid effect on nonselective cation channels (Santamarta et al., 2014). Furthermore, several oxidative mechanisms have been proposed to regulate MOR desensitization, including possible ROS-induced activation of PKC (Llorente et al., 2012).

It has been reported that NO modulates the firing activity of LC neurons by activation of sGC, the subsequent increase of cGMP levels and stimulation of PKG (Xu et al., 1998a; Pineda et al., 1996). Our work demonstrates that DEA/NO elevates by about 100% the firing rate of LC neurons and this excitatory effect is prevented by administration of the sGC inhibitor NS 2028. Furthermore, a 51% elevation of the spontaneous firing rate of LC cells was obtained after sGC stimulation with BAY 418543 and a slight reduction of the firing activity was observed after a combined perfusion with a sGC inhibitor (NS 2028) and an antioxidant (Trolox). Therefore, data obtained from the present work are compatible with an excitatory regulation of the firing activity of LC neurons by NO through the sGC/PKG pathway.

Morphine dependence and withdrawal are associated with neuroadaptive changes in the neuronal NOS activity (Vaupel et al., 1997). During conditions in which nNOS expression is raised (such as during morphine dependence), NO concentrations would be expected to be higher (Cuéllar et al., 2000). Our results demonstrate that submaximal MOR desensitization induced by an intermediate concentration of ME (3 μM) can be enhanced by raising the concentrations of NO and by activating the sGC in the LC. NO-induced enhancement appears to be blocked by a sGC inhibitor. Our previous work has

shown that antioxidant agents attenuate the enhancement of MOR desensitization induced by high concentrations of NO in the LC (Llorente et al., 2012). Removal of ROS also prevents the appearance of analgesic tolerance caused by opioids (Muscoli et al., 2007). Therefore, these data indicate that a combined activation of both signaling cascades, cGMP and ROS, may be needed to enhance MOR desensitization by high NO levels in this nucleus, so that inhibition of either of these pathways would disrupt the enhancement induced by NO. On the other hand, strong MOR desensitization obtained by high ME concentrations (10 μM) can be blocked by a combination of an antioxidant and a sGC inhibitor. Therefore, we conclude that endogenous NO derived from nNOS activity may mediate the development of strong MOR desensitization through downstream regulation of independent sGC/PKG and ROS pathways in the LC. Hypothetically, a pharmacological protection against NO-derived cGMP and ROS generation would result in prevention of opiate tolerance and maintaining a better control of pain with chronic opiates.

## 5.2 STUDY 2: STUDY OF THE INVOLVEMENT OF NEURONAL NITRIC OXIDE SYNTHASE IN MORPHINE-INDUCED DESENSITIZATION OF μ-OPIOID RECEPTORS IN THE RAT LOCUS COERULEUS

The ability of morphine to induce rapid MOR desensitization in native LC neurons has been a matter of debate (Alvarez et al., 2002; Bailey et al., 2003, 2009b). In addition, NO has been shown to regulate ME-induced MOR desensitization in the LC *in vitro* (Torrecilla et al., 2001; Llorente et al., 2012; Santamarta et al., 2014) and morphine-induced tolerance in this nucleus *in vivo* (Santamarta et al., 2005). However, the contribution of NO to MOR desensitization induced by non-peptide opioid agonists *in vitro* is unknown. In the present study, we used single-unit extracellular recordings in KCl-excited LC neurons from rat brain slices to characterize the desensitization of MOR induced by morphine and ME. We further explored the involvement of the neuronal NOS isoform in acute MOR desensitization. Our results show that morphine (30 μM) causes significant desensitization of MOR in the LC, so that the inhibitory effect of a supramaximal test concentration of ME (25.6 μM, applied before and after, or during the opioid perfusion) was markedly reduced. As expected, ME (10 μM) also induced substantial desensitization of MOR, since the inhibitory effect of ME (0.8 or 25.6 μM) was diminished. The inhibitory effect of GABA (1 mM) was unaltered after application of either ME (10 μM) or morphine (30 μM). Perfusion with a combination of two selective nNOS inhibitors (7-NI and SMTC) attenuated the induction of MOR desensitization induced by ME but, in contrast, it failed to alter the desensitization induced by morphine.

As previously mentioned, to study MOR desensitization, we evoked an excitation of LC neurons with KCl (14 mM). This procedure allows us to continously monitor morphine effects and, at the same time, to assess supramaximal test concentrations of ME by extracellular recording techniques. This would not have been feasible in spontaneously firing LC neurons from brain slices, since morphine would induce a complete inhibition of the firing activity that would not recover to baseline values. Apart from the postsynaptic action, it has been shown that KCl depolarizes nerve terminals, which triggers GABA and glutamate release in slice preparations (Liachenko et al., 1999). To avoid the interference of the KCl-induced glutamate release on MOR desensitization, all the experiments were performed in the presence of D-AP5 and CNQX (NMDA and non-

NMDA glutamate receptor antagonist, respectively), as described by Mendiguren and Pineda (2007). Under these experimental conditions, most of the excitation of LC cells by KCl is due to postsynaptic changes in membrane potassium equilibrium. Thus, we first characterized the acute inhibitory effects of ME and morphine on KCl-excited neurons. Concentration-effect curves showed that morphine has a smaller maximum inhibitory effect ($E_{max}$) than ME, which is consistent with previous studies that have shown that morphine behaves as partial agonist at the MOR in LC neurons (Osborne et al., 2000; Bailey et al., 2003). The $EC_{50}$ value for the inhibitory effect of ME effect in the presence of high $K^+$ was found to be slightly shifted to the right as compared to that from spontaneously firing LC neurons (Santamarta et al., 2005) or by intracellular electrodes under voltage-clamp mode in the LC (Osborne and Williams, 1995). Likewise, the $EC_{50}$ value for morphine in the presence of high $K^+$ is shifted rightward when compared to that reported using intracellular recording techniques in LC neurons (Chiu et al., 1993). This is likely due to a positive DC shift in the potassium equilibrium potential promoted by high concentrations of extracellular $K^+$ and the fact that we are able to follow the effect of ME or morphine at membrane potentials close to the reversal potential for $K^+$ (where GIRK channels show rectification).

To study MOR desensitization in the present study, we measured changes in the inhibitory effect of two test concentrations of the opioid agonist ME (0.8 or 25.6 μM). ME inhibits LC cell activity with high efficacy and almost exclusively through MOR (Williams and North, 1984). Moreover, it rapidly washes out from the slice so that MOR desensitization can be easily measured by extracellular recordings once the firing recovers from ME-induced inhibition. The use of an intermediate concentration of ME (0.8 μM), close to the $EC_{50}$ value, allowed us to detect any minimal change in the sensitivity of MOR associated with ME-induced desensitization. On the contrary, application of a supramaximal test concentration of ME (25.6 μM) made it possible to study reductions in the maximal activity of MOR associated with ME-induced desensitization (Osborne and Williams, 1995). In the case of morphine, as a concentration of 30 μM produces near maximal receptor occupancy, we had to use the supramaximal test concentration of ME (25.6 μM) to measure maximal activity of MOR, overcoming morphine's slow rate of receptor dissociation in the slice preparation.

As expected, ME (10 μM) strongly desensitized the inhibition induced by a test application of ME (0.8 μM). This degree of desensitization was found to be similar to that

reported in spontaneously firing LC neurons (Llorente et al., 2012; Santamarta et al., 2014). In addition, ME (10 μM) desensitized the inhibition induced by a supramaximal concentration of ME (25.6 μM), applied before and after the opioid perfusion. However, this degree of desensitization was less strong than that quantified by ME (0.8 μM), as a supramaximal test concentration is less sensitive to detect changes in MOR responsiveness associated with desensitization. Finally, the inhibitory effect of ME (25.6 μM), applied at two times during ME (10 μM, 10 min) administration, was also desensitized to a similar extent to that observed when the ME test was applied before and after.

On the other hand, morphine caused significant MOR desensitization, since the effect of ME (25.6 μM), applied before and after morphine (30 μM) perfusion, was significantly reduced. In fact, the degree of desensitization induced by morphine was stronger than that induced by ME under the same experimental design. This is likely because MOR signaling starts recovering once the sustained perfusion of ME finishes, whereas it does not recover for a long time after morphine perfusion. Likewise, morphine (30 μM) desensitized the inhibitory effect of ME (25.6 μM), when it was tested at two times during the opioid perfusion. Interestingly, the degree of desensitization induced by morphine using the latter protocol was not different from that induced by ME. This finding seems to contradict previous electrophysiological experiments that showed that morphine induces significantly weaker MOR desensitization than higher efficacy opioid agonists such as ME in LC neurons *in vitro* (Alvarez et al., 2002; Bailey et al., 2003). Interestingly, these authors have reported that morphine-induced desensitization is enhanced by concomitant activation of PKC (Bailey et al., 2004; Arttamangkul et al., 2015). In our assays, high $K^+$ concentration may facilitate calcium entry through voltage-dependent calcium channels (Meier et al., 1988), which has been shown to elevate PKC activity in different systems (Sakai et al., 1997; Dupont et al., 2000; Ratz and Miner, 2009). Other kinases such as CaMKII have been also reported to negatively regulate MOR signaling and to contribute to morphine-induced desensitization, tolerance and dependence (Mestek et al., 1995; Sánchez-Blázquez et al., 2008; Tang et al., 2006; Navidhamidi et al., 2012), with their activity being increased in a calcium-dependent manner (Kim et al., 2000; Song et al., 2010). However, it is unclear if they interact directly or indirectly with MOR in LC neurons (Wang and Wang, 2006; Feng et al., 2011; Arttamangkul et al., 2015). Given that the mean firing rate after KCl (14 mM) was ~4 Hz, we can speculate that these kinases

would be activated during KCl perfusion to a similar extent to that observed in waking animals, since tonic LC discharge rates up to 5 Hz are typically observed during normal waking in rats and monkeys (Foote et al., 1980; Berridge and Waterhouse, 2003).

On the contrary, our results suggest that, even in conditions where increased PKC activity would be expected (high $K^+$), ME-induced desensitization was not found to be stronger than in control tissues. In agreement, a recent study using intracellular recordings in LC neurons has reported that PKC activators do not affect the desensitization induced by a saturating concentration of ME (30 µM), when the test was applied before and after the ME perfusion (Arttamangkul et al., 2015). Finally, we observed that the inhibitory effect of GABA, which was tested as an internal control, was ~100% and was not affected by either morphine or ME perfusion. GABA has been shown to induce stronger inhibitory effects at depolarized than at hyperpolarized membrane potentials on LC neurons (Osmanovic and Shefner, 1990), but these actions are not changed by opioid agonists.

The NO system has been shown to modulate MOR signaling in the LC. We have previously reported that NO enhances ME-induced MOR desensitization (Llorente et al., 2012). Independent administration of 7-NI and SMTC, two structurally unrelated molecules that selectively inhibit the neuronal NOS isoform (Babbedge et al., 1993; Furfine et al., 1994), attenuated ME-induced MOR desensitization in spontaneously firing LC neurons *in vitro* (Santamarta et al., 2014). In the present study, nNOS inhibition by a combined perfusion with 7-NI and SMTC attenuated ME-induced MOR desensitization in KCl-excited LC neurons, which confirms the involvement of nNOS in this process. In addition, NO has been shown to play a critical role in the adaptations induced by chronic morphine administration. Thus, morphine treatment leads to an increased NOS expression in the central nervous system (Cuéllar et al., 2000; Wong et al., 2000). *In vivo* administration of 7-NI prevents the development of tolerance in morphine-treated rats (Santamarta et al., 2005) and reduced the hyperactivity of LC neurons typically found after chronic morphine exposure (Pineda et al., 1998). Morphine-induced analgesic tolerance has been also shown to be attenuated by NO-activated sGC/cGMP-dependent mechanisms (Ozdemir et al., 2011; Durmus et al., 2014) and ROS generation (Muscoli et al., 2007; Batinić-Haberle et al., 2009). Surprisingly, perfusion with the nNOS inhibitors 7-NI and SMTC failed to alter morphine-induced desensitization of MOR *in vitro* in our work. These results suggest that acute inhibition of neuronal NO synthesis does not affect

morphine-induced MOR desensitization *in vitro*, whereas it attenuates the induction of tolerance *in vivo*.

The mechanisms by which nNOS might be differentialy involved in ME-, but not morphine-induced MOR desensitization are unknown. Results obtained in our laboratory have indicated that NO mediates the development of ME-induced MOR desensitization through independent regulation of downstream sGC/PKG and ROS pathways in the LC (see Results, Study 1). One of the most remarkable differences between ME and morphine is that ME causes robust receptor internalization (Arttamangkul et al., 2008; 2012), whereas morphine fails to induce efficient internalization in adult rat LC neurons or HEK293 cells (Finn and Whistler, 2001; Alvarez et al., 2002; Bailey et al., 2003; Arttamangkul et al., 2008). It can be hypothesized that NO might act disrupting reinsertion of internalized receptors back into the plasma membrane, which would agree with the fact that morphine-induced desensitization is unaffected by nNOS inhibitors, since morphine does not promote efficient receptor endocytosis and recycling of the MOR.

On the other hand, the mechanisms by which nNOS inhibitors would attenuate morphine-induced cellular tolerance in LC neurons and morphine-induced analgesic tolerance, without affecting acute desensitization are unclear. One of the possibilities may involve alterations in MOR turnover in LC neurons, which has been suggested to underlie opioid tolerance (Dang and Christie, 2012). Thus, previous results from our group have reported that chronic treatment with morphine leads to a disruption in MOR functional recovery from complete receptor inactivation with β-funaltrexamine in the LC. Our preliminary data indicate that this modification of MOR turnover may be mediated by NO (M.T. Santamarta, Doctoral Thesis, unpublished data). In adition, several events dependent on NO signaling pathways have been reported to mediate *in vivo* morphine-induced antinociceptive tolerance, including glutamatergic activation (Sánchez-Blázquez et al., 2013), neuronal apoptosis (Bonfoco et al, 1995) or glial activation and induction of proinflammatory processes (Little et al., 2013). Thus, nNOS inhibitors could alleviate morphine tolerance *in vivo* by attenuating some of these processes, without altering morphine-induced desensitization.

In conclusion, the present study shows that morphine and ME induce acute MOR desensitization in LC neurons. On the basis of previous studies, we can hypothesize that

morphine-induced desensitization could be mediated by high firing rate-dependent activation of PKC and/or CaMKII, to a similar extent as *in vivo*, but the exact mechanism has yet to be determined. Selective nNOS inhibition attenuates the induction of MOR desensitization by the opioid agonist ME, but it failed to alter the desensitization promoted by morphine. These results highlight the agonist-selective acute regulation of MOR by nNOS. Further studies are needed to investigate the underlying mechanisms.

## 5.3 STUDY 3: EFFECT OF NEURONAL NITRIC OXIDE SYNTHASE INHIBITION AND ANTIOXIDANTS ON THE DEVELOPMENT OF TOLERANCE BY DIFFERENT OPIOID AGONISTS IN THE RAT LOCUS COERULEUS

The NO system has been involved in the underlying mechanisms of acute desensitization of MOR (Torrecilla et al., 2001; Llorente et al., 2012; Santamarta et al., 2014) and in the development of morphine-induced tolerance (Santamarta et al., 2005). The aim of this work was to investigate the role of neuronal NOS and NO-derived ROS in the development of tolerance induced by three different opioid agonists: morphine, methadone and fentanyl. For that purpose, we performed uni-extracellular recordings of LC neurons to test the effect of the nNOS inhibitor 7-NI and the ROS scavengers TX+AA and U-74389G on the induction of tolerance by chronic treatments with these three opioid agonists. Chronic treatments with morphine, methadone and fentanyl resulted in cellular tolerance in LC neurons, which was revealed by a rightward shift of 2-4 fold in the concentration-effect curves for the inhibitory effect of ME. Co-treatment with TX+AA and U-74389G attenuated the tolerance to the electrophysiological effect of ME induced by morphine. On the contrary, co-treatment with 7-NI or with U-74389G failed to modify the cellular tolerance induced by methadone or fentanyl.

It has been described that basal firing rates of LC neurons are significantly higher in slices from morphine-treated animals (Kogan et al., 1992), although they fire at control rates in morphine-treated rats that have been acutely pretreated with 7-NI (Pineda et al., 1998). In the present study, concentration-effect curves for ME were performed only in LC cells that spontaneously fired at slow rates (between 0.4 and 1.5 Hz, as in control animals), to avoid a biased quantification of opioid effects influenced by differences in the spontaneous activity of LC neurons. We used ME as an indicator of MOR function in the LC because it is a potent agonist that acts almost exclusively through MOR (Williams and North, 1984). Furthermore, it rapidly washes out after perfusion, which allows us to characterize the effect easily by extracellular recordings. Morphine tolerance was induced by s.c. implantation of an oily emulsion containing morphine base (200 mg/kg, a single administration, 72 h). These emulsions have been described to provide a slow drug release and prolonged exposure to the opioid (Salem and Hope, 1999). According to the time course described in mice, the emulsion promotes a rise in morphine concentration in

serum 3–12 h after implantation and a gradual clearance of morphine over 4–5 days (Garzón and Sánchez-Blázquez, 2001). In the present study, morphine caused a 4-fold shift to the right in the concentration-effect curves for ME in the LC. This degree of cellular tolerance is comparable to that reported previously in LC neurons *in vitro*, using the same morphine protocol (Santamarta et al., 2005). Likewise, in a previous study in the LC *in vivo*, we reported a 4-fold rightward shift in the morphine dose-effect curves after intraperitoneal administration of morphine hydrochloride solutions (10–100 mg/kg per injection, 15 injections, 5 days) (Pineda et al., 1998). However, Highfield and Grant (1998) implanted several slow-release pellets (75 mg morphine base per pellet, 6 pellets, 6 days) and found a 2-fold rightward shift in the concentration-effect curves for morphine in LC cells.

Chronic treatment with methadone osmotic pumps (60 mg/kg/day, 6 days) caused a 2-fold shift to the right in the concentration-effect curves for ME in the LC. Likewise, Quillinan et al. (2011) observed a 2-fold shift to the right in the concentration-effect curves for ME measured by intracellular recordings in LC cells using the same methadone administration protocol. Methadone has been reported to cause antinociception in the tail flick and hot plate tests with a potency similar to that of morphine when given s.c. to rats (Giusti et al., 1997; He et al., 2009). Furthermore, the peak hyperpolarization caused by methadone (30 μM) is approximately the same as the hyperpolarization induced by morphine (30 μM) measured by extracellular recordings in LC neurons (Alvarez et al., 2002). The dose of methadone that is delivered daily by the pump is comparable to that estimated to be released daily by the morphine emulsion (~66 mg/kg/day), but elicited a less profound degree of cellular tolerance. In behavioral experiments chronic methadone treatment has been also reported to cause a less strong degree of antinociceptive tolerance than morphine when given at equianalgesic doses (Enquist et al., 2012). In our results, morphine treatment exerted a stronger degree of cellular tolerance than methadone in LC neurons (see above). Studies comparing different MOR agonists have found that those that induce robust receptor endocytosis and recycling tend to produce reduced analgesic tolerance and dependence (Whistler et al., 1999). Morphine has a poor ability to promote internalization and recycling of the MOR (Alvarez et al., 2002; Arttamangkul et al., 2008), whereas methadone efficiently internalizes the MOR in different systems (Keith et al., 1998; Alvarez et al., 2002; Celver et al., 2004; Koch et al., 2005; Arttamangkul et al., 2008). In agreement with this

hyphothesis, mice with genetically modified MORs that have the ability to spontanelusly internalize and recycle develop a reduced tolerance to morphine (Kim et al., 2008). Similarly, animals with mutant MORs that show enhanced receptor degradation after endocytosis, developed stronger antinociceptive tolerance after methadone treatment (Enquist et al., 2012).

On the other hand, chronic treatment with fentanyl minipumps (0.2 mg/kg/day, 7 days) resulted in a 3-fold shift to the right in the concentration-effect curves for ME in LC neurons. Fentanyl has been reported to be up to 100 times more potent than morphine at producing analgesia (Vardanyan and Hruby, 2014). Surprisingly, this fentanyl administration protocol did not cause antinociceptive tolerance (see Results, Study 4). Paronis and Holtzman (1992) also observed that fentanyl (0.24 mg/kg/day) infused for 7 days by osmotic pumps failed to induce significant analgesic tolerance in rats. However, fentanyl has been found to induce analgesic tolerance when given at a dose of 0.04 mg/kg (s.c., 4 times a day, 3 days) in mice (Popik et al., 2000) and also at much higher doses, such as 2.4 mg/kg/day (72 h) or 3.2 mg/kg/day (5 days) by subcutaneously implanted pumps in neonatal rats and mice (Raehal and Bohn, 2011; Thornton and Smith, 1997). In our study, fentanyl elicited a weaker degree of cellular tolerance than morphine (see above). As it happens with methadone, fentanyl induces endocytosis and recycling of the MOR (Celver et al., 2004), which was been associated with a less potential to induce tolerance.

Thus, it can be hypothesized that differences between opioids in their ability to induce receptor internalization and recycling may contribute, at least in part, to the different degrees of cellular tolerance observed in this study. In contrast, other studies show that β-arrestin2 knockout mice, in which MOR endocytosis is presumably unpaired, fail to develop both cellular tolerance (Dang et al., 2011) and antinociceptive tolerance after morphine (Bohn et al., 2000), but not after methadone or fentanyl treatments (Raehal and Bohn, 2011). Interistingly, the impaired MOR recycling that was found in wild-type LC neurons from morphine-treated rats was attenuated in β-arrestin2 knockout animals (Quillinan et al., 2011). Thus, β-arrestin2 may disrupt the ability of receptors to recycle after endocytosis, and therefore, contribute to the development of tolerance.

Interactions between the opioid system and the NO cascade have been described in the brain (Pasternak et al., 1995; Sánchez-Blázquez et al., 2013). Thus, NOS activity and

expression in the central nervous system is up-regulated after chronic morphine administration (Machelska et al., 1997; Cuéllar et al., 2000). Previous data from our laboratory have shown that perfusion with non-selective and selective NOS inhibitors attenuates acute MOR desensitization induced by ME in LC cells *in vitro* (Torrecilla et al., 2001; Santamarta et al., 2014). Moreover, the nNOS inhibitor 7-NI attenuates the development of cellular and antinociceptive tolerance in morphine-treated rats (Santamarta et al., 2005). Likewise, nNOS-, but not eNOS-deficient mice, exhibit weak analgesic tolerance to morphine when compared to wild type animals (Heinzen and Pollack, 2004). NOS inhibitors also attenuated the withdrawal-induced hyperactivity of LC cells (Pineda et al., 1998). 7-NI is a heterocyclic compound that hardly distinguishes between nNOS and eNOS in brain homogenate preparations, but it exhibits a marked selectivity for neuronal NOS in intact cell models or *in vivo* (Babbedge et al., 1993; Hobbs et al., 1999), which is likely due to specific targets of 7-NI that are only present in neurons (Alderton et al., 2001; Handy and Moore, 1998). NO reacts with oxygen derivatives to produce ROS, such as the powerful oxidant peroxynitrite (Davis, 2001). ROS have been reported to regulate MOR desensitization in the LC (Llorente et al., 2012). In this study, we found that TX+AA (40 and 100 mg/kg/day, respectively, i.p.) and U-74389G (10 mg/kg/day, i.p.), attenuated morphine-induced cellular tolerance to the inhibitory effect of ME on LC neurons. Trolox is a cell-permeable vitamin E derivative with powerful antioxidant properties (Balogh et al., 2005). Ascorbic acid is a potent antioxidant and ROS chelator by itself, but we used it as a Trolox recycler from oxidation (Guo and Packer, 2000). Vitamin E (40 mg/kg) and ascorbic acid (100 mg/kg) are effective in preventing oxidative damage in the rat brain (Delwing et al., 2005). U-74389G is a 21-aminosteroid that potently inhibits ROS-mediated peroxidation and it has been shown to reduce cerebral superoxide anion concentration following brain injury (Villa and Gorini, 1997; Fabian et al., 1998). Similarly, TX+AA and U-74389G have been shown to block partially the development of antinociceptive tolerance induced by morphine (see Results, Study 4). In agreement, other ROS scavengers such as melatonin (Raghavendra and Kulkarni, 2000), alpha-lipoic acid (Abdel-Zaher et al., 2013) or metalloporphyrins (Muscoli et al., 2007; Batinić-Haberle et al., 2009) attenuate the development of morphine-induced antinociceptive tolerance.

The mechanisms by which NO modulates morphine-induced tolerance via ROS generation remain unclear. One possible mechanism might be ROS-mediated activation

of PKC. Opioids can induce a sustained increase in ROS (Koch et al., 2009) and PKC can be activated by raising the concentrations of ROS (Palumbo et al., 1992; Knapp and Klann, 2002). In the LC, PKC-induced phosphorylation enhances MOR desensitization induced by morphine without changing $\alpha_2$-adrenoceptor desensitization (Bailey et al., 2004). There is also good evidence that PKC-dependent mechanisms play a significant role in the development of morphine analgesic tolerance (Zeitz et al., 2001; Smith et al., 2003; Newton et al., 2007). Molecular data have reported that in brain areas such as the PAG, morphine-activated MOR increases NO concentrations via the Akt-nNOS pathway and activates PKC, which stimulates the activity of NMDARs (Sánchez-Blázquez et al., 2010). This increased NMDAR activity would induce the phosphorylation and uncoupling of MORs via nNOS/CaMKII pathway, which results in the development of morphine analgesic tolerance (Sánchez-Blázquez et al., 2013). Indeed, NMDAR antagonists and nNOS and CaMKII inhibitors attenuate opioid tolerance and withdrawal (Elliott et al., 1994; Herman et al., 1995). Future studies should test this hypothesis and the possible involvement of other kinases such as c-Jun N-terminal kinase (Melief et al., 2010).

Conversely, our results show that 7-NI and antioxidants did not affect the development of tolerance in rats treated chronically with methadone or fentanyl. Similarly, behavioral experiments showed that 7-NI and U-74389G failed to alter the development of antinociceptive tolerance in methadone-treated rats (see Results, Study 3). It has been described that methadone is a weak noncompetitive NMDAR antagonist (Ebert et al., 1998) and might counteract maladaptive changes in glutamate transmission. This might explain, at least in part, the less strong degree of cellular tolerance after methadone treatment and the lack of effects of NO/ROS modulators on methadone-induced tolerance. Methadone and fentanyl may induce cellular tolerance by different mechanisms and cellular pathways from those described for morphine, as they trigger internalization and recycling of the MOR. Further assays should unmask the mechanisms underlying methadone- and fentanyl-induced adaptations. In conclusion, our results show that chronic treatments with morphine, methadone and fentanyl induce different degrees of cellular tolerance in LC neurons. In addition, *in vivo* administration of antioxidant agents attenuates the development of morphine-, but not methadone- or fentanyl-induced cellular tolerance. Therefore, NO/ROS pathways seem to be differentially involved in opioid cellular tolerance. Taken together, our results highlight the interest of a

pharmacological protection against NO-derived ROS generation to attenuate the development of morphine tolerance and maintain a better control of pain.

## 5.4 STUDY 4: ROLE OF NEURONAL NITRIC OXIDE SYNTHASE AND REACTIVE OXYGEN SPECIES IN THE DEVELOPMENT OF ANTINOCICEPTIVE TOLERANCE INDUCED BY DIFFERENT OPIOID AGONISTS

In this study, we evaluated by the tail-flick technique the development of analgesic tolerance after chronic treatments with three different MOR agonists. We present behavioral evidence for a role of NO/ROS pathway in morphine-, but no other opioids-induced antinociceptive tolerance. Thus, morphine and methadone treatments induced tolerance to the antinociceptive effect of a challenge dose of morphine. In contrast, no tolerance to morphine effect was observed in fentanyl-treated animals. Co-administration of the antioxidant U-74389G partially prevented the development of antinociceptive tolerance in morphine-treated animals. On the contrary, co-treatment with neither the nNOS inhibitor 7-NI nor the antioxidant U-74389G affected the development of antinociceptive tolerance in methadone-treated rats.

Morphine tolerance was induced by subcutaneous implantation of an oily emulsion containing morphine base (200 mg/kg, a single administration, 72 h). Morphine base containing emulsions provide a slow drug release and prolonged exposure to the opioid (Salem and Hope, 1999). According to the time course described in treated mice, the oily emulsion promotes a rise in morphine concentration in serum 3–12 h after implantation and a gradual clearance of morphine over 4–5 days (Garzón and Sánchez-Blázquez, 2001). This morphine administration protocol has been reported to efficiently induce both analgesic and cellular tolerance in rats (Santamarta et al., 2005). The degree of tolerance was similar to that observed by Goodchild et al. (2009) who induced tolerance by a s.c. sustained release morphine emulsion (125 mg/kg/day, 2 days) in rats. Likewise, chronic administration of s.c. morphine (10 mg/kg, twice daily, 5 days) showed a similar degree of antinociceptive tolerance in thermal and mechanical test paradigms (Raghavendra et al., 2004).

Chronic treatment with methadone-filled osmotic pumps (60 mg/kg/day, 6 days) induced a less strong degree of tolerance. In agreement, chronic methadone treatment has been reported to cause substantially less antinociceptive tolerance than morphine when given at equianalgesic doses (Enquist et al., 2012). The dose was selected based on

previous studies where cellular tolerance was observed in LC neurons (Quillinan et al., 2011). Methadone has been reported to produce antinociception in the tail flick and hot plate tests with a potency similar to that of morphine when given s.c. to rats (Giusti et al., 1997; He et al., 2009). The dose of methadone that is daily administered by the osmotic pump in the present study is similar to that estimated to be released by the morphine emulsion (~66 mg/kg/day), yet induces a less profound degree of tolerance. Methadone has been found to induce analgesic tolerance at higher doses, such as 96 mg/kg/day (s.c., 5 days) (Raehal and Bohn, 2011) and also at much lower doses, such as 3 mg/kg/day (s.c., 4 days) in mice (Enquist et al., 2012). However, no tolerance was observed with 4 mg/kg (s.c., twice daily, 5 days) (Kim et al., 2008). It has been proposed that the degree of tolerance that an agonist can induce is inversely related to its ability to induce receptor internalization (Whistler et al., 1999). It could be hypothesized that in the present study methadone causes a less strong degree of tolerance because it induces endocytosis and recycling of the MOR, whereas morphine is less effective (Keith et al., 1998; Alvarez et al., 2002; Celver et al., 2004; Koch et al., 2005). Indeed, in an animal model in which the MOR is genetically modified to enhance receptor degradation after endocytosis, mice show a stronger degree of antinociceptive tolerance after methadone treatment (Enquist et al., 2012). In agreement, transgenic mice with genetically modified MORs that have the ability to internalize and recycle develop a reduced tolerance to morphine (Kim et al., 2008).

On the other hand, chronic treatment with fentanyl pumps (0.2 mg/kg/day, 7 days) did not cause antinociceptive tolerance. Fentanyl has been reported to be up to 100 times more potent than morphine as an analgesic (Vardanyan and Hruby, 2014). The dose of fentanyl used in the present study is sufficient to activate the MOR and promote behavioral changes and neuronal adaptations, as it was found to produce locomotor sensitization (Trujillo et al., 2004) and cellular tolerance in LC neurons (see Results, Study 3). In another study, fentanyl (0.24 mg/kg/day) infused for 7 days by osmotic pumps also failed to induce significant analgesic tolerance in rats (Paronis and Holtzman, 1992). However, it was found to cause tolerance when given at a dose of 0.04 mg/kg (s.c., 4 times a day, 3 days) in mice (Popik et al., 2000) and also at much higher doses, such as 2.4 mg/kg/day (72 h) or 3.2 mg/kg/day (5 days) by subcutaneously implanted pumps in neonatal rats and mice (Thornton and Smith, 1997; Raehal and Bohn, 2011). Our results suggest that fentanyl, at doses expected to activate MOR and promote neuronal

adaptations, is resistant to tolerance induction. Fentanyl induces endocytosis and recycling of the MOR (Celver et al., 2004), which was been associated with a less potential to induce tolerance. Furthermore, it could be hypothesized that the absence of antinociceptive tolerance may be the result of other adaptations in the whole animal caused by fentanyl that may counteract the development of cellular tolerance, as observed in LC neurons (see Results, Study 3).

Thus, we propose that the different magnitudes of tolerance among opioid agonists, may be explained, at least in part, by their different abilities to induce receptor internalization and recycling. However, β-arrestin2 knockout mice have been shown to develop attenuated analgesic tolerance to morphine but not to fentanyl or methadone (Bohn et al., 2000, 2002; Raehal and Bohn, 2011), which seems to contradict this hypothesis. Interistingly, Quillinan et al., (2011) showed that in morphine-treated rats recovery from acute ME-induced desensitization and receptor recycling was diminished, an effect that was not present in animals lacking β-arrestin2. Thus, it can be hypothesized that β-arrestin2 may disrupt the ability of receptors to recycle after endocytosis, which would contribute to tolerance development.

Previous studies have implicated the NO system in the adaptations triggered by chronic morphine treatment. Thus, chronic treatment with morphine has been found to increase NOS activity and expression in the brain and spinal cord (Machelska et al., 1997; Bhargava et al., 1998; Cuéllar et al., 2000). Our previous studies show that *in vivo* administration of the nNOS inhibitor 7-NI attenuates the development of cellular and analgesic tolerance in morphine-treated rats (Santamarta et al., 2005). Likewise, at the cellular level, non-selective and selective NOS inhibitors block opioid-induced MOR desensitization *in vitro* (Torrecilla et al., 2001; Santamarta et al., 2014). 7-NI hardly distinguishes between nNOS and eNOS in brain homogenate preparations, but it exhibits a marked selectivity for neuronal NOS in intact cell models (Babbedge et al., 1993), which seems to be due to specific targets of 7-NI that are only present in neurons (Handy and Moore, 1998; Alderton et al., 2001). In agreement, following sustained morphine administration, nNOS-, but not eNOS-deficient mice, exhibit weak analgesic tolerance development when compared to wild type animals (Heinzen and Pollack, 2004). It is well known that NO reacts with oxygen derivatives to produce ROS, such as the powerful oxidant peroxynitrite (Davis, 2001). Previous results obtained in our laboratory have indicated that the vitamin E analogue Trolox and U-74389G separately attenuated the

enhancement of MOR desensitization induced by NO donors in LC neurons (Llorente et al., 2012). Moreover, Trolox, administered together with ascorbic acid (TX+AA), blocked partially the development of antinociceptive tolerance in morphine-treated rats (J Llorente, Doctoral Thesis, unpublished data). Similarly, in the present study U-74389G blocked partially the development of analgesic tolerance induced by a subchronic treatment with morphine and it did not alter the animal pain threshold. The 21-aminosteroid U-74389G, whose molecular structure is unrelated to that of Trolox, potently inhibits ROS-mediated lipid peroxidation and has a strong antioxidant activity (Villa and Gorini, 1997; Fabian et al., 1998). Thus, we can assume that reduction of morphine tolerance by U-74389G is the consequence of prevention of ROS-induced effects. In agreement, targeting peroxynitrite by metalloporphyrins blocks the development of morphine-induced antinociceptive tolerance in mice (Muscoli et al., 2007; Batinić-Haberle et al., 2009). Likewise, antioxidant agents such as melatonin or alpha-lipoic acid have been reported to attenuate the development of morphine tolerance (Raghavendra and Kulkarni, 2000; Abdel-Zaher et al., 2013). Mice lacking NOX1, a major source of ROS formation, exhibited weaker analgesic tolerance induced by repeated administration of morphine than wild type animals (Ibi et al., 2011). NOX2 knockout mice developed antinociceptive tolerance similar to wild type mice after 3 days of continuous morphine, but showed restored morphine analgesia on day six, whereas wild type mice mice continued to develop tolerance (Doyle et al., 2013). In electrophysiological experiments, TX+AA and U-74389G separatedly blocked the development of cellular tolerance in LC neurons from morphine-treated rats (see Results, Study 3).

The mechanisms by which ROS modulate opioid tolerance remain unclear. The potent ROS peroxynitrite has emerged as a pivotal component of opioid antinociceptive tolerance and pain. (Salvemini and Neumann, 2009; Little et al., 2012). Thus, there are some mechanisms by which ROS formation might contribute to opioid tolerance. Peroxynitrite has been shown to alter glutamate homeostasis within the dorsal horn of the spinal cord by the post-translational nitration of key proteins involved in maintaining a normal glutamate balance, such as NMDARs, glutamate transporters or glutamine synthase (Trotti et al., 1996; Zanelli et al., 2000, 2002). Nitration of these proteins by peroxynitrite would lead to a constant potentiation of the glutamatergic system. There is general agreement that dysfunction of the NMDAR/NO pathway is a key component of

nociception. It has been described that morphine activation of MOR increases NO production via the Akt-nNOS pathway and activates PKC, which stimulates the activity of NMDARs (Sánchez-Blázquez et al., 2010). This increased NMDAR activity would induce the phosphorylation and uncoupling of MORs via nNOS/CaMKII pathway, which results in the development of morphine analgesic tolerance (Sánchez-Blázquez et al., 2013). In agreement, NMDAR antagonists and nNOS and CaMKII inhibitors attenuate opioid tolerance and dependence (Elliott et al., 1994; Herman et al., 1995). A second alternative would involve ROS-mediated activation of PKC (Palumbo et al., 1992; Knapp and Klann, 2000). Indeed, morphine tolerance is attenuated by administration of PKC inhibitors, or when PKC expression is reduced (Zeitz et al., 2001; Smith et al., 2003; Newton et al., 2007). A third potential ROS-dependent mechanism underlying tolerance might be glial activation and the consequent induction of proinflammatory processes. Chronic administration of morphine promotes neuroimmune activation as evidenced by activation of spinal cord glial cells and production of proinflammatory cytokines (Song and Zhao, 2001; Watkins et al., 2005, 2007; Zeng et al., 2014). The induction of those proinflammatory molecules would be relevant in the development of morphine tolerance, since the glial modulators propentofylline (Raghavendra et al., 2004), minocycline (Cui et al., 2008) or paeoniflorin (Jiang et al., 2014) attenuate morphine-induced antinociceptive tolerance. The possible mechanisms by which chronic morphine induces glial cell activation and cytokine production are not known, but a role for peroxynitrite as a signaling molecule involved in this process has been reported (Little et al., 2013). Resveratrol, a potent anti-inflammatory and antioxidant molecule, has been reported to attenuate morphine analgesic tolerance by inhibiting microglial activation and down-regulating NMDAR expression in the spinal cord (Han et al., 2014; Tsai et al., 2012). A fourth ROS-related mechanism might involve neuronal cell death, which is present in morphine-induced antinociceptive tolerance (Mao et al., 2002; Sharifipour et al., 2014). Chronic morphine exposure causes apoptosis within the spinal cord dorsal horn (Mao et al., 2002) and increases supraspinal apoptosis in the cortex and amygdala in neonatal rats (Bajic et al., 2013). The mechanisms involved in morphine-induced apoptosis remain unclear, but ROS seem to take part in this process. Thus, low concentrations of peroxynitrite trigger apoptotic death, whereas higher concentrations induce necrosis (Bonfoco et al., 1995; Virág et al., 2003). The nuclear enzyme poly(ADP-ribose) polymerase (PARP) has been shown to contribute to peroxynitrite-induced neuronal cell death in the spinal cord *in vitro* (Scott et al., 2004). Inhibitors of PARP, which is involved

in different paradigms of cell death (Aredia and Scovassi, 2014), prevent the development of morphine antinociceptive tolerance (Mayer et al., 1999).

On the other hand, we show that 7-NI and U-74389G did not affect the development of antinociceptive tolerance in methadone-treated rats. These findings are in agreement with electrophysiological experiments (see Results, Study 3), where 7-NI and U-74389G failed to alter the development of cellular tolerance in LC neurons from methadone-treated rats. These results suggest that the NO system is not involved in methadone-induced adaptations. Methadone has been described to behave as a weak noncompetitive NMDAR antagonist (Ebert et al., 1998). This ability of methadone to antagonize NMDA receptors and counteract maladaptive changes in glutamate transmission might explain, at least in part, the reduced tolerance after methadone treatment and lack of effects of NO/ROS modulators on methadone-induced tolerance. Further studies are needed to unmask the mechanisms underlying methadone-induced adaptations.

In conclusion, our results show that morphine treatment induces a stronger degree of antinociceptive tolerance than methadone in rats, whereas fentanyl was resistant to tolerance induction. In addition, *in vivo* administration of antioxidant agents partially prevents the development of morphine-, but not methadone-induced analgesic tolerance, suggesting that the NO/ROS pathway is differentially involved in opioid antinociceptive tolerance. We provide pharmacological basis for the potential use of antioxidants as useful co-adjuvants in the management of chronic pain to prevent or, at least, attenuate the development of morphine analgesic tolerance.

# 6. CONCLUSIONS

1. NO enhances ME-induced MOR desensitization in LC neurons by a mechanism that is blocked by sGC inhibition and mimicked by sGC activators. Although isolated inhibition of sGC/PKG pathways or ROS generation itself does not affect MOR desensitization in the LC, simultaneous inhibition of both sGC and ROS attenuates MOR desensitization. These results suggest that sGC/cGMP and ROS pathways independently mediate MOR desensitization and underlie the enhancing effect of NO on MOR desensitization in LC neurons.

2. ME and morphine induce acute desensitization of MOR in a model of KCl-evoked excitation of LC neurons *in vitro*, quantified by applying a test concentration of ME either before-after or during the desensitization period. These results contrast with literature reports that do not have shown any morphine-induced MOR desensitization by intracellular or patch-clamp recording techniques.

3. Neuronal NOS inhibitors attenuate ME-, but not morphine-induced MOR desensitization in LC neurons *in vitro*. This suggests a differential role of NO in mediating the acute desensitization of MOR induced by different opioid agonists.

4. Prolonged treatments with morphine, methadone and fentanyl induce a shift of the concentration-effect curves for ME to the right, with an increase of the $EC_{50}$ of 4, 2 and 3 folds, respectively, in LC neurons *in vitro*. This indicates that treatments with MOR agonists with different intrinsic efficacies cause variable degrees of cellular tolerance in LC cells.

5. Co-administration of antioxidants in morphine-treated animals prevents the development of tolerance to ME effects in LC neurons *in vitro*. Conversely, co-treatments with a neuronal NOS inhibitor or antioxidant agents fail to affect the induction of cellular tolerance in methadone- or fentanyl-treated animals. These results indicate a differential involvement of NO/ROS pathways in opioid tolerance *in vivo* after prolonged treatments with morphine, methadone and fentanyl.

6. Prolonged treatments with morphine and methadone cause tolerance to the analgesic effect of morphine, but the degree of tolerance induced by methadone is

weaker than that induced by morphine. On the contrary, no analgesic tolerance is observed after chronic fentanyl treatment. This indicates that MOR agonists with different intrinsic efficacies cause variable degrees of antinociceptive tolerance. Furthermore, the degree of opioid tolerance depends on the response measured, as suggested by the differential results observed with analgesic *vs* electrophysiological techniques (see fifth conclusion).

7. Co-administration of antioxidant agents in morphine-treated animals attenuates the development of tolerance to the antinociceptive effect of a challenge dose of morphine. In contrast, co-treatments with a neuronal NOS inhibitor or an antioxidant agent fail to affect the development of antinociceptive tolerance induced by methadone. These findings suggest that NO/ROS pathways are differentially involved in opioid tolerance, as measured by an *in vivo* function.

**Taken together, these results provide functional data supporting the involvement of neuronal NO and its downstream signaling pathways in the adaptations induced by opioids after acute or chronic exposure. We demonstrate that opioid agonists commonly prescribed in clinics for pain treatment have different profiles with respect to MOR regulation and promote agonist-specific activation of NO-related pathways.**

# 7. REFERENCES

# A

Abdel-Zaher AO, Mostafa MG, Farghaly HS, Hamdy MM, Abdel-Hady RH (2013) Role of oxidative stress and inducible nitric oxide synthase in morphine-induced tolerance and dependence in mice. Effect of alpha-lipoic acid. Behav Brain Res. 247:17–26.

Aghajanian GK, Rasmussen K (1989) Intracellular studies in the facial nucleus illustrating a simple new method for obtaining viable motoneurons in adult-rat brain-slices. Synapse. 3:331–338.

Alderton WK, Cooper CE, Knowles RG (2001) Nitric oxide synthases: structure, function and inhibition. Biochem J. 357:593–615.

Alagarsamy S, Lonart G, Johnson KM (1994) The role of P-type calcium channels in the depolarization-induced activation of nitric oxide synthase in frontal cortex. J Neurochem. 62:400–403.

Alvarez VA, Arttamangkul S, Dang V, Salem A, Whistler JL, Von Zastrow M, Grandy DK, and Williams JT (2002) mu-Opioid receptors: Ligand-dependent activation of potassium conductance, desensitization, and internalization. J Neurosci. 22:5769–5776.

Álvarez-Maubecin V, Garcia-Hernandez F, Williams JT, Van Bocksaele EJ (2000) Functional coupling between neurons and glia. J Neurosci. 20:4091–4098.

Andrade R, Vandermaelen CP, Aghajanian GK (1983) Morphine tolerance and dependence in the locus coeruleus: single cell studies in brain slices. Eur J Pharmacol. 91:161–169.

Andrade R, Aghajanian GK (1984) Locus coeruleus activity *in vitro*: intrinsic regulation by a calcium-dependent potassium conductance but not alpha 2-adrenoceptors. J. Neurosci. 4:161–170.

Anselmi L, Jaramillo I, Palacios M, Huynh J, Sternini C (2013) Ligand-induced μ opioid receptor internalization in enteric neurons following chronic treatment with the opiate fentanyl. J Neurosci Res. 91:854–860.

Arden JR, Segredo V, Wang Z, Lameh J, Sadée W (1995) Phosphorylation and agonist-specific intracellular trafficking of an epitope-tagged mu-opioid receptor expressed in HEK 293 cells. J Neurochem. 65:1636–1645.

Aredia F, Scovassi AI (2014) Poly(ADP-ribose): A signaling molecule in different paradigms of cell death. Biochem Pharmacol. 92:157–163.

Arima J, Kubo C, Ishibashi H, Akaike N (1998) alpha2-adrenoceptor-mediated potassium currents in acutely dissociated rat locus coeruleus neurons. J Physiol. 508:57–66.

Arnold WP, Mittal CK, Katsuki S, Murad F (1977) Nitric oxide activates guanylate cyclase and increases guanosine 3':5'-cyclic monophosphate levels in various tissue preparations. Proc Natl Acad Sci U S A. 74:3203–3207.

Arttamangkul S, Torrecilla M, Kobayashi K, Okano H, and Williams JT (2006) Separation of mu-opioid receptor desensitization and internalization: endogenous receptors in primary neuronal cultures. J Neurosci 26:4118–4125.

Arttamangkul S, Quillinan N, Low MJ, von Zastrow M, Pintar J, Williams JT (2008) Differential activation and trafficking of μ-opioid receptors in brain slices. Mol Pharmacol. 74:972–979.

Arttamangkul S, Lau EK, Lu H-W, and Williams JT (2012) Desensitization and trafficking of mu-opioid receptors in locus coeruleus neurons: Modulation by kinases. Mol Pharmacol. 81:348–355.

Arttamangkul S, Birdsong W, Williams JT (2015) Does PKC activation increase the homologous desensitization of μ opioid receptors? Br J Pharmacol. 172:583–592.

Arvidsson U, Riedl M, Chakrabarti S, Lee JH, Nakano AH, Dado RJ, Loh HH, Law PY, Wessendorf MW, Elde R (1995) Distribution and targeting of a mu-opioid receptor (MOR1) in brain and spinal cord. J Neurosci. 15(5 Pt 1):3328–3341.

Aston-Jones G, Bloom FE (1981) Activity of norepinephrine-containing locus coeruleus neurons in behaving rats anticipates fluctuations in the sleep-waking cycle. J. Neurosci. 1: 876–886.

Aston-Jones G, Cohen JD (2005) An integrative theory of locus coeruleus-norepinephrine function: adaptive gain and optimal performance. Annu Rev Neurosci. 28:403–450.

Aston-Jones G, Ennis M, Pieribone VA, Nickell WT, Shipley MT (1986) The brain nucleus locus coeruleus: restricted afferent control of a broad efferent network. Science 234:734–737.

Aston-Jones G, Shipley MT, Chouvet G, Ennis M, Van BE, Pieribone V, Shiekhattar R, Akaoka H, Drolet G, Astier B (1991) Afferent regulation of locus coeruleus neurons: anatomy, physiology and pharmacology. Prog Brain Res. 88:47–75.

Aston-Jones G, Rajkowski J, Cohen J (1999) Role of locus coeruleus in attention and behavioural flexibility. Biol. Psychiatry 46, 1309–1320.

Aston-Jones G, Zhu Y, Card JP (2004) Numerous GABAergic aferents to locus ceruleus in the pericerulear dendritic zone: Possible interneuronal pool. J Neurosci. 24:2313–2321.

Attramadal H, Arriza JL, Aoki C, Dawson TM, Codina J, Kwatra MM, Snyder SH, Caron MG, Lefkowitz RJ (1992) β-arrestin2, a novel member of the arrestin/β-arrestin gene family. J Biol Chem. 267:17882–17890.

# B

Babbedge RC, Bland-Ward PA, Hart SL, Moore PK (1993) Inhibition of rat cerebellar nitric oxide synthase by 7-nitro indazole and related substituted indazoles. Br J Pharmacol. 110:225–228.

Bailey CP, Couch D, Johnson E, Griffiths K, Kelly E, Henderson G (2003) Mu-opioid receptor desensitization in mature rat neurons: lack of interaction between DAMGO and morphine. J Neurosci. 23:10515–10520.

Bailey CP, Kelly E, Henderson G (2004) Protein kinase C activation enhances morphine-induced rapid desensitization of mu-opioid receptors in mature rat locus ceruleus neurons. Mol Pharmacol. 66:1592–1598.

Bailey CP, Llorente J, Gabra BH, Smith FL, Dewey WL, Kelly E, and Henderson G (2009a) Role of protein kinase C and mu-opioid receptor (MOPr) desensitization in tolerance to morphine in rat locus coeruleus neurons. Eur J Neurosci 29:307–318.

Bailey CP, Oldfield S, Llorente J, Caunt CJ, Teschemacher AG, Roberts L, McArdle CA, Smith FL, Dewey WL, Kelly E, Henderson G (2009b) Involvement of PKC alpha

and G-protein-coupled receptor kinase 2 in agonist-selective desensitization of mu-opioid receptors in mature brain neurons. Br J Pharmacol. 158:157–164.

Bajic D, Commons KG, Soriano SG (2013) Morphine-enhanced apoptosis in selective brain regions of neonatal rats. Int J Dev Neurosci. 31:258–266.

Balogh GT, Vukics K, Könczöl A, Kis-Varga A, Gere A, Fischer J (2005) Nitrone derivatives of trolox as neuroprotective agents. Bioorg Med Chem Lett. 15:3012–3015.

Bates TE, Loesch A, Burnstock, G, Clark JB (1995) Immunocytochemical evidence for a mitochondrially located nitric oxide synthase in brain and liver, Biochem. Biophys. Res. Commun. 213:896–900.

Bates TE, Loesch A, Burnstock G, Clark, JB (1996) Mitochondrial nitric oxide synthase: a ubiquitous regulator of oxidative phosphorylation? Biochem Biophys Res Commun. 218:40–44.

Batinić-Haberle I, Ndengele MM, Cuzzocrea S, Rebouças JS, Spasojević I, Salvemini D (2009) Lipophilicity is a critical parameter that dominates the efficacy of metalloporphyrins in blocking the development of morphine antinociceptive tolerance through peroxynitrite-mediated pathways. Free Radic Biol Med. 46:212–219.

Beckett AH, Casy AF (1954) Synthetic analgesics: stereochemical considerations J. Pharm. Pharmacol. 6:986–999.

Beckman JS (1996) Oxidative damage and tyrosine nitration from peroxynitrite. Chem Res Toxicol. 9:836–844.

Bellamy TC, Wood J, Goodwin DA, Garthwaite J (2000) Rapid desensitization of the nitric oxide receptor, soluble guanylyl cyclase, underlies diversity of cellular cGMP responses. Proc. Natl. Acad. Sci. USA. 97:2928–2933

Bender AT, Beavo JA (2006) Cyclic nucleotide phosphodiesterases: molecular regulation to clinical use. Pharmacol Rev. 58:488–520.

Bernstein MA, Welch SP (1997) Effects of spinal versus supraspinal administration of cyclic nucleotide-dependent protein kinase inhibitors on morphine tolerance in mice. Drug Alcohol Depend. 44:41–46.

Bernuci MP, Szawka RE, Helena CV, Leite CM, Lara HE, Anselmo-Franci JA (2008) Locus coeruleus mediates cold stress-induced polycystic ovary in rats. Endocrinology. 149:2907–2916.

Berridge CW, Foote SL (1996) Enhancement of behavioral and electroencephalographic indices of waking following stimulation of noradrenergic β-receptors within the medial septal region of the basal forebrain. J Neurosci. 16:6999–7009.

Berridge CW, Waterhouse BD (2003) The locus coeruleus-noradrenergic system: modulation of behavioral state and state-dependent cognitive processes. Brain Res Brain Res Rev. 42:33–84.

Bhargava HN, Kumar S, Barjavel MJ (1998) Kinetic properties of nitric oxide synthase in cerebral cortex and cerebellum of morphine tolerant mice. Pharmacology. 56:252–256.

Biel M (2009) Cyclic nucleotide-regulated cation channels. J Biol Chem. 284:9017–9021.

Bilsky EJ, Inturrisi CE, Sadee W, Hruby VJ, Porreca F (1996) Competitive and non-competitive NMDA antagonists block the development of antinociceptive tolerance to morphine, but not to selective mu or delta opioid agonists in mice. Pain. 68:229–237.

Blake AD, Bot G, Freeman JC, Reisine, T (1997) Differential opioid agonist regulation of the mouse mu opioid receptor. J Biol Chem. 272:782–790.

Blanchet C, Sollini M, Lüscher C (2003) Two distinct forms of desensitization of G-protein coupled inwardly rectifying potassium currents evoked by alkaloid and peptide mu-opioid receptor agonists. Mol Cell Neurosci. 24:517–523.

Bobker DH, Williams JT (1989) Serotonin agonists inhibit synaptic potentials in the rat locus ceruleus *in vitro* via 5-hydroxytryptamine$_{1A}$ and 5- hydroxytryptamine$_{1B}$ receptors. J. Pharmacol. Exp. Ther. 250:37–43.

Bohme GA, Bon C, Lemaire M, Reibaud M, Piot O, Stutzmann JM, Doble A, Blanchard, JC (1993) Altered synaptic plasticity and memory formation in nitric oxide synthase inhibitor-treated rats. Proc. Natl. Acad. Sci. U.S.A. 90:9191–9194.

Bohn LM, Gainetdinov RR, Lin FT, Lefkowitz RJ, Caron MG (2000) Mu-opioid receptor desensitization by beta-arrestin-2 determines morphine tolerance but not dependence. Nature. 408:720–723.

Bohn LM, Lefkowitz RJ, Caron MG (2002) Differential mechanisms of morphine antinociceptive tolerance revealed in (beta)arrestin-2 knock-out mice. J Neurosci 22:10494–10500.

Boissel JP, Schwarz PM, Förstermann U (1998) Neuronal-type NO synthase: transcript diversity and expressional regulation. Nitric Oxide 2:337–349.

Bonfoco E, Krainc D, Ankarcrona M, Nicotera P, Lipton SA (1995) Apoptosis and necrosis: two distinct events induced, respectively, by mild and intense insults with N-methyl-D-aspartate or nitric oxide/superoxide in cortical cell cultures. Proc Natl Acad Sci USA. 92:7162–7166.

Borgland SL, Connor M, Osborne PB, Furness JB, Christie MJ (2003) Opioid agonists have different efficacy profiles for G protein activation, rapid desensitization, and endocytosis of μ-opioid receptors. J Biol Chem. 278:18776–18784.

Bredt DS, Snyder SH (1989) Nitric oxide mediates glutamate-linked enhancement of cGMP levels in the cerebellum. Proc Natl Acad Sci USA. 86:9030–9033.

Bremner JD, Krystal JH, Southwick SM, Charney DS (1996) Noradrenergic mechanisms in stress and anxiety: I. Preclinical studies. Synapse. 23:28–38.

Brienza RS, Stein M, Chen MH, Gogineni A, Sobota M, Maksad J, Hu P and Clarke J (2000) Depression among needle exchange program and methadone maintenance clients. J Subst Abuse Treat. 18:331–337.

Brookes PS, Darley-Usmar VM (2004) Role of calcium and superoxide dismutase in sensitizing mitochondria to peroxynitrite-induced permeability transition. Am J Physiol Heart Circ Physiol. 286:H39–H46.

Bruinstroop E, Cano G, Vanderhorst VG, Cavalcante JC, Wirth J, Sena-Esteves M, Saper CB (2012) Spinal projections of the A5, A6 (locus coeruleus), and A7 noradrenergic cell groups in rats. J Comp Neurol. 520:1985–2001.

Buchen L (2012) Opioid receptors revealed. Nature. 483:383.

Butterfield DA, Howard BJ, LaFontaine MA (2001) Brain oxidative stress in animal models of accelerated aging and the age-related neurodegenerative disorders, Alzheimer's disease and Huntington's disease. Curr Med Chem. 8:815–828.

# C

Calabrese V, Mancuso C, Calvani M, Rizzarelli E, Butterfield DA, Stella AM (2007) Nitric oxide in the central nervous system: neuroprotection versus neurotoxicity. Nat Rev Neurosci. 8:766–775.

Carpenter JR (1986) A method for presenting and comparing dose-response curves. J Pharmacol Methods. 15:283–303.

Cedarbaum JM, Aghajanian GK (1976) Noradrenergic Neurons of Locus Coeruleus - Inhibition by Epinephrine and Activation by Alpha-Antagonist Piperoxane. Brain Res. 112:413–419.

Celver J, Xu M, Jin W, Lowe J, Chavkin C (2004) Distinct domains of the mu-opioid receptor control uncoupling and internalization. Mol Pharmacol. 65:528–537.

Chandler DJ, Gao WJ, Waterhouse BD (2014a) Heterogeneous organization of the locus coeruleus projections to prefrontal and motor cortices. Proc Natl Acad Sci USA. 111:6816–6821.

Chandler DJ, Waterhouse BD, Gao WJ (2014b) New perspectives on catecholaminergic regulation of executive circuits: evidence for independent modulation of prefrontal functions by midbrain dopaminergic and noradrenergic neurons. Front Neural Circuits. 8:53.

Chen Y, Mestek A, Liu J, Hurley JA, Yu L (1993) Molecular-Cloning and Functional Expression of A Mu-Opioid Receptor from Rat-Brain. Molecular Pharmacology 44:8–12.

Cherubini E, North RA, Williams JT (1988) Synaptic potentials in rat locus coeruleus neuronas. J. Physiol. 406:431–442.

Chiu TH, Yeh MH, Tsai SK, Mok MS (1993) Electrophysiological actions of alfentanil: intracellular studies in the rat locus coeruleus neurones. Br J Pharmacol. 110:903–909.

Christie MJ, Williams JT, North RA (1989) Electrical coupling synchronizes subthreshold activity in locus coeruleus neurons *in vitro* from neonatal rats. J. Neurosci. 10:3584–3589.

Ciccocioppo R, Angeletti S, Panocka I, Massi M (2000) Nociceptin/orphanin FQ and drugs of abuse. Peptides. 21:1071–1080.

Clayton EC, Williams CL (2000) Glutamatergic influences on the nucleus paragigantocellularis: contribution to performance in avoidance and spatial memory tasks. Behav. Neurosci. 114:707–712.

Codd EE, Shank RP, Schupsky JJ, Raffa RB (1995) Serotonin and norepinephrine uptake inhibiting activity of centrally acting analgesics; structural determinants and role in antinociception. J Pharmacol Exp Ther. 274:1263–1270.

Coleman JW (2001) Nitric oxide in immunity and inflammation. Int Immunopharmacol. 1:1397–1406.

Connor M, Osborne PB, Christie MJ (2004) μ-Opioid receptor desensitization: Is morphine different? Br J Pharmacol. 143:685–696.

Corbett AD, Henderson G, McKnight AT, Paterson SJ (2006) 75 years of opioid research: the exciting but vain quest for the Holy Grail. Br J Pharmacol. 147 Suppl 1:S153–S162.

Cox BM, Goldstein A, Li CH (1976) Opioid activity of a peptide, β-lipotropin-(61-91), derived from β-lipotropin. Proc. Natl. Acad. Sci. U.S.A. 73:1821–1823.

Cox BM, Christie MJ, Devi L, Toll L, Traynor JR (2015) Challenges for opioid receptor nomenclature: IUPHAR Review 9. Br J Pharmacol. 172:317–323.

Crain SM, Shen KF (1996) Modulatory effects of Gs-coupled excitatory opioid receptor functions on opioid analgesia, tolerance, and dependence. Neurochem Res. 21:1347–1351.

Cuéllar B, Fernández AP, Lizasoain I, Moro MA, Lorenzo P, Bentura ML, Rodrigo J, Leza JC (2000) Up-regulation of neuronal synthase immunoreactivity in opiate dependence and withdrawal. Psychopharmacology. 148:66–73.

Cui Y, Liao XX, Liu W, Guo RX, Wu ZZ, Zhao CM, Chen PX, Feng JQ (2008) A novel role of minocycline: attenuating morphine antinociceptive tolerance by inhibition of p38 MAPK in the activated spinal microglia. Brain Behav Immun. 22:114–123.

Curtis AL, Drolet G, Valentino RJ (1993) Hemodynamic stress activates locus coeruleus neurons of unanesthetized rats. Brain Res Bull. 31:737–744.

# D

Dahlström A, Fuxe K (1964) Evidence for the existence of monoamine neurons in the central nervous system. I. Demonstration of monoamine-containing neurons in the cell bodies of brainstem neurons. Acta Physiol Scand Suppl. SUPPL 232:1–55.

Dang VC, Williams JT (2004) Chronic morphine treatment reduces recovery from opioid desensitization. J Neurosci. 24:7699–7706.

Dang VC, Williams JT (2005) Morphine-Induced mu-opioid receptor desensitization. Mol Pharmacol. 68:1127–1132.

Dang VC, Napier IA, Christie MJ (2009) Two distinct mechanisms mediate acute mu-opioid receptor desensitization in native neurons. J Neurosci. 29:3322–3327.

Dang VC, Chieng B, Azriel Y, Christie MJ (2011) Cellular morphine tolerance produced by barrestin-2-dependent impairment of μ-opioid receptor resensitization. J Neurosci. 31:7122–7130.

Dang VC, Christie MJ (2012) Mechanisms of rapid opioid receptor desensitization, resensitization and tolerance in brain neurons. Br J Pharmacol. 165:1704–1716.

Davis KL, Martin E, Turko IV, Murad F (2001) Novel effects of nitric oxide. Annu Rev Pharmacol Toxicol. 41:203–236.

Dawson VL, Dawson TM, London ED, Bredt DS, Snyder SH (1991) Nitric oxide mediates glutamate neurotoxicity in primary cortical cultures. Proc Natl Acad Sci U S A. 88:6368–6371.

De Carvalho D, Patrone LG, Taxini CL, Biancardi V, Vicente MC, Gargaglioni LH (2014) Neurochemical and electrical modulation of the locus coeruleus: contribution to $CO_2$ drive to breathe. Front Physiol. 5:288.

De Conno F, Groff L, Brunelli C, Zecca E, Ventafridda V, Ripamonti C (1996) Clinical experience with oral methadone administration in the treatment of pain in 196 advanced cancer patients. J Clin Oncol. 14:2836–2842.

De Lecea L (2010) A decade of hypocretins: past, present and future of the neurobiology of arousal. Acta Physiol (Oxf). 198:203–208.

Del-Bel E, Padovan-Neto FE, Raisman-Vozari R, Lazzarini M (2011) Role of nitric oxide in motor control: implications for Parkinson's disease pathophysiology and treatment. Curr Pharm Des. 17:471–488.

Del Tredici K, Braak H (2013) Dysfunction of the locus coeruleus-norepinephrine system and related circuitry in Parkinson's disease-related dementia. J Neurol Neurosurg Psychiatry. 84:774–783.

Delwing D, Chiarani F, Bavaresco CS, Wannmacher CM, Wajner M, Dutra-Filho CS, Wyse AT (2005) Protective effect of antioxidants on brain oxidative damage caused by proline administration. Neurosci Res. 52:69–74.

Derbyshire ER and Marletta MA (2012) Structure and regulation of soluble guanylate cyclase. Annu Rev Biochem. 81:533–559.

Dhawan BN, Cesselin F, Raghubir R, Reisine T, Bradley PB, Portoghese PS, Hamon M (1996) Internationa Union of Pharmacology. XII classification of opioid receptors. Pharmacological Reviews 48: 567–592.

Dickenson AH (1991) Mechanisms of the analgesic actions of opiates and opioids. Br Med Bull. 47:690–702.

Dogrul A, Bilsky EJ, Ossipov MH, Lai J, Porreca F (2005) Spinal L-type calcium channel blockade abolishes opioid-induced sensory hypersensitivity and antinociceptive tolerance. Anesth Analg. 101:1730–1735.

Dole VP, Nyswander ME, Kreek MJ (1966) Narcotic blockade. Arch Intern Med. 118:304–309.

Doll C, Konietzko J, Pöll F, Koch T, Höllt V Schulz S (2011) Agonist-selective patterns of μ-opioid receptor phosphorylation revealed by phosphosite-specific antibodies. Br J Pharmacol. 164:298–307.

Donica CL, Awwad HO, Thakker DR, Standifer KM (2013) Cellular mechanisms of nociceptin/orphanin FQ (N/OFQ) peptide (NOP) receptor regulation and heterologous regulation by N/OFQ. Mol Pharmacol. 83:907–918.

Doyle T, Esposito E, Bryant L, Cuzzocrea S, Salvemini D (2013) NADPH-oxidase 2 activation promotes opioid-induced antinociceptive tolerance in mice. Neuroscience. 241:1–9.

Drolet G, Vanbockstaele EJ, Astonjones G (1992) Robust Enkephalin Innervation of the Locus-Ceruleus from the Rostral Medulla. J Neurosci. 12:3162–3174.

Duman RS, Tallman JF, Nestler EJ (1988) Acute and chronic opiate-regulation of adenylate cyclase in brain: specific effects in locus coeruleus. J Pharmacol Exp Ther. 246:1033–1039.

Dupont JL, Janoshazi A, Bellahcene M, Mykita S, de Barry J (2000) Reversible protein kinase C activation in PC12 cells: effect of NGF treatment. Eur J Neurosci. 12:215–226.

Durmus N, Bagcivan I, Ozdemir E, Altun A, Gursoy S (2014) Soluble guanylyl cyclase activators increase the expression of tolerance to morphine analgesic effect. Bratisl Lek Listy. 115:334–339.

# E

East SJ and Garthwaite J (1991) NMDA receptor activation in rat hippocampus induces cyclic GMP formation through the L-arginine-nitric oxidepathway. Neurosci Lett. 123:17–19.

Ebert B, Thorkildsen C, Andersen S, Christrup LL, Hjeds H (1998) Opioid analgesics as noncompetitive N-methyl-D-aspartate (NMDA) antagonists. Biochem Pharmacol. 56:553–559.

Eddy NB, May EL (1973) The search for a better analgesic. Science. 181:407–414.

Egan TM, Henderson G, North RA, Williams JT (1983) Noradrenaline- Mediated Synaptic Inhibition in Rat Locus Coeruleus Neurons. J Physiol. 345:477–488.

El-Husseini AE, Bladen C, Vincent SR (1995) Molecular characterization of a type II cyclic GMP-dependent protein kinase expressed in the rat brain. J Neurochem. 64:2814–2817.

Elliott K, Minami N, Kolesnikov YA, Pasternak GW, Inturrisi CE (1994) The NMDA receptor antagonists, LY274614 and MK-801, and the nitric oxide synthase inhibitor, NG-nitro-L-arginine, attenuate analgesic tolerance to the mu-opioid morphine but not to kappa opioids. Pain. 56:69–75.

Ennis M, Aston-Jones G, Shiekhattar R (1992) Activation of locus coeruleus neurons by nucleus paragigantocellularis or noxious sensory stimulation is mediated by intracoerulear excitatory amino acid neurotransmission. Brain Res. 598:185–195.

Enquist J, Ferwerda M, Milan-Lobo L, Whistler JL (2012) Chronic methadone treatment shows a better cost/benefit ratio than chronic morphine in mice. J Pharmacol Exp Ther. 340:386–392.

Escobales N, Crespo MJ (2005) Oxidative-nitrosative stress in hypertension. Curr Vasc Pharmacol. 3:231–246.

Esplugues JV (2002) NO as a signalling molecule in the nervous system. Br J Pharmacol. 135:1079–1095.

# F

Fabian RH, Dewitt DS, Kent TA (1998) The 21-aminosteroid U-74389G reduces cerebral superoxide anion concentration following fluid percussion injury of the brain. J Neurotrauma. 15:433–440.

Fallon JH, Loughlin SE (1982) Monoamine innervation of the forebrain: collateralization. Brain Res Bull. 9:295–307.

Feil R, Kemp-Harper B (2006) cGMP signalling: from bench to bedside. Conference on cGMP generators, effectors and therapeutic implications. EMBO Rep. 7:149–153.

Feil R, Lohmann SM, de Jonge H, Walter U, Hofmann F (2003) Cyclic GMP-dependent protein kinases and the cardiovascular system: insights from genetically modified mice. Circ Res. 93:907–916.

Fenalti G, Giguere PM, Katritch V, Huang XP, Thompson AA, Cherezov V, Roth BL, Stevens RC (2014) Molecular control of δ-opioid receptor signalling. Nature. 506:191–196.

Feng Y, He X, Yang Y, Chao D, Lazarus LH, Xia Y (2012) Current research on opioid receptor function. Curr Drug Targets. 13:230–246.

Feng B, Li Z, Wang JB (2011) Protein kinase C-mediated phosphorylation of the μ-opioid receptor and its effects on receptor signaling. Mol Pharmacol. 79:768–775.

Fernandez AP, Pozo-Rodrigalvarez A, Serrano J, Martinez-Murillo R (2010) Nitric oxide: target for therapeutic strategies in Alzheimer's disease. Curr Pharm Des. 16:2837–2850.

Finnerup NB, Sindrup SH, Jensen TS (2010) The evidence for pharmacological treatment of neuropathic pain. Pain 150:573–581.

Finn AK, Whistler JL (2001) Endocytosis of the mu opioid receptor reduces tolerance and a cellular hallmark of opiate withdrawal. Neuron. 32:829–839.

Florin-Lechner SM, Druhan JP, Aston-Jones G, Valentino RJ (1996) Enhanced norepinephrine release in prefrontal cortex with burst stimulation of the locus coeruleus. Brain Res. 742:89–97.

Foote SL, Aston-Jones G, Bloom FE (1980) Impulse activity of locus coeruleus neurons in awake rats and monkeys is a function of sensory stimulation and arousal. Proc Natl Acad Sci U S A. 77:3033–3037.

Foote SL, Bloom FE, Astonjones G (1983) Nucleus Locus Ceruleus - New Evidence of Anatomical and Physiological Specificity. Physiol Rev. 63:844–914.

Foran SE, Carr DB, Lipkowski AW, Maszczynska I, Marchand JE, Misicka A, Beinborn M, Kopin AS, Kream RM (2000) Inhibition of morphine tolerance development by a substance P-opioid peptide chimera. J Pharmacol Exp Ther. 295:1142–1148.

Forno LS (1996) Neuropathology of Parkinson's Disease. J Neuropathol Exp Neurol. 55:259–272.

Francis SH, Busch JL, Corbin JD, Sibley D (2010) cGMP-dependent protein kinases and cGMP phosphodiesterases in nitric oxide and cGMP action. Pharmacol Rev. 62:525–563.

Freedman NJ, Lefkowitz RJ (1996) Desensitization of G protein-coupled receptors. Recent Prog Horm Res. 51:319–351.

Fujita W, Gomes I, Devi LA (2014) Revolution in GPCR Signaling: Opioid receptor heteromers as novel therapeutic targets: IUPHAR Review 10. Br J Pharmacol. 171:4155–4176.

Fukuyama N, Takizawa S, Ishida H, Hoshiai K, Shino- Hara Y, Nakazawa H (1998) Peroxynitrite formation in focal cerebral ischemia-reperfusion in rats occurs predominantly in the peri-infarct region. J. Cereb. Blood Flow Metab. 18:123–129.

Furchgott RF, Zawadzki JV (1980) The obligatory role of endothelial cells in the relaxation of arterial smooth muscle by acetylcholine. Nature 288:373–376.

Furfine ES, Harmon MF, Paith JE, Knowles RG, Salter M, Kiff RJ, Duffy C, Hazelwood R, Oplinger JA, Garvey EP (1994) Potent and selective inhibition of human nitric oxide synthases: Selective inhibition of neuronal nitric oxide synthase by S-methyl-L-thiocitrulline and s-ethyl-L-thiocitrulline. J Biol Chem 269:26677–26683.

Furuyama T, Inagaki S, Takagi H (1993) Localizations of alpha-1 and beta-1 subunits of soluble guanylate cyclase in the rat brain. Mol Brain Res. 20:335–344.

# G

Gainetdinov RR, Premont RT, Bohn LM, Lefkowitz RJ, Caron MG (2004) Desensitization of G protein-coupled receptors and neuronal functions. Annu Rev Neurosci. 27:107–144.

Gardner-Nix JS (1996) Oral methadone for managing chronic nonmalignant pain. J Pain Symptom Manage. 11:321–328.

Gargaglioni LH, Hartzler LK, Putnam RW (2010) The Locus coeruleus and central chemosensitivity. Respir.Physiol.Neurobiol. 173:264–273.

Garthwaite J, Charles SL, Chess-Williams R (1988) Endothelium-derived relaxing factor release on activation of NMDA receptors suggests role as intracellular messenger in the brain. Nature. 336:385–388.

Garthwaite J, Southam E, Boulton CL, Nielsen EB, Schmidt K, Mayer B (1995) Potent and selective inhibition of nitric oxide-sensitive guanylyl cyclase by 1H-[1,2,4]oxadiazolo[4,3-a]quinoxalin-1-one. Mol Pharmacol. 48:184–188.

Garzón J, Castro M, Sánchez-Blázquez P (1998) Influence of Gz and Gi2 transducer proteins in the affinity of opioid agonists to mu receptors. Eur J Neurosci. 10:2557–2564.

Garzón J, Rodríguez-Díaz M, López-Fando A, Sánchez-Blázquez P (2001) RGS9 proteins facilitate acute tolerance to mu-opioid effects. Eur J Neurosci. 13:801–811.

Garzón J, Rodríguez-Díaz M, López-Fando A, García-España A, Sánchez-Blázquez P (2002) Glycosylated phosducin-like protein long regulates opioid receptor function in mouse brain. Neuropharmacology. 42:813–828.

Garzón J, Rodríguez-Muñoz M, de la Torre-Madrid E, Sánchez-Blázquez P (2005) Effector antagonism by the regulators of G protein signalling (RGS) proteins causes desensitization of mu-opioid receptors in the CNS. Psychopharmacology. 180:1–11.

Garzón J, Sánchez-Blázquez P (2001) Administration of myr$^{+}$-$G_{i2}\alpha$ subunits prevents acute tolerance (tachyphylaxis) to mu-opioid effects in mice. Neuropharmacology 40:560–569.

Geahlen RL, Krebs EG (1980) Studies on the phosphorylation of the type I cAMP-dependent protein kinase. J Biol Chem 255:9375–9379.

George SA, Knox D, Curtis AL, Aldridge JW, Valentino RJ, Liberzon I (2013) Altered locus coeruleus-norepinephrine function following single prolonged stress. Eur J Neurosci. 37:901–909.

Ghofrani HA, Galiè N, Grimminger F, Grünig E, Humbert M, Jing ZC, Keogh AM, Langleben D, Kilama MO, Fritsch A, Neuser D, Rubin LJ; PATENT-1 Study Group (2013) Riociguat for the treatment of pulmonary arterial hypertension. N Engl J Med. 369:330–340.

Gibbs ME, Hutchinson DS, Summers RJ (2010) Noradrenaline release in the locus coeruleus modulates memory formation and consolidation; roles for α- and β-adrenergic receptors. Neuroscience. 170:1209–1222.

Giusti P, Buriani A, Cima L, Lipartiti M (1997) Effect of acute and chronic tramadol on [3H]-5-HT uptake in rat cortical synaptosomes. Br J Pharmacol. 122:302–306.

Goldstein A, Tachibana S, Lowney LI, Hunkapiller M, Hood L (1979) Dynorphin-(1-13), an extraordinarily potent opioid peptide. Proc. Natl. Acad. Sci. U.S.A. 76:6666–6670.

Golebiewska U, Johnston JM, Devi L, Filizola M, Scarlata S (2011) Differential response to morphine of the oligomeric state of μ-opioid in the presence of δ-opioid receptors. Biochemistry 50:2829–2837.

Gomes I, Gupta A, Filipovska J, Szeto HH, Pintar JE, Devi LA (2004) A role for heterodimerization of mu and delta opiate receptors in enhancing morphine analgesia. Proc Natl Acad Sci U S A. 101:5135–5139.

Goodchild CS, Kolosov A, Geng L, Winter LL, Nadeson R (2009) Prevention and reversal of morphine tolerance by the analgesic neuroactive steroid alphadolone. Pain Med. 10:890–901.

Gorman AL, Elliott KJ, Inturrisi CE (1997) The d- and l-isomers of methadone bind to the non-competitive site on the N-methyl-D-aspartate (NMDA) receptor in rat forebrain and spinal cord. Neurosci Lett. 223:5–8.

Granier S, Manglik A, Kruse AC, Kobilka TS, Thian FS, Weis WI, Kobilka BK (2012) Structure of the δ-opioid receptor bound to naltrindole. Nature. 485:400–404.

Guo Q, Packer L (2000) Ascorbate-dependent recycling of the vitamin E homologue trolox by dihydrolipoate and glutathione in murine skin homogenates. Free Radic Biol Med. 29:368–374.

Gurtu S, Pant KK, Sinha JN, Bhargawa KP (1984) An investigation into the mechanism of cardiovascular responses elicited by electrical stimulation of locus coeruleus and subcoeruleus in the cat. Brain Res. 301:59–64.

# H

Han Y, Jiang C, Tang J, Wang C, Wu P, Zhang G, Liu W, Jamangulova N, Wu X, Song X (2014) Resveratrol reduces morphine tolerance by inhibiting microglial activation via AMPK signalling. Eur J Pain. 18:1458–1470.

Handy R LC and Moore PK (1998) Handy and Moore reply: 7-nitroindazole (7-NI) fails to increase blood pressure in animals: The 7-NI 'conundrum'. Trends Pharmacol Sci 19: 350.

Harris GC, Williams JT (1991) Transient homologous μ-opioid receptor desensitization in rat locus coeruleus neurons. J Neurosci 11:2574–2581.

Harrison LM, Kastin AJ, Zadina JE (1998) Opiate tolerance and dependence: receptors, G-proteins, and antiopiates. Peptides. 19:1603–1630.

Hasbi A, Nguyen T, Fan T, Cheng R, Rashid A, Alijaniaram M, Rasenick MM, O'Dowd BF, George SR (2007) Trafficking of preassembled opioid mu-delta heterooligomer-Gz signaling complexes to the plasma membrane: coregulation by agonists. Biochemistry 46: 12997–13009.

He L, Kim J, Ou C, McFadden W, van Rijn RM, Whistler JL (2009) Methadone antinociception is dependent on peripheral opioid receptors. J Pain. 10:369–379.

Hecker M, Mülsch A, Busse R (1994) Subcellular localization and characterization of neuronal nitric oxide synthase, J. Neurochem. 62:1524–1529.

Heinrich TA, da Silva RS, Miranda KM, Switzer CH, Wink DA, Fukuto JM (2013) Biological nitric oxide signaling: chemistry and terminology. Br J Pharmacol. 169:1417–1429.

Heinzen EL, Pollack GM (2004) The development of morphine antinociceptive tolerance in nitric oxide synthase-deficient mice. Biochem Pharmacol. 67:735–741.

Herman BH, Vocci F, Bridge P (1995) The effects of NMDA receptor antagonists and nitric oxide synthase inhibitors on opioid tolerance and withdrawal. Medication development issues for opiate addiction. Neuropsychopharmacology. 13:269–293.

Hickey L, Li Y, Fyson SJ, Watson TC, Perrins R, Hewinson J, Teschemacher AG, Furue H, Lumb BM, Pickering AE (2014) Optoactivation of locus ceruleus neurons evokes bidirectional changes in thermal nociception in rats. J Neurosci. 34:4148–4160.

Highfield DA, Grant S (1998) Ng-nitro-L-arginine, an NOS inhibitor, reduces tolerance to morphine in the rat locus coeruleus. Synapse. 29:233–239.

Hobbs AJ, Higgs A, Moncada S (1999) Inhibition of nitric oxide synthase as a potential therapeutic target. Annu Rev Pharmacol Toxicol. 39:191–220.

Hoffmann LS, Chen HH (2014) cGMP: transition from bench to bedside: a report of the 6th International Conference on cGMP Generators, Effectors and Therapeutic Implications. Naunyn Schmiedebergs Arch Pharmacol. 387:707–718.

Hofmann F, Wegener JW (2013) cGMP-dependent protein kinases (cGK). Methods Mol Biol. 1020:17–50.

Holscher C, Rose SP (1992) An inhibitor of nitric oxide synthesis prevents memory formation in the chick. Neurosci. Lett. 145:165–167.

Horvath TL, Diano S, and Van den Pol AN (1999) Synaptic interaction between hypocretin (orexin) and neuropeptide Y cells in the rodent and primate hypothalamus: a novel circuit implicated in metabolic and endocrine regulations. J. Neurosci. 19:1072–1087.

Hughes MN (2008) Chemistry of nitric oxide and related species. Methods Enzymol. 436:3–19.

Hughes J, Smith TW, Kosterlitz HW, Fothergill LA, Morgan BA, Morris HR (1975) Identification of two related pentapeptides from the brain with potent opiate agonist activity. Nature. 258: 577–579.

Huie RE, Padmaja S (1993) The reaction of NO with superoxide. Free Radic. Res. Commun. 18:195–199.

Hull LC, Llorente J, Gabra BH, Smith FL, Kelly E, Bailey C, Henderson G, Dewey WL (2010) The Effect of Protein Kinase C and G Protein-Coupled Receptor Kinase Inhibition on Tolerance Induced by μ-Opioid Agonists of Different Efficacy. J Pharmacol Exp Ther. 332:1127–1135.

# I

Ibi M, Matsuno K, Matsumoto M, Sasaki M, Nakagawa T, Katsuyama M, Iwata K, Zhang J, Kaneko S, Yabe-Nishimura C (2011) Involvement of NOX1/NADPH oxidase in morphine-induced analgesia and tolerance. J Neurosci. 31:18094–18103.

Ignarro LJ (1991) Heme-dependent activation of guanylate cyclase by nitric oxide: a novel signal transduction mechanism. Blood Vessels. 28:67–73.

Ignarro LJ (1999) Nitric oxide: a unique endogenous signaling molecule in vascular biology. Biosci Rep. 19:51–71.

Ignarro LJ, Adams JB, Horwitz PM, Wood KS (1986) Activation of soluble guanylate cyclase by NO-hemoproteins involves NO-heme exchange. Comparison of heme-containing and heme-deficient enzyme forms. J Biol Chem. 261:4997–5002.

Ignarro LJ, Buga GM, Wood KS, Byrns RE, Chaudhuri G (1987) Endothelium derived relaxing factor produced and released from artery and vein is nitric oxide. Proc. Natl. Acad. Sci. USA 84:9265–9269.

Illing S, Mann A, Schulz S (2014) Heterologous regulation of agonist-independent μ-opioid receptor phosphorylation by protein kinase C. Br J Pharmacol. 171:1330–1340.

Ingoglia NA and Dole VP (1970) Localization of d- and l-methadone after intraventricular injection into rat brains. J Pharmacol Exp Ther. 175:84–87.

Ishimatsu M, Williams JT (1996) Synchronous activity in locus coeruleus results from dendritic interactions in pericoerulear regions. J Neurosci. 16:5196–5204.

# J

Janes K, Neumann WL, Salvemini D (2012) Anti-superoxide and anti-peroxynitrite strategies in pain suppression. Biochim Biophys Acta. 1822:815–821.

Jean-Baptiste G, Yang Z, Greenwood MT (2006) Regulatory mechanisms involved in modulating RGS function. Cell Mol Life Sci. 63:1969–1985.

Jiang C, Xu L, Chen L, Han Y, Tang J, Yang Y, Zhang G, Liu W (2014) Selective suppression of microglial activation by paeoniflorin attenuates morphine tolerance. Eur J Pain. doi: 10.1002/ejp.617

Johnson EA, Oldfield S, Braksator E, Gonzalez-Cuello A, Couch D, Hall KJ, Mundell SJ, Bailey CP, Kelly E, and Henderson G (2006) Agonist-selective mechanisms of mu-opioid

receptor desensitization in human embryonic kidney 293 cells. Mol Pharmacol. 70:676–685.

Jones SL (1991) Descending noradrenergic influences on pain. Prog. Brain Res. 88:381–394.

Jones SL, Gebhart GF (1986) Characterization of coeruleospinal inhibition of the nociceptive tail-flick reflex in the rat: mediation by spinal alpha 2-adrenoceptors. Brain Res. 364:315–330.

# K

Kakizawa S, Yamazawa T, Chen Y, Ito A, Murayama T, Oyamada H, Kurebayashi N, Sato O, Watanabe M, Mori N, Oguchi K, Sakurai T, Takeshima H, Saito N, Iino M (2012) Nitric oxide-induced calcium release via ryanodine receptors regulates neuronal function. EMBO J. 31:417–428.

Kaupp UB, Seifert R (2002) Cyclic nucleotide-gated ion channels. Physiol Rev. 82:769–824.

Kawahara Y, Kawahara H, Westerink BH (1999) Tonic regulation of the activity of noradrenergic neurons in the locus coeruleus of the conscious rat studied by dual-probe microdialysis. Brain Res. 823:42–48.

Kelly E (2013) Efficacy and ligand bias at the μ-opioid receptor. Br J Pharmacol. 169:1430–1446.

Kenakin T (1995) Agonist-Receptor Efficacy II. Agonist Trafficking of Receptor Signals. Trends Pharmacol Sci. 16:232–238.

Keith DE, Anton B, Murray SR, Zaki PA, Chu PC, Lissin DV, Monteillet-Agius G, Stewart PL, Evans CJ, von Zastrow M (1998) μ-Opioid receptor internalization: opiate drugs have differential effects on a conserved endocytic mechanism in vitro and in the mammalian brain. Mol Pharmacol. 53:377–384.

Keith DE, Murray SR, Zaki PA, Chu PC, Lissin DV, Kang L, Evans CJ, von Zastrow M (1996) Morphine activates opioid receptors without causing their rapid internalization. J Biol Chem 271:19021–19024.

Kendrick KM, Guevara Guzman R, Zorrilla J, Hinton MR, Broad KD, Mimmack M, Ohkura S (1997) Formation of olfactory memories mediated by nitric oxide. Nature. 388:670–674.

Khalil A, Fortun A, Hebert S, Jay-Gerin JP, El Abbouyi A, Wallach J, Fulop T Jr (1998) Novel 21-aminosteroid U-74389G inhibits low-density lipoprotein peroxidation induced by $^{\cdot}OH$ and $O_2^{-\cdot}$ free radicals. Life Sci. 63:769–779.

Kim JA, Bartlett S, He L, Nielsen CK, Chang AM, Kharazia V, Waldhoer M, Ou CJ, Taylor S, Ferwerda M, Cado D, Whistler JL (2008) Morphine-induced receptor endocytosis in a novel knockin mouse reduces tolerance and dependence. Curr Biol. 18:129–135.

Kim I, Je HD, Gallant C, Zhan Q, Riper DV, Badwey JA, Singer HA, Morgan KG (2000) $Ca^{2+}$-calmodulin-dependent protein kinase II-dependent activation of contractility in ferret aorta. J Physiol. 526 Pt 2:367–374.

Kim J, Saravanakumar G, Choi HW, Park D, Kim WJ (2014) A platform for nitric oxide delivery. J Mater Chem B. 2:341–356.

Kim MA, Lee HS, Lee BY, Waterhouse BD (2004) Reciprocal connections between subdivisions of the dorsal raphe and the nuclear core of the locus coeruleus in the rat. Brain Res. 1026:56–67.

Klimek V, Stockmeier C, Overholser J, Meltzer HY, Kalka S, Dilley G, Ordway GA (1997) Reduced levels of norepinephrine transporters in the locus coeruleus in major depression. J Neurosci. 17:8451–8458.

Knapp LT, Klann E (2000) Superoxide-induced stimulation of protein kinase C via thiol modification and modulation of zinc content. J Biol Chem. 275:24136–24145.

Koch T, Widera A, Bartzsch K, Schulz S, Brandenburg LO, Wundrack N, Beyer A, Grecksch G, Höllt V (2005) Receptor endocytosis counteracts the development of opioid tolerance. Mol Pharmacol. 67:280–287.

Koch T, Seifert A, Wu DF, Rankovic M, Kraus J, Börner C, Brandenburg LO, Schröder H, Höllt V (2009) μ-opioid receptor-stimulated synthesis of reactive oxygen species is mediated via phospholipase D2. J Neurochem. 110:1288–1296.

Kogan JH, Nestler EJ, Aghajanian GK (1992) Elevated basal firing rates of locus coeruleus neurons in brain slices from opiate-dependent rats: Association with enhanced responses to 8-Br-cAMP. Eur J Pharmacol. 211:47–53.

Kornick CA, Santiago-Palma J, Moryl N, Payne R, Obbens EA (2003) Benefit-risk assessment of transdermal fentanyl for the treatment of chronic pain. Drug Saf. 26:951–973.

Kots AY, Martin E, Sharina IG, Murad F (2009) A short history of cGMP, guanylyl cyclases, and cGMP-dependent protein kinases. Handb Exp Pharmacol. 191:1–14.

Kovoor A, Celver JP, Wu A, and Chavkin C (1998) Agonist induced homologous desensitization of mu-opioid receptors mediated by G protein-coupled receptor kinases is dependent on agonist efficacy. Mol Pharmacol. 54:704–711.

Kreibich AS, Reyes BAS, Curtis AL, Ecke L, Chavkin C, Van Bockstaele EJ, Valentino RJ (2008) Presynaptic inhibition of diverse afferents to the locus ceruleus by kappa-opiate receptors: A novel mechanism for regulating the central norepinephrine system. J Neurosci. 28:6516–6525.

Kristensen K, Christensen CB, Christrup LL (1995) The mu1, mu2, delta, kappa opioid receptor binding profiles of methadone stereoisomers and morphine. Life Sci. 56:45–50.

# L

Lacza Z, Pankotai E, Csordás A, Gero D, Kiss L, Horváth EM, Kollai M, Busija DW, Szabó C (2006) Mitochondrial NO and reactive nitrogen species production: does mtNOS exist? Nitric Oxide. 14:162–168.

Lafon-cazal M, Pietri S, Culcasi M, Bockaert, J (1993) NMDA-dependent superoxide production and neuro-toxicity. Nature. 364:535–537.

Lane Ladd SB, Pineda J, Boundy VA, Pfeuffer T, Krupinski J, Aghajanian GK, Nestler EJ (1997) CREB (cAMP response element-binding protein) in the locus coeruleus: Biochemical, physiological, and behavioral evidence for a role in opiate dependence. J Neurosci 17:7890–7901.

Law PY, Hom DS, Loh HH (1982) Loss of opiate receptor activity in neuroblastoma ×glioma NG108-15 cells after chronic etorphine treatment: a multiple step process, Mol. Pharmacol.72:1–4.

Law PY, Wong YH, Loh HH (2000) Molecular mechanisms and regulation of opioid receptor signaling. Annu Rev Pharmacol Toxicol. 40:389–430.

Le Bars D, Gozariu M, Cadden SW (2001) Animal models of nociception. Pharmacol Rev. 53:597–652.

Lefkowitz RJ, Stadel JM, Caron MG (1983) Adenylate cyclase-coupled β-adrenergic receptors: structure and mechanisms of activation and desensitization. Annu Rev Biochem. 52:159–186.

Leitman DC, Waldman SA, Murad F (1994) Regulation of particulate guanylate cyclase by natriuretic peptides and Escherichia coli heat-stable enterotoxin. Adv Pharmacol. 26:67–86.

Levitt ES, Williams JT (2012) Morphine desensitization and cellular tolerance are distinguished in rat locus ceruleus neurons. Mol Pharmacol 82:983–992.

Liachenko S, Tang P, Somogyi GT, Xu Y (1999) Concentration-dependent isoflurane effects on depolarization-evoked glutamate and GABA outflows from mouse brain slices. Br J Pharmacol. 127:131–134.

Liang DY, Clark JD (2004) Modulation of the NO/CO-cGMP signaling cascade during chronic morphine exposure in mice. Neurosci Lett. 365:73–77.

Liang Y, Mestek A, Yu L, Carr LG (1995) Cloning and characterization of the promoter region of the mouse μ opioid receptor gene. Brain Res. 679:82–88.

Little JW, Cuzzocrea S, Bryant L, Esposito E, Doyle T, Rausaria S, Neumann WL, Salvemini D (2013) Spinal mitochondrial-derived peroxynitrite enhances neuroimmune activation during morphine hyperalgesia and antinociceptive tolerance. Pain. 154:978–986.

Little JW, Doyle T, Salvemini D (2012) Reactive nitroxidative species and nociceptive processing: determining the roles for nitric oxide, superoxide, and peroxynitrite in pain. Amino Acids. 42:75–94.

Llorente J, Santamarta MT, Henderson G, Pineda J (2012) Enhancement of mu-opioid receptor desensitization by nitric oxide in rat locus coeruleus neurons: involvement of reactive oxygen species. J Pharmacol Exp Ther. 342:552–560.

Lohmann SM, Vaandrager AB, Smolenski A, Walter U, De Jonge HR (1997) Distinct and specific functions of cGMP-dependent protein kinases. Trends Biochem. Sci. 22:307–312.

Lohse MJ, Andexinger S, Pitcher J, Trukawinski S, Codina J, Faure JP, Caron MG, Lefkowitz RJ (1993) Receptor specific desensitization with purified proteins. Kinase dependence and receptor specificity of β-arrestin and arrestin in the b2-adrenergic receptor and rhodopsin systems. J. Biol. Chem. 267:8558–8564.

Lohse MJ, Hein P, Hoffmann C, Nikolaev VO, Vilardaga JP, Bünemann M (2008) Kinetics of G-protein-coupled receptor signals in intact cells. Br J Pharmacol. 153 (Suppl 1): S125–S132.

Lucas KA, Pitari GM, Kazerounian S, Ruiz-Stewart I, Park J, Schulz S, Chepenik KP, Waldman SA (2000) Guanylyl cyclases and signaling by cyclic GMP. Pharmacol Rev. 52:375–414.

Luo ZD, Cizkova D (2000) The role of nitric oxide in nociception. Curr Rev Pain. 4:459–466.

# M

Machelska H, Ziolkowska B, Mika J, Przewlocka B, Przewlocki R (1997) Chronic morphine increases biosynthesis of nitric oxide synthase in the rat spinal cord. Neuroreport. 8:2743–2747.

Madia PA, Dighe SV, Sirohi S, Walker EA, Yoburn BC (2009) Dosing protocol and analgesic efficacy determine opioid tolerance in the mouse. Psychopharmacology. 207:413–422.

Maeda T, Kitahama K, Geffard M (1994) Dopaminergic innervation of rat locus coeruleus: a light and electron microscopic immunohistochemical study. Microsc. Res. Tech. 29:211–218.

Maldonado R (1997) Participation of noradrenergic pathways in the expression of opiate withdrawal: biochemical and pharmacological evidence. Neurosci Biobehav Rev. 21:91–104.

Malen PL, Chapman PF (1997) Nitric oxide facilitates long-term potentiation, but not long-term depression. J Neurosci. 17:2645–2651.

Manglik A, Kruse AC, Kobilka TS, Thian FS, Mathiesen JM, Sunahara RK, Pardo L, Weis WI, Kobilka BK, Granier S (2012) Crystal structure of the μ-opioid receptor bound to a morphinan antagonist. Nature. 485:321–326.

Mansour A, Fox CA, Burke S, Meng F, Thompson RC, Akil H, Watson SJ (1994) Mu, delta, and kappa opioid receptor mRNA expression in the rat CNS: an in situ hybridization study. J Comp Neurol. 350:412–438.

Mao J, Price DD, Hayes RL, Lu J, Mayer DJ (1992) Differential roles of NMDA and non-NMDA receptor activation in induction and maintenance of thermal hyperalgesia in rats with painful peripheral mononeuropathy. Brain Res 598:271–278.

Mao J, Sung B, Ji RR, Lim G (2002) Neuronal apoptosis associated with morphine tolerance: evidence for an opioid-induced neurotoxic mechanism. J Neurosci. 22:7650–7661.

Marletta MA (1994) Nitric oxide synthase: aspects concerning structure and catalysis. Cell. 78:927–930.

Martin WR, Eades CG, Thompson JA, Huppler RE, Gilbert PE (1976) The effects of morphine- and nalorphine- like drugs in the nondependent and morphine-dependent chronic spinal dog. J. Pharmacol. Exp. Ther. 197:517–532.

Mateo Y, Fernández-Pastor B, Meana JJ (2001) Acute and chronic effects of desipramine and clorgyline on alpha(2)-adrenoceptors regulating noradrenergic transmission in the rat brain: a dual-probe microdialysis study. Br J Pharmacol. 133:1362–1370.

Matsuda H, Iyanagi T (1999) Calmodulin activates intramolecular electron transfer between the two flavins of neuronal nitric oxide synthase flavin domain. Biochim. Biophys. Acta 1473:345–355.

Matsui A, Williams JT (2010) Activation of μ-opioid receptors and block of Kir3 potassium channels and NMDA receptor conductance by L- and D-methadone in rat locus coeruleus. Br J Pharmacol. 161:1403–1413.

Matsuoka I, Giuili G, Poyard M, Stengel D, Parma J, Guellaen G, Hanoune J (1992) Localization of adenylyl and guanylyl cyclase in rat brain by in situ hybridization: comparison with calmodulin mRNA distribution. J. Neurosci. 12:3350–3360.

Matthes HWD, Maldonado R, Simonin F, Valverde O, Slowe S, Kitchen I, Befort K, Dierich A, LeMeur M, Dolle P, Tzavara E, Hanoune J, Roques BP, Kieffer BL (1996) Loss of morphine-induced analgesia, reward effect and withdrawal symptoms in mice lacking the mu-opioid-receptor gene. Nature 383:819–823.

Mayer DJ, Mao J, Holt J, Price DD (1999) Cellular mechanisms of neuropathic pain, morphine tolerance, and their interactions. Proc Natl Acad Sci U S A. 96:7731–7736.

Mayer B, Koesling D (2001) cGMP signalling beyond nitric oxide. Trends Pharmacol Sci. 22:546–548.

Mazei-Robison MS, Nestler EJ (2012) Opiate-induced molecular and cellular plasticity of ventral tegmental area and locus coeruleus catecholamine neurons. Cold Spring Harb Perspect Med. 2:a012070.

McPherson J, Rivero G, Baptist M, Llorente J, Al-Sabah S, Krasel C, Dewey W L, Bailey CP, Rosethorne EM, Charlton SJ, Henderson G, Kelly E (2010) μ-opioid receptors: correlation of agonist efficacy for signalling with ability to activate internalization. Mol Pharmacol. 78:756–766.

Meier K, Knepel W, Schöfl C (1988) Potassium depolarization elevates cytosolic free calcium concentration in rat anterior pituitary cells through 1,4-dihydropyridine-sensitive, omega-conotoxin-insensitive calcium channels. Endocrinology. 122:2764–2770.

Melief EJ, Miyatake M, Bruchas MR, Chavkin C (2010) Ligand-directed c-Jun N-terminal kinase activation disrupts opioid receptor signaling. Proc Natl Acad Sci U S A. 107:11608–11613.

Mendiguren A, Pineda J (2004) Cannabinoids enhance N-methyl-D-aspartate-induced excitation of locus coeruleus neurons by CB1 receptors in rat brain slices. Neurosci Lett. 363:1–5.

Mendiguren A, Pineda J (2006) Systemic effect of cannabinoids on the spontaneous firing rate of locus coeruleus neurons in rats. Eur J Pharmacol. 534:83–88.

Mendiguren A, Pineda J (2007) CB1 cannabinoid receptors inhibit the glutamatergic component of KCl-evoked excitation of locus coeruleus neurons in rat brain slices. Neuropharmacology. 52:617–625.

Mergia E, Russwurm M, Zoidl G, Koesling D (2003) Major occurrence of the new $\alpha_2\beta_1$ isoform of NO-sensitive guanylyl cyclase in brain. Cell Signal 15:189–195

Mestek A, Hurley JH, Bye LS, Campbell AD, Chen Y, Tian M, Liu J, Schulman H, Yu L (1995) The human mu opioid receptor: modulation of functional desensitization by calcium/calmodulin dependent protein kinase and protein kinase C. J Neurosci. 15:2396–2406.

Miguelez C, Aristieta A, Cenci MA, Ugedo L (2011) The locus coeruleus Is Directly Implicated in L-DOPA-Induced Dyskinesia in Parkinsonian Rats: An Electrophysiological and Behavioural Study. Plos One 6:e24679

Milan-Lobo L, Enquist J, van Rijn RM, Whistler JL (2013) Anti-analgesic effect of the mu/delta opioid receptor heteromer revealed by ligand-biased antagonism. PLoS One. 8:e58362.

Millan MJ (2002) Descending control of pain. Prog Neurobiol. 66:355-474.

Miller JF, Proudfit HK (1990) Antagonism of stimulation-produced antinociception from ventrolateral pontine sites by intrathecal administration of alpha-adrenergic antagonists and naloxone. Brain Res 530:20–34.

Minnis JG, Patierno S, Kohlmeier SE, Brecha NC, Tonini M, Sternini C (2003) Ligand-induced mu opioid receptor endocytosis and recycling in enteric neurons. Neuroscience. 119:33–42.

Mogil JS, Pasternak GW (2001) The molecular and behavioral pharmacology of the orphanin FQ/nociceptin peptide and receptor family. Pharmacol Rev 53: 381–415.

Monassier L, Bousquet P (2002) Sigma receptors: from discovery to highlights of their implications in the cardiovascular system. Fundam Clin Pharmacol. 16:1–8.

Muraki T, Uzumaki H, Kato R (1982) Strain difference in morphine-induced increase in plasma cyclic AMP and cyclic GMP levels in relation to locomotor activity in male mice. Psychopharmacology. 76:316–319.

Muscoli C, Cuzzocrea S, Ndengele MM, Mollace V, Porreca F, Fabrizi F, Esposito E, Masini E, Matuschak GM, Salvemini D (2007) Therapeutic manipulation of peroxynitrite attenuates the development of opiate-induced antinociceptive tolerance in mice. J Clin Invest. 117:3530–3539.

# N

Nagi K, Pineyro G (2014) Kir3 channel signaling complexes: focus on opioid receptor signaling. Front Cell Neurosci. 8:186.

Nakane M, Mitchell J, Förstermann U, Murad F (1991) Phosphorylation by calcium calmodulin-dependent protein kinase II and protein kinase C modulates the activity of nitric oxide synthase. Biochem Biophys Res Commun. 180:1396–1402.

Napoli C, Paolisso G, Casamassimi A, Al-Omran M, Barbieri M, Sommese L, Infante T, Ignarro LJ (2013) Effects of nitric oxide on cell proliferation: novel insights. J Am Coll Cardiol. 62:89–95.

Navidhamidi M, Semnanian S, Javan M, Goudarzvand M, Rohampour K, Azizi H (2012) Examining the effect of the CaMKII inhibitor administration in the locus coeruleus on the naloxone-precipitated morphine withdrawal signs in rats. Behav Brain Res. 226:440–444.

Nayebi AM, Rezazadeh H, Parsa Y (2009) Effect of fluoxetine on tolerance to the analgesic effect of morphine in mice with skin cancer. Pharmacol Rep. 61:453–458.

Nestler EJ, Tallman JF (1988) Chronic morphine treatment increases cyclic AMP-dependent protein kinase activity in the rat locus coeruleus. Mol Pharmacol. 33:127–132.

Nestler EJ, Alreja M, Aghajanian GK (1994) Molecular and cellular mechanisms of opiate action: studies in the rat locus coeruleus. Brain Res Bull. 35:521–528.

Nestler EJ, Aghajanian GK (1997) Molecular and cellular basis of addiction. Science. 278: 58–63.

Nestler EJ, Alreja M, Aghajanian GK (1999) Molecular control of locus coeruleus neurotransmission. Biol. Psychiatry. 46:1131–1139.

Newton PM, Kim JA, McGeehan AJ, Paredes JP, Chu K, Wallace MJ, Roberts AJ, Hodge CW, Messing RO (2007). Increased response to morphine in mice lacking protein kinase C epsilon. Genes Brain Behav. 6:329–338.

Noda Y, Mori A, Liburdy R, Packer L (1999) Melatonin and its precursors scavenge nitric oxide. J Pineal Res. 27:159–163.

North RA, Williams JT, Surprenant A, Christie MJ (1987) Mu-receptor and delta-receptor belong to a family of receptors that are coupled to potassium channels. Proceedings of the National Academy of Sciences of the United States of America 84:5487–5491.

# O

Olesen SP, Drejer J, Axelsson O, Moldt P, Bang L, Nielsen-Kudsk JE, Busse R, Mülsch A (1998) Characterization of NS 2028 as a specific inhibitor of soluble guanylyl cyclase. Br J Pharmacol. 123:299–309.

Ordway GA, Schenk J, Stockmeier CA, May W, Klimek V (2003) Elevated agonist binding to alpha(2)-adrenoceptors in the locus coeruleus in major depression. Biol Psychiatry. 53:315–323.

Ortega JE, Mendiguren A, Pineda J, Meana JJ (2012) Regulation of central noradrenergic activity by 5-HT3 receptors located in the locus coeruleus of the rat Neuropharmacology 62:2472–2479.

Osborne PB, Williams JT (1995) Characterization of acute homologous desensitization of mu-opioid receptor-induced currents in locus coeruleus neurones. Br J Pharmacol. 115:925–932.

Osborne PB, Chieng B, Christie MJ (2000) Morphine-6 beta-glucuronide has a higher efficacy than morphine as a mu-opioid receptor agonist in the rat locus coeruleus. Br J Pharmacol. 131:1422–1428.

Osmanovic SS, Shefner SA (1990) γ-Aminobutyric-acid responses in rat locus coeruleus neurons *in vitro*: a current-clamp and voltage-clamp study. J Physiol. 421:151–170.

Ota KT, Pierre VJ, Ploski JE, Queen K, Schafe GE (2008) The NO-cGMP-PKG signaling pathway regulates synaptic plasticity and fear memory consolidation in the lateral amygdala via activation of ERK/MAP kinase. Learn Mem. 15:792–805.

Ozdemir E, Bagcivan I, Durmus N, Altun A, Gursoy S (2011) The nitric oxide-cGMP signaling pathway plays a significant role in tolerance to the analgesic effect of morphine. Can J Physiol Pharmacol. 89:89–95.

# P

Pacher P, Beckman JS, Liaudet L (2007) Nitric oxide and peroxynitrite in health and disease. Physiol Rev. 87:315–424.

Pak Y, O'Dowd BF, Wang JB, George SR (1999) Agonist-induced, G protein-dependent and -independent down-regulation of the mu opioid receptor. The receptor is a direct substrate for protein-tyrosine kinase. J Biol Chem. 274:27610–27616.

Palmer RM, Ferrige AG, Moncada S (1987) Nitric oxide release accounts for the biological activity of endothelium derived relaxing factor. Nature. 327:524–526.

Palumbo EJ, Sweatt JD, Chen SJ, Klann E (1992) Oxidation-induced persistent activation of protein kinase C in hippocampal homogenates. Biochem Biophys Res Commun. 187:1439–1445.

Pan W, Kastin AJ (2007) From MIF-1 to endomorphin: the Tyr-MIF-1 family of peptides. Peptides. 28:2411–2434.

Pan YX, Xu J, Xu M, Rossi GC, Matulonis JE, Pasternak GW (2009) Involvement of exon 11-associated variants of the mu opioid receptor MOR-1 in heroin, but not morphine, actions. Proc Natl Acad Sci U S A. 106:4917–4922.

Paravicini TM, Touyz RM (2006) Redox signaling in hypertension. Cardiovasc Res. 71:247–258.

Parlato R, Cruz H, Otto C, Murtra P, Parkitna JR, Martin M, Bura SA, Begus- Nahrmann Y, Von Bohlen Und Halbach O, Maldonado R, Schutz G, Luscher C (2010) Effects of the cell type-specific ablation of the cAMP-responsive transcription factor in noradrenergic neurons on locus coeruleus firing and withdrawal behavior after chronic exposure to morphine. J Neurochem. 115:563–573.

Paronis CA, Holtzman SG (1992) Development of tolerance to the analgesic activity of mu agonists after continuous infusion of morphine,meperidine or fentanyl in rats. J Pharmacol Exp Ther. 262:1–9.

Pasternak GW, Kolesnikov YA, Babey AM (1995) Perspectives on the N-methyl-D-aspartate/nitric oxide cascade and opioid tolerance. Neuropsychopharmacology. 13:309–313.

Pasternak GW (2014) Opioids and their receptors: Are we there yet? Neuropharmacology. 76:198–203.

Peles E, Schreiber S, Naumovsky Y, Adelson M (2007) Depression in methadone maintenance treatment patients: Rate and risk factors. J Affect Disord. 99:213–220.

Pepper CM, Henderson G (1980) Opiates and opioid peptides hyperpolarize locus coeruleus neurons in vitro. Science. 209:394–395.

Pergolizzi J, Böger RH, Budd K, Dahan A, Erdine S, Hans G, Kress HG, Langford R, Likar R, Raffa RB, Sacerdote P (2008) Opioids and the management of chronic severe pain in the elderly: consensus statement of an International Expert Panel with focus on the six clinically most often used World Health Organization Step III opioids (buprenorphine, fentanyl, hydromorphone, methadone, morphine, oxycodone). Pain Pract 8:287–313.

Pert CB, Snyder SH (1973) Opiate receptor: demonstration in nervous tissue. Science, 179: 1011–1014.

Pertovaara A (2006) Noradrenergic pain modulation. Prog Neurobiol. 80:53–83.

Pfeiffer A, Brantl V, Herz A, Emrich HM (1986) Psychotomimesis mediated by kappa opiate receptors. Science. 233:774–776.

Phillips MA, Szabadi E, Bradshaw CM (2000) Comparison of the effects of clonidine and yohimbine on spontaneous pupillary fluctuations in healthy human volunteers. Psychopharmacology. 150:85–89.

Pifarré P, García A, Mengod G (2007) Species differences in the localization of soluble guanylyl cyclase subunits in monkey and rat brain. J Comp Neurol. 500:942–957.

Pineda J, Ugedo L, García-Sevilla JA (1993) Stimulatory effects of clonidine, cirazoline and rilmenidine on locus coeruleus noradrenergic neurons: posible involvement of imidazoline-preferring receptors. Naunyn Schmiedebergs Arch. Pharmacol. 348:134–140.

Pineda J, Aghajanian GK (1997) Carbon dioxide regulates the tonic activity of locus coeruleus neurons by modulating a proton- and polyamine-sensitive inward rectifier potassium current. Neuroscience. 77:723–743.

Pineda J, Kogan JH, Aghajanian GK (1996) Nitric oxide and carbon monoxide activate locus coeruleus neurons through a cGMP-dependent protein kinase: involvement of a nonselective cationic channel. J Neurosci. 16:1389–1399.

Pineda J, Torrecilla M, Martín-Ruiz R, Ugedo L (1998) Attenuation of withdrawal-induced hyperactivity of locus coeruleus neurones by inhibitors of nitric oxide synthase in morphine-dependent rats. Neuropharmacology. 37:759–767.

Poderoso JJ, Carreras MC, Lisdero C, Riobó N, Schöpfer F, Boveris A (1996) Nitric oxide inhibits electron transfer and increases superoxide radical production in rat heart mitochondria and submitochondrial particles. Arch. Biochem. Biophys. 328:85–92.

Pöhler D, Butt E, Meissner J, Müller S, Lohse M, Walter U, Lohmann SM, Jarchau T (1995) Expression, purification, and characterization of the cGMP-dependent protein kinases I beta and II using the baculovirus system. FEBS Lett. 374:419–425.

Polakiewicz RD, Schieferl SM, Dorner LF, Kansra V, Comb MJ (1998) A mitogen-activated protein kinase pathway is required for mu-opioid receptor desensitization. J Biol Chem. 273:12402–12406.

Pollard H, Llorens-Cortes C, Barbin G, Garbarg M, Schwartz JC (1978) Histamine and histidine decarboxylase in brain stem nuclei: distribution and decrease after lesions. Brain Res. 157:178–181.

Popik P, Kozela E, Pilc A (2000) Selective agonist of group II glutamate metabotropic receptors, LY354740, inhibits tolerance to analgesic effects of morphine in mice. Br J Pharmacol. 130:1425–1431.

Potenza MN, Gold SJ, Roby-Shemkowitz A, Lerner MR, Nestler EJ (1999) Effects of regulators of G protein-signaling proteins on the functional response of the mu-opioid receptor in a melanophore-based assay. J Pharmacol Exp Ther. 291:482–491.

Potter LR (2011) Guanylyl cyclase structure, function and regulation. Cell Signal. 23:1921–1926.

Powell KJ, Ma W, Sutak M, Doods H, Quirion R, Jhamandas K (2000) Blockade and reversal of spinal morphine tolerance by peptide and non-peptide calcitonin gene-related peptide receptor antagonists. Br J Pharmacol. 131:875–884.

Punch LJ, Self DW, Nestler EJ, Taylor JR (1997) Opposite modulation of opiate withdrawal behaviors on microinfusion of a protein kinase A inhibitor versus activator into the locus coeruleus or periaqueductal gray. J Neurosci. 17:8520–8527.

# Q

Quillinan N, Lau EK, Virk M, von Zastrow M, Williams JT (2011) Recovery from mu-Opioid Receptor Desensitization after Chronic Treatment with Morphine and Methadone. J Neurosci. 31:4434–4443.

# R

Radi R, Beckman JS, Bush KM, Freeman BA (1991a) Peroxynitrite oxidation of sulfhydryls. The cytotoxic potential of superoxide and nitric oxide. J Biol Chem. 266:4244–4250.

Radi R, Beckman JS, Bush KM, Freeman BA (1991b) Peroxynitrite-induced membrane lipid peroxidation: the cytotoxic potential of superoxide and nitric oxide. Arch Biochem Biophys. 288:481–487.

Radi R (2013) Peroxynitrite, a stealthy biological oxidant. J Biol Chem. 288:26464–26472.

Raehal KM, Bohn LM (2011) The role of β-arrestin2 in the severity of antinociceptive tolerance and physical dependence induced by different opioid pain therapeutics. Neuropharmacology. 60:58–65.

Raehal KM, Schmid CL, Groer CE, Bohn LM (2011) Functional selectivity at the μ-opioid receptor: implications for understanding opioid analgesia and tolerance. Pharmacol Rev. 63:1001–1019.

Raghavendra V, Kulkarni SK (2000) Possible mechanisms of action in melatonin reversal of morphine tolerance and dependence in mice. Eur J Pharmacol. 409:279–289.

Raghavendra V, Tanga FY, DeLeo JA (2004) Attenuation of morphine tolerance, withdrawal-induced hyperalgesia, and associated spinal inflammatory immune responses by propentofylline in rats. Neuropsychopharmacology. 29:327–334.

Rameau GA, Chiu LY, Ziff EB (2004) Bidirectional regulation of neuronal nitric-oxide synthase phosphorylation at serine 847 by the N-methyl-D-aspartate receptor. J Biol Chem. 279:14307–14314.

Rasmussen K (1991) Afferent effects on locus coeruleus in opiate withdrawal. Prog Brain Res. 88:207–216.

Rasmussen K, Beitner-Johnson DB, Krystal JH, Aghajanian GK, Nestler EJ (1990) Opiate withdrawal and the rat locus coeruleus: Behavioral, electrophysiological, and biochemical correlates. J Neurosci 10:2308–2317.

Ratz PH, Miner AS (2009) Role of protein kinase Czeta and calcium entry in KCl-induced vascular smooth muscle calcium sensitization and feedback control of cellular calcium levels. J Pharmacol Exp Ther. 328:399–408.

Raveh A, Cooper A, Guy-David L, Reuveny E (2010) Nonenzymatic rapid control of GIRK channel function by a G protein-coupled receptor kinase. Cell. 143:750–760.

Raynor K, Kong H, Chen Y, Yasuda K, Yu L, Bell GI, Reisine T (1994) Pharmacological characterization of the cloned κ-, δ-, and μ-opioid receptors. Mol Pharmacol 45:330–334.

Reil JC (1809) Untersuchungen uber den Bau des grossen Gehims im Menschen. Arch.Physiol. 9:136–524.

Reyes BA, Chavkin C, van Bockstaele EJ (2009) Subcellular targeting of kappa-opioid receptors in the rat nucleus locus coeruleus. J Comp Neurol. 512:419–431.

Ripamonti C, Zecca E, Bruera E (1997) An update on the clinical use of methadone for cancer pain. Pain. 70:109–115.

Robertson SD, Plummer NW, de Marchena J, Jensen P (2013) Developmental origins of central norepinephrine neuron diversity. Nat Neurosci. 16:1016–1023.

Rodríguez-Martín I, Braksator E, Bailey CP, Goodchild S, Marrion NV, Kelly E, Henderson G (2008) Methadone: does it really have low efficacy at μ-opioid receptors? Neuroreport. 19:589–593.

Rojas-Corrales MO, Berrocoso E, Gibert-Rahola J, Mico JA (2002) Antidepressant-like effects of tramadol and other central analgesics with activity on monoamines reuptake, in helpless rats. Life Sci. 72:143–152.

Roman LJ, Masters BS (2006) Electron transfer by neuronal nitric-oxide synthase is regulated by concerted interaction of calmodulin and two intrinsic regulatory elements, J. Biol. Chem. 281:23111–23118.

Rothe F, Canzler U, Wolf G (1998) Subcellular localization of the neuronal isoform of nitric oxide synthase in the rat brain: a critical evaluation, Neuroscience. 83:259–269.

Rozenfeld R, Devi LA (2007) Receptor heterodimerization leads to a switch in signaling: β-arrestin2-mediated ERK activation by mu-delta opioid receptor heterodimers. FASEB J 21:2455–2465.

Russell GV (1955) The nucleus locus coeruleus (dorsolateralis tegmenti). Tex. Rep.Biol.Med. 13:939–988.

Russwurm M, Koesling D (2002) Isoforms of NO-sensitive guanylyl cyclase. Mol Cell Biochem. 230:159–164.

Russwurm M, Russwurm C, Koesling D, Mergia E (2013) NO/cGMP: the past, the present, and the future. Methods Mol Biol. 1020:1–16.

# S

Sakai N, Sasaki K, Ikegaki N, Shirai Y, Ono Y, Saito N (1997) Direct visualization of the translocation of the γ-subspecies of protein kinase C in living cells using fusion proteins with green fluorescent protein. J Cell Biol. 139:1465–1476.

Salem A, Hope W (1999) Role of endogenous adenosine in the expression of opiate withdrawal in rats. Eur J Pharmacol. 369:39–42.

Salvemini D, Neumann WL (2009) Peroxynitrite: a strategic linchpin of opioid analgesic tolerance. Trends Pharmacol Sci. 30:194–202.

Salvemini D, Neumann W (2010) Targeting peroxynitrite driven nitroxidative stress with synzymes: A novel therapeutic approach in chronic pain management. Life Sci. 86:604–614.

Salvemini D, Little JW, Doyle T, Neumann WL (2011) Roles of reactive oxygen and nitrogen species in pain. Free Radic Biol Med. 51:951–966.

Samuels ER, Szabadi E (2008) Functional neuroanatomy of the noradrenergic locus coeruleus: its roles in the regulation of arousal and autonomic function part I: principles of functional organization. Curr Neuropharmacol 6: 235–253.

Samuels ER, Szabadi E (2008) Functional neuroanatomy of the noradrenergic locus coeruleus: its roles in the regulation of arousal and autonomic function part II: physiological and pharmacological manipulations and pathological alterations of locus coeruleus activity in humans Curr Neuropharmacol. 6:254–285.

Sánchez-Blázquez P, Rodríguez-Muñoz M, Montero C, de la Torre-Madrid E, Garzón J (2008) Calcium/calmodulin-dependent protein kinase II supports morphine antinociceptive tolerance by phosphorylation of glycosylated phosducin-like protein. Neuropharmacology. 54:319–330.

Sánchez-Blázquez P, Rodríguez-Muñoz M, Garzón J (2010) Mu-opioid receptors transiently activate the Akt-nNOS pathway to produce sustained potentiation of PKC-mediated NMDAR-CaMKII signaling. PLoS One. 5:e11278.

Sánchez-Blázquez P, Rodríguez-Muñoz M, Berrocoso E, Garzón J (2013) The plasticity of the association between mu-opioid receptor and glutamate ionotropic receptor N in opioid analgesic tolerance and neuropathic pain. Eur J Pharmacol. 716:94–105.

Santamarta MT, Llorente J, Mendiguren A, Pineda J (2014) Involvement of neuronal nitric oxide synthase in desensitisation of μ-opioid receptors in the rat locus coeruleus. J Psychopharmacol. 28:903–914.

Santamarta MT, Ulibarri I, Pineda J (2005) Inhibition of neuronal nitric oxide synthase attenuates the development of morphine tolerance in rats. Synapse. 57:38–46.

Santin JM, Hartzler LK (2013) Respiratory signaling of locus coeruleus neurons during hypercapnic acidosis in the bullfrog, *Lithobates catesbeianus*. Respir. Physiol. Neurobiol. 185:553–561

Scarlett JL, Packer MA, Porteous CM, Murphy MP (1996) Alterations to glutathione and nicotinamide nucleotides during the mitochondrial permeability transition induced by peroxynitriten. Biochem Pharmacol. 52:1047–1055.

Schuller AG, King MA, Zhang J, Bolan E, Pan YX, Morgan DJ, Chang A, Czick ME, Unterwald EM, Pasternak GW, Pintar JE (1999) Retention of heroin and morphine-6β-glucuronide analgesia in a new line of mice lacking exon 1 of MOR-1. Nat Neurosci. 2:151–156.

Schroder H, Leitman DC, Bennett BM, Waldman SA, Murad F (1988) Glyceryl trinitrate-induced desensitization of guanylate cyclase in cultured rat lung fibroblasts. J. Pharmacol. Exp. Ther. 245:413–418.

Scott CC, Robbins EB and Chen KK (1948) Pharmacologic comparison of the optical isomers of methadone. J Pharmacol Exp Ther. 93:282–286.

Scott GS, Szabó C, Hooper DC (2004) Poly(ADP-ribose) polymerase activity contributes to peroxynitrite-induced spinal cord neuronal cell death in vitro. J Neurotrauma. 21:1255–1263.

Shacka JJ, Sahawneh MA, Gonzalez JD, Ye YZ, D'Alessandro TL, Estévez AG (2006) Two distinct signaling pathways regulate peroxynitrite-induced apoptosis in PC12 cells. Cell Death Differ. 13:1506–1514.

Sharifipour M, Izadpanah E, Nikkhoo B, Zare S, Abdolmaleki A, Hassanzadeh K, Moradi F, Hassanzadeh K (2014) A new pharmacological role for donepezil: attenuation of morphine-induced tolerance and apoptosis in rat central nervous system. J Biomed Sci. 21:6.

Shipley MT, Fu L, Ennis M, Liu WL, Aston-Jones G (1996) Dendrites of locus coeruleus neurons extend preferentially into two pericoerulear zones. J. Comp. Neurol. 365:56-68.

Simon EJ, Hiller JM, Edelman I (1973) Stereospecific binding of the potent narcotic analgesic (3H) Etorphine to rat-brain homogenate. Proc Natl Acad Sci USA. 70:1947–1949.

Simson PE, Weiss JM (1988) Altered activity of the locus coeruleus in an animal model of depression. Neuropsychopharmacology. 1:287–295.

Singewald N, Kaehler ST, Philippu A (1999) Noradrenaline release in the locus coeruleus of conscious rats is triggered by drugs, stress and blood pressure changes. Neuroreport. 10:1583–1587.

Singewald N, Philippu A (1998) Release of neurotransmitters in the locus coeruleus. Prog Neurobiol 56:237–267.

Sirohi S, Dighe SV, Walker EA, Yoburn BC (2008) The analgesic efficacy of fentanyl: relationship to tolerance and mu-opioid receptor regulation. Pharmacol Biochem Behav 91: 115–120.

Sittl R, Nuijten M, Nautrup BP (2006) Patterns of dosage changes with transdermal buprenorphine and transdermal fentanyl for the treatment of noncancer and cancer pain: a retrospective data analysis in Germany. Clin Therapeut 28:1144–1154.

Smith FL, Javed RR, Elzey MJ, Dewey WL (2003) The expression of a high level of morphine antinociceptive tolerance in mice involves both PKC and PKA. Brain Res 985:78–88.

Smolenski A, Burkhardt AM, Eigenthaler M, Butt E, Gambaryan S, Lohmann SM, Walter U (1998) Functional analysis of cGMP-dependent protein kinases I and II as mediators of NO/cGMP effects. Naunyn Schmiedebergs Arch Pharmacol. 358:134–139.

Song P, Zhao ZQ (2001) The involvement of glial cells in the development of morphine tolerance. Neurosci Res. 39:281–286.

Song B, Lai B, Zheng Z, Zhang Y, Luo J, Wang C, Chen Y, Woodgett JR, Li M (2010) Inhibitory phosphorylation of GSK-3 by CaMKII couples depolarization to neuronal survival. J Biol Chem. 285:41122–41134.

Stasch JP, Alonso-Alija C, Apeler H, Dembowsky K, Feurer A, Minuth T, Perzborn E, Schramm M, Straub A (2002) Pharmacological actions of a novel NO-independent guanylyl cyclase stimulator, BAY 418543: in vitro studies. Br J Pharmacol. 135:333–343.

Stein C (1991) Peripheral analgesic actions of opioids. J Pain Symptom Manage. 6:119–124.

Steininger TL, Gong H, McGinty D, Szymusiak R (2001) Subregional organization of preoptic area/anterior hypothalamic projections to arousal-related monoaminergic cell groups. J Comp Neurol. 429:638–653.

Sternini C, Spann M, Anton B, Keith DE Jr, Bunnett NW, von Zastrow M, Evans C, and Brecha NC (1996) Agonist-selective endocytosis of mu opioid receptor by neurons *in vivo*. Proc Natl Acad Sci USA 93:9241–9246.

Stone JR, Marletta MA (1996) Spectral and kinetic studies on the activation of soluble guanylate cyclase by nitric oxide. Biochemistry 35:1093–1099.

Szabadi E, Tavernor S (1999) Hypo- and hypersalivation induced by psychoactive drugs - Incidence, mechanisms and therapeutic implications. Cns Drugs 11:449–466.

Szabo C, Zingarelli B, O'Connor M, Salzman AL (1996) DNA strand breakage, activation of poly (ADPribose) synthetase, cellular energy depletion are involved in the cytotoxicity of macrophages and smooth muscle cells exposed to peroxynitrite. Proc Natl Acad Sci USA 93:1753–1758.

Szabo ST, de Montigny C, Blier P (1999) Modulation of noradrenergic neuronal firing by selective serotonin reuptake blockers. Br J Pharmacol. 126:568–571.

Szabo ST, Blier P (2001) Functional and pharmacological characterization of the modulatory role of serotonin on the firing activity of locus coeruleus norepinephrine neurons. Brain Res. 922:9–20.

# T

Tang L, Shukla PK, Wang LX, Wang ZJ (2006) Reversal of morphine antinociceptive tolerance and dependence by the acute supraspinal inhibition of Ca2+/calmodulin-dependent protein kinase II. J Pharmacol Exp Ther. 317:901–909.

Taherzadeh M, Fradette C, Bleau AM, Jomphe C, Trudeau LE, du Souich P (2006) The 21-aminosteroid U74389G prevents the down-regulation and decrease in activity of CYP1A1, 1A2 and 3A6 induced by an inflammatory reaction Biochem. Pharmacol. 71:366–376.

Takahashi K, Kayama Y, Lin JS, Sakai K (2010) Locus coeruleus neuronal activity during the sleep-waking cycle in mice. Neuroscience 169:1115–1126.

Takasago T, Imagawa T, Furukawa K, Ogurusu T, and Shigekawa M (1991) Regulation of the cardiac ryanodine receptor by protein kinase-dependent phosphorylation. J Biochem 109:163–170.

Tanaka K, Shirai T, Nagata E, Dembo T, Fukuuchi Y (1997) Immunohistochemical detection of nitrotyrosine in postischemic cerebral cortex in gerbil. Neurosci. Lett. 235:85–88.

Tanaka M, Yoshida M, Emoto H, Ishii H (2000) Noradrenaline systems in the hypothalamus, amygdala and locus coeruleus are involved in the provocation of anxiety: basic studies. Eur. J. Pharmacol. 405:397–406.

Tayfun-Uzbay I, Oglesby MW (2001) Nitric oxide and substance dependence. Neurosci. Biobehav. Rev. 25:43–52.

Terenius L (1973) Stereospecific interaction between narcotic analgesics and a synaptic plasma membrane fraction of rat cerebral cortex. Acta Pharmacol. Toxicol. 32:317–320.

Terman GW, Jin W, Cheong YP, Lowe J, Caron MG, Lefkowitz RJ, Chavkin C (2004) G-protein receptor kinase 3 (GRK3) influences opioid analgesic tolerance but not opioid withdrawal. Br J Pharmacol. 141:55–64.

Thomas MK, Francis SH, and Corbin JD (1990) Substrate- and kinase-directed regulation of phosphorylation of a cGMP-binding phosphodiesterase by cGMP. J Biol Chem 265:14971–14978.

Thompson AA, Liu W, Chun E, Katritch V, Wu H, Vardy E, Huang XP, Trapella C, Guerrini R, Calo G, Roth BL, Cherezov V, Stevens RC (2012) Structure of the nociceptin/orphanin FQ receptor in complex with a peptide mimetic. Nature. 485:395–399.

Thornton SR, Smith FL (1997) Characterization of neonatal rat fentanyl tolerance and dependence. J Pharmacol Exp Ther. 281:514–521.

Toda N, Kishioka S, Hatano Y, Toda H (2009) Modulation of opioid actions by nitric oxide signaling. Anesthesiology. 110:166–181.

Torrecilla M, Pineda J, Ugedo L (2001) NO synthase inhibitors reduce opioid desensitization in rat locus coeruleus neurons in vitro. Neuroreport. 12:1601–1604.

Torrecilla M, Marker CL, Cintora SC, Stoffel M, Williams JT, Wickman K (2002) G-protein-gated potassium channels containing Kir3.2 and Kir3.3 subunits mediate the acute inhibitory effects of opioids on locus ceruleus neurons. J Neurosci. 22:4328–4334.

Torrecilla M, Ruiz-Ortega JA, Ugedo L, Pineda J (2007) Excitatory regulation of noradrenergic neurons by L-arginine/nitric oxide pathway in the rat locus coeruleus in vivo. Naunyn Schmiedebergs Arch Pharmacol. 375:337–347.

Tortorella S, Rodrigo-Angulo ML, Núnez A, Garzón M (2013) Synaptic interactions between perifornical lateral hypothalamic area, locus coeruleus nucleus and the oral pontine reticular nucleus are implicated in the stage succession during sleep wakefulness cycle. Front Neurosci. 7:216.

Trapaidze N, Gomes I, Cvejic S, Bansinath M, Devi LA (2000) Opioid receptor endocytosis and activation of MAP kinase pathway. Brain Res Mol Brain Res. 76:220–228.

Trotti D, Rossi D, Gjesdal O, Levy LM, Racagni G, Danbolt NC, Volterra A (1996) Peroxynitrite inhibits glutamate transporter subtypes. J. Biol Chem. 271:5976–5979.

Trujillo KA, Akil H (1991) Inhibition of morphine tolerance and dependence by the NMDA receptor antagonist MK-801. Science. 251:85–87.

Trujillo KA, Kubota KS, Warmoth KP (2004) Continuous administration of opioids produces locomotor sensitization. Pharmacol Biochem Behav. 79:661–669.

Truong W, Cheng C, Xu QG, Li XQ, Zochodne DW (2003) Mu opioid receptors and analgesia at the site of a peripheral nerve injury. Ann Neurol. 53:366–375.

Tsai RY, Chou KY, Shen CH, Chien CC, Tsai WY, Huang YN, Tao PL, Lin YS, Wong CS (2012) Resveratrol regulates N-methyl-D-aspartate receptor expression and suppresses neuroinflammation in morphine-tolerant rats. Anesth Analg. 115:944–952.

Tsao P, von Zastrow M (2000) Downregulation of G protein-coupled receptors. Curr Opin Neurobiol. 10:365–369.

Tsujino N, Tsunematsu T, Uchigashima M, Konno K, Yamanaka A, Kobayashi K, Watanabe M, Koyama Y, Sakurai T (2013) Chronic alterations in monoaminergic cells in the locus coeruleus in orexin neuron-ablated narcoleptic mice. PLoS One. 8:e70012.

# U

Ugedo L, Pineda J, Ruiz-Ortega JA, Martin-Ruiz R (1998) Stimulation of locus coeruleus neurons by non-I-1/I-2-type imidazoline receptors: an in vivo and in vitro electrophysiological study. Br J Pharmacol. 125:1685–1694.

Urushitani M, Shimohama S (2001) The role of nitric oxide in amyotrophic lateral sclerosis. Amyotroph Lateral Scler Other Motor Neuron Disord. 2:71–81.

# V

Valentino RJ, Chen S, Zhu Y, Aston-Jones G (1996) Evidence for divergent projections to the brain noradrenergic system and the spinal parasympathetic system from Barrington's nucleus. Brain Res. 732:1–15.

Valverde O, Mantamadiotis T, Torrecilla M, Ugedo L, Pineda J, Bleckmann S, Gass P, Kretz O, Mitchell JM, Schutz G, Maldonado R (2004) Modulation of anxiety-like

behavior and morphine dependence in CREB-deficient mice. Neuropsychopharmacology. 29:1122–1133.

Van Bockstaele EJ, Colago EE, Cheng P, Moriwaki A, Uhl GR, Pickel VM (1996) Ultrastructural evidence for prominent distribution of the mu-opioid receptor at extrasynaptic sites on noradrenergic dendrites in the rat nucleus locus coeruleus. J Neurosci. 16:5037–5048.

Van Bockstaele EJ, Commons K, Pickel VM (1997) Delta-opioid receptor is present in presynaptic axon terminals in the rat nucleus locus coeruleus: relationships with methionine 5-enkephalin. J Comp Neurol. 388:575–586.

Vardanyan RS, Hruby VJ (2014) Fentanyl-related compounds and derivatives: current status and future prospects for pharmaceutical applications. Future Med Chem. 6:385–412.

Vaupel DB, Kimes AS, London ED (1997) Further in vivo studies on attenuating morphine withdrawal: isoform-selective nitric oxide synthase inhibitors differ in efficacy. Eur J Pharmacol. 324:11–20.

Villa RF, Gorini A (1997) Pharmacology of lazaroids and brain energy metabolism: a review. Pharmacol Rev. 49:99–136.

Virág L, Szabo E, Gergely P, Szabo C (2003) Peroxynitrite-induced cytotoxicity: mechanism and opportunities for intervention. Toxicol Lett. 140-141:113–124.

Virk MS, Williams JT (2008) Agonist-specific regulation of mu-opioid receptor desensitization and recovery from desensitization. Mol Pharmacol. 73:1301–1308.

Von Zastrow M (2010) Regulation of opioid receptors by endocytic membrane traffic: Mechanisms and translational implications. Drug Alcohol Depend. 108:166–171.

Vulliemoz Y, Whittington RA, Virag L (1999) The nitric oxide-cGMP system of the locus coeruleus and the hypnotic action of alpha-2 adrenergic agonists. Brain Res. 849:169–174.

# W

Waldhoer M, Bartlett SE, Whistler JL (2004) Opioid receptors. Annu Rev Biochem. 73:953–990.

Wang YY, Aghajanian GK (1987) Excitation of locus coeruleus neurons by an adenosine 3',5'-cyclic monophosphate-activated inward current: extracellular and intracellular studies in rat brain slices. Synapse. 1:481–487.

Wang HY, Friedman E, Olmstead MC, and Burns LH (2005) Ultra-low-dose naloxone suppresses opioid tolerance, dependence and associated changes in mu opioid receptor-G protein coupling and Gβγ signaling. Neuroscience. 135:247–261.

Wang HY and Burns LH (2006) Gβγ that interacts with adenylyl cyclase in opioid tolerance originates from a Gs protein. J Neurobiol. 66:1302–1310.

Wang ZJ, Wang LX (2006) Phosphorylation: a molecular switch in opioid tolerance. Life Sci. 79:1681–1691.

Watkins LR, Hutchinson MR, Johnston IN, Maier SF (2005) Glia: novel counter-regulators of opioid analgesia. Trends Neurosci. 28:661–669.

Watkins LR, Hutchinson MR, Ledeboer A, Wieseler-Frank J, Milligan ED, Maier SF (2007) Norman Cousins Lecture. Glia as the "bad guys": implications for improving clinical pain control and the clinical utility of opioids. Brain Behav Immun. 21:131–146.

Weiss JM, Boss-Williams KA, Moore JP, Demetrikopoulos MK, Ritchie JC, West CHK (2005) Testing the hypothesis that locus coeruleus hyperactivity produces depression-related changes via galanin. Neuropeptides. 39:281–287.

Wendel B, Hoehe MR (1998) The human μ opioid receptor gene: 5' regulatory and intronic sequences. J Mol Med. 76:525–532.

West WL, Yeomans DC, Proudfit HK (1993) The function of noradrenergic neurons in mediating antinociception induced by electrical stimulation of the locus coeruleus in two different sources of Sprague-Dawley rats. Brain Res. 626:127–135.

Whistler JL, Chuang HH, Chu P, Jan LY, von Zastrow M (1999) Functional dissociation of mu opioid receptor signaling and endocytosis: implications for the biology of opiate tolerance and addiction. Neuron. 23:737–746.

Williams JT, Egan TM, North RA (1982) Enkephalin opens potassium channels on mammalian central neurons. Nature. 299:74–77.

Williams JT, North RT (1984) Opiate-receptor interactions on single locus coeruleus neurons. Mol Pharmacol. 26:489–497.

Williams JT, North RA, Shefner SA, Nishi S, Egan TM (1984) Membrane properties of rat locus coeruleus neurones. Neuroscience. 13:137–156.

Williams JT, Bobker DH, Harris GC (1991) Synaptic potentials in the locus coeruleus neurons in brain slices. Prog. Brain Res. 88:167–172.

Williams JT, Ingram SL, Henderson G, Chavkin C, von Zastrow M, Schulz S, Koch T, Evans CJ, Christie MJ (2013) Regulation of μ-opioid receptors: desensitization, phosphorylation, internalization, and tolerance. Pharmacol Rev. 65:223–254.

Wink DA, Mitchell JB (1998) Chemical biology of nitric oxide: insights into regulatory, cytotoxic, and cytoprotective mechanisms of nitric oxide. Free Radic. Biol. Med. 25:434–456.

Wolin MS (2005) Loss of vascular regulation by soluble guanylate cyclase is emerging as a key target of the hypertensive disease process. Hypertension. 45:1068–1069.

Wolozin BL, Pasternak GW (1981) Classification of multiple morphine and encephalin binding sites in the central nervous system. Proc Natl Acad Sci USA. 78:6181–6185.

Wong CS, Hsu MM, Chou YY, Tao PL, Tung CS (2000) Morphine tolerance increases [3H]MK-801 binding affinity and constitutive neuronal nitric oxide synthase expression in rat spinal cord. Br J Anaesth. 85:587–591.

Wu H, Wacker D, Mileni M, Katritch V, Han GW, Vardy E, Liu W, Thompson AA, Huang XP, Carroll FI, Mascarella SW, Westkaemper RB, Mosier PD, Roth BL,Cherezov V, Stevens RC (2012) Structure of the human κ-opioid receptor in complex with JDTic. Nature. 485:327–332.

Wüster M, Schulz R, Herz A (1979) Specificity of opioids towards the mu-, delta- and epsilon-opiate receptors. Neurosci Lett. 15:193–198.

# X

Xu ZQ, de Vente J, Steinbusch H, Grillner S, Hokfelt T (1998a) The NO-cGMP pathway in the rat locus coeruleus: electrophysiological, immunohistochemical and in situ hybridization studies. Eur J Neurosci. 10:3508–3516.

Xu JY, Hill KP, Bidlack JM (1998b) The nitric oxide/cyclic GMP system at the supraspinal site is involved in the development of acute morphine antinociceptive tolerance. J Pharmacol Exp Ther. 284:196–201.

Xu W, Liu LZ, Loizidou M, Ahmed M, Charles IG (2002) The role of nitric oxide in cancer. Cell Res. 12:311–320.

# Y

Yaksh TL (1987) Spinal opiates: a review of their effect on spinal function with emphasis on pain processing. Acta Anaesthesiol Scand Suppl. 85:25–37.

Yamamoto T, Maruyama W, Kato Y, Yi H, Shamoto-Nagai M, Tanaka M, Sato Y, Naoi M (2002) Selective nitration of mitochondrial complex I by peroxynitrite: involvement in mitochondria dysfunction and cell death of dopaminergic SHSY5Y cells. J. Neural Transm. 109:1–13.

Yekkirala AS, Lunzer MM, McCurdy CR, Powers MD, Kalyuzhny AE, Roerig SC, Portoghese PS (2011) N-naphthoyl-β-naltrexamine (NNTA), a highly selective and potent activator of mu/kappa-opioid heteromers. Proc Natl Acad Sci U S A. 108:5098–5103.

Yuan Z, Liu B, Yuan L, Zhang Y, Dong X, Lu J (2004) Evidence of nuclear localization of neuronal nitric oxide synthase in cultured astrocytes of rats. Life Sci. 74:3199–3209.

# Z

Zabel U, Hausler C, Weeger M, Schmidt HHHW (1999) Homodimerization of soluble guanylyl cyclase subunits. Dimerization analysis using a glutathione s-transferase affinity tag. J Biol Chem. 274:18149–18152.

Zadina JE, Hackler L, Ge LJ, Kastin AJ (1997) A potent and selective endogenous agonist for the mu-opiate receptor. Nature. 386:499–502.

Zagon IS, Verderame MF, Allen SS, McLaughlin PJ (2000) Cloning, sequencing, chromosomal location, and function of cDNAs encoding an opioid growth factor receptor (OGFr) in humans. Brain Res. 856:75–83.

Zaki PA, Keith DE Jr, Brine GA, Carroll FI, Evans CJ (2000) Ligand-induced changes in surface mu-opioid receptor number: relationship to G protein activation? J Pharmacol Exp Ther. 292:1127–1134.

Zanelli SA, Ashraf QM, Delivoria-Papadopoulos M, Mishra OP (2000) Peroxynitrite-induced modification of the N-methyl-D-aspartate receptor in the cerebral cortex of the guinea pig fetus at term. Neurosci Lett. 296:5–8.

Zanelli SA, Ashraf QM, Mishra OP (2002) Nitration is a mechanism of regulation of the NMDA receptor function during hypoxia. Neuroscience. 112:869–877.

Zaobornyj T, Ghafourifar P (2012) Strategic localization of heart mitochondrial NOS: a review of the evidence. Am J Physiol Heart Circ Physiol. 303:H1283–1293.

Zarow C, Lyness SA, Mortimer JA, Chui HC (2003) Neuronal loss is greater in the locus coeruleus than nucleus basalis and substantia nigra in Alzheimer and Parkinson diseases. Arch Neurol. 60:337–341.

Zeitz KP, Malmberg AB, Gilbert H, Basbaum AI (2001) Reduced development of tolerance to the analgesic effects of morphine and clonidine in PKCγ mutant mice. Pain. 94:245–253.

Zeng X, Lin MY, Wang D, Zhang Y, Hong Y (2014) Involvement of adrenomedullin in spinal glial activation following chronic administration of morphine in rats. Eur J Pain. 18:1323–1332.

Zhang J, Ferguson SS, Barak LS, Bodduluri SR, Laporte SA, Law PY, and Caron MG (1998) Role for G protein-coupled receptor kinase in agonist-specific regulation of mu-opioid receptor responsiveness. Proc Natl Acad Sci USA. 95:7157–7162.

Zhou L, Zhu DY (2009) Neuronal nitric oxide synthase: structure, subcellular localization, regulation, and clinical implications. Nitric Oxide. 20:223–230.

Zhou D, Chen ML, Zhang YQ, Zhao ZQ (2010) Involvement of spinal microglial P2X7 receptor in generation of tolerance to morphine analgesia in rats. J Neurosci. 30:8042–8047.

Zhu MY, Klimek V, Dilley GE, Haycock JW, Stockmeier C, Overholser JC, Meltzer HY, Ordway GA (1999) Elevated levels of tyrosine hydroxylase in the locus coeruleus in major depression. Biol Psychiatry. 46:1275–1286.

# 8. ACCOMPANYING MANUSCRIPTS

# MANUSCRIPT 1

Submitted to Neuropharmacology

**Title:**

# CONTRIBUTION OF NITRIC OXIDE-DEPENDENT GUANYLATE CYCLASE AND REACTIVE OXYGEN SPECIES SIGNALING PATHWAYS TO DESENSITIZATION OF μ-OPIOID RECEPTORS IN THE RAT LOCUS COERULEUS

**Running title:**

Involvement of NO/sGC and ROS in MOR desensitization

**Authors:**

Patricia Pablos, Aitziber Mendiguren and Joseba Pineda*

*Department of Pharmacology, Faculty of Medicine and Odontology, University of the Basque Country (UPV/EHU), E-48940 Leioa, Bizkaia, Spain*

*Corresponding author: J Pineda, M.D., Ph.D., Dept. of Pharmacology, Fac. of Medicine and Odontology, Univ. of the Basque Country (UPV / EHU), Bº Sarriena s/n, E-48940 Leioa, Bizkaia, Spain. Tel.: +34 94 6015577; fax: +34 94 6013220.

E-mail address: joseba.pineda@ehu.es (Dr. Joseba Pineda).

**Abstract**

Nitric oxide (NO) is involved in desensitization of μ-opioid receptors (MOR) in the locus coeruleus (LC). We used extracellular recordings *in vitro* to unmask the NO-dependent pathways involved in MOR desensitization in the rat LC. Perfusion with ME (3 and 10 μM) reduced ME (0.8 μM) effect in a concentration-related manner, indicative of MOR desensitization. ME (3 μM)-induced desensitization was enhanced by the NO donor DEA/NO (100 μM) and the soluble guanylate cyclase (sGC) activators A 350619 (30 μM) or BAY 418543 (1 μM). DEA/NO-induced enhancement was blocked by the sGC inhibitor NS 2028 (10 μM). The neuronal NO synthase inhibitor 7-NI (100 μM) reduced ME (10 μM)-induced desensitization, an effect that was prevented by the cGMP-dependent protein kinase (PKG) activator 8-Br-cGMP (100 and 300 μM). Paradoxically, ME (10 μM)-induced desensitization was not modified by several sGC inhibitors (NS 2028 and ODQ), PKG inhibitors (H8 and Rp-8-Br-PET-cGMP) or antioxidant agents (Trolox, U-74389G and melatonin), but it was attenuated by a combination of a sGC inhibitor (NS 2028 10 μM) and an antioxidant (Trolox 200 μM). Our results suggest that MOR desensitization in the LC may be mediated or regulated by NO through sGC and reactive oxygen species signaling pathways.

*Keywords*: nitric oxide; μ-opioid receptor; locus coeruleus; cyclic guanosine monophosphate; slice; firing.

*Abbreviations*: A350619, 3-[2-[(4-chlorophenyl)thiophenyl]-*N*-[4-(dimethylamino)butyl]-2-propenamide hydrochloride; aCSF, artificial cerebrospinal fluid; BAY 418543, 2-[1-[(2-fluorophenyl)methyl]-1H-pyrazolo[3,4-b]pyridin-3-yl]-5-(4-morpholinyl)-4,6 pyrimidinediamine; cGMP, cyclic guanosine monophosphate; 8-Br-cGMP, 8-

bromoguanosine 3′,5′-cyclic monophosphate**;** DEA/NO, diethylamine NONOate; H8, N-(2-[methylamino]ethyl)-5-isoquinoline-sulfonamide; LC, locus coeruleus; ME, $Met^5$-enkephalin; MOR, μ-opioid receptor; 7-NI, 7-nitroindazole; NO, nitric oxide; NOS, nitric oxide synthase; nNOS, neuronal nitric oxide synthase; NS 2028, 8-bromo-1H,4H-[1,2,4]oxadiazolo[3,4-*c*][1,4]benzoxazin-1-one; ODQ, 1H-[1,2,4]oxadiazolo[4,3-a]quinoxalin-1-one; PKG, cGMP-dependent protein kinase; ROS, reactive oxygen species; Rp-8-Br-PET-cGMP, Rp-β-phenyl-1,$N^2$-etheno-8-bromoguanosine 3′,5′-cyclic monophosphorothioate; S.E.M., standard error of the mean; sGC, soluble guanylate cyclase; U-74389G, 21-[4-(2,6-di-1-pyrrolidinyl-4-pyrrimidinyl)-1-piperazinyl]-pregna-1,4,9(11)-triene-3,20-dione(Z)-2-butenedioate.

## 1. Introduction

Opioids have long been used to alleviate severe, acute and chronic pain due to their high analgesic efficacy. However, the major limitation of their long-term use is the development of tolerance and dependence. Despite extensive research, the mechanisms responsible for opioid tolerance have been only partially unmasked. The analgesic effects of opioids are mediated by μ-opioid receptors (MOR). Accumulating evidence suggests a close relation between the induction of opioid tolerance and the appearance of MOR desensitization. Classical mechanisms underlying MOR desensitization include receptor phosphorylation, β-arrestin binding, receptor/effector uncoupling and receptor internalization (Taylor and Fleming, 2001). Additionally, nitric oxide (NO) cascade seems to be involved in the adaptations occurring during tolerance to opioids (Pasternak et al., 1995; Taylor and Fleming, 2001). NO production in the brain is catalyzed from L-arginine mainly by the neuronal NO synthase (nNOS) and is followed by different direct and indirect effects. Direct effects involve the interaction of NO with the soluble protein guanylate cyclase (sGC) to increase the production of 3´,5´-cyclic guanosine monophosphate (cGMP) (Hoffmann and Chen, 2014), which in turn regulates especific protein kinases (PKG) (Kots et al., 2009; Lohmann et al., 1997), phosphodiesterases (Degerman et al., 1997) and nucleotide-gated cationic channels (Zagotta and Siegelbaum, 1996). On the contrary, the indirect effects of NO are triggered by interaction of this molecule with oxygen ($O_2$) or superoxide radicals ($O_2^-$), which form nitrogen and oxygen species (ROS) when high concentrations of NO are reached (Davis et al., 2001).

The locus coeruleus (LC), which represents the major noradrenergic cluster in the brain, contains a high density of somatodendritic MOR and therefore it has been used to explore the molecular and cellular mechanisms of opioid effects (Nestler et al., 1994). MOR activation by opioid agonists inhibits LC neurons through $G_{i/o}$ protein-coupled

inwardly rectifying $K^+$ channels (Nestler and Aghajanian., 1997). Short-term exposure to high concentrations of opioid agonists desensitizes MOR in the LC *in vitro* (Harris and Williams, 1991; Torrecilla et al., 2001). Furthermore, chronic treatments with opiates induce various adaptive changes in the LC that lead to cellular tolerance (Santamarta et al., 2005), including up-regulation of cAMP pathway (Cao et al., 2010), desensitization by protein kinase-dependent phosphorylation (Dang and Christie, 2012) or changes in receptor trafficking and resensitization (Arttamangkul et al., 2012). Moreover, previous reports have described the involvement of NO cascade in the LC in the induction of cellular withdrawal (Pineda et al., 1998) and tolerance (Highfield and Grant, 1998; Santamarta et al., 2005) in morphine-dependent animals. Accordingly, prolonged treatment with morphine increases the expression of nNOS in the LC (Cuéllar et al., 2000) and non-selective and neuronal NOS inhibitors reduce MOR desensitization in the LC *in vitro* (Santamarta et al., 2014; Torrecilla et al., 2001). Recent work has suggested that ROS may mediate part of NO effects during opioid desensitization in the LC (Llorente et al., 2012). Thus, the ROS-generating molecule $H_2O_2$ enhances ME-induced MOR desensitization without affecting $\alpha_2$-adrenoceptor desensitization. However, a further characterization of NO-dependent pathways causing MOR desensitization has not been previously undertaken in the LC.

Therefore, the aim of this work was to investigate the contribution of NO-dependent sGC and ROS signaling to MOR desensitization induced by ME in the LC. We explored, by single-unit extracellular recordings of LC neurons, the effect of different activators or inhibitors of sGC/PKG and ROS pathways on opioid desensitization in the rat *in vitro*.

## 2. Materials and Methods

### *2.1. Animals*

Adult male Sprague-Dawley rats weighing 200–300 g were housed under controlled laboratory conditions (22 °C and 12-h light/dark cycles) with free access to food and water. All experimental procedures reported in this manuscript were conducted in accordance with U.K. Animals (Scientific Procedures) Act, 1986, and associated guidelines, and with the European Community Council Directive on "Protection of Animals Used in Experimental and Other Scientific Purposes" of 24 November 1986 (86/609/EEC). The procedures were approved by the *Animal Care and Use Committee* of the University of the Basque Country. All efforts were made to minimize animal suffering and to reduce the number of animals used. The animals for this study were obtained from the animal house of the University of the Basque Country (Leioa, Spain).

### *2.2. In vitro* electrophysiology

#### *2.2.1. Brain slice preparation*

*In vitro* experiments were performed as previously described (Mendiguren and Pineda, 2007). Briefly, animals were first anaesthetized with chloral hydrate (400 mg/kg, i.p.) and sacrificed by decapitation. The brain was removed and a block of tissue containing the brainstem was placed in ice-cold modified artificial cerebrospinal fluid (aCSF) where NaCl was equiosmotically substituted with sucrose to improve neuronal viability. Coronal slices of around 500 μm thickness containing the LC were cut by an oscillating vibratome (FHC Inc., Brunswick, USA) and then allowed to recover from the slicing for 90 min in oxygenated aCSF. Next, slices were placed on a nylon mesh and

maintained at 33 ± 0.5 ºC in a modified Haas-type interface chamber continuously perfused with oxygenated aCSF (95% $O_2$/5% $CO_2$, pH 7.34-7.38) at a flow rate of 1-1.5 ml/min. The aCSF contained (in mM): NaCl 130, KCl 3, $NaH_2PO_4$ 1.25, D-glucose 10, $NaHCO_3$ 21, $CaCl_2$ 2, and $MgSO_4$ 2.

*2.2.2. Recording procedures*

Extracellular recordings of single neurons were performed as previously described (Grandoso et al., 2004). The recording electrode consisted of an Omegadot glass micropipette (Sutter Instrument Co., Novato, CA, USA) that was pulled and filled with a solution of 50 mM NaCl (tip size of 2-5 μm, 3–5 MΩ). The microelectrode was placed in the LC, which was visually identified in the rostral pons as a dark oval area on the lateral borders of the central gray and the 4th ventricle, just anterior to the genu of the facial nerve (–9.48 to –9.96 mm from Bregma; Paxinos and Watson, 2005: figures 112–116). The extracellular signal recorded by the microelectrode was passed through a high-input impedance amplifier system (Axoclamp 2A, Axon Instruments, Foster City, CA) and monitored on an oscilloscope and by an audioanalyzer (Cibertec S.A., Madrid, Spain). Individual (single-unit) neuronal spikes were isolated from the background noise with a window discriminator and counted. The firing rate was represented and analyzed by a PC-based custom-made program (HFCP®; Cibertec S.A. Madrid, Spain), which generated histogram bars representing the cumulative number of spikes in consecutive 10 s bins. Noradrenergic neurons in the LC were identified by the following electrophysiological criteria: a spontaneous and regular discharge, a slow firing rate and a positive-negative biphasic waveform of 3–4 ms duration (Andrade and Aghajanian, 1984). We only recorded cells that showed stable firing rates between 0.4 and 1.5 Hz for at least 3–5 min

and strong inhibitory effects induced by ME (0.8 μM, 1 min) (higher than 80%). Only one neuron was recorded per slice and only one slice was obtained from each animal.

*2.3 Pharmacological procedures*

Acute MOR desensitization in LC neurons was studied by testing the inhibitory effect of ME (0.8 μM; 1 min) before (basal effect) and 5 min after perfusion with a high, desensitizing concentration of ME (3 or 10 μM, 10 min) (Santamarta et al., 2014). ME was selected on the basis of its good efficacy in inhibiting the firing of LC neurons almost exclusively through MOR (Williams and North, 1984), and because it rapidly washes out from the tissue after its perfusion (Santamarta et al., 2014). ME concentrations were chosen on the basis of previous studies (Harris and Williams, 1991; Santamarta et al., 2014; Torrecilla et al., 2001).

To characterize the involvement of the NO-dependent sGC/PKG and ROS pathways in ME-induced desensitization, the following drugs were perfused for at least 20-30 min before inducing the desensitization with ME (3 or 10 μM) and, then, during the whole experiment: BAY 418543 (1 μM) and A 350619 (30 μM) (sGC activators), NS 2028 (10 or 30 μM) and ODQ (10 or 30 μM) (sGC inhibitors), 8-Br-cGMP (100 or 300 μM) (PKG activator), Rp-8-Br-PET-cGMP (1 μM) and H8 (30 or 100 μM) (PKG inhibitors), or Trolox (200 μM), melatonin (100 μM) and U-74389G (10 μM) (antioxidants). In some assays, the NO donor DEA/NO (100 μM) or the nNOS inhibitor 7-NI (100 μM) were perfused to induce enhancement or blockade, respectively, of ME-induced desensitization and thereby to explore their interaction with drugs targeting sGC/PKG pathway. Finally, in one series of experiments, Trolox (200 μM) was administered together with NS 2028 (10 μM) to further evaluate the involvement of both sGC/PKG and ROS pathways in

MOR desensitization. The desensitization induced by ME (3 μM) was used to investigate the effect of sGC/PKG activators, since we have previously demonstrated that this protocol of desensitization (by ME 3 μM) can be readily enhanced by NO donors (Llorente et al., 2012). Moreover, the desensitization induced by a higher concentration of ME (10 μM) was tested to explore the effect of sGC/PKG inhibitors or antioxidants, because this paradigm of desensitization (by ME 10 μM) has been shown to be sensitive to NOS inhibitors (Santamarta et al., 2014; Torrecilla et al., 2001).

*2.4 Drugs and Reagents*

8-Bromoguanosine 3′,5′-cyclic monophosphate (8-Br-cGMP), chloral hydrate, diethylamine NONOate (DEA/NO), N-(2-[methylamino]ethyl)-5-isoquinoline-sulfonamide (H8), 7-nitroindazole (7-NI), 1H-[1,2,4]oxadiazolo[4,3-a]quinoxalin-1-one (ODQ) and Rp-β-Phenyl-1,$N^2$-etheno-8-bromoguanosine 3′,5′-cyclic monophosphorothioate (Rp-8-Br-PET-cGMP) were obtained from Sigma-Aldrich Química S.A. (Madrid, Spain). 8-Bromo-1H,4H-[1,2,4]oxadiazolo[3,4-*c*][1,4]benzoxazin-1-one (NS 2028) and 3-[2-[(4-chlorophenyl)thiophenyl]-*N*-[4-(dimethylamino)butyl]-2-propenamide hydrochloride (A 350619) were purchased from Tocris Bioscience (Bristol, UK). $Met^5$-enkephalin (ME) was obtained from Bachem (Weil am Rhein, Germany) and 2-[1-[(2-fluorophenyl)methyl]-1H-pyrazolo[3,4-b]pyridin-3-yl]-5-(4-morpholinyl)-4,6 pyrimidinediamine (BAY 418543), from Biotrend Chemikalien GMBH (Köln, Germany). 21-[4-(2,6-Di-1-pyrrolidinyl-4-pyrrimidinyl)-1-piperazinyl]-pregna-1,4,9(11)-triene-3,20-dione(Z)-2-butenedioate (U-74389G), melatonin and Trolox were purchased from Enzo Life Sciences Inc. (New York, USA). All other chemicals

were obtained from standard sources and were of the highest purity commercially available.

Drugs were dissolved in the final volume of aCSF just before each assay, to ensure full potency, and applied by turning a three-way valve that switched from aCSF to the test solution. DEA/NO was first dissolved in NaOH (25 mM; pH = 12) to prevent the spontaneous release of NO and then it was neutralized with HCl 1M and diluted in aCSF to its final concentration just before the assay. 8-Br-cGMP, 7-NI and Trolox were directly dissolved in aCSF on the day of the experiment. 7-NI required prolonged sonication to facilitate homogeneity. The rest of the drugs were prepared as stock solutions in milliQ water (ME, A 350619, H8, Rp-8-Br-PET-cGMP), ethanol (melatonin) or DMSO (NS 2028, U-74389G, BAY 418543, ODQ), stored at -25 ºC and, on the day of the experiment, diluted in aCSF to their final volume. The maximal final concentration of DMSO or ethanol was 0.1%, which fails to significantly affect the firing rate of LC neurons (Wang and Aghajanian, 1987). Drugs were administered for enough time (10–30 min) to reach a steady-state response and maintained during the whole experiment.

*2.5. Data analysis and statistics*

Values are expressed as the mean ± standard error of the mean (S.E.M) of *n* (number) experiments. The firing rate of LC cells was recorded before (baseline), during and after drug applications and throughout the experiment. The inhibitory effect of ME (0.8 µM, 1 min) was calculated as follows: $E = [(FR_{basal} - FR_{post}) \cdot 100] / FR_{basal}$, where $FR_{basal}$ is the mean firing rate for a 60 s period immediately before ME (0.8 µM, 1 min) application and $FR_{post}$ is the average firing rate for a 90 s period after onset of ME (0.8 µM, 1 min) perfusion. The degree of ME (3 or 10 µM)-induced opioid desensitization was calculated

as follows: desensitization percentage = 100 · [ 1 - ($E_{post}$)/$E_{basal}$)], where $E_{basal}$ and $E_{post}$ are the inhibitory effects of the test agonist (ME 0.8 μM, 1 min) before (*basal*) and 5 min after (*post*) the perfusion with the desensitizing concentrations of ME (3 or 10 μM). This value indicates the reduction in the inhibitory effect of the opioid agonist after perfusion with a high agonist concentration as compared with its basal effect.

To validate statistically the development of desensitization, the test effects of ME before and after the high concentration of ME were compared by a paired Student's *t* test. In addition, to evaluate the differences in the degree of ME-induced desensitization between groups, we compared the desensitization percentage values in the absence (control) or the presence of the drug by a two-sample Student's *t* test. Possible changes induced by drugs in the basal firing rates or the acute effects of ME (0.8 μM) were evaluated by a paired Student's *t* test when compared within the same cell or by a two-sample Student's *t* test when compared between different cells. The level of significance was considered as $p = 0.05$.

## 3. Results

### *3.1. Involvement of soluble guanylate cyclase in opioid-induced MOR desensitization in the locus coeruleus*

We have previously reported that NO donors enhance ME (3 μM)-induced MOR desensitization (Llorente et al., 2012). It is well known that NO targets the heme group of the sGC to elevate cGMP concentrations (Ignarro et al., 1991). To study the involvement of sGC in NO-induced regulation of MOR desensitization, we tested the effect of DEA/NO, a nucleophile complex that spontaneously releases NO in aqueous solution, in the absence and the presence of the sGC inhibitor NS 2028. Perfusion with ME (3 μM, 10 min) desensitized by 30 ± 6% the inhibitory effect of ME (0.8 μM) ($n$ = 5, $P$ < 0.05), whereas DEA/NO (100 μM) enhanced by 65 ± 18% the degree of ME (3 μM)-induced desensitization ($n$ = 5, $p$ < 0.05 *vs* control) (Figs. 1A, 1B and 1D). The firing rate of LC cells was elevated by 101 ± 14% ($n$ = 5, $p$ < 0.05) during DEA/NO (100 μM) perfusion (see baselines in Fig 1A and 1B), which is in agreement with previous studies showing a neuronal activation by various NO donors (Llorente et al., 2012; Pineda et al., 1996; Torrecilla et al., 2007). More importantly, administration of NS 2028 (10 μM) fully prevented both DEA/NO (100 μM)-induced enhancement of MOR desensitization (ME 3 μM) ($n$ = 5, $p$ < 0.05 DEA/NO + NS 2028 *vs* DEA/NO) (Figs. 1C and 1D) and DEA/NO (100 μM)-evoked activation of LC neurons (firing rate change by DEA/NO, after NS 2028: -9 ± 5%, $n$ = 5, $p$ < 0.005 *vs* control, see above). NS 2028 (10 μM) itself did not modify MOR desensitization ($n$ = 3) (Fig. 1D). Finally, no changes were found in the acute effects of ME (0.8 μM) between the different groups (ME effect, control: 86 ± 3%, $n$ = 5; NS 2028: 90 ± 2%, $n$ = 3; DEA/NO: 87 ± 5%, $n$ = 5; and DEA/NO + NS 2028: 92

± 2%, $n$ = 5). These data suggest the contribution of sGC in the enhancement of MOR desensitization and hyperactivity of LC cells induced by NO.

To further explore the involvement of sGC in MOR desensitization, we evaluated the direct effect of sGC activation on ME (3 and 10 μM)-induced desensitization. Perfusion with the sGC activators A 350619 (30 μM) and BAY 418543 (1 μM) enhanced by 93 ± 15% and 90 ± 6%, respectively, the ME (3 μM)-induced MOR desensitization ($n$ = 5, $p$ < 0.01 *vs* control; and $n$ = 5, $p$ < 0.005 *vs* control; respectively) (Figs. 2A, 2B and 2C). BAY 418543 (1 μM) elevated by 51 ± 16% the firing activity of LC neurons ($n$ = 5, $p$ < 0.05). There was no change in the acute effects of ME (0.8 μM) between the different groups (ME effect, A 350619: 88 ± 3%, $n$ = 5; BAY 418543: 94 ± 2%, $n$ = 5). On the other hand, perfusion with a higher concentration of ME (10 μM, 10 min) reduced by 61 ± 3% the inhibitory effect of ME (0.8 μM) ($n$ = 8, $p$ < 0.005), which was a significantly stronger desensitization ($p$ < 0.005) than that induced by ME (3 μM) (see above; Figs. 3A and 3C). Unexpectedly, administration of two different concentrations of the sGC inhibitors NS 2028 (10 and 30 μM) and ODQ (10 and 30 μM) failed to modify the degree of ME (10 μM)-induced MOR desensitization, so that opioid effects were still desensitized in the presence of these inhibitors (NS 2028 10 and 30 μM: $n$ = 6, $p$ < 0.005 and $n$ = 3, $p$ < 0.005, respectively; ODQ 10 and 30 μM: $n$ = 5, $p$ < 0.005 and $n$ = 6, $p$ < 0.005, respectively) (Figs. 3B and 3C).

### *3.2. Involvement of cyclic GMP-dependent protein kinase in opioid-induced MOR desensitization in the locus coeruleus*

We have previously postulated that endogenous NO may mediate MOR desensitization and tolerance in the LC (Santamarta et al., 2005; 2014). To investigate the

contribution of cGMP/PKG pathway to NO-mediated MOR desensitization, we explored the effect of a soluble cGMP analogous that activates the PKG (8-Br-cGMP). Herein, administration of the neuronal NOS inhibitor 7-NI (100 μM) reduced by 60 ± 8% the degree of ME (10 μM)-induced desensitization in LC neurons ($n$ = 4, $p$ < 0.005 *vs* control desensitization) (Fig. 4A and 4D, see above for control). Perfusion 8-Br-cGMP (100 and 300 μM) fully prevented 7-NI from blocking MOR desensitization, so that ME (10 μM)-induced desensitization in the presence of 8-Br-cGMP (100 or 300 μM) + 7-NI (100 μM) was significantly greater than in the presence of 7-NI (100 μM) alone ($n$ = 3, $p$ < 0.05; and $n$ = 5, $p$ < 0.01, respectively) (Figs. 4B and 4D). Therefore, cGMP-dependent events (i.e., PKG) may take part in NO-mediated MOR desensitization. Unexpectedly, administration of the PKG inhibitors H8 (30 and 100 μM) or Rp-8-Br-PET-cGMP (1 μM) failed to modify the degree of ME (10 μM)-induced desensitization (Fig. 4C and 4D) and, thereby, ME (10 μM) caused standard desensitization in the presence of H8 (30 and 100 μM) or Rp-8-Br-PET-cGMP (1 μM) ($n$ = 5, $p$ < 0.005; $n$ = 3, $p$ < 0.05; and $n$ = 4, $p$ < 0.005, respectively) (Fig. 4D).

### *3.3. Involvement of reactive oxygen species in opioid-induced MOR desensitization in the locus coeruleus*

NO reacts with oxygen derivatives to produce reactive nitrogen and oxygen species (ROS) (Davis et al., 2001), which have been shown to contribute to NO-induced enhancement of MOR desensitization in the LC (Llorente et al., 2012). We further explored whether ROS would itself mediate ME (10 μM)-induced desensitization by administration of three structurally unrelated antioxidants. Thus, perfusion of the antioxidants U-74389G (10 μM), melatonin (100 μM) or Trolox (200 μM) failed to

modify the degree of ME (10 μM)-induced desensitization ($n$ = 4 in each group) when compared with the corresponding control group (Figs. 5A and 5C). However, combined perfusion of the antioxidant Trolox (200 μM) and the sGC inhibitor NS 2028 (10 μM) reduced by 37 ± 6% the magnitude of ME (10 μM)-induced desensitization ($n$ = 5, $p$ < 0.005 *vs* control) (Figs. 5B and 5C). This combination (Trolox 200 μM + NS 2028 10 μM) slightly decreased the firing activity of LC neurons (firing rate reduction: 22 ± 4%, $n$ = 5, $p$ < 0.005), although the basal firing rate after perfusion with Trolox + NS 2028 was not significantly different from control (basal firing rate before desensitization, control: 0.72 ± 0.09 Hz, n = 8; Trolox + NS 2028: 0.67 ± 0.13 Hz, $n$ = 5). Finally, no changes in the acute ME (0.8 μM) effects were found between the groups (ME effect, control: 93 ± 1%, $n$ = 8; Trolox + NS 2028: 91 ± 3%, $n$ = 5). This indicates that activation of either of the NO-dependent ROS and sGC/PKG signaling cascades may be enough for induction of MOR desensitization and, therefore, both pathways may be independently triggered by NO to mediate this process.

## 4. Discussion

Previous electrophysiological experiments have shown that NO regulates MOR desensitization in the LC (Llorente et al., 2012; Santamarta et al., 2014; Torrecilla et al., 2001). We have used single-unit extracellular recording techniques in brain slices to characterize the NO-dependent pathways (i.e., sGC and ROS) involved in MOR desensitization in the LC *in vitro*. Our results confirm that ME (3–10 μM) causes a concentration-related desensitization of MOR in the LC, so that the inhibitory effect of ME (0.8 μM) was markedly reduced. ME (3 μM)-induced MOR desensitization was enhanced by perfusion with the NO donor DEA/NO, whereas this enhancement was blocked by the sGC inhibitor NS 2028. Accordingly, ME (3 μM)-induced MOR desensitization was enhanced by two activators of sGC, A 350619 and BAY 418543. On the other hand, ME (10 μM)-induced MOR desensitization was blocked by the nNOS inhibitor 7-NI, a blockade that was prevented by the PKG activator 8-Br-cGMP. In contrast, ME (10 μM)-induced desensitization was not modified by inhibition of sGC (with NS 2028 and ODQ) or PKG (with H8 and Rp-8-Br-PET-cGMP). Perfusion with the antioxidants Trolox, melatonin or U-74389G failed to change ME (10 μM)-induced desensitization, but a combination of an antioxidant (Trolox) with a sGC inhibitor (NS 2028) was able to attenuate ME (10 μM)-induced desensitization.

To study MOR desensitization in the LC, we measured the inhibitory effect of a test concentration of the opioid agonist ME (0.8 μM). ME was used as an indicator of MOR function, because it exerts a full inhibition of the firing activity of LC neurons almost exclusively through MOR (McPherson et al., 2010; Williams and North, 1984). Moreover, ME effect can be tested several times in the same cell, since it rapidly washes out from the tissue after bath perfusion. Therefore, MOR desensitization can be readily measured by extracellular recordings after recovery of the firing from ME-induced

inhibition. Our results confirm that sustained application of ME (3 and 10 μM) causes MOR desensitization in the LC, expressed as a concentration-related decline in the test ME effect (30% and 61%, respectively). This protocol including variable desensitization degrees (i.e., by ME 3 and 10 μM) allowed us to investigate possible regulation of this phenomenon by activators or inhibitors of sGC pathway. Similar degrees of MOR desensitization by ME (3 and 10 μM) have been described by both intracellular electrodes measuring ion currents (Harris and Williams, 1991) and extracellular electrodes recording cell firing rates (Llorente et al., 2012; Santamarta et al., 2014). The firing activity recorded by extracellular techniques may be considered as a closer physiological end-point of MOR desensitization at the synaptic level of the neuron.

ME (3 μM)-induced MOR desensitization was enhanced by 65% in the presence of the NO donor DEA/NO. Likewise, previous electrophysiological experiments *in vitro* have shown that the NO donor sodium nitroprusside also enhances MOR desensitization in the LC (Llorente et al., 2012). The main direct target of NO is the sGC, which catalyzes the production of cGMP from GTP (Hoffmann and Chen, 2014; Kots et al., 2009). The LC has been reported to express the $\alpha_1$ and ß$_1$ subunits of the sGC (Furuyama et al., 1993; Matsuoka et al., 1992; Pifarré et al., 2007) and, accordingly, detectable concentrations of cGMP are measured in the LC (Vulliemoz et al., 1999; Xu et al., 1998a). Herein, ME (3 μM)-induced MOR desensitization in LC neurons was enhanced by ~90% after perfusion with two structurally unrelated sGC activators, A 350619 or BAY 418543. Both activators enhance the catalytic function of sGC in an NO-independent manner, although they can also act synergically with NO (Mayer and Koesling, 2001; Stasch et al. 2002). BAY 418543 lacks any effect on phosphodiesterase activity (Stasch et al., 2002). Accordingly, we found that DEA/NO-induced enhancement of MOR desensitization was prevented by NS 2028, an irreversible inhibitor of NO-

dependent sGC activation in homogenates and slice preparations of the brain (Olesen et al., 1998). A high concentration of NO in the LC as that reached during DEA/NO administration could be obtained when nNOS expression is elevated in this nucleus, as described by chronic morphine treatments (Cuéllar et al., 2000). None of the drugs targeting the NO/sGC pathway in the present work (DEA/NO, NS 2028, A 350619 or BAY 418543) altered the acute effects of ME (0.8 μM) (before desensitization). Therefore, our data indicate that activation of sGC signaling can enhance MOR desensitization and also mediate the enhancement of MOR desensitization induced by raising the NO concentration in the LC. Other authors have reported *in vivo* that treatment with sGC activators enhances the development and expression of analgesic tolerance to morphine (Ozdemir et al., 2011) and administration of sGC inhibitors prevents the development of analgesic tolerance to morphine (Durmus et al., 2014; Xu et al., 1998b).

As discussed above, perfusion with high concentrations of ME (10 μM) induce a near-maximal degree of MOR desensitization in the absence of NO enhancers ("high MOR desensitization") (Harris and Williams, 1991; Santamarta et al., 2014). We herein found that the neuronal-selective NOS inhibitor 7-NI reduced by more than 50% the magnitude of high MOR desensitization. Previous *in vitro* reports have described that lowering the endogenous production of NO by different neuronal-selective NOS inhibitors also attenuates the development of high MOR desensitization in the LC (Santamarta et al., 2014; Torrecilla et al., 2001). Likewise, inhibition of nNOS *in vivo* has been described to reduce the induction of morphine tolerance (Highfield and Grant, 1998; Santamarta et al., 2005) and morphine withdrawal (Pineda et al., 1998) in the LC. A high amount of type II PKG mRNA, one of the main cGMP targets (Kots et al., 2009), has been detected in the LC (El-Husseini et al., 1995). In the present study, we observed that high MOR desensitization was restored from 7-NI-induced blockade by addition of 8-Br-

cGMP, a cell permeable cGMP analog with high potency for type II PKG activation (Pöhler et al., 1995). This suggests that downstream regulation of cGMP/PKG pathway by NO may account for the effect of nNOS inhibitors on high MOR desensitization in the LC. Interestingly, sGC activity and type II PKG expression are up-regulated by morphine treatments in mice (Liang and Clarck, 2004; Muraki et al., 1982) and, therefore, the contribution of cGMP to MOR desensitization mediated by endogenous NO could be functionally relevant *in vivo*. Paradoxically, we did not detect any change in the extent of high MOR desensitization after independent administrations of high concentrations of sGC inhibitors (NS 2028 10–30 μM or ODQ 10–30 μM) or PKG inhibitors (H8 30-100 μM or Rp-8-Br-PET-cGMP 1 μM). These drugs have been previously used as effective inhibitors of cGMP/PKG signaling. Thus, ODQ is a NS 2028 analog that inhibits brain sGC activity *in vitro* with lower potency than NS 2028 (Garthwaite et al., 1995; Olesen et al., 1998). H8 and Rp-8-Br-PET-cGMP are two cell-permeable, potent inhibitors of PKG that show 3- and 300-fold higher selectivities for PKG, respectively, than for PKA (Hidaka et al., 1984; Smolenski et al., 1998). H8 has been shown to antagonize the electrophysiological effects of cGMP but not cAMP on LC neurons (Pineda et al., 1996). Similarly, intracerebroventricular administration of the PKG inhibitor KT-5823 fails to alter morphine tolerance *in vivo* (Bernstein and Welch, 1997).

On the other hand, ROS have been reported to regulate MOR desensitization in the LC (Llorente et al., 2012). We found no change in the degree of high MOR desensitization (ME 10 μM) after separate administrations of antioxidant agents (U-74389G, melatonin or Trolox). U-74389G and melatonin are two lipid-soluble antioxidants that protect against the effects induced by ROS (Khalil et al., 1998; Noda et al., 1999; Taherzadeh et al., 2006), whereas Trolox is a cell-permeable vitamin E derivative that prevents oxidative stress in rat models (Balogh et al., 2005). In contrast,

combined administrations of a sGC inhibitor (NS 2028) and an antioxidant agent (Trolox) significantly attenuated the development of high MOR desensitization, whereas they did not affect the acute effect of ME. Therefore, these results (together with 8-Br-cGMP data, see above) indicate that endogenous production of NO from nNOS purportedly caused by high ME concentrations would induce MOR desensitization by independent activation of sGC/PKG and ROS signaling pathways. Either of these cascades would be enough by itself to trigger the induction of high MOR desensitization by endogenous NO, so that both pathways should be simultaneously blocked to observe a reduced desensitization. The mechanism by which NO is generated and the exact NO-dependent events regulated by sGC/PKG and ROS remain as yet to be elucidated. Thus, NO-dependent activation of PKG has been speculated to mediate MOR desensitization by phosphorylating a substrate that affects MOR/G protein interaction or by counteracting the opioid effect on nonselective cation channels (Santamarta et al., 2014). Furthermore, several oxidative mechanisms have been proposed to regulate MOR desensitization, including possible ROS-induced activation of PKC (Llorente et al., 2012).

It has been reported that NO modulates the firing activity of LC neurons by activation of sGC, the subsequent increase of cGMP levels and stimulation of PKG (Pineda et al., 1996; Xu et al., 1998a). Our work demonstrates that DEA/NO elevates by about 100% the firing rate of LC neurons and this excitatory effect is prevented by administration of the sGC inhibitor NS 2028. Furthermore, a 51% elevation of the spontaneous firing rate of LC cells was obtained after sGC stimulation with BAY 418543 and a slight reduction of the firing activity was observed after a combined perfusion with a sGC inhibitor (NS 2028) and an antioxidant (Trolox). Therefore, data obtained from the present work are compatible with an excitatory regulation of the firing activity of LC neurons by NO through the sGC/PKG pathway.

Morphine dependence and withdrawal are associated with neuroadaptive changes in the neuronal NOS activity (Vaupel et al., 1997). During conditions in which nNOS expression is raised (such as during morphine dependence), NO concentrations would be expected to be higher (Cuéllar et al., 2000). Our results demonstrate that submaximal MOR desensitization induced by an intermediate concentration of ME (3 μM) can be enhanced by raising the concentrations of NO and by activating the sGC in the LC. NO-induced enhancement appears to be blocked by a sGC inhibitor. Our previous work has shown that antioxidant agents attenuate the enhancement of MOR desensitization induced by high concentrations of NO in the LC (Llorente et al., 2012). Removal of ROS also prevents the appearance of analgesic tolerance caused by opioids (Muscoli et al., 2007). Therefore, these data indicate that a combined activation of both signaling cascades, cGMP and ROS, may be needed to enhance MOR desensitization by high NO levels in this nucleus, so that inhibition of either of these pathways would disrupt the enhancement induced by NO. On the other hand, strong MOR desensitization obtained by high ME concentrations (10 μM) can be blocked by nNOS inhibition or by a combination of an antioxidant and a sGC inhibitor. MOR desensitization is restored from nNOS inhibition by activation of PKG. Therefore, we conclude that endogenous NO derived from nNOS activity may mediate the development of strong MOR desensitization through downstream regulation of independent sGC/PKG and ROS pathways in the LC. Hypothetically, a pharmacological protection against NO-derived cGMP and ROS generation would result in prevention of opiate tolerance and maintaining a better control of pain with chronic opiates.

**Acknowledgements**

This work was supported by the Ministerio de Ciencia e Innovación [Grant SAF2008-03612] and the University of the Basque Country (UPV/EHU) [Grant GIU11/27 and Grant GIU14/29]. Pineda´s research group takes part in a network unit supported by the University of the Basque Country [UFI 11/35]. I. P. Pablos was supported by a predoctoral fellowship from the Basque Government. There is no conflict of interest and no financial relationship with the Organization that sponsored the research. The experiments comply with the current laws of Spain. We want to thank to Dr. M. T. Santamarta for her preliminary contribution to this work.

**Conflict of interest**

The authors declare that there is no conflict of interest.

**References**

Andrade, R., Aghajanian, G.K., 1984. Locus coeruleus activity *in vitro*: intrinsic regulation by a calcium-dependent potassium conductance but not alpha 2-adrenoceptors. J. Neurosci. 4, 161–170.

Arttamangkul, S., Lau, E. K., Lu, H. W., Williams, J. T., 2012. Desensitization and trafficking of μ-opioid receptors in locus ceruleus neurons: modulation by kinases. Mol. Pharmacol. 81, 348–355.

Balogh, G. T., Vukics, K., Könczöl, A., Kis-Varga, A., Gere, A., Fischer, J., 2005. Nitrone derivatives of Trolox as neuroprotective agents. Bioorg. Med. Chem. Lett. 15, 3012–3015.

Bernstein, M. A., Welch, S. P., 1997. Effects of spinal versus supraspinal administration of cyclic nucleotide-dependent protein kinase inhibitors on morphine tolerance in mice. Drug Alcohol Depend. 44, 41–46.

Cao, J. L., Vialou, V. F., Lobo, M. K., Robison, A. J., Neve, R. L., Cooper, D. C., Nestler, E. J., Han, M. H., 2010. Essential role of the cAMP-cAMP response-element binding protein pathway in opiate-induced homeostatic adaptations of locus coeruleus neurons. Proc. Natl. Acad. Sci. U.S.A. 107, 17011–17016.

Cuéllar, B., Fernández, A. P., Lizasoain, I., Moro, M. A., Lorenzo, P., Bentura, M. L., Rodrigo, J., and Leza, J. C., 2000. Up-regulation of neuronal synthase immunoreactivity in opiate dependence and withdrawal. Psychopharmacology 148, 66–73.

Dang, V. C., Christie, M. J., 2012. Mechanisms of rapid opioid receptor desensitization, resensitization and tolerance in brain neurons. Br. J. Pharmacol. 165, 1704–1716.

Davis, K. L., Martin, E., Turko, I. V., Murad, F., 2001. Novel effects of nitric oxide. Annu. Rev. Pharmacol. Toxicol. 41, 203–236.

Degerman, E., Belfrage, P., Manganiello, V. C., 1997. Structure, localization, and regulation of cGMP-inhibited phosphodiesterase (PDE3). J. Biol. Chem. 272, 6823–6826.

Durmus, N., Bagcivan, I., Ozdemir, E., Altun, A., Gursoy, S., 2014. Soluble guanylyl cyclase activators increase the expression of tolerance to morphine analgesic effect. Bratisl. Lek. Listy. 115, 334–339.

El-Husseini, A. E., Bladen, C., Vincent S. R., 1995. Molecular characterization of a type II cyclic GMP-dependent protein kinase expressed in the rat brain. J. Neurochem. 64, 2814–2817.

Furuyama, T., Inagaki, S., Takagi, H., 1993. Localizations of alpha-1 and beta-1 subunits of soluble guanylate cyclase in the rat brain. Mol. Brain Res. 20, 335–344.

Garthwaite, J., Southam, E., Boulton, C.L., Nielsen, E.B., Schmidt, K., Mayer, B., 1995. Potent and selective inhibition of nitric oxide-sensitive guanylyl cyclase by 1H-[1,2,4]oxadiazolo[4,3-a]quinoxalin-1-one. Mol. Pharmacol. 48, 184–188.

Grandoso, L., Pineda, J., Ugedo, L., 2004. Comparative study of the effects of desipramine and reboxetine on locus coeruleus neurons in rat brain slices. Neuropharmacology 46, 815–823.

Harris, G. C., Williams, J. T., 1991. Transient homologous mu-opioid receptor desensitization in rat locus coeruleus neurons. J. Neurosci. 11, 2574–2581.

Hidaka, H., Inagaki, M., Kawamoto, S., Sasaki, Y., 1984. Isoquinolinesulfonamides, novel and potent inhibitors of cyclic nucleotide dependent protein kinase and protein kinase C. Biochemistry 23, 5036–5041.

Highfield, D. A., Grant, S., 1998. $N^{\omega}$-nitro-L-arginine, an NOS inhibitor, reduces tolerance to morphine in the rat locus coeruleus. Synapse 29, 233–239.

Hoffmann, L. S., Chen, H. H., 2014. cGMP: transition from bench to bedside: a report of the 6th International Conference on cGMP Generators, Effectors and Therapeutic Implications. Naunyn Schmiedebergs Arch. Pharmacol. 387, 707–718.

Ignarro, L. J., 1991. Heme-dependent activation of guanylate cyclase by nitric oxide: a novel signal transduction mechanism. Blood Vessels 28, 67–73.

Khalil, A., Fortun, A., Hebert, S., Jay-Gerin, J. P., El Abbouyi, A., Wallach, J., Fulop, T., Jr., 1998. Novel 21-aminosteroid U-74389G inhibits low-density lipoprotein peroxidation induced by $^{\cdot}OH$ and $O_2^{-\cdot}$ free radicals. Life Sci. 63, 769–779.

Kots, A.Y., Martin, E., Sharina, I. G., Murad, F., 2009. A short history of cGMP, guanylyl cyclases, and cGMP-dependent protein kinases. Handb. Exp. Pharmacol. 191, 1–14.

Liang, D. Y., Clark, J. D., 2004. Modulation of the NO/CO-cGMP signaling cascade during chronic morphine exposure in mice. Neurosci. Lett. 365, 73–77.

Llorente, J., Santamarta, M. T., Henderson, G., Pineda, J., 2012. Enhancement of μ opioid receptor desensitization by nitric oxide in rat locus coeruleus neurons: involvement of reactive oxygen species. J. Pharmacol. Exp. Ther. 342, 552–560.

Lohmann, S. M., Vaandrager, A. B., Smolenski, A., Walter, U., de Jonge H. R., 1997. Distinct and specific functions of cGMP-dependent protein kinases. Trends Biochem. Sci. 22, 307–312.

Matsuoka, I., Giuili, G., Poyard, M., Stengel, D., Parma, J., Guellaen, G., Hanoune J., 1992. Localization of adenylyl and guanylyl cyclase in rat brain by in situ hybridization: comparison with calmodulin mRNA distribution. J. Neurosci. 12, 3350–3360.

Mayer, B., Koesling, D., 2001. cGMP signalling beyond nitric oxide. Trends Pharmacol. Sci. 22, 546–548.

McPherson, J., Rivero, G., Baptist, M., Llorente, J., Al-Sabah, S., Krasel, C., Dewey, W. L., Bailey, C. P., Rosethorne, E.M., Charlton, S.J., Henderson, G., Kelly, E., 2010. μ-opioid receptors: correlation of agonist efficacy for signalling with ability to activate internalization. Mol. Pharmacol. 78, 756–766.

Mendiguren, A., Pineda J., 2007. $CB_1$ cannabinoid receptors inhibit the glutamatergic component of KCl-evoked excitation of locus coeruleus neurons in rat brain slices. Neuropharmacology 52, 617–625.

Muraki, T., Uzumaki, H., Kato, R., 1982. Strain difference in morphine-induced increase in plasma cyclic AMP and cyclic GMP levels in relation to locomotor activity in male mice. Psychopharmacology 76, 316–319.

Muscoli, C., Cuzzocrea, S., Ndengele, M. M., Mollace, V., Porreca, F., Fabrizi, F., Esposito, E., Masini, E., Matuschak, G. M., Salvemini, D., 2007. Therapeutic manipulation of peroxynitrite attenuates the development of opiate-induced antinociceptive tolerance in mice. J. Clin. Invest. 117, 3530–3539.

Nestler, E. J., Aghajanian, G. K., 1997. Molecular and cellular basis of addiction. Science 278, 58–63.

Nestler, E. J., Alreja, M., Aghajanian, G. K., 1994. Molecular and cellular mechanisms of opiate action: studies in the rat locus coeruleus. Brain Res. Bull. 35, 521–528.

Noda, Y., Mori, A., Liburdy, R., Packer, L., 1999. Melatonin and its precursors scavenge nitric oxide. J. Pineal Res. 27, 159–163.

Olesen, S. P., Drejer, J., Axelsson, O., Moldt, P., Bang, L., Nielsen-Kudsk, J. E., Busse, R., Mülsch, A., 1998. Characterization of NS 2028 as a specific inhibitor of soluble guanylyl cyclase. Br. J. Pharmacol. 123, 299–309.

Ozdemir, E., Bagcivan, I., Durmus, N., Altun, A., Gursoy, S., 2011. The nitric oxide-cGMP signaling pathway plays a significant role in tolerance to the analgesic effect of morphine. Can. J. Physiol. Pharmacol. 89, 89–95.

Pasternak, G. W., Kolesnikov, Y. A., Babey, A. M., 1995. Perspectives on the N-methyl-D aspartate/nitric oxide cascade and opioid tolerance. Neuropsychopharmacology 13, 309–313.

Paxinos, G., Watson, C., 2005. The Rat Brain in Stereotaxic Coordinates. 5th ed, Burlington, Massachusetts: Elsevier Academic Press.

Pifarré, P., García, A., Mengod, G., 2007. Species differences in the localization of soluble guanylyl cyclase subunits in monkey and rat brain. J. Comp. Neurol. 500, 942–957.

Pineda, J., Kogan, J. H., Aghajanian, G. K., 1996. Nitric oxide and carbon monoxide activate locus coeruleus neurons through a cGMP-dependent protein kinase: involvement of a nonselective cationic channel. J. Neurosci. 16, 1389–1399.

Pineda, J., Torrecilla, M., Martín-Ruiz, R., Ugedo, L., 1998. Attenuation of withdrawal-induced hyperactivity of locus coeruleus neurones by inhibitors of nitric oxide synthase in morphine-dependent rats. Neuropharmacology 37, 759–767.

Pöhler, D., Butt, E., Meissner, J., Müller, S., Lohse, M., Walter, U., Lohmann, S. M., Jarchau, T., 1995. Expression, purification, and characterization of the cGMP-dependent protein kinases I beta and II using the baculovirus system. FEBS Lett. 374, 419–425.

Santamarta, M. T., Llorente, J., Mendiguren, A., Pineda, J., 2014. Involvement of neuronal nitric oxide synthase in desensitisation of μ-opioid receptors in the rat locus coeruleus. J. Psychopharmacol. 28, 903–914.

Santamarta, M. T., Ulibarri, I., Pineda J., 2005. Inhibition of neuronal nitric oxide synthase attenuates the development of morphine tolerance in rats. Synapse 57, 38–46.

Smolenski, A., Burkhardt, A.M., Eigenthaler, M., Butt, E., Gambaryan, S., Lohmann, S. M., Walter, U., 1998. Functional analysis of cGMP-dependent protein kinases I and II as mediators of NO/cGMP effects. Naunyn Schmiedebergs Arch. Pharmacol. 358, 134–139.

Stasch, J. P., Alonso-Alija, C., Apeler, H., Dembowsky, K., Feurer, A., Minuth, T., Perzborn, E., Schramm, M., Straub, A., 2002. Pharmacological actions of a novel

NO-independent guanylyl cyclase stimulator, BAY 418543: in vitro studies. Br. J. Pharmacol. 135, 333–343.

Taherzadeh, M., Fradette, C., Bleau, A. M., Jomphe, C., Trudeau, L.E., du Souich P., 2006. The 21-aminosteroid U74389G prevents the down-regulation and decrease in activity of CYP1A1, 1A2 and 3A6 induced by an inflammatory reaction. Biochem. Pharmacol. 71, 366–376.

Taylor, D. A., Fleming, W.W., 2001. Unifying perspectives of the mechanisms underlying the development of tolerance and physical dependence to opioids. J. Pharmacol. Exp. Ther. 297, 11–18.

Torrecilla, M., Pineda, J., Ugedo, L., 2001. NO synthase inhibitors reduce opioid desensitization in rat locus coeruleus neurons in vitro. Neuroreport 12, 1601–1604.

Torrecilla, M., Ruiz-Ortega, J. A., Ugedo, L., Pineda, J., 2007. Excitatory regulation of noradrenergic neurons by L-arginine/nitric oxide pathway in the rat locus coeruleus in vivo. Naunyn Schmiedebergs Arch. Pharmacol. 375, 337–347.

Vaupel, D.B., Kimes, A.S., London, E.D., 1997. Further in vivo studies on attenuating morphine withdrawal: isoform-selective nitric oxide synthase inhibitors differ in efficacy. Eur. J. Pharmacol. 324, 11–20.

Vulliemoz, Y., Whittington, R. A., Virag, L., 1999. The nitric oxide-cGMP system of the locus coeruleus and the hypnotic action of alpha-2 adrenergic agonists. Brain Res. 849, 169–174.

Wang, Y.Y., Aghajanian, G.K., 1987. Excitation of locus coeruleus neurons by an adenosine 3',5'-cyclic monophosphate-activated inward current: extracellular and intracellular studies in rat brain slices. Synapse 1, 481–487.

Williams, J. T., North, R. T., 1984. Opiate-receptor interactions on single locus coeruleus neurons. Mol. Pharmacol. 26, 489–497.

Xu, Z. Q., de Vente, J., Steinbusch, H., Grillner, S., Hokfelt, T., 1998a. The NO-cGMP pathway in the rat locus coeruleus: electrophysiological, immunohistochemical and in situ hybridization studies. Eur. J. Neurosci. 10, 3508–3516.

Xu, J. Y., Hill, K. P., Bidlack, J. M., 1998b. The nitric oxide/cyclic GMP system at the supraspinal site is involved in the development of acute morphine antinociceptive tolerance. J. Pharmacol. Exp. Ther. 284, 196–201.

Zagotta, W. N., Siegelbaum, S.A., 1996. Structure and function of cyclic nucleotide-gated channels. Annu. Rev. Neurosci. 19, 235–263.

**Figure legends**

**Figure 1.** Effect of DEA/NO and DEA/NO + NS 2028 on ME (3 μM, 10 min)-induced MOR desensitization. **A, B, C.** Representative examples of firing-rate recordings of LC cells showing the effect of ME (0.8 μM, 1 min) before and 5 min after application of ME (3 μM, 10 min) in control slices (**A**), in slices perfused with DEA/NO (100 μM (**B**) or DEA/NO (100 μM) + NS 2028 (10 μM) (**C**). The horizontal bars indicate the period of drug applications and the vertical lines show the number of spikes recorded every 10 s. **D.** Bar histograms show the mean ± S.E.M of ME (3 μM, 10 min)-induced desensitization in the absence ($n$ = 5) or the presence of NS 2028 (10 μM, $n$ = 3), DEA/NO (100 μM, $n$ = 5) or NS 2028 (10 μM) + DEA/NO (100 μM) ($n$ = 5). Desensitization degrees were calculated as percentage values (see *Data analysis and statistics*). Note that DEA/NO markedly enhanced MOR desensitization and NS 2028 fully prevented the enhancement of MOR desensitization induced by DEA/NO. *$p < 0.05$ when compared with the control group (two-sample Student's $t$ test), and † $p < 0.05$ when compared with the DEA/NO group (two-sample Student's $t$ test).

**Figure 2.** Effect of A 350619 and BAY 418543 on ME (3 μM, 10 min)-induced desensitization. **A, B.** Representative examples of firing-rate recordings of LC cells showing the effect of ME (0.8 μM, 1 min) before and 5 min after application of ME (3 μM, 10 min) in slices perfused with A 350619 (30 μM) (**A**) or BAY 418543 (1 μM) (**B**). The horizontal bars indicate the period of drug applications and the vertical lines show the number of spikes recorded every 10 s. **C.** Bar histograms show the mean ± S.E.M of ME (3 μM, 10 min)-induced desensitization in the presence of A 350619 (30 μM, $n$ = 5) or BAY 418543 (1 μM, $n$ = 5). Desensitization degrees were calculated as percentage values

(see *Data analysis and statistics*). Note that A 350619 and BAY 418543 markedly enhanced MOR desensitization. *$p < 0.01$ and **$p < 0.005$ when compared with the control group (two-sample Student's *t* test).

**Figure 3.** Effect of NS 2028 and ODQ on ME (10 μM, 10 min)-induced desensitization. **A, B.** Representative examples of firing-rate recordings of LC cell showing the inhibitory effect of ME (0.8 μM, 1 min) before (basal) and 5 min after application of ME (10 μM, 10 min) in control slices (**A**) and in slices perfused with NS 2028 (10 μM) (**B**). The horizontal bars indicate the period of drug applications and the vertical lines show the number of spikes recorded every 10 s. **C.** Bar histograms show the mean ± S.E.M of ME (10 μM, 10 min)-induced desensitization in the absence ($n = 8$, control) or the presence of ODQ (10 μM, $n = 5$ and 30 μM, $n = 6$) or NS 2028 (10 μM, $n = 6$ and 30 μM, $n = 3$). Desensitization degrees were calculated as percentage values (see *Data analysis and statistics*). Note that ME-induced desensitization was not changed in the presence of NS 2028 or ODQ.

**Figure 4.** Effect of 7-NI, 8-Br-cGMP + 7-NI, H8 and Rp-8-Br-PET-cGMP on ME (10 μM, 10 min)-induced desensitization of LC neurons *in vitro*. **A, B, C** Representative examples of firing-rate recordings of LC cells showing the effect of ME (0.8 μM, 1 min) before and 5 min after application of ME (10 μM, 10 min) in slices perfused with 7-NI (100 μM) (**A**) 8-Br-cGMP (300 μM) + 7-NI (100 μM) (**B**) or H8 (100 μM) (**C**). The horizontal bars indicate the period of drug applications and the vertical lines show the number of spikes recorded every 10 s. **D.** Bar histograms show the mean ± S.E.M of ME

(10 μM)-induced desensitization in the absence ($n$ = 8, control) or the presence of 7-NI (100 μM, $n$ = 4), 8-Br-cGMP (100 μM and 300 μM) + 7-NI (100 μM) ($n$ = 3 and $n$ = 5, respectively), H8 (30 μM, $n$ = 5 and 100 μM, $n$ = 3) or Rp-8-Br-PET-cGMP (1 μM, $n$ = 4). Desensitization degrees were calculated as percentage values (see *Data analysis and statistics*). Note that 7-NI attenuated MOR desensitization and that both concentrations of 8-Br-cGMP (100 μM or 300 μM) restored the desensitization. *$p$ < 0.005 compared with the control group (two-sample Student's $t$ test), and †$p$ < 0.05, ††$p$ < 0.01 compared with the 7-NI group (two-sample Student's $t$ test).

**Figure 5.** Effect of Trolox, Trolox + NS 2028, U-74389G and melatonin on ME (10 μM, 10 min)-induced desensitization. **A, B.** Representative examples of firing-rate recordings of LC cells showing the effect of ME (0.8 μM, 1 min) before and 5 min after application of ME (10 μM, 10 min) in slices perfused with Trolox (200 μM) (**A**) or Trolox (200 μM) + NS 2028 (10 μM) (**B**). Drugs were bath applied for the time indicated by the horizontal bars. Vertical lines represent the number of spikes recorded every 10 s. **C**. Bar histograms show the mean ± S.E.M of ME (10 μM)-induced desensitization in the absence ($n$ = 8, control) or the presence of U-74389G (10 μM, $n$ = 4), melatonin (100 μM, $n$ = 4), Trolox (200 μM, $n$ = 4) or Trolox (200 μM) + NS 2028 (10 μM) ($n$ = 5). Desensitization degrees were calculated as percentage values (see *Data analysis and statistics*). Note that in the presence of Trolox + NS 2028 MOR desensitization was markedly attenuated. *$p$ < 0.005 compared with the control group (two-sample Student's $t$ test).

**Highlights**

- The involvement of sGC/PKG and ROS in MOR desensitization was explored by extracellular recordings in the rat LC.
- MOR desensitization was enhanced by a NO donor and sGC activators. NO effect was blocked by a sGC inhibitor.
- MOR desensitization was blocked by a nNOS inhibitor and also a combination of an antioxidant and a sGC inhibitor. A PKG activator restored MOR desensitization.
- NO derived from nNOS would mediate MOR desensitization through independent regulation of PKG and ROS pathways in the LC.

**FIGURE 1**

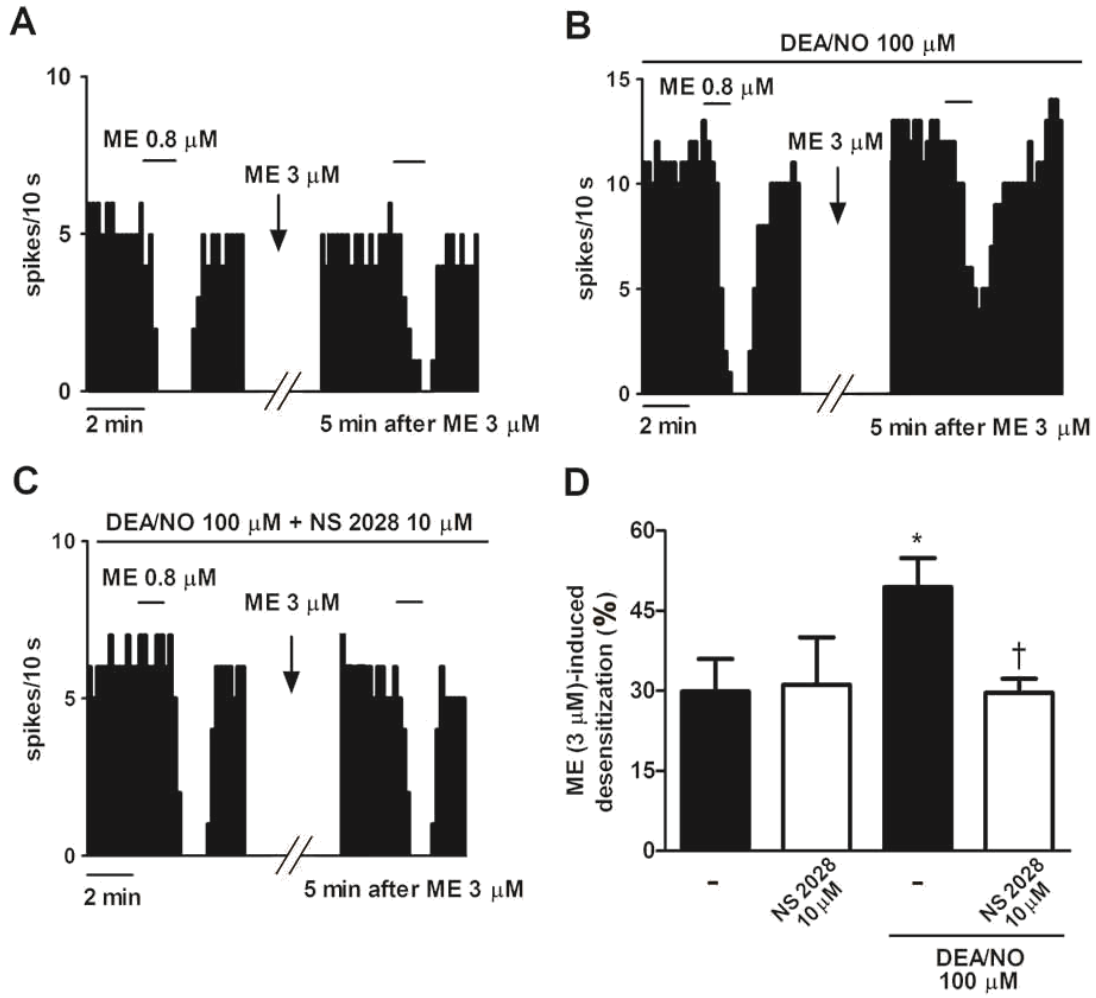
A
10
5
0
spikes/10 s
ME 0.8 μM
ME 3 μM
2 min
5 min after ME 3 μM
B
DEA/NO 100 μM
15
10
5
0
spikes/10 s
ME 0.8 μM
ME 3 μM
2 min
5 min after ME 3 μM
C
DEA/NO 100 μM + NS 2028 10 μM
10
5
0
spikes/10 s
ME 0.8 μM
ME 3 μM
2 min
5 min after ME 3 μM
D
60
45
30
15
0
ME (3 μM)-induced desensitization (%)
*
†
-
NS 2028 10 μM
-
NS 2028 10 μM
DEA/NO 100 μM

**FIGURE 2**

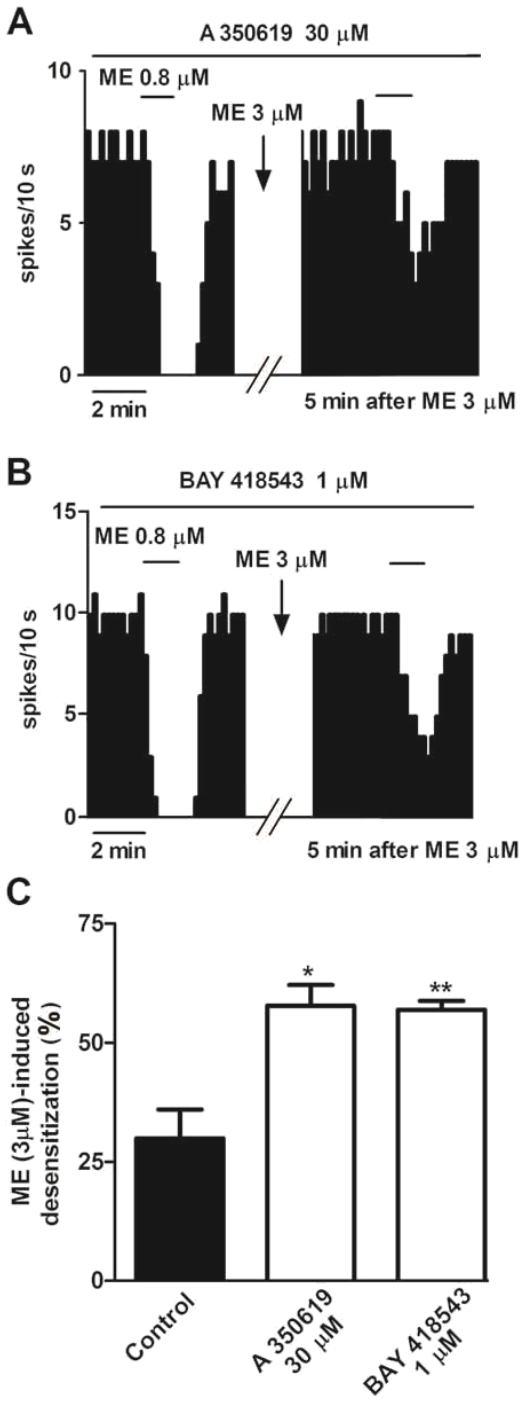
A
A 350619 30 μM
ME 0.8 μM
ME 3 μM
spikes/10 s
10
5
0
2 min
5 min after ME 3 μM
B
BAY 418543 1 μM
ME 0.8 μM
ME 3 μM
spikes/10 s
15
10
5
0
2 min
5 min after ME 3 μM
C
ME (3μM)-induced desensitization (%)
75
50
25
0
*
**
Control
A 350619 30 μM
BAY 418543 1 μM

**FIGURE 3**

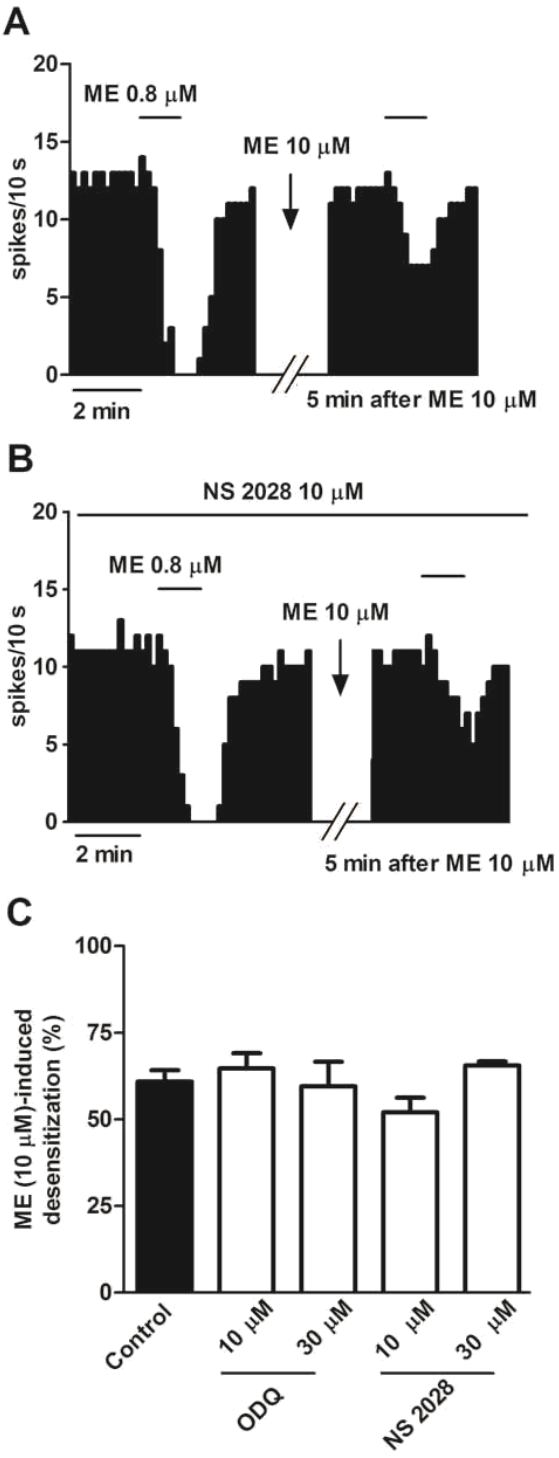
A
ME 0.8 μM
ME 10 μM
spikes/10 s
20
15
10
5
0
2 min
5 min after ME 10 μM
B
NS 2028 10 μM
ME 0.8 μM
ME 10 μM
spikes/10 s
2 min
5 min after ME 10 μM
C
ME (10 μM)-induced desensitization (%)
100
75
50
25
0
Control
10 μM
30 μM
10 μM
30 μM
ODQ
NS 2028

**FIGURE 4**

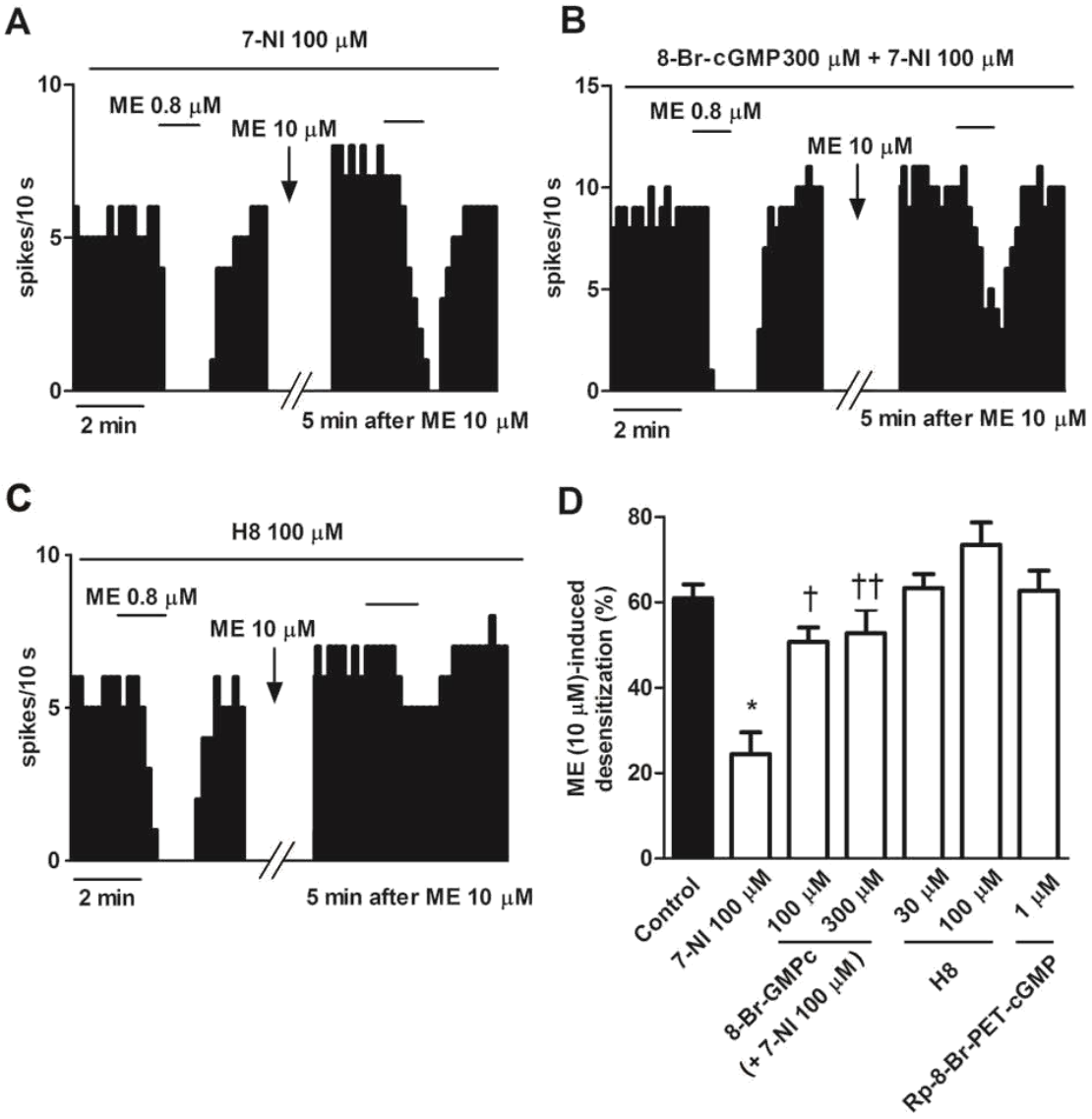
A
7-NI 100 μM
ME 0.8 μM
ME 10 μM
spikes/10 s
10
5
0
2 min
5 min after ME 10 μM
B
8-Br-cGMP300 μM + 7-NI 100 μM
ME 0.8 μM
ME 10 μM
spikes/10 s
15
10
5
0
2 min
5 min after ME 10 μM
C
H8 100 μM
ME 0.8 μM
ME 10 μM
spikes/10 s
10
5
0
2 min
5 min after ME 10 μM
D
ME (10 μM)-induced desensitization (%)
80
60
40
20
0
*
†
††
Control
7-NI 100 μM
100 μM
300 μM
8-Br-cGMPc (+ 7-NI 100 μM)
30 μM
100 μM
H8
1 μM
Rp-8-Br-PET-cGMP

**FIGURE 5**

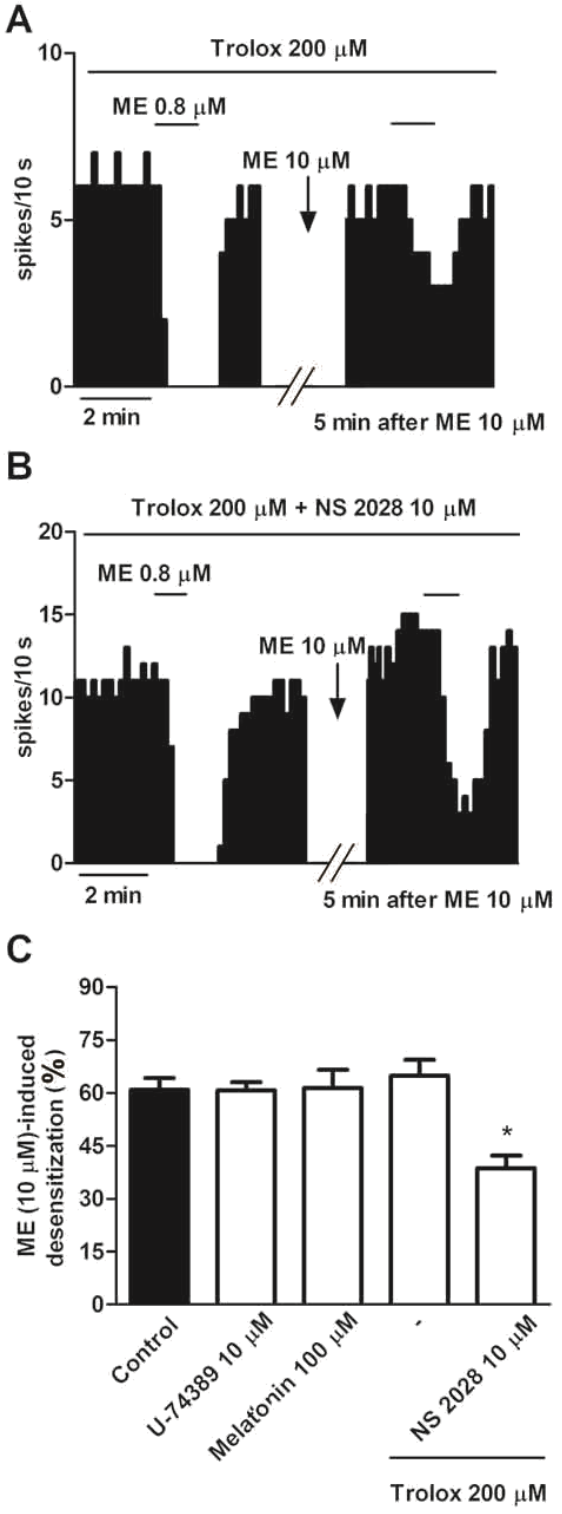
A
Trolox 200 μM
ME 0.8 μM
ME 10 μM
spikes/10 s
10
5
0
2 min
5 min after ME 10 μM
B
Trolox 200 μM + NS 2028 10 μM
ME 0.8 μM
ME 10 μM
spikes/10 s
20
15
10
5
0
2 min
5 min after ME 10 μM
C
ME (10 μM)-induced desensitization (%)
90
75
60
45
30
15
0
*
Control
U-74389 10 μM
Melatonin 100 μM
-
NS 2028 10 μM
Trolox 200 μM

# MANUSCRIPT 2

To be submitted to *British Journal of Pharmacology*

**Title:** STUDY OF THE INVOLVEMENT OF NEURONAL NITRIC OXIDE IN MORPHINE-INDUCED DESENSITIZATION OF μ-OPIOID RECEPTORS IN THE RAT LOCUS COERULEUS

**Authors:** Patricia Pablos[1], Aitziber Mendiguren[1] and Joseba Pineda[1*].

[1]Department of Pharmacology, Faculty of Medicine and Odontology, University of the Basque Country (UPV/EHU), E-48940 Leioa, Bizkaia, Spain

**Short running title:** Nitric oxide and morphine desensitization

*__Corresponding author details__:

Name: Dr. Joseba Pineda

Email: joseba.pineda@ehu.es

Phone: (+34) 94 6015577 Fax: (+34) 94 6013220

Adress: Dept. of Pharmacology, Fac. of Medicine and Odontology, Univ. of the Basque Country (UPV / EHU), Bº Sarriena s/n, E-48940 Leioa, Bizkaia, Spain.

**Authorship contribution:**

- IPP performed the research and analysed the data.
- AM and JP designed the research study
- IPP, AM and JP wrote the manuscript

## Abstract

### BACKGROUND AND PURPOSE

The ability of morphine to induce rapid MOR desensitization in native LC neurons has been questioned. The signaling messenger nitric oxide (NO) is a key mediator in the mechanisms underlying acute and chronic regulation of MOR. The aim of this study was to examine the involvement of neuronal nitric oxide synthase (nNOS) in morphine-induced acute desensitization of MOR in LC neurons *in vitro*.

### EXPERIMENTAL APPROACH

We studied by single-unit extracellular recordings the effect of nNOS inhibition on acute desensitization of MOR induced by morphine or ME in KCl-excited neurons from rat brain slices. To characterize desensitization, the reduction in the inhibition of a test concentration of [Met]$^5$enkephalin (ME; 0.8 or 25.6 μM, 1 min) was measured before and after or during the application of a saturating concentration of the opioid agonist.

### KEY RESULTS

Morphine (30 μM) induces significant desensitization of MOR in the LC, so that the inhibitory effect of a supramaximal test concentration of ME (25.6 μM, applied before and after or during the opioid perfusion) was markedly reduced. As expected, ME (10 μM, 10 min) desensitized the inhibitory effect of a test application of ME (0.8 or 25.6 μM, 1 min). Conversely, the inhibitory effect promoted by gamma-aminobutyric acid (GABA; 1 mM) was unaltered after either ME or morphine perfusion. A combination of the nNOS inhibitors 7-nitroindazole (7-NI, 100 μM) and S-methyl-L-thiocitrulline (SMTC, 10 μM) failed to affect the desensitization promoted by morphine, but attenuated ME (10 μM)-induced desensitization of MOR.

### CONCLUSIONS AND IMPLICATIONS

These results demonstrate the ability of morphine to induce MOR desensitization *in vitro* and highlight the agonist-selective acute regulation of MOR desensitization by neuronal NOS.

### Abbreviations.

aCSF, artificial CSF; CNQX, 6-cyano-7-notroquinoxaline-2, 3-dione; D-AP5, D-(–)-2-amin-5-phosponopentanoic acid; GABA, gamma-aminobutyric acid; LC, locus coeruleus; ME, [Met]$^5$enkephalin; MOR, μ-opioid receptor; 7-NI, 7-nitroindazole; nNOS, neuronal nitric oxide synthase; NMDA, N-methyl-D-aspartate; NO, nitric oxide; PKC, protein kinase C; ROS, reactive oxygen species; SMTC, S-methyl-L-thiocitrulline.

## Introduction

Opioids are potent analgesics used for acute and chronic pain. The major problem with the use of opioids in the clinic is the rapid development of tolerance, which requires escalating doses to maintain the same therapeutic effect. Despite extensive research, the cellular mechanisms underlying opioid tolerance are not fully understood (Dang and Christie, 2012). There is good evidence that desensitization of μ-opioid receptors (MOR) is intimately related to the development of tolerance (Allouche *et al.,* 2014). Molecular mechanisms involved in opioid receptor desensitization include receptor phosphorylation, G protein uncoupling and receptor internalization (Williams *et al.,* 2013). In addition, the nitric oxide (NO) cascade has been proposed to be involved in opioid tolerance (Pasternak, 2007). NO production in the brain is catalyzed from L-arginine principally by the neuronal NO synthase (nNOS). NO interacts with several effectors, including guanylate cyclase to elevate cGMP concentrations or with oxygen or superoxide anion, which enhances reactive oxygen species (ROS) and reactive nitrogen species production.

The locus coeruleus (LC), which provides the most extensive noradrenergic projections in the central nervous system, contains a high density of MOR. For that reason, it has long been used to explore the cellular mechanisms underlying acute and chronic effects of opioids (Nestler, 2001). Acutely, MOR agonists hyperpolarize LC neurons through $G_{i/o}$ protein-coupled inwardly rectifying $K^+$ channels (GIRK) (Torrecilla *et al.,* 2002). Short-term application of high concentrations of opioid agonists desensitizes MOR-mediated responses in the LC *in vitro* (Harris and Williams, 1991). Opioids differ in their ability to desensitize the MOR. Thus, the highly efficacious endogenous peptide agonist [Met]$^5$enkephalin (ME) causes profound desensitization in LC neurons (Alvarez *et al.,* 2002; Santamarta *et al.,* 2014). In contrast, morphine has been described as a partial agonist that induces desensitization and endocytosis to a lesser degree in the brain slice (Alvarez *et al.,* 2002; Bailey *et al.,* 2004), although it efficiently induces tolerance in the LC after chronic administration *in vivo* (Santamarta *et al.,* 2005). On the other hand, the NO pathway has been shown to regulate the functional activity of LC neurons (Pineda *et al.,* 1996; Torrecilla *et al.,* 2007). ROS have been reported to mediate some of the NO-mediated effects on MOR desensitization in the LC (Llorente *et al.,* 2012). Furthermore, nNOS inhibitors have been found to attenuate ME-induced MOR desensitization in the LC *in vitro* (Santamarta *et al.,* 2014) and reduce cellular tolerance in morphine-treated animals (Santamarta *et al.,* 2005). However, there is no information regarding the implication of the NO system in morphine-induced acute desensitization. Therefore, the aim of this study was to evaluate by single-unit extracellular recordings *in vitro*, the involvement of the neuronal isoform of NOS in MOR desensitization induced by morphine.

## Methods

### *Animals and treatments*

Adult male Sprague–Dawley rats (200–300 g) were housed under standard laboratory conditions (22°C, 12:12 h light/dark cycles) with free access to food and water. All experimental procedures reported in this manuscript were carried out in accordance with UK Animals (Scientific Procedures) Act, 1986, and associated guidelines (86/609/EEC) and approved by the Animal Care and Use Committee of the University of the Basque Country. All efforts were made to minimize the suffering of the animals and to reduce the number of animals used. The animals for this study were obtained from the animal house of the University of the Basque Country (Leioa, Spain). All studies involving animals are reported in accordance with the ARRIVE guidelines for reporting experiments involving animals (Kilkenny *et al.*, 2010; McGrath *et al.*, 2010).

### *In vitro electrophysiology: brain slice preparation and extracellular recordings*

Animals were anaesthetized with chloral hydrate (400 mg/kgi.p.) and sacrificed by decapitation. The brain was rapidly removed, and a block of tissue containing the brainstem was obtained. Coronal slices of 500–600 μm thickness including the LC were cut using a vibratome. The tissue was then allowed to recover from the slicing for 90 min in a modified Haas-type interface chamber continuously perfused with artificial cerebrospinal fluid (aCSF) at 33°C, saturated with a mixture of 95% $O_2$ and 5% $CO_2$ , at a flow rate of 1.5 $mL \cdot min^{-1}$ (final pH = 7.34). The aSCF contained (in mM): NaCl 130, KCl 3, $NaH_2PO_4$ 1.25, D-glucose 10, $NaHCO_3$ 21, $CaCl_2$ 2, and $MgSO_4$ 2. Single-unit extracellular recordings of LC cells were performed as described (Pineda *et al.*, 1996). The recording electrode, an Omegadot glass micropipette, was pulled and filled with NaCl (0.05 M). The tip was broken back to a size of 2–5 μm (3–5 MΩ).

The electrode was positioned on the LC, which was identified visually in the rostral pons as a dark oval area on the lateral borders of the central grey and the fourth ventricle, just anterior to the genu of the facial nerve. The extracellular signal from the electrode was passed through a high-input impedance amplifier and monitored on an oscilloscope and an audio unit. Individual neuronal spikes were isolated from the background noise with a window discriminator. The firing rate was analysed by means of a PC-based custom-made software, which generated histogram bars representing the cumulative number of spikes in consecutive 10 s bins (HFCP®, Cibertec S.A., Madrid, Spain). Noradrenergic cells were identified by their spontaneous and regular discharge activity, the slow firing rate and the long-lasting, positive-negative waveform (Andrade *et al.*, 1983).

### *Pharmacological procedures*

The desensitization model that we have previously used in spontaneously firing neurons (Llorente *et al*., 2012; Santamarta *et a*l., 2014) was particularly suitable to study the desensitization induced by ME because it rapidly washes out from the preparation, so that the effect of a test concentration of ME (0.8 μM, 1 min) can be evaluated several times in the same neuron within few minutes. However, that protocol is not suitable to

evaluate morphine effects repeatedly in the same neuron, since it does not quickly wash out from slices (Levitt and Williams, 2012). For those reasons, we quantified the extent of receptor desensitization induced by morphine by evoking a positive DC shift in the resting potential of LC neurons with a KCl (14 mM) containing aCSF, so that the maximal effect of morphine could be monitored. In these assays, the osmolarity of KCl was compensated with a lower concentration of NaCl (119 mM). All the experiments were performed in the presence of 6-cyano-7-notroquinoxaline-2 (CNQX, a non- N-methyl-D-aspartate (NMDA) glutamate receptor antagonist, 30 μM) and D-(–)-2-amin-5-phosponopentanoic acid (D-AP5, a NMDA receptor antagonist, 100 μM) to avoid the interference of KCl-induced glutamate release on MOR desensitization. In each of the experiments, GABA (1 mM) was tested as an internal control before and after the desensitization with ME (10 μM, 10 min) or morphine (30 μM, 10 min).

ME and morphine effects on KCl-excited LC neurons were characterized by performing concentration-effect curves for the inhibitory effects of ME (0.1-25.6 μM, 2x, 1 min) and morphine (0.1-30 μM, 3x, 5 min) on the firing rate of LC neurons from rat brain slices. To characterize the acute desensitization of MOR induced by ME or morphine under these experimental conditions, two possible designs were used. First, we compared the inhibitory effect of a supramaximal concentration of ME (25.6 μM, 1 min) before and 3-5 min after inducing desensitization with ME (10 μM, 10 min) or morphine (30 μM, 10 min). Once the last test concentration of ME (25.6 μM, 1 min) was applied, naloxone (1 μM) was perfused to reverse the morphine-induced hyperpolarization and to return the firing rate to control conditions. The decrease in the ME (25.6 μM, 1 min) effect after ME (10 μM) or morphine (30 μM) was taken as a measure of the degree of desensitization (see figure 1). With the purpose of comparisons, in some experiments, we used ME (0.8 μM, 1 min) as a test concentration before and after inducing desensitization with ME (10 μM, 10 min). Second, we measured the maximal response to ME (25.6 μM) at two times during a prolonged application of ME (10 μM, 10 min) or morphine (30 μM, 10 min): (1) 40-60 s after initiating the 10 min ME (10 μM) or morphine (30 μM) perfusion and (2) just after finishing it (see figure 2). Finally, naloxone (1 μM) was applied to reverse morphine-induced effects. The decrease in the ME (25.6 μM, 1 min) effect after ME (10 μM) or morphine (30 μM) was taken as a measure of the degree of desensitization. In all cases, the application of the supramaximal test concentration of ME (25.6 μM) was limited to 1 min and a washout period of approximately 10 min was set between applications in order to reduce the induction of desensitization by test ME applications alone.

To evaluate the effect of nNOS inhibitors on ME- and morphine-induced acute desensitization of MOR under KCl-induced activation, SMTC (10 μM) was perfused together with 7-NI (100 μM) for 20 min before starting the experiment and during the entire desensitization assay with ME (10 μM, 10 min) or morphine (30 μM, 10 min). MOR desensitization in the presence of nNOS inhibitors was explored using the two experimental designs of MOR desensitization.

*Data analysis and statistics*

Values are expressed as the mean ± standard error of the mean (S.E.M) of n (number) experiments. The firing rate of LC cells was recorded before (baseline), during and after drug applications and throughout the experiment. The inhibitory effect of ME (0.8 or 25.6 μM, 1 min) or GABA (1 mM, 1 min) was calculated as follows: $E = [(FR_{basal} - FR_{post}) \cdot$

100] / $FR_{basal}$, where $FR_{basal}$ is the mean firing rate for a 60 s period immediately before ME or GABA application and $FR_{post}$ is the average firing rate for a 30 s period after onset of ME (0.8 or 25.6 μM, 1 min) or GABA (1 mM, 1 min) perfusion. The degree of ME (10 μM)- or morphine (30 μM)-induced opioid desensitization was calculated as follows: desensitization percentage = $100 \cdot [ 1 - (E_{post})/E_{basal})]$, where $E_{basal}$ and $E_{post}$ are the inhibitory effects of the agonist test concentrations (ME 0.8 or 25.6 μM; GABA 1 mM) when applied before (basal) and after (post) inducing desensitization with ME (10 μM) or morphine (30 μM); or the initial (basal) or final (post) inhibitory effects of (ME 25.6 μM) when applied during a continuous desensitizing concentration of ME (10 μM) or morphine (30 μM). This value indicates the reduction in the inhibitory effect of the opioid agonist after perfusion with a high agonist concentration (as compared with the basal effect).

To validate statistically the development of desensitization, the effects of ME before and after inducing desensitization were compared by a paired Student's t test. In addition, to evaluate the differences in the degree of ME- or morphine-induced desensitization between groups, we compared the desensitization percentage values in the absence (control) or in the presence of the drug by a two-sample Student's t test. Possible changes induced by drugs in the basal firing rates or the acute effect of ME (0.8 or 25.6 μM) or GABA (1 mM, 1 min) were evaluated by a paired Student's t test when compared within the same cell or by a two-sample Student's t test when compared between different cells. The level of significance was considered as $p = 0.05$.

*Drugs and reagents*

ME was purchased from Bachem (Bodendorf, Germany). Morphine hydrochloride was purchased from Alcaliber (Madrid, Spain). 7-NI and SMTC were obtained from Sigma-Aldrich Quimica S.A. (Madrid, Spain). Chloral hydrate and GABA were obtained from Sigma-Aldrich Quimica S.A. (Madrid, Spain). D-(-)-2-Amino-5-phosphonopentanoic acid (D-AP5) and 6-Cyano-7-nitroquinoxaline-2,3-dione disodium salt (CNQX) were purchased from Tocris (Bristol, UK). ME, SMTC, GABA, D-AP5 and CNQX were prepared as stock solutions in water, stored at –25 ºC and, on the day of the experiment, diluted in the final volume. 7-NI was directly dissolved in KCl (14 mM) containing aCSF and required prolonged sonication to facilitate homogeneity. All drugs were administered for enough time to reach a steady-state response and during the whole experiment.

## Results

*Characterization of acute inhibitory effects of ME and morphine on KCl-excited LC neurons in vitro*

A sustained perfusion with KCl (14 mM) increased by 6 fold the firing rate of LC neurons (firing rate before KCl: 0.80 ± 0.04 Hz; after KCl: 4.29 ± 0.16 Hz, $n = 52$, $p < 0.005$). In order to characterize the acute inhibitory effects of ME and morphine, increasing concentrations of ME (0.1-25.6 μM, 2x, 1 min) or morphine (0.1-30 μM, 3x, 5 min) were perfused in the slice (Figs. 3A and B). No differences were found in the KCl-excited basal firing rate between groups (basal firing rate, before ME: 3.08 ± 0.44 Hz, $n = 5$; before morphine: 3.27 ± 0.56 Hz, $n = 5$). The $pEC_{50}$ value for ME effect obtained by nonlinear analysis was 6.12 ± 0.02 ($EC_{50}$ = 0.75 μM, n = 5), whereas the $pEC_{50}$ for morphine effect was 6.41 ± 0.09 ($EC_{50}$ = 0.39 μM, $n = 5$). The maximum inhibitory effects ($E_{max}$) induced by ME and morphine were 81 ± 8% and 55 ± 5% from the KCl-excited basal firing rate, respectively (Figs. 3C and D). GABA promoted a 100% inhibition from baseline in all cases. These results suggest that ME has a higher efficacy at the MOR than morphine.

*Characterization of acute MOR desensitization induced by ME and morphine in LC neurons*

First, we evaluated the effect of short applications of two test concentrations of ME (0.8 μM or 25.6 μM, 1 min) before and after perfusing with a high, desensitizing concentration of ME (10 μM, 10 min) or morphine (30 μM, 10 min). ME (0.8 μM) is a concentration that is close to the $EC_{50}$ in this KCl model and ME (25.6 μM) allows us to see changes in the maximum response. Thus, after finishing the ME (10 μM, 10 min) administration, the inhibitory effect of ME (0.8 μM) was desensitized by 55 ± 3% ($n = 5$, $p < 0.005$), whereas the effect of ME (25.6 μM) was reduced by 26 ± 3% ($n = 5$, $p < 0.005$) (Figs. 4A, C and G). On the other hand, after finishing the morphine (30 μM, 10 min) perfusion, the inhibitory effect of (25.6 μM) was desensitized by 39 ± 4% ($n = 5$, $p < 0.005$) (Figs. 4D and G). This degree of desensitization was higher than that induced by ME (10 μM) ($p < 0.05$, Fig. 4G). Since morphine (30 μM) produces 100% receptor occupancy and it does not quickly wash out from the slice, we only studied changes in the maximum response caused by desensitization and therefore, ME (0.8 μM) was not tested in morphine experiments. After inducing desensitization with morphine, naloxone was applied to return to control firing rate values in the absence of MOR activation. In fact, the firing rate after naloxone (1 μM) was not different when compared to the firing rate before desensitization (firing rate, before desensitization: 4.1 ± 0.5 Hz, $n = 5$; after naloxone (1 μM): 4.0 ± 0.5 Hz, $n = 5$).

Second, we compared the maximal response to ME (25.6 μM) applied at two times during a continuous application of ME (10 μM, 10 min) or morphine (30 μM, 10 min). By this approach the inhibitory effect of ME (25.6 μM, 1 min) was desensitized by 36 ± 4% ($n = 5$, $p < 0.05$) following ME (10 μM, 10 min) perfusion and by 32 ± 5% ($n = 5$, $p < 0.01$) after morphine (30 μM, 10 min) (Figs. 4E, F and G). The firing rate after naloxone (1 μM) did not differ from the firing rate before desensitization (firing rate, before desensitization: 4.7 ± 0.4 Hz, $n = 5$; after naloxone (1 μM): 4.5 ± 0.4 Hz, $n = 5$).

In each desensitization experiment, GABA (1 mM) was tested as an internal control. The inhibitory effect of GABA (1 mM, 1 min) was close to 100% from baseline (>95%) both before and after perfusion with ME (10 μM, 10 min) ($n$ = 15) (Figs. 4B and G) or morphine (30 μM, 10 min) ($n$ = 9) (Figs. 4G).

*Effect of neuronal NOS inhibitors on acute MOR desensitization induced by ME and morphine*

It has been shown that nNOS contributes to ME-induced MOR desensitization in spontaneously active LC neurons (Santamarta *et al*., 2014). To further study the involvement of nNOS on morphine (30 μM)-induced desensitization, we perfused a combination of two nNOS inhibitors 7-NI (100 μM) and SMTC (10 μM). Perfusion with the nNOS inhibitors did not alter the firing rate of LC neurons (firing rate change: 2 ± 1%, $n$ = 17). Moreover, acute effects of both test concentrations of ME (0.8 and 25.6 μM) in the presence of nNOS inhibitors were not different from those in the control group (change in acute effect, ME (0.8 μM): 15 ± 7%, $n$ = 5; ME (25.6 μM): 5 ± 7%, $n$ = 15).

As in spontaneously firing neurons, administration of nNOS inhibitors in KCl-excited LC neurons reduced by 27 ± 6% ($n$ = 5, $p$ < 0.05 vs control) the desensitization induced by ME (10 μM) when ME (0.8 μM) was applied before and after inducing desensitization. In addition, nNOS inhibitors blocked the desensitization by 58 ± 8% ($n$ = 5, $p$ < 0.005 vs control) when ME (25.6 μM) was applied before and after ME (10 μM), (Figs. 5B and E). Finally, nNOS inhibitors reduced by 43 ± 8% ($n$ = 5, $p$ < 0.05 vs control) the desensitization when ME (25.6 μM) was applied during ME (10 μM), (Figs. 5D and E). The basal firing rate in the presence of nNOS inhibitors was not significantly different when compared to the control group (basal firing rate, control: 4.35 ± 0.26 Hz, $n$ = 15; in the presence of nNOS inhibitors: 4.92 ± 0.32 Hz, $n$ = 15). GABA (1 mM, 1 min) caused a 100% reduction from baseline before and after inducing desensitization ($n$ = 14) (Fig. 5C and E). These results reaffirm that nNOS contributes to ME-induced MOR desensitization in rat LC neurons.

On the contrary, perfusion with 7-NI (100 μM) together with SMTC (10 μM) failed to alter morphine (30 μM)-induced desensitization. Thus, desensitization induced by morphine (30 μM) in the presence of nNOS inhibitors was significant ($n$ = 5, $p$ < 0.005) (Fig. 6A and B). No differences were found between the firing rate before morphine (30 μM) and after naloxone (1 μM) (firing rate before morphine (30 μM): 5.0 ± 0.2 Hz, $n$ = 5; firing rate after naloxone (1 μM): 4.8 ± 0.3 Hz, $n$ = 5). GABA (1 mM) promoted a 100% inhibition from baseline before and after inducing desensitization ($n$ = 5) (Fig. 6A and B). These results suggest that nNOS is not involved in acute MOR desensitization induced by morphine in LC neurons.

## Discussion

The ability of morphine to induce rapid MOR desensitization in native LC neurons has been a matter of debate (Alvarez *et al*., 2002; Bailey *et al*., 2003, 2009b). In addition, NO has been shown to regulate ME-induced MOR desensitization in the LC *in vitro* (Torrecilla *et al*., 2001; Llorente *et al*., 2012; Santamarta *et al*., 2014) and morphine-induced tolerance in this nucleus *in vivo* (Santamarta *et al*., 2005). However, the contribution of NO to MOR desensitization induced by non-peptide opioid agonists *in vitro* is unknown. In the present study, we used single-unit extracellular recordings in KCl-excited LC neurons from rat brain slices to characterize the desensitization of MOR induced by morphine and ME. We further explored the involvement of the neuronal NOS isoform in acute MOR desensitization. Our results show that morphine (30 μM) causes significant desensitization of MOR in the LC, so that the inhibitory effect of a supramaximal test concentration of ME (25.6 μM, applied before and after, or during the opioid perfusion) was markedly reduced. As expected, ME (10 μM) also induced substantial desensitization of MOR, since the inhibitory effect of ME (0.8 or 25.6 μM) was diminished. The inhibitory effect of GABA (1 mM) was unaltered after application of either ME (10 μM) or morphine (30 μM). Perfusion with a combination of two selective nNOS inhibitors (7-NI and SMTC) attenuated the induction of MOR desensitization induced by ME but, in contrast, it failed to alter the desensitization induced by morphine.

As previously mentioned, to study MOR desensitization, we evoked an excitation of LC neurons with KCl (14 mM). This procedure allows us to continously monitor morphine effects and, at the same time, to assess supramaximal test concentrations of ME by extracellular recording techniques. This would not have been feasible in spontaneously firing LC neurons from brain slices, since morphine would induce a complete inhibition of the firing activity that would not recover to baseline values. Apart from the postsynaptic action, it has been shown that KCl depolarizes nerve terminals, which triggers GABA and glutamate release in slice preparations (Liachenko *et al*., 1999). To avoid the interference of the KCl-induced glutamate release on MOR desensitization, all the experiments were performed in the presence of D-AP5 and CNQX (NMDA and non-NMDA glutamate receptor antagonist, respectively), as described by Mendiguren and Pineda (2007). Under these experimental conditions, most of the excitation of LC cells by KCl is due to postsynaptic changes in membrane potassium equilibrium. Thus, we first characterized the acute inhibitory effects of ME and morphine on KCl-excited neurons. Concentration-effect curves showed that morphine has a smaller maximum inhibitory effect (Emax) than ME, which is consistent with previous studies that have shown that morphine behaves as partial agonist at the MOR in LC neurons (Osborne *et al*., 2000; Bailey *et al*., 2003). The EC50 value for the inhibitory effect of ME effect in the presence of high K+ was found to be slightly shifted to the right as compared to that from spontaneously firing LC neurons (Santamarta *et al*., 2005) or by intracellular electrodes under voltage-clamp mode in the LC (Osborne and Williams, 1995). Likewise, the EC50 value for morphine in the presence of high K+ is shifted rightward when compared to that reported using intracellular recording techniques in LC neurons (Chiu *et al*., 1993). This is likely due to a positive DC shift in the potassium equilibrium potential promoted by high concentrations of extracellular K+ and the fact that we are able to follow the effect of ME or morphine at membrane potentials close to the reversal potential for K+ (where GIRK channels show rectification).

To study MOR desensitization in the present study, we measured changes in the inhibitory effect of two test concentrations of the opioid agonist ME (0.8 or 25.6 μM). ME inhibits LC cell activity with high efficacy and almost exclusively through MOR (Williams and North, 1984). Moreover, it rapidly washes out from the slice so that MOR desensitization can be easily measured by extracellular recordings once the firing recovers from ME-induced inhibition. The use of an intermediate concentration of ME (0.8 μM), close to the EC50 value, allowed us to detect any minimal change in the sensitivity of MOR associated with ME-induced desensitization. On the contrary, application of a supramaximal test concentration of ME (25.6 μM) made it possible to study reductions in the maximal activity of MOR associated with ME-induced desensitization (Osborne and Williams, 1995). In the case of morphine, as a concentration of 30 μM produces near maximal receptor occupancy, we had to use the supramaximal test concentration of ME (25.6 μM) to measure maximal activity of MOR, overcoming morphine's slow rate of receptor dissociation in the slice preparation.

As expected, ME (10 μM) strongly desensitized the inhibition induced by a test application of ME (0.8 μM). This degree of desensitization was found to be similar to that reported in spontaneously firing LC neurons (Llorente *et al*., 2012; Santamarta *et al*., 2014). In addition, ME (10 μM) desensitized the inhibition induced by a supramaximal concentration of ME (25.6 μM), applied before and after the opioid perfusion. However, this degree of desensitization was less strong than that quantified by ME (0.8 μM), as a supramaximal test concentration is less sensitive to detect changes in MOR responsiveness associated with desensitization. Finally, the inhibitory effect of ME (25.6 μM), applied at two times during ME (10 μM, 10 min) administration, was also desensitized to a similar extent to that observed when the ME test was applied before and after.

On the other hand, morphine caused significant MOR desensitization, since the effect of ME (25.6 μM), applied before and after morphine (30 μM) perfusion, was significantly reduced. In fact, the degree of desensitization induced by morphine was stronger than that induced by ME under the same experimental design. This is likely because MOR signaling starts recovering once the sustained perfusion of ME finishes, whereas it does not recover for a long time after morphine perfusion. Likewise, morphine (30 μM) desensitized the inhibitory effect of ME (25.6 μM), when it was tested at two times during the opioid perfusion. Interestingly, the degree of desensitization induced by morphine using the latter protocol was not different from that induced by ME. This finding seems to contradict previous electrophysiological experiments that showed that morphine induces significantly weaker MOR desensitization than higher efficacy opioid agonists such as ME in LC neurons *in vitro* (Alvarez *et al*., 2002; Bailey *et al*., 2003). Interestingly, these authors have reported that morphine-induced desensitization is enhanced by concomitant activation of PKC (Bailey *et al*., 2004; Arttamangkul *et al*., 2015). In our assays, high K+ concentration may facilitate calcium entry through voltage-dependent calcium channels (Meier *et al*., 1988), which has been shown to elevate PKC activity in different systems (Sakai *et al*., 1997; Dupont *et al*., 2000; Ratz and Miner, 2009). Other kinases such as CaMKII have been also reported to negatively regulate MOR signaling and to contribute to morphine-induced desensitization, tolerance and dependence (Mestek *et al*., 1995; Sánchez-Blázquez *et al*., 2008; Tang *et al*., 2006; Navidhamidi *et al*., 2012), with their activity being increased in a calcium-dependent manner (Kim *et al*., 2000; Song *et al*., 2010). However, it is unclear if they interact directly or indirectly with MOR in LC neurons (Wang and Wang, 2006; Feng *et al*., 2011; Arttamangkul *et al*., 2015). Given that the mean firing rate after KCl (14 mM) was ~4 Hz, we can speculate that these kinases

would be activated during KCl perfusion to a similar extent to that observed in waking animals, since tonic LC discharge rates up to 5 Hz are typically observed during normal waking in rats and monkeys (Foote *et al*., 1980; Berridge and Waterhouse, 2003).

On the contrary, our results suggest that, even in conditions where increased PKC activity would be expected (high K+), ME-induced desensitization was not found to be stronger than in control tissues. In agreement, a recent study using intracellular recordings in LC neurons has reported that PKC activators do not affect the desensitization induced by a saturating concentration of ME (30 μM), when the test was applied before and after the ME perfusion (Arttamangkul *et al*., 2015). Finally, we observed that the inhibitory effect of GABA, which was tested as an internal control, was ~100% and was not affected by either morphine or ME perfusion. GABA has been shown to induce stronger inhibitory effects at depolarized than at hyperpolarized membrane potentials on LC neurons (Osmanovic and Shefner, 1990), but these actions are not changed by opioid agonists.

The NO system has been shown to modulate MOR signaling in the LC. We have previously reported that NO enhances ME-induced MOR desensitization (Llorente *et al*., 2012). Independent administration of 7-NI and SMTC, two structurally unrelated molecules that selectively inhibit the neuronal NOS isoform (Babbedge *et al*., 1993; Furfine *et al*., 1994), attenuated ME-induced MOR desensitization in spontaneously firing LC neurons *in vitro* (Santamarta *et al*., 2014). In the present study, nNOS inhibition by a combined perfusion with 7-NI and SMTC attenuated ME-induced MOR desensitization in KCl-excited LC neurons, which confirms the involvement of nNOS in this process. In addition, NO has been shown to play a critical role in the adaptations induced by chronic morphine administration. Thus, morphine treatment leads to an increased NOS expression in the central nervous system (Cuéllar *et al*., 2000; Wong *et al*., 2000). *In vivo* administration of 7-NI prevents the development of tolerance in morphine-treated rats (Santamarta *et al*., 2005) and reduced the hyperactivity of LC neurons typically found after chronic morphine exposure (Pineda *et al*., 1998). Morphine-induced analgesic tolerance has been also shown to be attenuated by NO-activated sGC/cGMP-dependent mechanisms (Ozdemir *et al*., 2011; Durmus *et al*., 2014) and ROS generation (Muscoli *et al*., 2007; Batinić-Haberle *et al*., 2009). Surprisingly, perfusion with the nNOS inhibitors 7-NI and SMTC failed to alter morphine-induced desensitization of MOR *in vitro* in our work. These results suggest that acute inhibition of neuronal NO synthesis does not affect morphine-induced MOR desensitization *in vitro*, whereas it attuenuates the induction of tolerance *in vivo*.

The mechanisms by which nNOS might be differentialy involved in ME-, but not morphine-induced MOR desensitization are unknown. Results obtained in our laboratory have indicated that NO mediates the development of ME-induced MOR desensitization through independent regulation of downstream sGC/PKG and ROS pathways in the LC (see Results, Study 1). One of the most remarkable differences between ME and morphine is that ME causes robust receptor internalization (Arttamangkul *et al*., 2008; 2012), whereas morphine fails to induce efficient internalization in adult rat LC neurons or HEK293 cells (Finn and Whistler, 2001; Alvarez *et al*., 2002; Bailey *et al*., 2003; Arttamangkul *et al*., 2008). It can be hypothesized that NO might act disrupting reinsertion of internalized receptors back into the plasma membrane, which would agree with the fact that morphine-induced desensitization is unaffected by nNOS inhibitors, since morphine does not promote efficient receptor endocytosis and recycling of the MOR.

On the other hand, the mechanisms by which nNOS inhibitors would attenuate morphine-induced cellular tolerance in LC neurons and morphine-induced analgesic tolerance, without affecting acute desensitization are unclear. One of the possibilities may involve alterations in MOR turnover in LC neurons, which has been suggested to underlie opioid tolerance (Dang and Christie, 2012). Thus, previous results from our group have reported that chronic treatment with morphine leads to a disruption in MOR functional recovery from complete receptor inactivation with β-funaltrexamine in the LC. Our preliminary data indicate that this modification of MOR turnover may be mediated by NO (M.T. Santamarta, Doctoral Thesis, unpublished data). In adition, several events dependent on NO signaling pathways have been reported to mediate *in vivo* morphine-induced antinociceptive tolerance, including glutamatergic activation (Sánchez-Blázquez *et al*., 2013), neuronal apoptosis (Bonfoco *et al*, 1995) or glial activation and induction of proinflammatory processes (Little *et al*., 2013). Thus, nNOS inhibitors could alleviate morphine tolerance *in vivo* by attenuating some of these processes, without altering morphine-induced desensitization.

In conclusion, the present study shows that morphine and ME induce acute MOR desensitization in LC neurons. On the basis of previous studies, we can hypothesize that morphine-induced desensitization could be mediated by high firing rate-dependent activation of PKC and/or CaMKII, to a similar extent as *in vivo*, but the exact mechanism has yet to be determined. Selective nNOS inhibition attenuates the induction of MOR desensitization by the opioid agonist ME, but it failed to alter the desensitization promoted by morphine. These results highlight the agonist-selective acute regulation of MOR by nNOS. Further studies are needed to investigate the underlying mechanisms.

## References


Allouche S, Noble F, Marie N (2014). Opioid receptor desensitization: mechanisms and its link to tolerance. Front Pharmacol 5:280.

Arttamangkul S, Birdsong W, Williams JT (2015). Does PKC activation increase the homologous desensitization of μ opioid receptors? Br J Pharmacol 172: 583–592.

Arttamangkul S, Lau EK, Lu H-W, and Williams JT (2012). Desensitization and trafficking of mu-opioid receptors in locus coeruleus neurons: Modulation by kinases. Mol Pharmacol 81: 348–355.

Arttamangkul S, Quillinan N, Low MJ, von Zastrow M, Pintar J, Williams JT (2008). Differential activation and trafficking of μ-opioid receptors in brain slices. Mol Pharmacol 74: 972–979.

Alvarez VA, Arttamangkul S, Dang V, Salem A, Whistler JL, Von Zastrow M, Grandy DK, and Williams JT (2002). mu-Opioid receptors: Ligand-dependent activation of potassium conductance, desensitization, and internalization. J Neurosci. 22: 5769–5776.

Andrade R, Vandermaelen CP, Aghajanian GK (1983). Morphine tolerance and dependence in the locus coeruleus: single cell studies in brain slices. Eur J Pharmacol 91: 161–169.

Babbedge RC, Bland-Ward PA, Hart SL, Moore PK (1993). Inhibition of rat cerebellar nitric oxide synthase by 7-nitro indazole and related substituted indazoles. Br J Pharmacol 110: 225–228.

Bailey CP, Couch D, Johnson E, Griffiths K, Kelly E, Henderson G (2003). Mu-opioid receptor desensitization in mature rat neurons: lack of interaction between DAMGO and morphine. J Neurosci 23: 10515–10520.

Bailey CP, Kelly E, Henderson G (2004). Protein kinase C activation enhances morphine-induced rapid desensitization of mu-opioid receptors in mature rat locus ceruleus neurons. Mol Pharmacol 66: 1592–1598.

Batinić-Haberle I, Ndengele MM, Cuzzocrea S, Rebouças JS, Spasojević I, Salvemini D (2009). Lipophilicity is a critical parameter that dominates the efficacy of metalloporphyrins in blocking the development of morphine antinociceptive tolerance through peroxynitrite-mediated pathways. Free Radic Biol Med 46: 212–219.

Berridge CW, Waterhouse BD (2003). The locus coeruleus-noradrenergic system: modulation of behavioral state and state-dependent cognitive processes. Brain Res Brain Res Rev 42: 33–84.

Bonfoco E, Krainc D, Ankarcrona M, Nicotera P, Lipton SA (1995). Apoptosis and necrosis: two distinct events induced, respectively, by mild and intense insults with N-methyl-D-aspartate or nitric oxide/superoxide in cortical cell cultures. Proc Natl Acad Sci USA 92: 7162–7166.

Chiu TH, Yeh MH, Tsai SK, Mok MS (1993). Electrophysiological actions of alfentanil: intracellular studies in the rat locus coeruleus neurones. Br J Pharmacol 110: 903–909.

Cuéllar B, Fernández AP, Lizasoain I, Moro MA, Lorenzo P, Bentura ML, Rodrigo J, Leza JC (2000). Up-regulation of neuronal synthase immunoreactivity in opiate dependence and withdrawal. Psychopharmacology 148: 66–73.

Dang VC, Christie MJ (2012). Mechanisms of rapid opioid receptor desensitization, resensitization and tolerance in brain neurons. Br J Pharmacol 165: 1704 –1716.

Dupont JL, Janoshazi A, Bellahcene M, Mykita S, de Barry J (2000). Reversible protein kinase C activation in PC12 cells: effect of NGF treatment. Eur J Neurosci 12: 215–226.

Durmus N, Bagcivan I, Ozdemir E, Altun A, Gursoy S (2014). Soluble guanylyl cyclase activators increase the expression of tolerance to morphine analgesic effect. Bratisl Lek Listy 115: 334–339.

Feng B, Li Z, Wang JB (2011). Protein kinase C-mediated phosphorylation of the μ-opioid receptor and its effects on receptor signaling. Mol Pharmacol 79: 768–775.

Finn AK, Whistler JL (2001). Endocytosis of the mu opioid receptor reduces tolerance and a cellular hallmark of opiate withdrawal. Neuron 32:829–839.

Foote SL, Aston-Jones G, Bloom FE (1980). Impulse activity of locus coeruleus neurons in awake rats and monkeys is a function of sensory stimulation and arousal. Proc Natl Acad Sci U S A 77: 3033–3037.

Furfine ES, Harmon MF, Paith JE, Knowles RG, Salter M, Kiff RJ, Duffy C, Hazelwood R, Oplinger JA, Garvey EP (1994). Potent and selective inhibition of human nitric oxide synthases: Selective inhibition of neuronal nitric oxide synthase by S-methyl-L-thiocitrulline and s-ethyl-L-thiocitrulline. J Biol Chem 269: 26677–26683.

Harris GC, Williams JT (1991). Transient homologous μ-opioid receptor desensitization in rat locus coeruleus neurons. J Neurosci 11: 2574–2581.

Kilkenny C, Browne W, Cuthill IC, Emerson M, Altman DG, NC3Rs Reporting Guidelines Working Group (2010). Animal research: reporting in vivo experiments: the ARRIVE guidelines. Br J Pharmacol 160: 1577–1579.

Kim I, Je HD, Gallant C, Zhan Q, Riper DV, Badwey JA, Singer HA, Morgan KG (2000). $Ca^{2+}$-calmodulin-dependent protein kinase II-dependent activation of contractility in ferret aorta. J Physiol 526 Pt 2: 367–374.

Levitt ES, Williams JT (2012). Morphine desensitization and cellular tolerance are distinguished in rat locus ceruleus neurons. Mol Pharmacol 82: 983–992.

Liachenko S, Tang P, Somogyi GT, Xu Y (1999). Concentration-dependent isoflurane effects on depolarization-evoked glutamate and GABA outflows from mouse brain slices. Br J Pharmacol 127: 131–134.

Little JW, Cuzzocrea S, Bryant L, Esposito E, Doyle T, Rausaria S, Neumann WL, Salvemini D (2013). Spinal mitochondrial-derived peroxynitrite enhances neuroimmune activation during morphine hyperalgesia and antinociceptive tolerance. Pain 154: 978–986.

Llorente J, Santamarta MT, Henderson G, Pineda J (2012). Enhancement of mu-opioid receptor desensitization by nitric oxide in rat locus coeruleus neurons: involvement of reactive oxygen species. J Pharmacol Exp Ther 342: 552–560.

McGrath JC, Drummond GB, McLachlan EM, Kilkenny C, Wainwright CL (2010). Guidelines for reporting experiments involving animals: the ARRIVE guidelines. Br J Pharmacol 160: 1573–1576.

Meier K, Knepel W, Schöfl C (1988). Potassium depolarization elevates cytosolic free calcium concentration in rat anterior pituitary cells through 1,4-dihydropyridine-sensitive, omega-conotoxin-insensitive calcium channels. Endocrinology 122: 2764–2770.

Mendiguren A, Pineda J (2007). CB1 cannabinoid receptors inhibit the glutamatergic component of KCl-evoked excitation of locus coeruleus neurons in rat brain slices. Neuropharmacology 52: 617–625.

Mestek A, Hurley JH, Bye LS, Campbell AD, Chen Y, Tian M, Liu J, Schulman H, Yu L (1995). The human mu opioid receptor: modulation of functional desensitization by calcium/calmodulin dependent protein kinase and protein kinase C. J Neurosci 15: 2396–2406.

Muscoli C, Cuzzocrea S, Ndengele MM, Mollace V, Porreca F, Fabrizi F, Esposito E, Masini E, Matuschak GM, Salvemini D (2007). Therapeutic manipulation of peroxynitrite attenuates the development of opiate-induced antinociceptive tolerance in mice. J Clin Invest 117: 3530–3539.

Navidhamidi M, Semnanian S, Javan M, Goudarzvand M, Rohampour K, Azizi H (2012). Examining the effect of the CaMKII inhibitor administration in the locus coeruleus on the naloxone-precipitated morphine withdrawal signs in rats. Behav Brain Res 226: 440–444.

Nestler EJ (2001). Molecular neurobiology of addiction. Am J Addict 10: 201–217.

Osborne PB, Williams JT (1995). Characterization of acute homologous desensitization of mu-opioid receptor-induced currents in locus coeruleus neurones. Br J Pharmacol 115: 925–932.

Osborne PB, Chieng B, Christie MJ (2000). Morphine-6 beta-glucuronide has a higher efficacy than morphine as a mu-opioid receptor agonist in the rat locus coeruleus. Br J Pharmacol 131: 1422–1428.

Osmanovic SS, Shefner SA (1990). γ-Aminobutyric-acid responses in rat locus coeruleus neurons in vitro: a current-clamp and voltage-clamp study. J Physiol 421: 151–170.

Ozdemir E, Bagcivan I, Durmus N, Altun A, Gursoy S (2011). The nitric oxide-cGMP signaling pathway plays a significant role in tolerance to the analgesic effect of morphine. Can J Physiol Pharmacol 89: 89–95.

Pasternak GW (2007). When it comes to opiates, just say NO. J Clin Invest 117: 3185–3187.

Pineda J, Kogan JH, Aghajanian GK (1996). Nitric oxide and carbon monoxide activate locus coeruleus neurons through a cGMP-dependent protein kinase: involvement of a nonselective cationic channel. J Neurosci 16: 1389–1399.

Pineda J, Torrecilla M, Martín-Ruiz R, Ugedo L (1998). Attenuation of withdrawal-induced hyperactivity of locus coeruleus neurones by inhibitors of nitric oxide synthase in morphine-dependent rats. Neuropharmacology 37: 759–767.

Ratz PH, Miner AS (2009). Role of protein kinase Czeta and calcium entry in KCl-induced vascular smooth muscle calcium sensitization and feedback control of cellular calcium levels. J Pharmacol Exp Ther 328: 399–408.

Sakai N, Sasaki K, Ikegaki N, Shirai Y, Ono Y, Saito N (1997). Direct visualization of the translocation of the γ-subspecies of protein kinase C in living cells using fusion proteins with green fluorescent protein. J Cell Biol 139: 1465–1476.

Sánchez-Blázquez P, Rodríguez-Muñoz M, Montero C, de la Torre-Madrid E, Garzón J (2008). Calcium/calmodulin-dependent protein kinase II supports morphine antinociceptive tolerance by phosphorylation of glycosylated phosducin-like protein. Neuropharmacology 54: 319–330.

Sánchez-Blázquez P, Rodríguez-Muñoz M, Berrocoso E, Garzón J (2013). The plasticity of the association between mu-opioid receptor and glutamate ionotropic receptor N in opioid analgesic tolerance and neuropathic pain. Eur J Pharmacol 716: 94–105.

Santamarta MT, Llorente J, Mendiguren A, Pineda J (2014). Involvement of neuronal nitric oxide synthase in desensitisation of μ-opioid receptors in the rat locus coeruleus. J Psychopharmacol 28: 903–914.

Santamarta MT, Ulibarri I, Pineda J (2005). Inhibition of neuronal nitric oxide synthase attenuates the development of morphine tolerance in rats. Synapse 57: 38–46.

Song B, Lai B, Zheng Z, Zhang Y, Luo J, Wang C, Chen Y, Woodgett JR, Li M (2010). Inhibitory phosphorylation of GSK-3 by CaMKII couples depolarization to neuronal survival. J Biol Chem 285: 41122–41134.

Tang L, Shukla PK, Wang LX, Wang ZJ (2006). Reversal of morphine antinociceptive tolerance and dependence by the acute supraspinal inhibition of Ca2+/calmodulin-dependent protein kinase II. J Pharmacol Exp Ther 317: 901–909.

Torrecilla M, Pineda J, Ugedo L (2001). NO synthase inhibitors reduce opioid desensitization in rat locus coeruleus neurons in vitro. Neuroreport 12: 1601–1604.

Torrecilla M, Marker CL, Cintora SC, Stoffel M, Williams JT, Wickman K (2002). G-protein-gated potassium channels containing Kir3.2 and Kir3.3 subunits mediate the acute inhibitory effects of opioids on locus ceruleus neurons. J Neurosci 22: 4328–4334.

Torrecilla M, Ruiz-Ortega JA, Ugedo L, Pineda J (2007). Excitatory regulation of noradrenergic neurons by L-arginine/nitric oxide pathway in the rat locus coeruleus in vivo. Naunyn Schmiedebergs Arch Pharmacol 375: 337–347.

Wang ZJ, Wang LX (2006). Phosphorylation: a molecular switch in opioid tolerance. Life Sci 79: 1681–1691.

Williams JT, Ingram SL, Henderson G, Chavkin C, von Zastrow M, Schulz S, Koch T, Evans CJ, Christie MJ (2013). Regulation of μ-opioid receptors: desensitization, phosphorylation, internalization, and tolerance. Pharmacol Rev 65: 223–254.

Williams JT, North RT (1984). Opiate-receptor interactions on single locus coeruleus neurons. Mol Pharmacol 26: 489–497.

Wong CS, Hsu MM, Chou YY, Tao PL, Tung CS (2000). Morphine tolerance increases [3H]MK-801 binding affinity and constitutive neuronal nitric oxide synthase expression in rat spinal cord. Br J Anaesth 85:587–591.

**Figure legends**

**Figure 1.** Scheme of one of the experimental designs used to evaluate the degree of opioid desensitization induced by ME or morphine in LC neurons under KCl-evoked excitation. The acute effect of ME (0.8 or 25.6 μM) was tested before and after inducing desensitization with ME (10 μM, 10 min) or morphine (30 μM, 10 min). The inhibitory effect induced by morphine was reversed by naloxone (1 μM). The decrease in the effect of ME (25.6 μM, 1 min) was taken as a measure of the degree of desensitization. All the experiments were performed in the presence of CNQX (non-NMDA glutamate receptor antagonist, 30 μM) and D-AP5 (NMDA receptor antagonist, 100 μM) to avoid the interference of KCl-induced glutamate release on MOR desensitization.

**Figure 2.** Scheme of one of the experimental designs used to evaluate the degree of opioid desensitization induced by ME or morphine in LC neurons under KCl-evoked excitation. The maximal effect induced by ME (25.6 μM) was tested during the continuous perfusion with ME (10 μM, 10 min) or morphine (30 μM, 10 min). The inhibitory effect induced by morphine was reversed by naloxone (1 μM). The decrease in the effect of ME (25.6 μM, 1 min) was taken as a measure of the degree of desensitization. All the experiments were performed in the presence of CNQX (non-NMDA glutamate receptor antagonist, 30 μM) and D-AP5 (NMDA receptor antagonist, 100 μM) to avoid the effects of KCl-induced glutamate release on MOR desensitization.

**Figure 3.** Characterization of acute ME and morphine effects under KCl-evoked activation of LC neurons *in vitro*. **A, B.** Examples of firing-rate recordings of LC cells showing the inhibitory effect of ME (**A**) and morphine (**B**). Each horizontal bar represents the period of application of each ME (0.1 - 25.6 μM, 2x) or morphine concentration (0.1 - 30 μM, 3x) and the vertical lines show the number of spikes recorded every 10 s. **C, D.** Concentration-effect curves for the inhibitory effect of ME (**C**) and morphine (**D**) in KCl-excited LC neurons. The horizontal axis represents the logarithms of ME and morphine concentrations in linear scale. The vertical axis expresses the reduction in the firing rate of LC neurons as a percentage from the KCl-induced basal firing rate. Symbols are the mean ± SEM of ME or morphine effects at each concentration obtained from n animals. The lines through the data are the theoretical curves constructed from the mean of the individual concentration-effect curve parameters, as estimated by nonlinear regression (see Methods for details).

**Figure 4.** Characterization of acute desensitization of MOR induced by ME and morphine in KCl-excited LC neurons *in vitro*. **A, B, C.** Examples of firing-rate recordings of LC cells showing the effect of ME (0.8 μM, 1 min) (**A**), GABA (1 mM, 1 min) (**B**) or ME (25.6 μM, 1 min) (**C**) before and after inducing desensitization with ME (10 μM, 10 min). **D,** Example of firing-rate recording of a LC neuron showing the effect of ME (25.6 μM, 1 min) before and after inducing desensitization with morphine (30 μM, 10 min). **E, F.** Examples of firing-rate recordings of LC cells showing the effect of ME (25.6 μM, 1 min) applied at two times during a sustained perfusion with ME (10 μM, 10 min) (**E**) or morphine (30 μM, 10 min) (**F**). The horizontal bars indicate the period of drug applications and the vertical lines show the number of spikes recorded every 10 s. G. Bar histograms show the mean ± S.E.M of ME (10 μM)-, or morphine (30 μM)-induced desensitization. Different test concentrations and experimental designs were used (see Pharmacological procedures). GABA was used as an internal control. All the experiments were performed in the presence of the glutamate receptor antagonists CNQX (30 μM) and D-AP5 (100 μM). Desensitization degrees were calculated as percentage values (see Data analysis and statistics). Note that significant reductions in the effect of ME (0.8 μM, 1

min) or ME (25.6 μM, 1 min) were observed when applied before and after or during ME (10 μM, 10 min) ($n$ = 5, in all cases), but the degree of desensitization was greater when it was quantified by ME (0.8 μM). Likewise, substantial reduction in ME (25.6 μM) effect was observed when applied before and after ($n$ = 5) or during ($n$ = 5) morphine (30 μM, 10 min). The desensitization induced by morphine (30 μM) was greater than that induced by ME (10 μM) when the test concentration was applied before and after. The effect of GABA (1 mM) was unaltered after perfusion with either ME (10 μM) or morphine (30 μM) ($n$ = 15 and $n$ = 9, respectively). *$p$ < 0.01, *$p$ < 0.01 and **$p$ < 0.005 when the effect of the test concentration of ME after desensitization was compared to the basal effect by a paired Student's t test. $^{\#}p$ < 0.005 when compared to the ME (0.8 μM) group by a two-sample Student's t test; $^{\dagger}p$ < 0.05 when compared to the corresponding ME (10 μM) group by a two-sample Student's t test.

**Figure 5.** Effect of nNOS inhibitors on acute MOR desensitization induced by ME in KCl-excited LC neurons *in vitro*. **A, B, C.** Representative examples of firing-rate recordings of LC cells showing the effect of ME (0.8 μM, 1 min) (**A**), ME (25.6 μM, 1 min) (**B**) or GABA (1 mM, 1 min) (**C**) applied before and after inducing desensitization with ME (10 μM, 10 min) in the presence of 7-NI (100 μM) and SMTC (10 μM). D. Example of firing-rate recording of LC cell showing the effect of ME (25.6 μM, 1 min) applied at two times during a sustained perfusion with ME (10 μM, 10 min) in the presence of 7-NI (100 μM) and SMTC (10 μM). The horizontal bars indicate the period of drug applications and the vertical lines show the number of spikes recorded every 10 s. E. Bar histograms show the mean ± S.E.M of ME (10 μM)-induced desensitization in the absence and in the presence of nNOS inhibitors. Different test concentrations and experimental designs were used (see Pharmacological procedures). GABA was used as an internal control. All the experiments were performed in the presence of the glutamate receptor antagonists CNQX (30 μM) and D-AP5 (100 μM). Desensitization degrees were calculated as percentage values (see Data analysis and statistics). Note that nNOS inhibitors attenuated ME (10 μM)-induced desensitization when it was quantified by ME (0.8 μM, $n$ = 5), or ME (25.6 μM) applied before and after ($n$ = 5) or during ME 10 μM ($n$ = 5). In contrast, GABA (1 mM) effect was not affected ($n$ = 14). *$p$ < 0.05 and **$p$ < 0.005 when compared to the corresponding control group by two-sample Student's t test.

**Figure 6.** Effect of nNOS inhibitors on acute MOR desensitization induced by morphine in KCl-excited LC neurons *in vitro*. **A.** Representative example of a firing-rate recording of LC cell showing the effect of ME (25.6 μM, 1 min) applied at two times during a sustained perfusion with morphine (30 μM, 10 min) in the presence of 7-NI (100 μM) and SMTC (10 μM). The horizontal bars indicate the period of drug applications and the vertical lines show the number of spikes recorded every 10 s. **B.** Bar histograms show the mean ± S.E.M of morphine (30 μM)-induced desensitization in the absence and in the presence of nNOS inhibitors. GABA was used as an internal control. All the experiments were performed in the presence of the glutamate receptor antagonists CNQX (30 μM) and D-AP5 (100 μM). Desensitization degrees were calculated as percentage values (see Data analysis and statistics). Note that nNOS inhibitors failed to block morphine (30 μM)-induced desensitization ($n$ = 5). The effect of GABA (1 mM) was not affected by morphine perfusion ($n$ = 5).

**FIGURE 1**

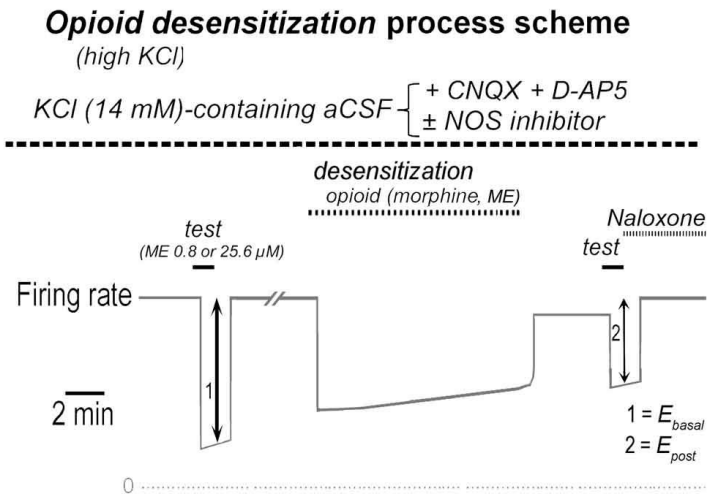


**FIGURE 2**

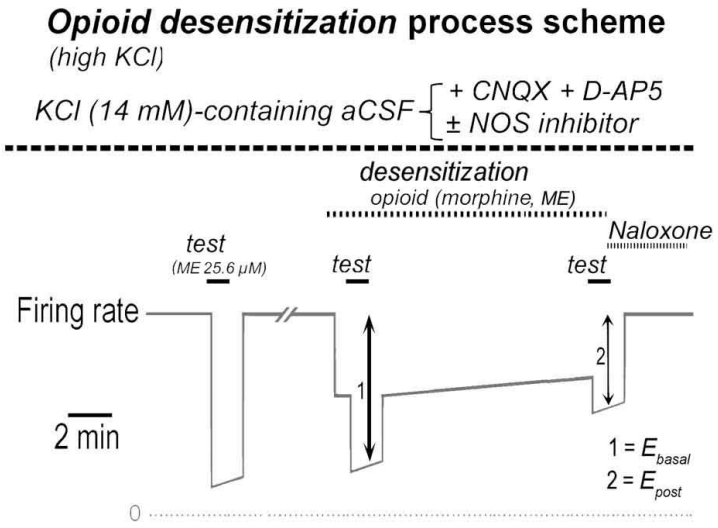

**FIGURE 3**

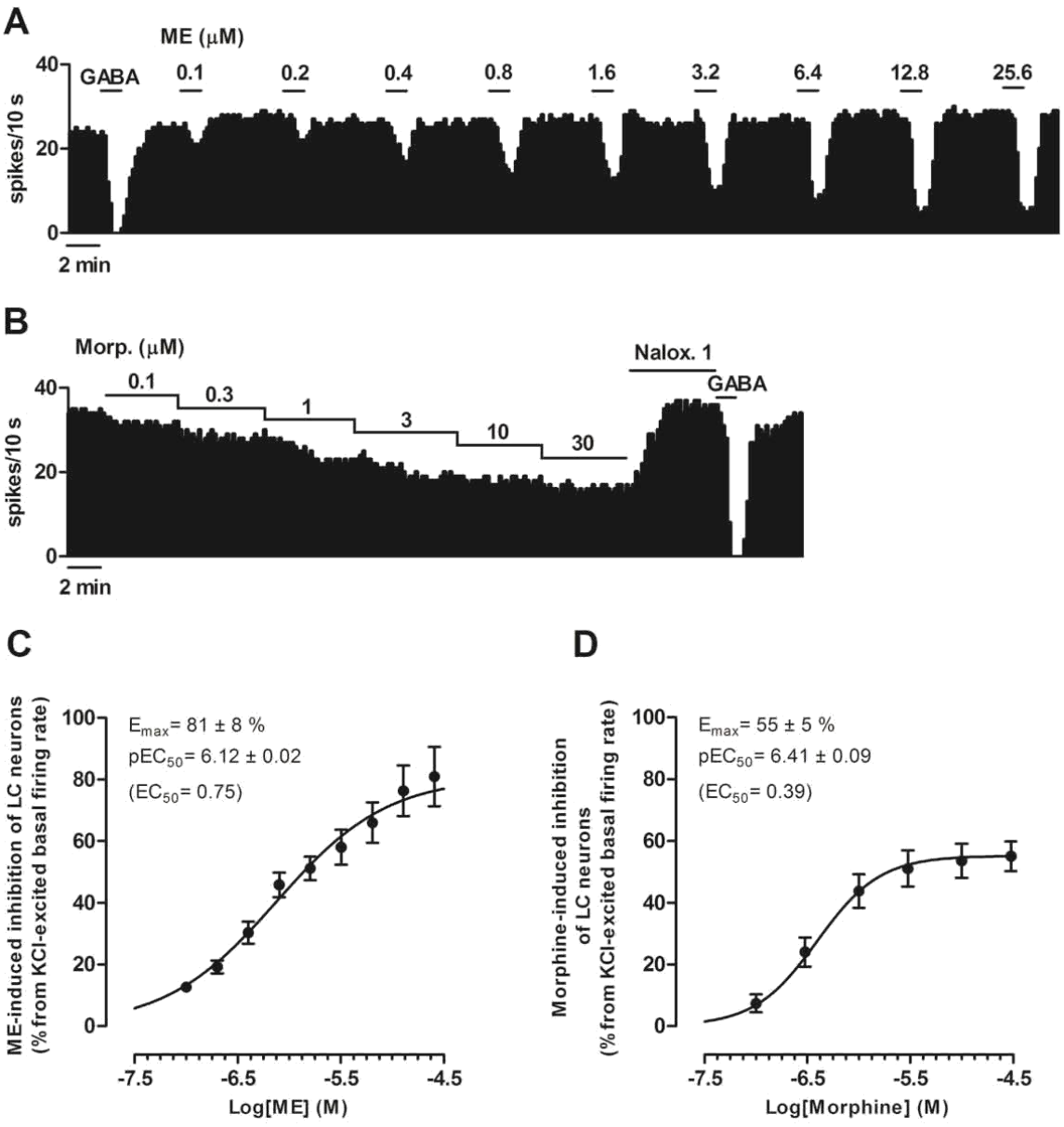
A
ME (μM)
GABA
0.1
0.2
0.4
0.8
1.6
3.2
6.4
12.8
25.6
spikes/10 s
40
20
0
2 min
B
Morp. (μM)
0.1
0.3
1
3
10
30
Nalox. 1
GABA
spikes/10 s
40
20
0
2 min
C
ME-induced inhibition of LC neurons (% from KCl-excited basal firing rate)
Emax= 81 ± 8 %
pEC50= 6.12 ± 0.02
(EC50= 0.75)
100
80
60
40
20
0
-7.5
-6.5
-5.5
-4.5
Log[ME] (M)
D
Morphine-induced inhibition of LC neurons (% from KCl-excited basal firing rate)
Emax= 55 ± 5 %
pEC50= 6.41 ± 0.09
(EC50= 0.39)
100
80
60
40
20
0
-7.5
-6.5
-5.5
-4.5
Log[Morphine] (M)

**FIGURE 4**

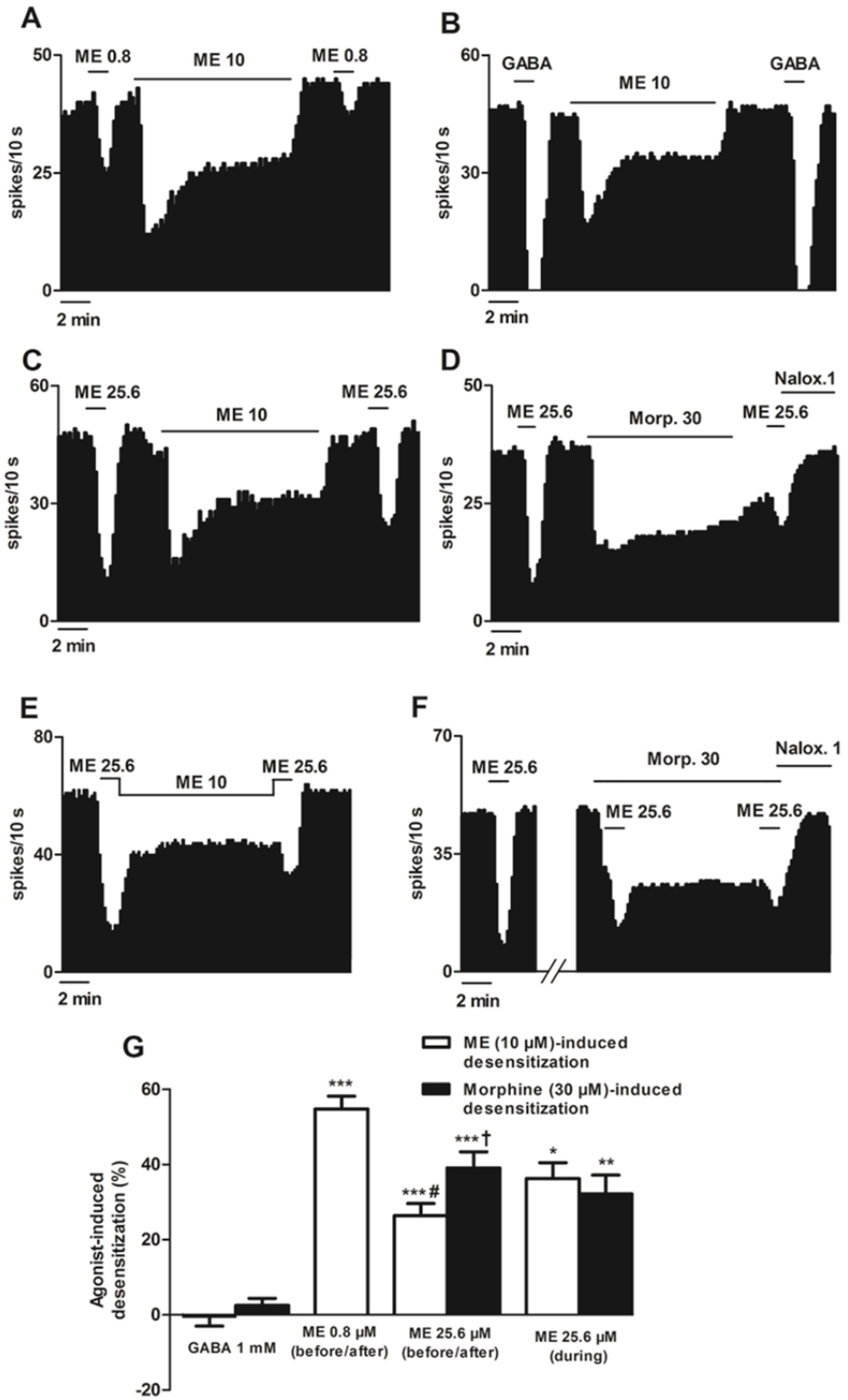
A
ME 0.8
ME 10
ME 0.8
spikes/10 s
50
25
0
2 min
B
GABA
ME 10
GABA
spikes/10 s
60
30
0
2 min
C
ME 25.6
ME 10
ME 25.6
spikes/10 s
60
30
0
2 min
D
ME 25.6
Morp. 30
ME 25.6
Nalox.1
spikes/10 s
50
25
0
2 min
E
ME 25.6
ME 10
ME 25.6
spikes/10 s
80
40
0
2 min
F
ME 25.6
Morp. 30
Nalox. 1
ME 25.6
ME 25.6
spikes/10 s
70
35
0
2 min
G
ME (10 µM)-induced desensitization
Morphine (30 µM)-induced desensitization
Agonist-induced desensitization (%)
60
40
20
0
-20
***
***#
***†
*
**
GABA 1 mM
ME 0.8 µM (before/after)
ME 25.6 µM (before/after)
ME 25.6 µM (during)

**FIGURE 5**

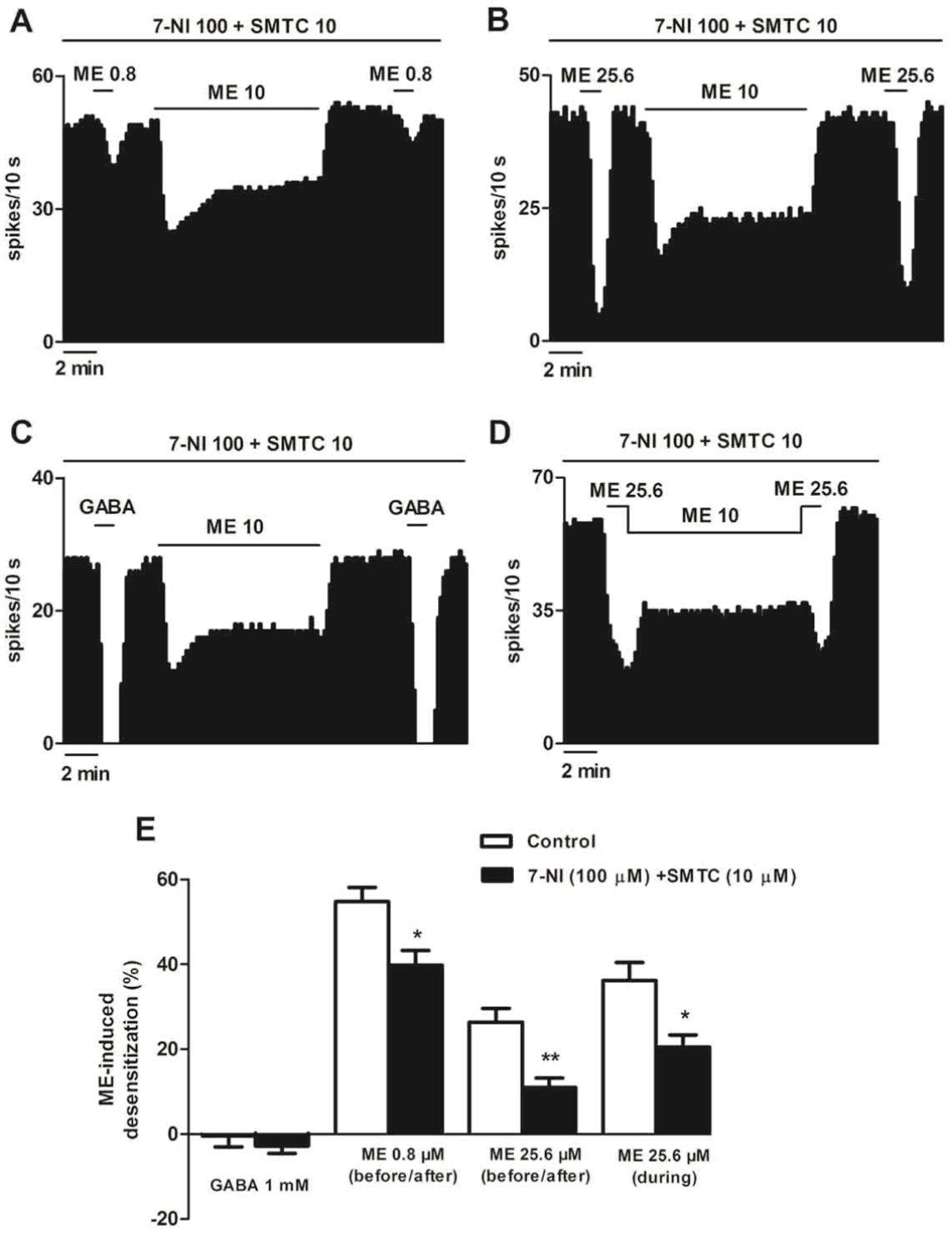
A
7-NI 100 + SMTC 10
ME 0.8
ME 10
ME 0.8
60
30
0
spikes/10 s
2 min
B
7-NI 100 + SMTC 10
ME 25.6
ME 10
ME 25.6
50
25
0
spikes/10 s
2 min
C
7-NI 100 + SMTC 10
GABA
ME 10
GABA
40
20
0
spikes/10 s
2 min
D
7-NI 100 + SMTC 10
ME 25.6
ME 10
ME 25.6
70
35
0
spikes/10 s
2 min
E
Control
7-NI (100 μM) +SMTC (10 μM)
ME-induced desensitization (%)
60
40
20
0
-20
*
**
*
GABA 1 mM
ME 0.8 μM (before/after)
ME 25.6 μM (before/after)
ME 25.6 μM (during)

**FIGURE 6**

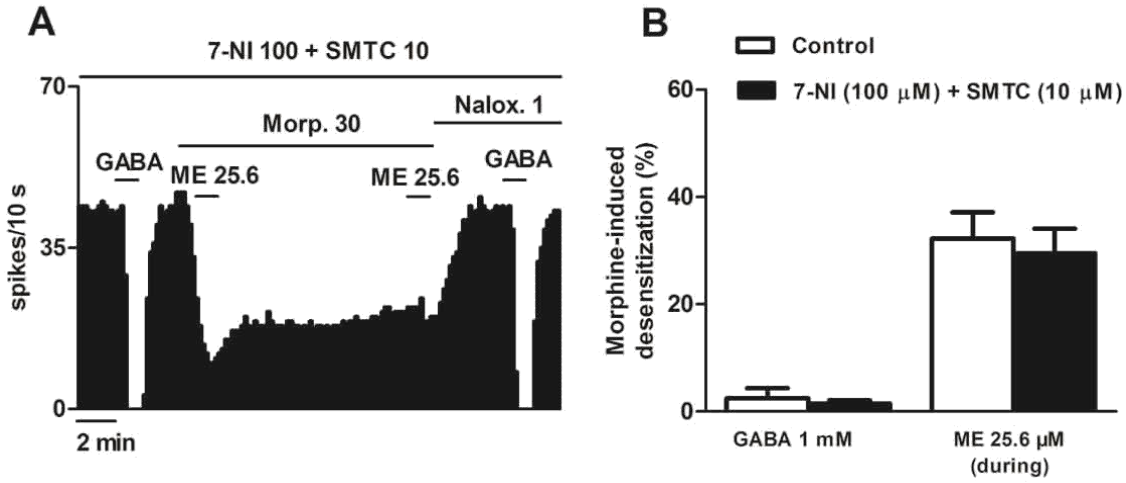
A
7-NI 100 + SMTC 10
Morp. 30
Nalox. 1
GABA
ME 25.6
ME 25.6
GABA
70
35
0
spikes/10 s
2 min
B
Control
7-NI (100 μM) + SMTC (10 μM)
60
40
20
0
Morphine-induced desensitization (%)
GABA 1 mM
ME 25.6 μM (during)

# MANUSCRIPT 3

To be submitted to *Neuropharmacology*

**Title:**

# EFFECT OF NEURONAL NITRIC OXIDE SYNTHASE INHIBITION AND ANTIOXIDANTS ON THE DEVELOPMENT OF TOLERANCE BY DIFFERENT OPIOID AGONISTS IN THE RAT LOCUS COERULEUS

**Authors:**

Patricia Pablos[1], Aitziber Mendiguren[1] and Joseba Pineda[1*].

[1]*Department of Pharmacology, Faculty of Medicine and Odontology, University of the Basque Country (UPV/EHU), E-48940 Leioa, Bizkaia, Spain*

*Corresponding author: J Pineda, M.D., Ph.D., Dept. of Pharmacology, Fac. of Medicine and Odontology, Univ. of the Basque Country (UPV / EHU), Bº Sarriena s/n, E-48940 Leioa, Bizkaia, Spain. Tel.: +34 94 6015577; fax: +34 94 6013220.

E-mail address: joseba.pineda@ehu.es (Dr. Joseba Pineda).

**Abstract**

Nitric oxide (NO) has been implicated in acute μ-opioid receptor (MOR) desensitization in the locus coeruleus (LC) and in the neuroadaptations following chronic morphine administration. Herein, we examined by extracellular recording techniques in LC neurons the effect of 7-nitroindazole (7-NI; 30 mg/kg/12 h, i.p.), a selective neuronal nitric oxide synthase (nNOS) inhibitor, and the antioxidants Trolox + ascorbic acid (TX+AA; 40 and 100 mg/kg/day, respectively, i.p.) and U-74389G (10 mg/kg/day, i.p.), on the development of cellular tolerance induced by three different opioid agonists (morphine, methadone and fentanyl). For induction of morphine tolerance, rats were treated subcutaneously (s.c.) with a slow release emulsion containing free base morphine (200 mg/kg) for 72 h. For methadone (60 mg/kg/day, 6 days) and fentanyl (0.2 mg/kg/day, 7 days), tolerance was induced by s.c. implantation of osmotic pumps. Concentration-effect curves for the inhibitory effect of the opioid agonist $Met^5$-enkephalin (ME) on the cell firing rate was evaluated by single-unit extracellular recordings of LC neurons from brain slices. Morphine, methadone and fentanyl treatments shifted concentration-effect curves for ME to the right and increased the $EC_{50}$ by 2-4 folds, as compared to those in sham-treated animals. This suggests that opioids induce different degrees of cellular tolerance in LC neurons. Tolerance to ME effect by morphine was attenuated by co-administration of TX+AA or U-74389G, when compared to the control (morphine/vehicle group). In contrast, Co-treatment with either U-74389G or 7-NI failed to alter the tolerance to the inhibitory effect of ME in methadone- or fentanyl-treated animals. Taken together, our results suggest that NO/ROS pathways differentially modulate the development of cellular tolerance in LC neurons.

*Keywords*: slice; μ-opioid receptor; tolerance; reactive oxygen species; locus coeruleus; nitric oxide.

*Abbreviations*: LC: locus coeruleus; i.p.: intraperitoneal; 7-NI: 7-nitroindazole; NMDA: N-methyl-D-aspartate; NO: nitric oxide; NOS: nitric oxide synthase; nNOS: neuronal nitric oxide synthase; ROS: reactive oxygen species; s.c.: subcutaneous; Trolox: 6-hydroxy-2,5,7,8-tetramethylchroman-2-carboxylic acid; TX+AA: Trolox and ascorbic acid; U-74389G: 21-[4-(2,6-di-1-pyrrolidinyl-4-pyrrimidinyl)-1-piperazinyl]-pregna-1,4,9(11)-triene-3,20-dione(Z)-2 butenedioate

## 1. Introduction

Morphine, methadone or fentanyl are among the most common clinically used opioid agonists. However, their long-term utility is greatly compromised because of the development of tolerance and dependence (Inturrisi, 2002). Opioid tolerance requires dose escalation to maintain adequate analgesia, which is associated with side effects, such as severe constipation or nausea. Understanding the mechanisms underlying opioid tolerance is essential to design better therapeutic approaches to improve pain management. Numerous mechanisms have been reported to contribute to opioid tolerance and it is difficult to integrate them into a unified theory. Tolerance may result from adaptive changes such as enhanced MOR desensitization, receptor internalization or receptor down-regulation, among other mechanisms (Dang and Christie, 2012; Williams et al., 2013). In addition, the N-methyl-D-aspartate receptor (NMDAR)/nitric oxide (NO) system has been proposed to be involved in opioid tolerance (Heinzen and Pollack, 2004). In the brain, NO is produced by the neuronal NO synthase (nNOS) and targets the heme group of guanylate cyclase, which elevates cGMP concentrations. Moreover, high, sustained concentrations of NO promote the generation of reactive nitrogen species and reactive oxygen species (ROS), such as the extremely oxidant molecule peroxynitrite ($ONOO^-$), originated from the reaction of NO with superoxide anion (Davis et al., 2001; Radi, 2013). Both peroxynitrite and superoxide have been implicated in the development of pain of several etiologies including pain associated with chronic use of opioids such as morphine (Salvemini et al., 2011).

The locus coeruleus (LC), the major noradrenergic nucleus in the brain, has long been used as a model for examining the cellular mechanisms of opioid tolerance and dependence (Nestler et al., 1994). It contains a homogeneous population of neurons that almost exclusively express the MOR (Williams and North, 1984). In brain slices, opioid

agonists induce a marked inhibition of LC neurons through a $G_{i/o}$ protein-dependent activation of inwardly rectifying $K^+$ channel (GIRK) conductance (Williams et al. 1982; Torrecilla et al., 2002). The NO system participates in the adaptive mechanisms underlying opioid tolerance in the LC. Thus, inhibition of neuronal NO synthase attenuates acute MOR desensitization induced by the opiod agonist $Met^5$-enkephalin (ME) (Santamarta et al., 2014) and attenuates cellular tolerance in morphine-treated animals (Santamarta et al., 2005). Futthermore, ROS seem to contribute to the enhancement on MOR desensitization induced by NO in LC neurons (Llorente et al., 2012). However, there is lacking evidence regarding the implication of NO/ROS pathway in the adaptations triggered by chronic treatments with other different opioid agonists in the LC. Morphine, methadone and fentanyl are opioid agonists that exert their effects mainly through MOR, but they promote quantitatively different actions at the cellular level. Thus, methadone and fentanyl have been reported to promote efficient desensitization and internalization of MOR in the LC (Alvarez et al., 2002; Arttamangkul et al., 2008, Virk and Williams, 2008). In contrast, morphine seems to be relatively inefficient at producing acute desensitization and internalization in this nucleus (Alvarez et al., 2002; Arttamangkul et al., 2008).

The aim of this work was to investigate whether NO and ROS regulate the tolerance induced by opioids with different pharmacologic profiles, such as morphine, methadone and fentanyl. For that purpose, we performed uni-extracellular recordings *in vitro* to evaluate the effect of chronic treatment with 7-nitroindazole (7-NI), a relatively selective inhibitor of neuronal NO synthase (Moore et al., 1993; Moore and Handy, 1997) on methadone- and fentanyl-induced tolerance. Moreover, the effect of treatment with the antioxidants 6-hydroxy-2,5,7,8-tetramethylchroman-2-carboxylic acid (Trolox) administered together with ascorbic acid (TX+AA) or 21-[4-(2,6-di-1-pyrrolidinyl-4-

pyrrimidinyl)-1-piperazinyl]-pregna-1,4,9(11)-triene-3,20-dione(*Z*)-2-butenedioate (U-74389G) was also evaluated on morphine-, methadone- and fentanyl-treated animals.

## 2. Materials and Methods

### *2.1 Animals and treatments.*

Male adult Sprague-Dawley rats (200-300 g) were housed under standard laboratory conditions (22ºC, 12:12 h light/dark cycles) with free access to food and water. All experimental procedures reported in this manuscript were carried out in accordance with the European Community Council Directive on "Protection of Animals Used in Experimental and Other Scientific Purposes" (86/609/EEC) and approved by the Research Committee of the Faculty of Medicine and Odontology (University of the Basque Country, Spain). Every effort was made to minimize animal suffering and use the fewest possible number of animals.

For induction of morphine tolerance, an oily emulsion of morphine base (200 mg/kg) was subcutaneously injected in the back of the rat, under chloral hydrate (200 mg/kg, intraperitoneal (i.p.)) anesthesia. Sham animals were administered the same vehicle emulsion without morphine. Then, morphine or sham animals were daily injected with the antioxidants Trolox (40 mg/kg) and ascorbic acid (100 mg/kg) (TX+AA), U-74389G (10 mg/kg) or 0.9% NaCl (saline) intraperitoneally (i.p.). Electrophysiological experiments were performed 72 h after emulsion implantation.

For chronic treatments with methadone or fentanyl, osmotic mini-pumps (Alzet 2ML1) were implanted subcutaneously, as described by Quillinan et al. (2011) and Trujillo et al. (2004), respectively. The mini-pumps have a 2 ml reservoir that delivers the content continuously at the rate of 10 µl/h. Pumps were filled with the required concentration of methadone (60 mg/kg/day) or fentanyl (0.2 mg/kg/day), dissolved in saline. Animals were first anaesthetized with isoflurane and an incision was made in the midscapular region to insert the minipump. Sham animals were implanted with saline-

filled osmotic pumps under the same experimental conditions. For induction of methadone tolerance, rats were given methadone i.p injections before the implantation of the pump, as follows: the day before, they received 5 mg/kg at 9:00 h and 7 mg/kg at 18:00 h. Next day, they received 7 mg/kg at 9:00 h and the osmotic pump was implanted at 18:00 h. Once the minipump was inserted, sham, methadone-, or fentanyl-treated animals were treated every 12 h with the nNOS inhibitor 7-NI (30 mg/kg) or its vehicle (peanut oil), i.p. In another group of experiments, sham, methadone-, or fentanyl-receiving rats were daily injected with the antioxidant U-74389G (10 mg/kg) or its vehicle (saline), i.p. Experiments were carried out on day 7 in methadone-treated rats (6 days after minipump implantation) and on day 8 in fentanyl-treated rats (7 days after minipump implantation).

*2.2 In vitro electrophysiology*

*2.2.1 Brain slice preparation*.

Animals were anaesthetized with chloral hydrate (400 mg/kg, i.p.) and decapitated. The brain was rapidly removed and a block of tissue containing the brainstem was placed in ice-cold artificial cerebrospinal fluid (aCSF) containing 130 mM NaCl, 3 mM KCl, 1.25 mM $NaH_2PO_4$, 10 mM D-glucose, 21 mM $NaHCO_3$, 2 mM $CaCl_2$, and 2 mM $MgSO_4$. Coronal slices of 600 µm thickness containing the LC were cut using a vibratome. The tissue was allowed to recover from the slicing for 90 min in oxygenated aCSF. Next, slices were placed on a nylon mesh in a modified Haas-type interface chamber maintained at 33 °C and continuously perfused with aCSF saturated with 95% $O_2$/ 5% $CO_2$ (pH = 7.34) at a flow rate of 1.5 ml/min.

*2.2.2 Recording procedures*

Single-unit extracellular recordings of LC cells were performed as described previously (Mendiguren and Pineda, 2004). The recording electrode, an Omegadot glass micropipette, was pulled and filled with NaCl (50 mM). The tip was broken back to a diameter of 2 – 5 μm (3 – 5 MΩ). The electrode was placed in the LC, visually identified as a dark oval area on the lateral borders of the central gray and the fourth ventricle, just anterior to the genu of the facial nerve. The extracellular signal from the electrode was passed through a high-input impedance amplifier and displayed on an oscilloscope and monitored with an audio unit. Individual neuronal spikes were isolated from the background noise with a window discriminator. The firing rate was analyzed by a PC-based custom-made software, which generated histogram bars representing the cumulative number of spikes in consecutive 10 s bins (HFCP®, Cibertec S.A., Madrid, Spain). Noradrenergic cells were identified by their spontaneous and regular discharge activity, the slow firing rate and the long-lasting, positive-negative waveform (Andrade et al., 1983).

*2.3 Pharmacological procedures*

To assess the effect of 7-NI and antioxidants on the development of opioid tolerance in LC neurons, we performed concentration-effect curves for the inhibitory effect of the MOR agonist ME in sham and opioid-treated animals. Thus, we perfused increasing concentrations of ME (2x, 0.05 – 12.8 μM, each concentration applied for 1 min) at 5-min intervals. ME was chosen because its washout is fast even at high concentrations and its action is mediated almost exclusively by MOR in LC neurons

(Williams and North, 1984). The inhibitory effect of each ME concentration was calculated as follows:

$$E = (FR_{basal} - FR_{post}) \cdot 100 / FR_{initial}$$

where $FR_{basal}$ is the average firing rate for 60 s before each ME application, $FR_{post}$ is the average firing rate for 60 s after each ME perfusion, and $FR_{initial}$ is the firing rate of each cell at the beginning of the recording. Curve fitting analysis was performed by the computer program GraphPad Prism (version 5.0 for Windows, San Diego, CA, USA) to obtain the best simple nonlinear fit to the following three-parameter logistic equation:

$$E = E_{max} / [1 + (EC_{50}/A)^n]$$

in which E and A are the observed effect and the concentration of the agonist (ME), respectively; $E_{max}$ is the maximal effect, expressed in percentage values; $EC_{50}$ is the concentration of ME needed to elicit a 50% of the maximal effect, and n represents the slope factor of the function. $EC_{50}$ values were finally expressed as negative logarithm ($pEC_{50}$).

*2.4 Drugs and reagents*

The following drugs were purchased from Sigma-Aldrich Química (Madrid, Spain): Fentanyl, methadone, L-ascorbic acid and 7-nitroindazole (7-NI). $Met^5$-enkephalin acetate salt (ME) was obtained from Bachem (Weil am Rhein, Germany). Morphine base was purchased from Alcaliber (Madrid, Spain). Trolox and U-74389G were obtained from Enzo Life Sciences (Lausen, Switzerland). For electrophysiological recordings, ME stock solutions were firstly prepared in miliQ water and then then diluted in aCSF to their final concentration. The aCSF contained (in mM): NaCl 129, KCl 3, $NaH_2PO_4$ 1.25, D-glucose 10, $NaHCO_3$ 21, $CaCl_2$ 2 and $MgSO_4$ 2 For subchronic treatment with morphine,

an oily emulsion of morphine free base (200 mg ml-1) containing mannide monooleate, liquid parafine, and 0.9% NaCl (0.08: 0.42: 0.5, v/v/v) was made (Santamarta et al., 2005). All the drugs were dissolved in saline except 7-NI, which was dissolved in peanut oil.

*2.5 Data analysis and statistics*

Data are expressed as mean ± standard error of the mean (SEM). For statistical analysis, the $EC_{50}$ values were transformed to the corresponding logarithmic data to convert them to a Gaussian distribution. Data among groups were compared by one-way analysis of variance (ANOVA) followed by Tukey´s *post hoc* test using the computer program GraphPad Prism (version 5.0). A probability level of 0.05 was accepted as statistically significant.

## 3. Results

### Effect of chronic treatments with morphine, methadone and fentanyl on concentration-effect curves for ME in rat LC neurons

To evaluate the development of tolerance, concentration-effect curves for the inhibitory effect of ME were performed. It has been reported that the firing rate of LC neurons is elevated in brain slices from opioid-treated rats (Kogan et al., 1992). In this study we attempted to minimize the differences in firing rates among groups by performing concentration-effect curves only in cells that displayed standard spontaneous firing rates in the range of 0.4-1.5 Hz (mean ± SEM: 0.80 ± 0.02 Hz, $n$ = 95). This procedure attempted to avoid the possibility that a change in the spontaneous activity of LC cells could influence the quantification of opioid effects (Andrade et al., 1983). Thus, the firing rate of LC neurons from morphine-, methadone- and fentanyl-treated animals was not different when compared to the corresponding sham groups (Tables 1 and 2). Subchronic treatment with morphine (200 mg/kg, s.c., 72 h) induced a strong degree of tolerance in the LC, which was revealed by a substantial rightward shift in the concentration-effect curves for ME and an increase in the $EC_{50}$ of about 4 fold, as compared to the corresponding sham group ($p < 0.005$) (Figs. 1A and 2A; Table 2). Similarly, chronic treatment with methadone (60 mg/kg/day, s.c., 6 days) induced a rightward shift in the concentration-effect curves for ME and increased by about 2 fold the $EC_{50}$ value when compared to the corresponding sham group ($p < 0.005$) (Figs. 1B and 2B; Table 2). Finally, chronic treatment with fentanyl (0.2 mg/kg/day, s.c., 7 days) also caused a rightward shift in the concentration-effect curves for ME with an increase of the $EC_{50}$ of about 3 fold, as compared to the corresponding sham group ($p < 0.005$) (Figs. 1B and 2C; Table 2). These results indicate that morphine, methadone and fentanyl

induce different degrees of tolerance to the inhibitory effect of ME in LC neurons. In all groups, the maximal effect of ME was 100% of baseline, which corresponded with an absolute inhibition from the basal firing rate.

**Effect of the nNOS inhibitor 7-NI on opioid tolerance in rat LC neurons**

*In vivo* administration of the nNOS inhibitor 7-NI has been shown to attenueate the development of cellular tolerance in LC neurons from morphine-treated rats (Santamarta et al., 2005). Herein, we tested the effect of 7-NI on the tolerance induced by chronic treatments with other opioid agonists such as methadone and fentanyl. Co-administration of 7-NI in methadone- and fentanyl-treated rats (methadone/7-NI group and fentanyl/7-NI group) failed to prevent the development of tolerance. Thus, the $pEC_{50}$ values of concentration-effect curves for ME in the methadone/7-NI or fentanyl/7-NI group were statistically lower than those in the corresponding sham group ($p < 0.005$ *vs* sham/7-NI; in both cases), but they were not different from the corresponding vehicle groups (i.e., *vs* methadone/vehicle and fentanyl/vehicle) (Fig. 3; Table 1). 7-NI administration in sham-treated animals (sham-7-NI group) did not modify the concentration-effect curves for ME in the LC as compared to the sham-vehicle group (Fig. 3; Table 1). No differences were found in the basal firing rate among groups (Table 1). Therefore, unlike morphine (Santamarta et al., 2005), the neuronal NOS inhibitor 7-NI fails to affect the development of opioid tolerance after methadone or fentanyl treatments.

**Effect of antioxidants on opioid tolerance in rat LC neurons**

Previous results from our group have shown that the co-administration of the free radical scavenger Trolox together with ascorbic acid (TX+AA) blocked partially the development of analgesic tolerance in morphine-treated rats (J. Llorente, Doctoral Thesis,

unpublished data). To verify these results with other antioxidants and other opioid agonists, we evaluated the effect of co-administration of TX+AA or U-74389 on the development of tolerance in morphine-, methadone- and fentanyl-treated animals. In agreement with previous results, co-administration of the vitamin E analogue Trolox, together with ascorbic acid in morphine-treated rats (morphine/TX+AA group) attenuated the development of cellular tolerance, which was shown by a blockade of the rightward shift of the concentration-effect curve in this group. Thus, the $pEC_{50}$ value for ME effect in the morphine/TX+AA group did not differ statistically from the value in the sham/TX+AA group, but it was significantly less than that in the morphine/vehicle group ($p < 0.05$), indicating that the blockade of morphine tolerance by TX+AA was complete (Figs. 4A and C; Table 2). In contrast, TX+AA administration in sham-treated animals (sham/TX+AA) did not modify the concentration-effect curves for ME in the LC, as compared to the sham/vehicle group (Figs. 4A and C; Table 2). Likewise, co-treatment with U-74389G, a structurally unrelated antioxidant in morphine-treated rats (morphine/U-74389G group), attenuated the development of morphine tolerance, revealed by a blockade of the rightward shift of the concentration-effect curves in this group and an overlap with sham curves. Hence, the $pEC_{50}$ for ME effect in the morphine/U-74389G group was not different from that in the sham/U-74389G group, but was significantly less than that in the morphine/vehicle group ($p < 0.01$) (Figs. 4B and C; Table 2). Administration of U-74389G in sham animals (sham/U-74389G) failed to modify the concentration-effect curves for ME when compared to the sham/vehicle group (Figs. 4B and C; Table 2). No differences were found in the basal firing rate among groups (Table 2).

On the contrary, co-treatment with U-74389G in rats treated chronically with methadone or fentanyl (methadone/U-74389G and fentanyl/U-74389G group) did not prevent the development of cellular tolerance induced by these opioids, so that the concentration-effect curves from either methadone/U-74389G or fentanyl/U-74389G group were overlapped with those from their respective vehicle groups (methadone/vehicle and fentanylvehicle, respectively). Thus, the $pEC_{50}$ values for ME effect in the methadone/U-74389G or fentanyl/U-74389G groups were statistically different from the corresponding sham group (sham/ U-74389G; $p < 0.05$ and $p < 0.01$, respectively), but they were not different from the corresponding vehicle groups (methadone/vehicle and fentanyl/vehicle, respectively) (Fig. 5; Table 2). U-74389G administration in sham animals (sham/U-74389G) failed to modify the concentration-effect curves for ME when compared to the sham/vehicle group (Fig. 5; Table 2). No differences were found in the basal firing rate among groups (Table 2).

Taken together, these data indicate that antioxidants reduce the development of opioid tolerance after morphine, but not methadone or fentanyl, and therefore, ROS seem to be differentially involved in opioid-induced cellular tolerance in the LC.

## 4. Discussion

The NO system has been involved in the underlying mechanisms of acute desensitization of MOR (Llorente et al., 2012; Santamarta et al., 2014; Torrecilla et al., 2001) and in the development of morphine-induced tolerance (Santamarta et al., 2005). The aim of this work was to investigate the role of neuronal NOS and NO-derived ROS in the development of tolerance induced by three different opioid agonists: morphine, methadone and fentanyl. For that purpose, we performed uni-extracellular recordings of LC neurons to test the effect of the nNOS inhibitor 7-NI and the ROS scavengers TX+AA and U-74389G on the induction of tolerance by chronic treatments with these three opioid agonists. Chronic treatments with morphine, methadone and fentanyl resulted in cellular tolerance in LC neurons, which was revealed by a rightward shift of 2-4 fold in the concentration-effect curves for the inhibitory effect of ME. Co-treatment with TX+AA and U-74389G attenuated the tolerance to the electrophysiological effect of ME induced by morphine. On the contrary, co-treatment with 7-NI or with U-74389G failed to modify the cellular tolerance induced by methadone or fentanyl.

It has been described that basal firing rates of LC neurons are significantly higher in slices from morphine-treated animals (Kogan et al., 1992), although they fire at control rates in morphine-treated rats that have been acutely pretreated with 7-NI (Pineda et al., 1998). In the present study, concentration-effect curves for ME were performed only in LC cells that spontaneously fired at slow rates (between 0.4 and 1.5 Hz, as in control animals), to avoid a biased quantification of opioid effects influenced by differences in the spontaneous activity of LC neurons. We used ME as an indicator of MOR function in the LC because it is a potent agonist that acts almost exclusively through MOR (Williams and North, 1984). Furthermore, it rapidly washes out after perfusion, which allows us to characterize the effect easily by extracellular recordings. Morphine tolerance was induced

by s.c. implantation of an oily emulsion containing morphine base (200 mg/kg, a single administration, 72 h). These emulsions have been described to provide a slow drug release and prolonged exposure to the opioid (Salem and Hope, 1999). According to the time course described in mice, the emulsion promotes a rise in morphine concentration in serum 3–12 h after implantation and a gradual clearance of morphine over 4–5 days (Garzón and Sánchez-Blázquez, 2001). In the present study, morphine caused a 4-fold shift to the right in the concentration-effect curves for ME in the LC. This degree of cellular tolerance is comparable to that reported previously in LC neurons *in vitro*, using the same morphine protocol (Santamarta et al., 2005). Likewise, in a previous study in the LC *in vivo*, we reported a 4-fold rightward shift in the morphine dose-effect curves after intraperitoneal administration of morphine hydrochloride solutions (10–100 mg/kg per injection, 15 injections, 5 days) (Pineda et al., 1998). However, Highfield and Grant (1998) implanted several slow-release pellets (75 mg morphine base per pellet, 6 pellets, 6 days) and found a 2-fold rightward shift in the concentration-effect curves for morphine in LC cells.

Chronic treatment with methadone osmotic pumps (60 mg/kg/day, 6 days) caused a 2-fold shift to the right in the concentration-effect curves for ME in the LC. Likewise, Quillinan et al. (2011) observed a 2-fold shift to the right in the concentration-effect curves for ME measured by intracellular recordings in LC cells using the same methadone administration protocol. Methadone has been reported to cause antinociception in the tail flick and hot plate tests with a potency similar to that of morphine when given s.c. to rats (Giusti et al., 1997; He et al., 2009). Furthermore, the peak hyperpolarization caused by methadone (30 μM) is approximately the same as the hyperpolarization induced by morphine (30 μM) measured by extracellular recordings in LC neurons (Alvarez et al., 2002). The dose of methadone that is delivered daily by the

pump is comparable to that estimated to be released daily by the morphine emulsion (~66 mg/kg/day), but elicited a less profound degree of cellular tolerance. In behavioral experiments chronic methadone treatment has been also reported to cause a less strong degree of antinociceptive tolerance than morphine when given at equianalgesic doses (Enquist et al., 2012). In our results, morphine treatment exerted a stronger degree of cellular tolerance than methadone in LC neurons (see above). Studies comparing different MOR agonists have found that those that induce robust receptor endocytosis and recycling tend to produce reduced analgesic tolerance and dependence (Whistler et al., 1999). Morphine has a poor ability to promote internalization and recycling of the MOR (Alvarez et al., 2002; Arttamangkul et al., 2008), whereas methadone efficiently internalizes the MOR in different systems (Alvarez et al., 2002; Arttamangkul et al., 2008; Celver et al., 2004; Keith et al., 1998; Koch et al., 2005). In agreement with this hyphothesis, mice with genetically modified MORs that have the ability to spontanelusly internalize and recycle develop a reduced tolerance to morphine (Kim et al., 2008). Similarly, animals with mutant MORs that show enhanced receptor degradation after endocytosis, developed stronger antinociceptive tolerance after methadone treatment (Enquist et al., 2012).

On the other hand, chronic treatment with fentanyl minipumps (0.2 mg/kg/day, 7 days) resulted in a 3-fold shift to the right in the concentration-effect curves for ME in LC neurons. Fentanyl has been reported to be up to 100 times more potent than morphine at producing analgesia (Vardanyan and Hruby, 2014). Surprisingly, this fentanyl administration protocol did not cause antinociceptive tolerance (Pablos et al., unpublished results). Paronis and Holtzman (1992) also observed that fentanyl (0.24 mg/kg/day) infused for 7 days by osmotic pumps failed to induce significant analgesic tolerance in rats. However, fenatnyl has been found to induce analgesic tolerance when given at a

dose of 0.04 mg/kg (s.c., 4 times a day, 3 days) in mice (Popik et al., 2000) and also at much higher doses, such as 2.4 mg/kg/day (72 h) or 3.2 mg/kg/day (5 days) by subcutaneously implanted pumps in neonatal rats and mice (Raehal and Bohn, 2011; Thornton and Smith, 1997). Fentanyl induces endocytosis and recycling of the MOR (Celver et al., 2004), which was been associated with a less potential to induce tolerance. In our study, fentanyl elicited a slightly less stronger rightward shift in the concentration-effect curves than morphine in LC neurons (see above).

Thus, it can be hypothesized that differences between opioids in their ability to induce receptor internalization and recycling may contribute, at least in part, to the different degrees of cellular tolerance observed in this study. In contrast, other studies show that β-arrestin2 knockout mice, in which MOR endocytosis is presumably unpaired, fail to develop both cellular tolerance (Dang et al., 2011) and antinociceptive tolerance after morphine (Bohn et al., 2000), but not after methadone or fentanyl treatments (Raehal and Bohn, 2011). Interistingly, the impaired MOR recycling that was found in wild-type LC neurons from morphine-treated rats was attenuated in β-arrestin2 knockout animals (Quillinan et al., 2011). Thus, β-arrestin2 may disrupt the ability of receptors to recycle after endocytosis, and therefore, contribute to the development of tolerance.

Interactions between the opioid system and the NO cascade have been described in the brain (Pasternak et al., 1995; Sánchez-Blázquez et al., 2013). Thus, NOS activity and expression in the central nervous system is up-regulated after chronic morphine administration (Cuéllar et al., 2000; Machelska et al., 1997). Previous data from our laboratory have shown that perfusion with non-selective and selective NOS inhibitors attenuates acute MOR desensitization induced by ME in LC cells *in vitro* (Santamarta et al., 2014; Torrecilla et al., 2001). Moreover, the nNOS inhibitor 7-NI attenuates the development of cellular and antinociceptive tolerance in morphine-treated rats

(Santamarta et al., 2005). Likewise, nNOS-, but not eNOS-deficient mice, exhibit weak analgesic tolerance to morphine when compared to wild type animals (Heinzen and Pollack, 2004). NOS inhibitors also attenuated the withdrawal-induced hyperactivity of LC cells (Pineda et al., 1998). 7-NI is a heterocyclic compound that hardly distinguishes between nNOS and eNOS in brain homogenate preparations, but it exhibits a marked selectivity for neuronal NOS in intact cell models or *in vivo* (Babbedge et al., 1993; Hobbs et al., 1999), which is likely due to specific targets of 7-NI that are only present in neurons (Alderton et al., 2001; Handy and Moore, 1998). NO reacts with oxygen derivatives to produce ROS, such as the powerful oxidant peroxynitrite (Davis, 2001). ROS have been reported to regulate MOR desensitization in the LC (Llorente et al., 2012). In this study, we found that TX+AA (40 and 100 mg/kg/day, respectively, i.p.) and U-74389G (10 mg/kg/day, i.p.), attenuated morphine-induced cellular tolerance to the inhibitory effect of ME on LC neurons. Trolox is a cell-permeable vitamin E derivative with powerful antioxidant properties (Balogh et al., 2005). Ascorbic acid is a potent antioxidant and ROS chelator by itself, but we used it as a Trolox recycler from oxidation (Guo and Packer, 2000). Vitamin E (40 mg/kg) and ascorbic acid (100 mg/kg) are effective in preventing oxidative damage in the rat brain (Delwing et al., 2005). U-74389G is a 21-aminosteroid that potently inhibits ROS-mediated peroxidation and it has been shown to reduce cerebral superoxide anion concentration following brain injury (Fabian et al., 1998; Villa and Gorini, 1997). Similarly, TX+AA and U-74389G have been shown to block partially the development of antinociceptive tolerance induced by morphine (Pablos et al.,unpublished results). In agreement, other ROS scavengers such as melatonin (Raghavendra and Kulkarni, 2000), alpha-lipoic acid (Abdel-Zaher et al., 2013) or metalloporphyrins (Muscoli et al., 2007; Batinić-Haberle et al., 2009) attenuate the development of morphine-induced antinociceptive tolerance.

The mechanisms by which NO modulates morphine-induced tolerance via ROS generation remain unclear. One possible mechanism might be ROS-mediated activation of PKC. Opioids can induce a sustained increase in ROS (Koch et al., 2009) and PKC can be activated by raising the concentrations of ROS (Palumbo et al., 1992; Knapp and Klann, 2002). In the LC, PKC-induced phosphorylation enhances MOR desensitization induced by morphine without changing $\alpha_2$-adrenoceptor desensitization (Bailey et al., 2004). There is also good evidence that PKC-dependent mechanisms play a significant role in the development of morphine analgesic tolerance (Newton et al., 2007; Smith et al., 2003; Zeitz et al., 2001). Molecular data have reported that in brain areas such as the PAG, morphine-activated MOR increases NO concentrations via the Akt-nNOS pathway and activates PKC, which stimulates the activity of NMDARs (Sánchez-Blázquez et al., 2010). This increased NMDAR activity would induce the phosphorylation and uncoupling of MORs via nNOS/CaMKII pathway, which results in the development of morphine analgesic tolerance (Sánchez-Blázquez et al., 2013). Indeed, NMDAR antagonists and nNOS and CaMKII inhibitors attenuate opioid tolerance and withdrawal (Elliott et al., 1994; Herman et al., 1995). Future studies should test this hypothesis and the possible involvement of other kinases such as c-Jun N-terminal kinase (Melief et al., 2010).

Conversely, our results show that 7-NI and antioxidants did not affect the development of tolerance in rats treated chronically with methadone or fentanyl. Similarly, behavioral experiments showed that 7-NI and U-74389G failed to alter the development of antinociceptive tolerance in methadone-treated rats (Pablos et al., unpublished results). It has been described that methadone is a weak noncompetitive NMDAR antagonist (Ebert et al., 1998) and might counteract maladaptive changes in glutamate transmission. This might explain, at least in part, the less strong degree of

cellular tolerance after methadone treatment and the lack of effects of NO/ROS modulators on methadone-induced tolerance. Methadone and fentanyl may induce cellular tolerance by different mechanisms and cellular pathways from those described for morphine, as they trigger internalization and recycling of the MOR. Further assays should unmask the mechanisms underlying methadone- and fentanyl-induced adaptations. In conclusion, our results show that chronic treatments with morphine, methadone and fentanyl induce different degrees of cellular tolerance in LC neurons. In addition, *in vivo* administration of antioxidant agents attenuates the development of morphine-, but not methadone- or fentanyl-induced cellular tolerance. Therefore, NO/ROS pathways seem to be differentially involved in opioid cellular tolerance. Taken together, our results highlight the interest of a pharmacological protection against NO-derived ROS generation to attenuate the development of morphine tolerance and maintain a better control of pain.

**Acknowledgements**

This work was supported by the Ministerio de Ciencia e Innovación [Grant SAF2008-03612] and the University of the Basque Country (UPV/EHU) [Grant GIU11/27 and Grant GIU14/29]. Pineda´s research group takes part in a network unit supported by the University of the Basque Country [UFI 11/35]. I. P. Pablos was supported by a predoctoral fellowship from the Basque Government. There is no conflict of interest and no financial relationship with the Organization that sponsored the research. The experiments comply with the current laws of Spain.

**Conflict of interest**

The authors declare that there is no conflict of interest.

## References

Abdel-Zaher, A.O., Mostafa, M.G., Farghaly, H.S., Hamdy, M.M., Abdel-Hady, R.H., 2013. Role of oxidative stress and inducible nitric oxide synthase in morphine-induced tolerance and dependence in mice. Effect of alpha-lipoic acid. Behav Brain Res. 247, 17–26.

Alderton, W.K., Cooper, C.E., Knowles, R.G., 2001. Nitric oxide synthases: structure, function and inhibition. Biochem J. 357, 593–615.

Alvarez, V.A., Arttamangkul, S., Dang, V., Salem, A., Whistler, J.L., Von Zastrow, M., Grandy, D.K., Williams, J.T., 2002. mu-Opioid receptors: Ligand-dependent activation of potassium conductance, desensitization, and internalization. J. Neurosci. 22, 5769–5776.

Andrade, R., Vandermaelen, C.P., Aghajanian, G.K., 1983. Morphine tolerance and dependence in the locus coeruleus: single cell studies in brain slices. Eur. J. Pharmacol. 91, 161–169.

Arttamangkul, S., Quillinan, N., Low, M.J., von Zastrow, M., Pintar, J., Williams, J.T., 2008. Differential activation and trafficking of mu-opioid receptors in brain slices. Mol. Pharmacol. 74, 972–979.

Babbedge, R.C., Bland-Ward, P.A., Hart, S.L., Moore, P.K., 1993. Inhibition of rat cerebellar nitric oxide synthase by 7-nitro indazole and related substituted indazoles. Br. J. Pharmacol. 110, 225–228.

Bailey, C.P., Kelly, E., Henderson G., 2004. Protein kinase C activation enhances morphine-induced rapid desensitization of mu-opioid receptors in mature rat locus ceruleus neurons. Mol. Pharmacol. 66, 1592–1598.

Balogh, G.T., Vukics, K., Könczöl, A., Kis-Varga, A., Gere, A., Fischer, J., 2005. Nitrone derivatives of trolox as neuroprotective agents. Bioorg. Med. Chem. Lett. 15, 3012–3015.

Batinić-Haberle, I., Ndengele, M.M., Cuzzocrea, S., Rebouças, J.S., Spasojević, I., Salvemini, D., 2009. Lipophilicity is a critical parameter that dominates the efficacy of metalloporphyrins in blocking the development of morphine antinociceptive tolerance through peroxynitrite-mediated pathways. Free Radic. Biol. Med. 46, 212–219.

Bohn, L.M., Gainetdinov, R.R., Lin, F.T., Lefkowitz, R.J., Caron, M.G., 2000. Mu-opioid receptor desensitization by beta-arrestin-2 determines morphine tolerance but not dependence. Nature. 408, 720–723.

Celver, J., Xu, M., Jin, W., Lowe, J., Chavkin, C., 2004. Distinct domains of the mu-opioid receptor control uncoupling and internalization. Mol Pharmacol. 65, 528–537.

Cuéllar, B., Fernández, A.P., Lizasoain, I., Moro, M.A., Lorenzo, P., Bentura, M.L., Rodrigo, J., Leza, J.C., 2000. Up-regulation of neuronal synthase immunoreactivity in opiate dependence and withdrawal. Psychopharmacology 148, 66–73.

Dang, V.C., Chieng, B., Azriel, Y., Christie, M.J., 2011. Cellular morphine tolerance produced by barrestin-2-dependent impairment of μ-opioid receptor resensitization. J Neurosci. 31, 7122–7130.

Dang, V.C., Christie, M.J., 2012. Mechanisms of rapid opioid receptor desensitization, resensitization and tolerance in brain neurons. Br. J. Pharmacol. 165, 1704–1716.

Davis, K.L., Martin, E., Turko, I.V., Murad, F., 2001. Novel effects of nitric oxide. Annu. Rev. Pharmacol. Toxicol. 41, 203–236.

Delwing, D., Chiarani, F., Bavaresco, C.S., Wannmacher, C.M., Wajner, M., Dutra-Filho, C.S., Wyse, A.T., 2005. Protective effect of antioxidants on brain oxidative damage caused by proline administration. Neurosci. Res. 52, 69–74.

Ebert, B., Thorkildsen, C., Andersen, S., Christrup, L.L., Hjeds, H., 1998. Opioid analgesics as noncompetitive N-methyl-D-aspartate (NMDA) antagonists. Biochem Pharmacol. 56, 553–559.

Elliott, K., Minami, N., Kolesnikov, Y.A., Pasternak, G.W., Inturrisi, C.E., 1994. The NMDA receptor antagonists, LY274614 and MK-801, and the nitric oxide synthase inhibitor, NG-nitro-L-arginine, attenuate analgesic tolerance to the mu-opioid morphine but not to kappa opioids. Pain. 56, 69–75.

Enquist, J., Ferwerda, M., Milan-Lobo, L., Whistler, J.L., 2012. Chronic methadone treatment shows a better cost/benefit ratio than chronic morphine in mice. J Pharmacol Exp Ther. 340, 386–392.

Fabian, R.H., Dewitt, D.S., Kent, T.A., 1998. The 21-aminosteroid U-74389G reduces cerebral superoxide anion concentration following fluid percussion injury of the brain. J. Neurotrauma. 15, 433–440.

Garzón, J., Sánchez-Blázquez, P., 2001 Administration of $myr^{+}$-$G_{i2}\alpha$ subunits prevents acute tolerance (tachyphylaxis) to mu-opioid effects in mice. Neuropharmacology 40, 560–569.

Giusti, P., Buriani, A., Cima, L., Lipartiti, M., 1997. Effect of acute and chronic tramadol on [3H]-5-HT uptake in rat cortical synaptosomes. Br J Pharmacol. 122, 302–306.

Guo, Q., Packer, L., 2000. Ascorbate-dependent recycling of the vitamin E homologue trolox by dihydrolipoate and glutathione in murine skin homogenates. Free Radic. Biol. Med. 29, 368–374.

Handy, R..L.C., Moore, P.K., 1998. Handy and Moore reply: 7-nitroindazole (7-NI) fails to increase blood pressure in animals: The 7-NI 'conundrum'. Trends Pharmacol Sci 19, 350.

He, L., Kim, J., Ou, C., McFadden, W., van Rijn, R.M., Whistler, J.L., 2009. Methadone antinociception is dependent on peripheral opioid receptors. J Pain. 10, 369–379.

Heinzen, E.L., Pollack, G.M., 2004. The development of morphine antinociceptive tolerance in nitric oxide synthase-deficient mice. Biochem. Pharmacol. 67, 735–741.

Herman, B.H., Vocci, F., Bridge, P., 1995. The effects of NMDA receptor antagonists and nitric oxide synthase inhibitors on opioid tolerance and withdrawal. Medication development issues for opiate addiction. Neuropsychopharmacology 13, 269–293.

Highfield, D.A., Grant, S., 1998. Ng-nitro-L-arginine, an NOS inhibitor, reduces tolerance to morphine in the rat locus coeruleus. Synapse 29, 233–239.

Hobbs, A.J., Higgs, A., Moncada, S., 1999. Inhibition of nitric oxide synthase as a potential therapeutic target. Annu. Rev. Pharmacol. Toxicol. 39, 191–220.

Inturrisi, C.E., 2002. Clinical pharmacology of opioids for pain. Clin. J. Pain 18(Suppl 4), 3S–13S.

Keith, D.E., Anton, B., Murray, S.R., Zaki, P.A., Chu, P.C., Lissin, D.V., Monteillet-Agius, G., Stewart, P.L., Evans, C.J., von Zastrow, M., 1998. μ-Opioid receptor

internalization: opiate drugs have differential effects on a conserved endocytic mechanism in vitro and in the mammalian brain. Mol Pharmacol. 53, 377–384.

Kim, J.A., Bartlett, S., He, L., Nielsen, C.K., Chang, A.M., Kharazia, V., Waldhoer, M., Ou, C.J., Taylor, S., Ferwerda, M., Cado, D., Whistler, J.L., 2008. Morphine-induced receptor endocytosis in a novel knockin mouse reduces tolerance and dependence. Curr Biol. 18, 129–135.

Knapp, L.T., Klann, E., 2000. Superoxide-induced stimulation of protein kinase C via thiol modification and modulation of zinc content. J. Biol. Chem. 275, 24136–24145.

Koch, T., Seifert, A., Wu, D.F., Rankovic, M., Kraus, J., Börner, C., Brandenburg, L.O., Schröder, H., Höllt, V., 2009. μ-opioid receptor-stimulated synthesis of reactive oxygen species is mediated via phospholipase D2. J Neurochem. 110, 1288–1296.

Koch, T., Widera, A., Bartzsch, K., Schulz, S., Brandenburg, L.O., Wundrack, N., Beyer, A., Grecksch, G., Höllt, V., 2005. Receptor endocytosis counteracts the development of opioid tolerance. Mol Pharmacol. 67, 280–287.

Kogan, J.H., Nestler, E.J., Aghajanian, G.K., 1992. Elevated basal firing rates of locus coeruleus neurons in brain slices from opiate-dependent rats: Association with enhanced responses to 8-Br-cAMP. Eur. J. Pharmacol. 211, 47–53.

Llorente, J., Santamarta, M.T., Henderson, G., Pineda J., 2012. Enhancement of mu-opioid receptor desensitization by nitric oxide in rat locus coeruleus neurons: involvement of reactive oxygen species. J. Pharmacol. Exp. Ther. 342, 552–560.

Machelska, H., Ziolkowska, B., Mika, J., Przewlocka, B., Przewlocki, R., 1997. Chronic morphine increases biosynthesis of nitric oxide synthase in the rat spinal cord. Neuroreport 8, 2743–2747.

Melief, E.J., Miyatake, M., Bruchas, M.R., Chavkin, C., 2010. Ligand-directed c-Jun N-terminal kinase activation disrupts opioid receptor signaling. Proc Natl Acad Sci U S A. 107, 11608–11613.

Mendiguren, A., Pineda, J., 2004. Cannabinoids enhance N-methyl-D-aspartate-induced excitation of locus coeruleus neurons by CB1 receptors in rat brain slices. Neurosci. Lett. 363, 1–5.

Moore, P.K., Handy, R.L., 1997. Selective inhibitors of neuronal nitric oxide synthase-is no NOS really good NOS for the nervous system? Trends Pharmacol. Sci. 18, 204–211.

Moore, P.K., Wallace, P., Gaffen, Z.A., Hart, S.L., Babbedge, R.C., 1993. Characterization of the novel nitric oxide synthase inhibitor 7-nitro indazole and related indazoles: antinociceptive and cardiovascular effects. Br. J. Pharmacol. 110, 219–224.

Muscoli, C., Cuzzocrea, S., Ndengele, M.M., Mollace, V., Porreca, F., Fabrizi, F., Esposito, E., Masini, E., Matuschak, G.M., Salvemini, D., 2007 Therapeutic manipulation of peroxynitrite attenuates the development of opiate-induced antinociceptive tolerance in mice. J. Clin. Invest. 117, 3530–3539.

Nestler, E.J., Alreja, M., Aghajanian, G.K., 1994. Molecular and cellular mechanisms of opiate action: studies in the rat locus coeruleus. Brain Res. Bull. 35, 521–528.

Newton, P.M., Kim, J.A., McGeehan, A.J., Paredes, J.P., Chu, K., Wallace, M.J., Roberts, A.J., Hodge, C.W., Messing, R.O., 2007. Increased response to morphine in mice lacking protein kinase C epsilon. Genes Brain Behav. 6, 329–338.

Palumbo, E.J., Sweatt, J.D., Chen, S.J., Klann, E., 1992. Oxidation-induced persistent activation of protein kinase C in hippocampal homogenates. Biochem. Biophys. Res. Commun. 187, 1439–1445.

Paronis, C.A., Holtzman, S.G., 1992. Development of tolerance to the analgesic activity of mu agonists after continuous infusion of morphine,meperidine or fentanyl in rats. J Pharmacol Exp Ther. 262, 1–9.

Pasternak, G.W., Kolesnikov, Y.A., Babey, A.M., 1995. Perspectives on the N-methyl-D-aspartate/nitric oxide cascade and opioid tolerance. Neuropsychopharmacology 13, 309–313.

Pineda, J., Torrecilla, M., Martín-Ruiz, R., Ugedo, L., 1998. Attenuation of withdrawal-induced hyperactivity of locus coeruleus neurones by inhibitors of nitric oxide synthase in morphine-dependent rats. Neuropharmacology 37, 759–767.

Quillinan, N., Lau, E.K., Virk, M., von Zastrow, M., Williams, J.T., 2011. Recovery from mu-Opioid Receptor Desensitization after Chronic Treatment with Morphine and Methadone. J. Neurosci. 31, 4434–4443.

Radi, R., 2013. Peroxynitrite, a stealthy biological oxidant. J. Biol. Chem. 288, 26464–26472.

Raehal, K.M., Bohn, L.M., 2011. The role of β-arrestin2 in the severity of antinociceptive tolerance and physical dependence induced by different opioid pain therapeutics. Neuropharmacology 60, 58–65.

Raghavendra, V., Kulkarni, S.K., 2000. Possible mechanisms of action in melatonin reversal of morphine tolerance and dependence in mice. Eur J Pharmacol. 409, 279–289.

Salem, A., Hope, W., 1999. Role of endogenous adenosine in the expression of opiate withdrawal in rats. Eur J Pharmacol. 369, 39–42.

Salvemini, D., Little, J.W., Doyle, T., Neumann, W.L., 2011. Roles of reactive oxygen and nitrogen species in pain. Free. Radic. Biol. Med. 51, 951–966.

Sánchez-Blázquez, P., Rodríguez-Muñoz, M., Garzón, J., 2010. Mu-opioid receptors transiently activate the Akt-nNOS pathway to produce sustained potentiation of PKC-mediated NMDAR-CaMKII signaling. PLoS One. 5:e11278.

Sánchez-Blázquez, P., Rodríguez-Muñoz, M., Berrocoso, E., Garzón, J., 2013. The plasticity of the association between mu-opioid receptor and glutamate ionotropic receptor N in opioid analgesic tolerance and neuropathic pain. Eur. J. Pharmacol. 716, 94–105.

Santamarta, M.T., Llorente, J., Mendiguren, A., Pineda, J., 2014. Involvement of neuronal nitric oxide synthase in desensitisation of mu-opioid receptors in the rat locus coeruleus. J Psychopharmacol. 28, 903–914.

Santamarta, M.T., Ulibarri, I., Pineda, J., 2005. Inhibition of neuronal nitric oxide synthase attenuates the development of morphine tolerance in rats. Synapse 57, 38–46.

Smith, F.L., Javed, R.R., Elzey, M.J., Dewey, W.L., 2003. The expression of a high level of morphine antinociceptive tolerance in mice involves both PKC and PKA. Brain Res. 985, 78–88.

Thornton, S.R., Smith, F.L., 1997. Characterization of neonatal rat fentanyl tolerance and dependence. J Pharmacol Exp Ther. 281, 514–521.

Torrecilla, M., Marker, C.L., Cintora, S.C., Stoffel, M., Williams, J.T., Wickman, K., 2002. G-protein-gated potassium channels containing Kir3.2 and Kir3.3 subunits mediate the acute inhibitory effects of opioids on locus ceruleus neurons. J. Neurosci. 22, 4328–4334.

Torrecilla, M., Pineda, J., Ugedo, L., 2001. NO synthase inhibitors reduce opioid desensitization in rat locus coeruleus neurons in vitro. Neuroreport 12, 1601–1604.

Trujillo, K.A., Kubota, K.S., Warmoth, K.P., 2004. Continuous administration of opioids produces locomotor sensitization. Pharmacol. Biochem. Behav. 79, 661–669.

Vardanyan, R.S., Hruby, V.J., 2014. Fentanyl-related compounds and derivatives: current status and future prospects for pharmaceutical applications. Future Med Chem. 6, 385–412.

Villa, R.F., Gorini, A., 1997. Pharmacology of lazaroids and brain energy metabolism: a review. Pharmacol. Rev. 49, 99–136.

Virk, M.S., Williams, J.T., 2008. Agonist-specific regulation of mu-opioid receptor desensitization and recovery from desensitization. Mol. Pharmacol. 73, 1301–1308.

Whistler, J.L., Chuang, H.H., Chu, P., Jan, L.Y., von Zastrow, M., 1999. Functional dissociation of mu opioid receptor signaling and endocytosis: implications for the biology of opiate tolerance and addiction. Neuron 23, 737–746.

Williams, J.T., North, R.T., 1984. Opiate-receptor interactions on single locus coeruleus neurons. Mol. Pharmacol. 26, 489–497.

Williams, J.T., Ingram, S.L., Henderson, G., Chavkin, C., von Zastrow, M., Schulz, S., Koch, T., Evans, C.J., Christie, M.J., 2013. Regulation of mu-opioid receptors: desensitization, phosphorylation, internalization, and tolerance. Pharmacol. Rev. 65, 223–254.

Zeitz, K.P., Malmberg, A.B., Gilbert, H., Basbaum, A.I., 2001. Reduced development of tolerance to the analgesic effects of morphine and clonidine in PKCγ mutant mice. Pain 94, 245–253.

**Figure legends**

**Figure 1.** Effect of chronic treatments with morphine, methadone or fentanyl on the acute ME effect in rat LC neurons. Rats were treated for 72 h with a morphine (*n* = 5) or sham emulsion (*n* = 5). Another group of animals were treated for 6 days with methadone (*n* = 7), 7 days with fentanyl (*n* = 5) or sham (*n* = 5) minipumps. **A, B**. Representative examples of firing-rate recording of LC cells from rats receiving the following treatments: sham (emulsion) or morphine (**A**), sham (minipump), methadone or fentanyl (**B**). Each horizontal bar represents the period of application of each ME concentration (0.05 - 12.8 μM, 2x) and the vertical lines show the number of spikes recorded every 10 s. The inhibitory effect induced by each application was calculated as a percentage from the basal firing rate. Note that greater concentrations of ME are needed to inhibit the neuron activity in rats treated with morphine, methadone and fentanyl, compared with sham animals, indicative of tolerance.

**Figure 2.** Concentration-effect curves for the inhibitory effect of ME in LC neurons from rats treated chronically with morphine, methadone or fentanyl. Rats were treated for 72 h with a morphine (*n* = 5) or sham emulsion (*n* = 5). Another group of animals were treated for 6 days with methadone (*n* = 7), 7 days with fentanyl (*n* = 5) or sham (*n* = 5) minipumps. **A, B, C**. Concentration-effect curves for the inhibitory effect of ME in LC neurons from rats receiving morphine (**A**), methadone (**B**), fentanyl (**C**) or sham treatment. The horizontal axis represents the logarithms of ME concentrations (0.05 - 12.8 μM, 2x) in linear scale. The vertical axis expresses the reduction in the firing rate of LC neurons as a percentage from the basal firing rate. Symbols are the mean ± SEM of ME effect at each concentration obtained from n animals. The lines through the data are the theoretical curves in each group constructed from the mean of the individual concentration-effect curve parameters, as estimated by nonlinear regressions (see

Materials and Methods for details and Table 2 for mean values). Note that administration of morphine, methadone or fentanyl induces a shift to the right of the ME curves, representative of tolerance. In all groups, the maximal effect of ME was 100% of baseline, which corresponded with an absolute inhibition from the basal firing rate.

**Figure 3.** Effect of 7-nitroindazole (7-NI) on the concentration-effect curves for the inhibitory effect of ME and $pEC_{50}$ values for ME in LC neurons from methadone- and fentanyl-treated rats. Animals were co-treated with methadone or fentanyl minipumps and 7-NI injections for 6 and 7 days, respectively (methadone/7-NI group, $n = 5$; fentanyl/7-NI group, $n = 5$) or with their vehicles (sham/vehicle group, $n = 5$; sham/7-NI group, $n = 5$; methadone/vehicle group, $n = 5$ and fentanyl/vehicle group, $n = 6$). **A, B**. Concentration-effect curves for the inhibitory effect of ME in LC neurons from rats receiving 7-NI together with methadone (**A**), fentanyl (**B**) or sham treatment. The horizontal axis represents the logarithms of ME concentration (0.05 - 12.8 μM, 2x) in linear scale. The vertical axis expresses the reduction in the firing rate of LC neurons as a percentage from the basal firing rate. Symbols are the mean ± SEM at each ME concentration obtained from *n* rats. The lines through the data are the theoretical curves in each group constructed from the mean of the individual concentration-effect curve parameters, as estimated by nonlinear regressions (see Materials and Methods for details and Table 1 for mean values). **C, D**. Ordinate represents $pEC_{50}$ values for ME effect in sham-, methadone- or fentanyl-treated rats. Bars are mean ± S.E.M. of *n* rats. Note that administration of methadone and fentanyl induces a rightward shift to the right of the ME curves, but co-administration of the nNOS inhibitor 7-NI does not prevent this change. In all groups, the maximal effect of ME was 100% of baseline, which corresponded with an absolute inhibition from the basal firing rate. $*p < 0.005$ when compared to the corresponding sham group (one-way ANOVA followed by a post-hoc Tukey's test).

**Figure 4**. Effect of Trolox + ascorbic acid (TX+AA) and U-74389G on the concentration-effect curves for the inhibitory effect of ME and $pEC_{50}$ values for ME in LC neurons from morphine-treated rats. Animals were co-treated for 72 h with a morphine emulsion and TX+AA or U-74389G injections (morphine/TX+AA group, $n$ = 5; morphine/U-74389G group, $n$ = 5) or with their vehicles (sham/vehicle group, $n$ = 5; morphine/vehicle group, $n$ = 5; sham/TX+AA group, $n$ = 5; sham/U-74389G group, $n$ = 5). **A, B**. Concentration-effect curves for the inhibitory effect of ME in LC neurons from morphine-treated rats receiving TX+AA (**A**) or U-74389G (**B**). The horizontal axis represents the logarithms of ME concentration (0.05 - 12.8 μM, 2x) in linear scale. The vertical axis expresses the reduction in the firing rate of LC neurons as a percentage from the basal firing rate. Data points are the mean ± SEM at each ME concentration obtained from n animals. The lines through the data are the theoretical curves in each group constructed from the mean of the individual concentration-effect curve parameters, as estimated by nonlinear regressions (see Materials and Methods for details and Table 2 for mean values). **C**. Ordinate represents pEC50 values for ME effect in sham- and morphine-treated animals. Bars are mean ± S.E.M. of $n$ rats. Note that administration of morphine induces a strong shift to the right of the ME curves, and co-administration of antioxidants TX+AA and U-74389G blocks this rightward displacement. In all groups, the maximal effect of ME was 100% of baseline, which corresponded with an absolute inhibition from the basal firing rate. $^{*}p < 0.005$, when compared to the corresponding sham group, $^{\dagger}p < 0.05$ and $^{\dagger\dagger}p < 0.01$, when compared to the vehicle group (one-way ANOVA followed by a post-hoc Tukey's test).

**Figure 5.** Effect of U-74389G on the concentration-effect curves for the inhibitory effect of ME and $pEC_{50}$ values for ME in LC neurons from methadone- or fentanyl-treated rats. Animals were co-treated with methadone or fentanyl minipumps for 6 and 7 days, respectively, and U-74389G injections (methadone/U-74389G group, $n$ = 7; fentanyl/U-

74389G group, $n$ = 5) or with their vehicles (sham/vehicle group, $n$ = 5; sham/U-74389G group, $n$ = 5; methadone/vehicle group, $n$ = 7 and fentanyl/vehicle group, $n$ = 5). **A, B.** Concentration-effect curves for the inhibitory effect of ME in LC neurons from rats receiving U-74389G together with methadone (**A**), fentanyl (**B**) or sham treatment The horizontal axis represents the logarithms of ME concentration (0.05 - 12.8 μM, 2x) in linear scale. The vertical axis expresses the reduction in the firing rate of LC neurons as a percentage from the basal firing rate. Symbols are the mean ± SEM at each ME concentration obtained from $n$ rats. The lines through the data are the theoretical curves in each group constructed from the mean of the individual concentration-effect curve parameters, as estimated by nonlinear regressions (see Materials and Methods for details and Table 2 for mean values). **C, D.** Ordinate represents $pEC_{50}$ values for ME effect in sham-, methadone- and fentanyl-treated rats. Bars are mean ± S.E.M. of $n$ rats. Note that administration of methadone of fentanyl induces a rightward shift to the right of the ME curves, but co-administration of the antioxidant U-74389G does not block this change. In all groups, the maximal effect of ME was 100% of baseline, which corresponded with an absolute inhibition from the basal firing rate. *$p < 0.05$, **$p < 0.01$ and ***$p < 0.005$ when compared to the corresponding sham group (one-way ANOVA followed by a post-hoc Tukey's test).

**Table 1. Effect of 7-nitroindazole (7-NI) on the basal firing rate and the inhibition induced by ME in the LC of sham- and opioid-treated rats.**

| | | Concentration-effect curves[2] | | | |
|---|---|---|---|---|---|
| **Treatment groups[1]** | **Basal firing rate (Hz)** | **$pEC_{50}$ (M)** | **($EC_{50}$, µM)** | **Slope factor** | **n** |
| Sham (minipump) | | | | | |
| Vehicle (peanut oil) | 0.74 ± 0.03 | 6.66 ± 0.03 | (0.22) | 1.15 ± 0.07 | 5 |
| 7-NI | 0.69 ± 0.06 | 6.84 ± 0.04 | (0.15) | 0.93 ± 0.07 | 5 |
| Methadone | | | | | |
| Vehicle (peanut oil) | 0.75 ± 0.06 | 6.29 ± 0.09* | (0.52) | 0.96 ± 0.03 | 5 |
| 7-NI | 0.57 ± 0.02 | 6.43 ± 0.04* | (0.37) | 1.02 ± 0.13 | 5 |
| Fentanyl | | | | | |
| Vehicle (peanut oil) | 0.96 ± 0.08 | 6.23 ± 0.05* | (0.58) | 1.03 ± 0.09 | 6 |
| 7-NI | 0.82 ± 0.10 | 6.38 ± 0.05* | (0.42) | 0.97 ± 0.04 | 5 |

[1]Animals were co-treated for 6 days with methadone or 7 days with fentanyl by an osmotic minipump and 7-NI injections (methadone/7-NI group, fentanyl/7-NI group), or with their vehicles (sham/vehicle group, sham/7-NI group, methadone/vehicle group, and fentanyl/vehicle group).

[2]Parameters of concentration-effect curves for ME were estimated in each experiment by nonlinear regression. $pEC_{50}$ values (negative logarithm of the concentration needed to elicit a 50% of maximal effect) and slope factors are shown as mean ± SEM of *n* experiments. Maximal effect values were 100% in all cases. *$p < 0.005$ when compared to the corresponding sham group (one-way ANOVA followed by a post-hoc Tukey's test).

**Table 2. Effect of antioxidants (Trolox + ascorbic acid and U-74389G) on the basal firing rate and the inhibition induced by ME in the LC of sham- and opioid-treated rats.**

| | | Concentration-effect curves[2] | | | |
|---|---|---|---|---|---|
| **Treatment groups[1]** | **Basal firing rate (Hz)** | **$pEC_{50}$ (M)** | **($EC_{50}$, µM)** | **Slope factor** | **n** |
| Sham (emulsion) | | | | | |
| Vehicle (saline) | 0.87 ± 0.05 | 6.66 ± 0.05 | (0.22) | 1.01 ± 0.05 | 5 |
| TX+AA | 0.71 ± 0.04 | 6.58 ± 0.10 | (0.26) | 1.06 ± 0.06 | 5 |
| U-74389G | 0.72 ± 0.05 | 6.52 ± 0.01 | (0.30) | 1.14 ± 0.05 | 5 |
| Morphine | | | | | |
| Vehicle (saline) | 1.05 ± 0.14 | 6.02 ± 0.10*** | (0.95) | 0.91 ± 0.04 | 5 |
| TX+AA | 0.89 ± 0.09 | 6.41 ± 0.11$^{\dagger}$ | (0.39) | 0.92 ± 0.06 | 5 |
| U-74389G | 0.85 ± 0.06 | 6.42 ± 0.08$^{\dagger\dagger}$ | (0.38) | 1.03 ± 0.09 | 5 |
| Sham (minipump) | | | | | |
| Vehicle (saline) | 0.78 ± 0.04 | 6.64 ± 0.03 | (0.23) | 1.05 ± 0.08 | 5 |
| U-74389G | 0.78 ± 0.03 | 6.58 ± 0.06 | (0.27) | 1.06 ± 0.05 | 5 |
| Methadone | | | | | |
| Vehicle (saline) | 0.81 ± 0.06 | 6.31 ± 0.05*** | (0.49) | 1.05 ± 0.04 | 7 |
| U-74389G | 0.68 ± 0.09 | 6.34 ± 0.04* | (0.45) | 1.16 ± 0.10 | 7 |
| Fentanyl | | | | | |
| Vehicle (saline) | 0.93 ± 0.09 | 6.19 ± 0.03*** | (0.64) | 1.02 ± 0.11 | 5 |
| U-74389G | 0.81 ± 0.09 | 6.19 ± 0.09** | (0.65) | 1.04 ± 0.11 | 5 |

[1]Animals were co-treated for 72 h with a morphine emulsion, for 6 days with methadone and 7 days with fentanyl by an osmotic minipump and Trolox + ascorbic acid or U-74389G injections (morphine/TX+AA group, morphine/U-74389G group, methadone/U-74389G group, fentanyl/U-74389G group), or with their vehicles (sham/vehicle group, sham/TX+AA group, sham/U-74389G group, morphine/vehicle group, methadone/vehicle group and fentanyl/vehicle group).

[2]Parameters of concentration-effect curves for ME were estimated in each experiment by nonlinear regression. $pEC_{50}$ values (negative logarithm of the concentration needed to elicit a 50% of maximal effect) and slope factors are shown as mean ± SEM of *n* experiments. Maximal effect values were 100% in all cases. $*p < 0.05$, $**p < 0.01$ and $***p < 0.005$ when compared to the corresponding sham group. $^{\dagger}p < 0.05$ and $^{\dagger\dagger}p < 0.01$ when compared to the corresponding vehicle group (one-way ANOVA followed by a post-hoc Tukey's test).

**FIGURE 1**

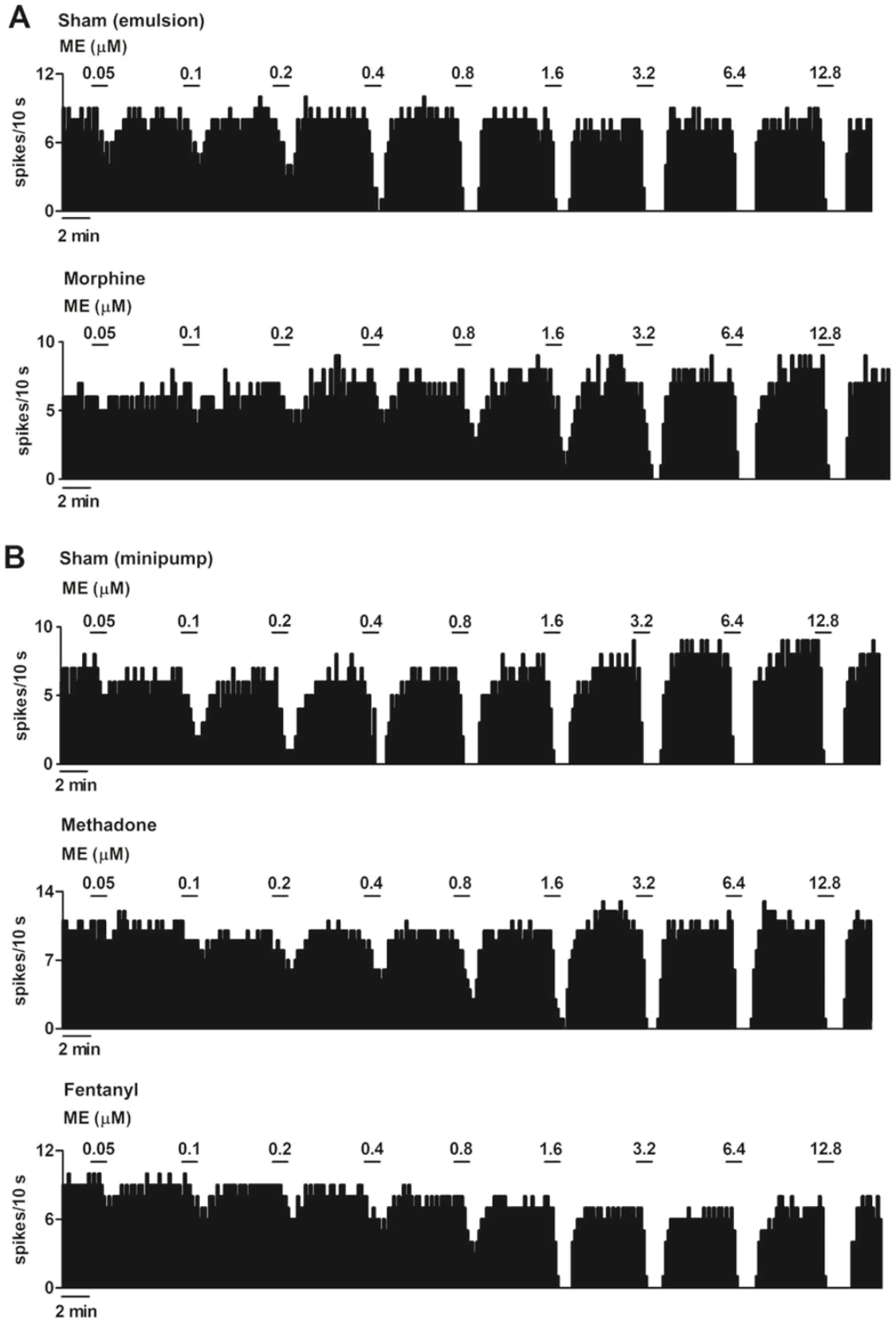
A
Sham (emulsion)
ME (μM)
0.05
0.1
0.2
0.4
0.8
1.6
3.2
6.4
12.8
spikes/10 s
12
6
0
2 min
Morphine
ME (μM)
0.05
0.1
0.2
0.4
0.8
1.6
3.2
6.4
12.8
spikes/10 s
10
5
0
2 min
B
Sham (minipump)
ME (μM)
0.05
0.1
0.2
0.4
0.8
1.6
3.2
6.4
12.8
spikes/10 s
10
5
0
2 min
Methadone
ME (μM)
0.05
0.1
0.2
0.4
0.8
1.6
3.2
6.4
12.8
spikes/10 s
14
7
0
2 min
Fentanyl
ME (μM)
0.05
0.1
0.2
0.4
0.8
1.6
3.2
6.4
12.8
spikes/10 s
12
6
0
2 min

**FIGURE 2**

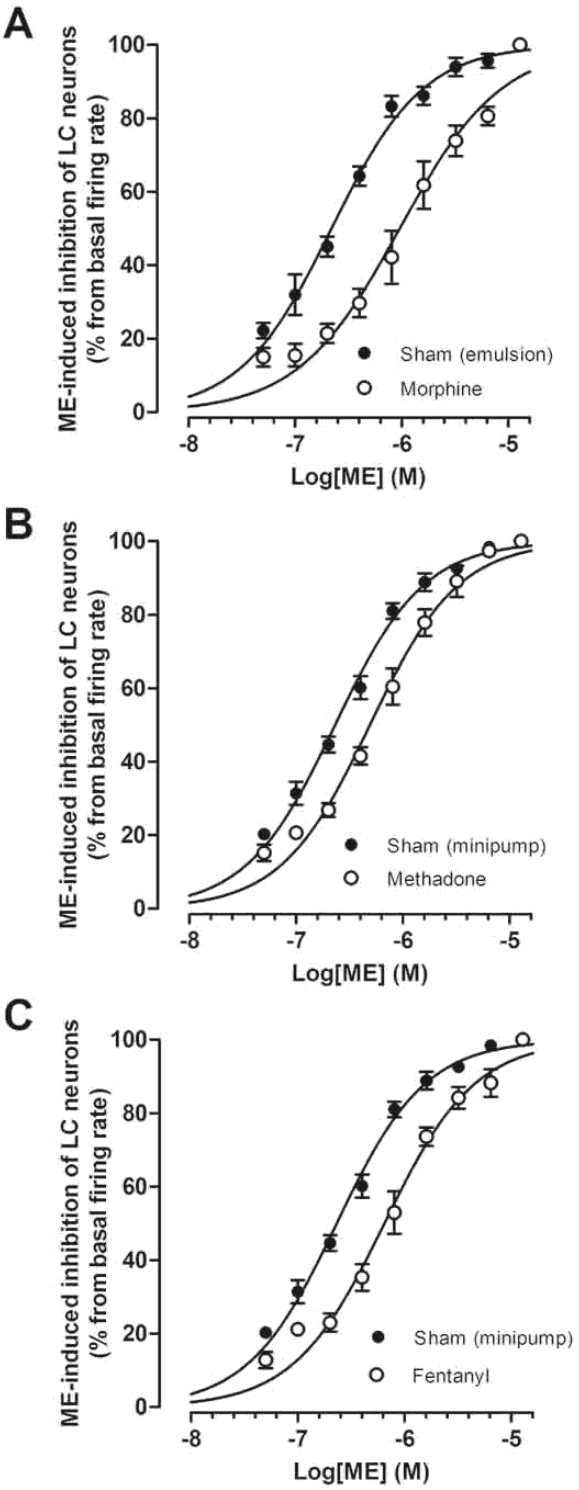
A
ME-induced inhibition of LC neurons (% from basal firing rate)
100
80
60
40
20
0
-8
-7
-6
-5
Log[ME] (M)
Sham (emulsion)
Morphine
B
ME-induced inhibition of LC neurons (% from basal firing rate)
Log[ME] (M)
Sham (minipump)
Methadone
C
ME-induced inhibition of LC neurons (% from basal firing rate)
Log[ME] (M)
Sham (minipump)
Fentanyl

**FIGURE 3**

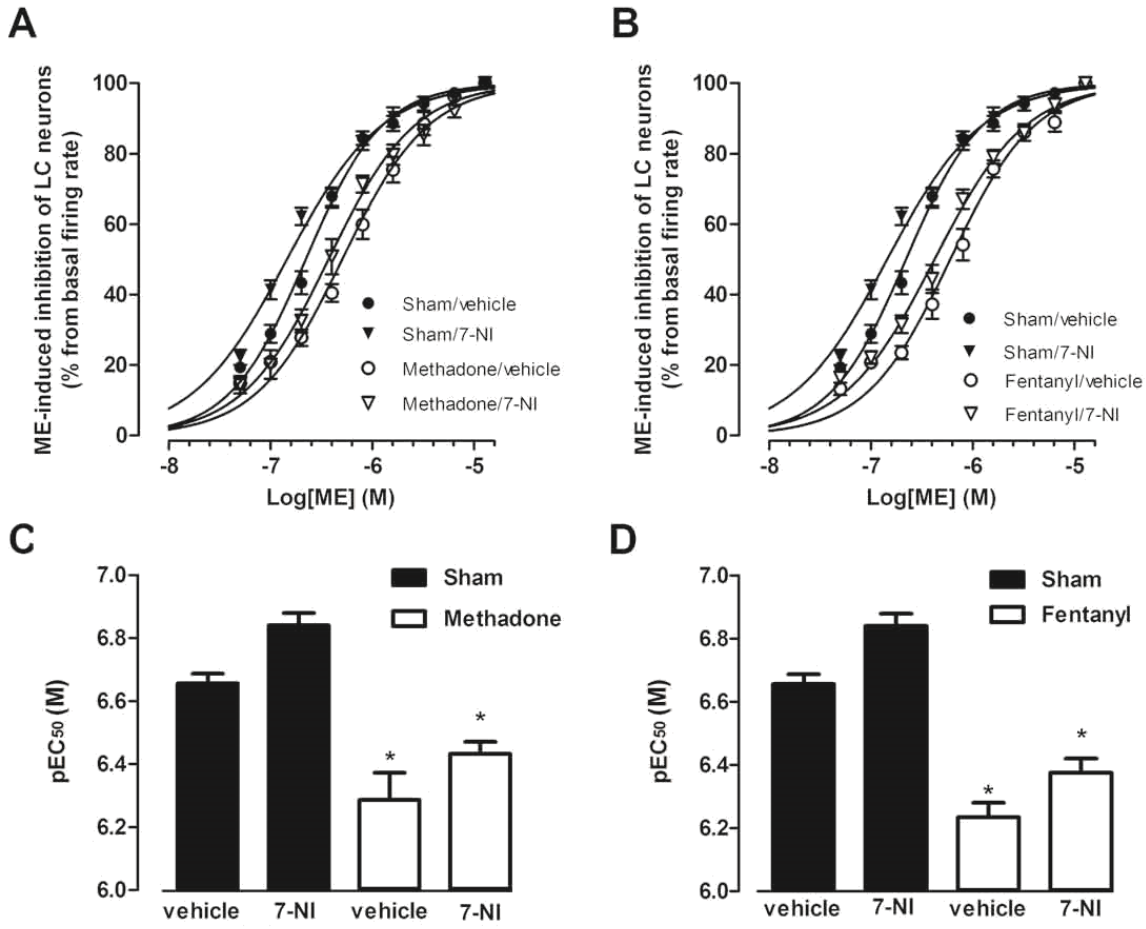
A
ME-induced inhibition of LC neurons (% from basal firing rate)
100
80
60
40
20
0
-8
-7
-6
-5
Log[ME] (M)
Sham/vehicle
Sham/7-NI
Methadone/vehicle
Methadone/7-NI
B
ME-induced inhibition of LC neurons (% from basal firing rate)
Log[ME] (M)
Sham/vehicle
Sham/7-NI
Fentanyl/vehicle
Fentanyl/7-NI
C
pEC50 (M)
7.0
6.8
6.6
6.4
6.2
6.0
Sham
Methadone
vehicle
7-NI
vehicle
7-NI
*
D
pEC50 (M)
Sham
Fentanyl
vehicle
7-NI
vehicle
7-NI

**FIGURE 4**

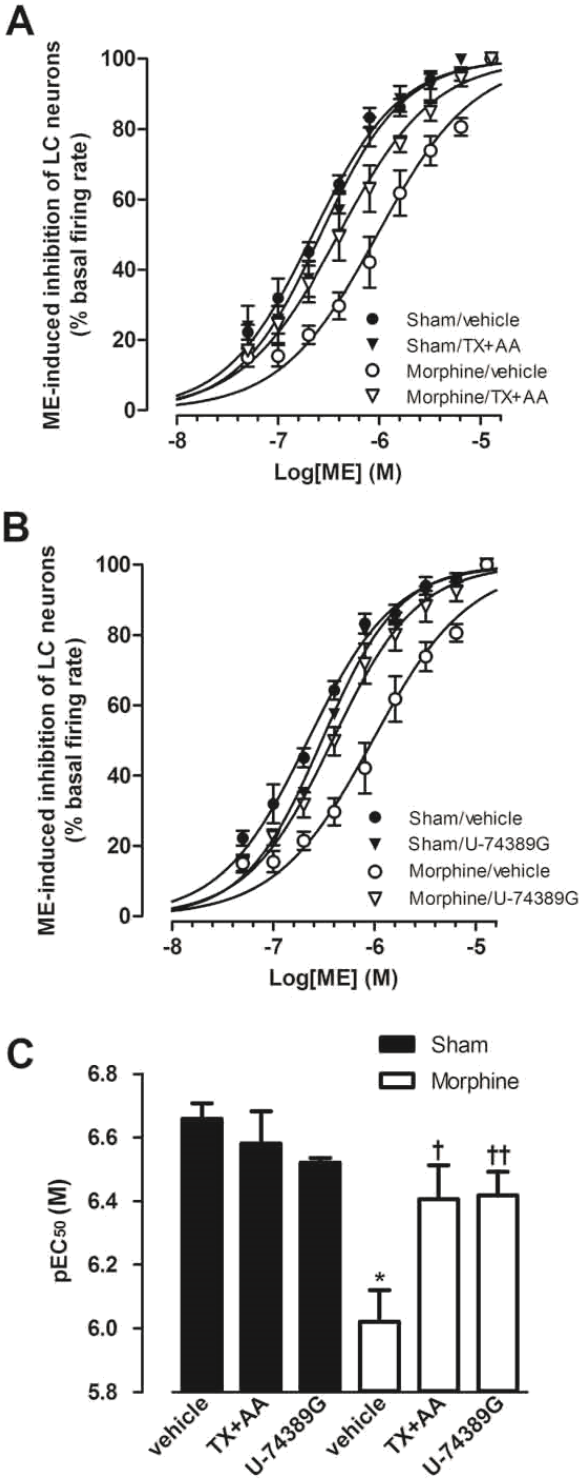
A
ME-induced inhibition of LC neurons
(% basal firing rate)
100
80
60
40
20
0
-8
-7
-6
-5
Log[ME] (M)
Sham/vehicle
Sham/TX+AA
Morphine/vehicle
Morphine/TX+AA
B
ME-induced inhibition of LC neurons
(% basal firing rate)
Log[ME] (M)
Sham/vehicle
Sham/U-74389G
Morphine/vehicle
Morphine/U-74389G
C
Sham
Morphine
pEC50 (M)
6.8
6.6
6.4
6.2
6.0
5.8
*
†
††
vehicle
TX+AA
U-74389G
vehicle
TX+AA
U-74389G

**FIGURE 5**

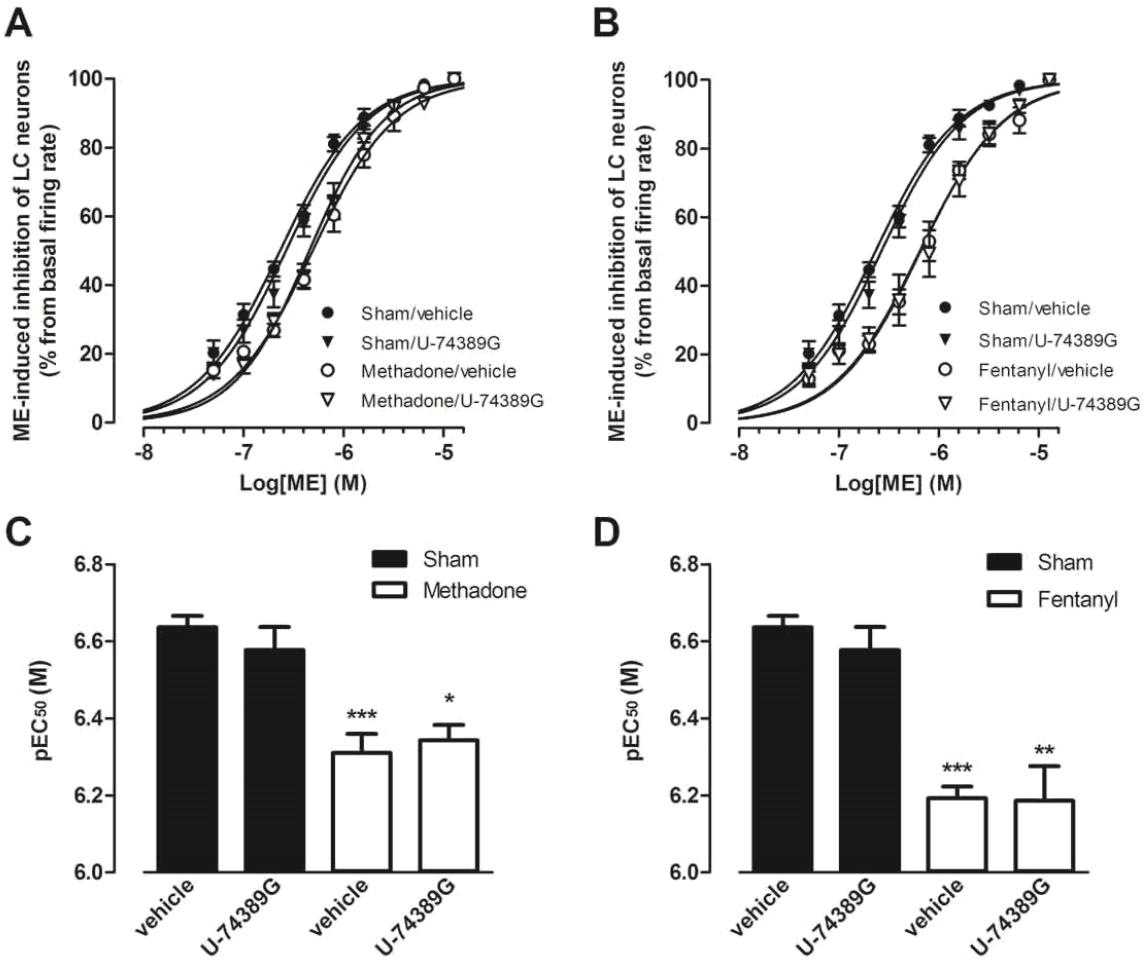
A
ME-induced inhibition of LC neurons (% from basal firing rate)
Log[ME] (M)
Sham/vehicle
Sham/U-74389G
Methadone/vehicle
Methadone/U-74389G
B
ME-induced inhibition of LC neurons (% from basal firing rate)
Log[ME] (M)
Sham/vehicle
Sham/U-74389G
Fentanyl/vehicle
Fentanyl/U-74389G
C
pEC50 (M)
Sham
Methadone
***
*
vehicle
U-74389G
vehicle
U-74389G
D
pEC50 (M)
Sham
Fentanyl
***
**
vehicle
U-74389G
vehicle
U-74389G

# MANUSCRIPT 4

To be submitted to *European Journal of Pharmacology*

**Title:**

# ROLE OF NEURONAL NITRIC OXIDE SYNTHASE AND REACTIVE OXYGEN SPECIES IN THE DEVELOPMENT OF ANTINOCICEPTIVE TOLERANCE INDUCED BY DIFFERENT OPIOID AGONISTS

**Running title:**

Involvement of nNOS and ROS in opioid analgesic tolerance

**Authors:**

Patricia Pablos, Javier Llorente, Aitziber Mendiguren and Joseba Pineda*

*Department of Pharmacology, Faculty of Medicine and Odontology, University of the Basque Country (UPV/EHU), E-48940 Leioa, Bizkaia, Spain*

*Corresponding author: J Pineda, M.D., Ph.D., Dept. of Pharmacology, Fac. of Medicine and Odontology, Univ. of the Basque Country (UPV / EHU), Bº Sarriena s/n, E-48940 Leioa, Bizkaia, Spain. Tel.: +34 94 6015577; fax: +34 94 6013220.

E-mail address: joseba.pineda@ehu.es (Dr. Joseba Pineda).

**Abstract**

Previous studies have shown that nitric oxide (NO) is involved in the adaptations induced by chronic morphine treatment. In the present study, we used the tail-flick technique in rats to examine the effect of 7-nitroindazole (7-NI; 30 mg/kg/12 h, i.p.), a selective neuronal nitric oxide synthase (nNOS) inhibitor, and the antioxidant agents Trolox and ascorbic acid (TX+AA; 40 and 100 mg/kg/day, respectively i.p.) and U-74389G (10 mg/kg/day, i.p.), on the development of opioid antinociceptive tolerance induced by prolonged treatments with morphine, methadone and fentanyl. For induction of morphine tolerance, rats were treated subcutaneously (s.c.) with a slow release emulsion containing free base morphine (200 mg/kg) for 72 h. For methadone (60 mg/kg/day, 6 days) and fentanyl (0.2 mg/kg/day, 7 days), tolerance was induced by s.c. implantation of osmotic pumps. Morphine treatments induced a strong degree of tolerance to the antinociceptive effect of a challenge dose of morphine. Methadone treatments induced a weaker degree of antinociceptive tolerance. On the contrary, no tolerance to morphine challenge effects was observed in fentanyl-treated animals. Co-treatment with the antioxidants TX+AA or U-74389G partially blocked morphine-induced analgesic tolerance. On the contrary, 7-NI or U-74389G administration failed to affect the development of antinociceptive tolerance induced by methadone. Our results suggest that NO/ROS pathways are differentially involved in the development of opioid antinociceptive tolerance.

*Keywords:* morphine, methadone, fentanyl, tolerance, nitric oxide, ROS.

*Abbreviations*: LC: locus coeruleus; i.p.: intraperitoneal; 7-NI: 7-nitroindazole; NMDA: N-methyl-D-aspartate; NO: nitric oxide; NOS: nitric oxide synthase; nNOS: neuronal nitric oxide synthase; NOX: NADPH-oxidase; ROS: reactive oxygen species; s.c.:

subcutaneous; Trolox: 6-hydroxy-2,5,7,8-tetramethylchroman-2-carboxylic acid; TX+AA: Trolox and ascorbic acid; U-74389G: 21-[4-(2,6-di-1-pyrrolidinyl-4-pyrrimidinyl)-1-piperazinyl]-pregna-1,4,9(11)-triene-3,20-dione(Z)-2 butenedioate

## 1. Introduction

Opioids are efficacious analgesics clinically used for pain management. However, one of the major problems associated with chronic opioid use is the significant risk of developing drug tolerance and dependence. When opioid tolerance develops, a dose escalation is needed to obtain equivalent pain relief, with the resulting risk of undesired effects. For that reason, it is necessary to unmask the mechanisms underlying tolerance to increase the efficacy of analgesic therapy. Since its isolation, chemistry research efforts have yielded thousands of morphine related opioids, resulting in a rich pharmacology (Corbett et al., 2006). Methadone is a good alternative to morphine for pain relief in cancer patients (Shelton et al., 2008). Fentanyl is estimated to be up to 100 fold more potent than morphine as an analgesic (Vardanyan and Hruby, 2014). Transdermal formulation of fentanyl is effective and well tolerated for the treatment of chronic pain caused by malignancy and non-malignant conditions (Kornick et al., 2003). Different regulatory events occurring at the MOR, including receptor desensitization, internalization, recovery from desensitization or down-regulation are though to be cellular mechanisms underlying opioid tolerance (Williams et al., 2013). Opioid agonists have widely differing signaling efficacies in each of these processes (Kelly, 2013; Von Zastrow, 2010). Other mechanisms including spinal glia activation and neuronal apoptotis also seem to contribute to opioid analgesic tolerance (Mao et al., 2002; Song and Zhao, 2001; Watkins et al., 2005; Zhou et al., 2010).

The chemical messenger NO is produced from L-arginine by the enzyme NO synthase (NOS), which can be classified as constitutive (neuronal and endothelial isoforms) or inducible (Alderton et al., 2001). Considerable evidence implicates the nitric oxide (NO) system in nociceptive processes either in the periphery or within the central nervous system (Haley et al. 1992) and in opioid-induced tolerance. Thus, inhibition of

the neuronal nitric oxide synthase (nNOS) attenuates the tolerance to the cellular and analgesic effects of MOR agonists after morphine treatment (Heinzen and Pollack, 2004; Santamarta et al., 2005). NO has been shown to react with oxygen derivatives, resulting in the formation of reactive oxygen species (ROS) and reactive nitrogen species (Davis et al., 2001). One of the most remarkable proinflammatory and proapoptotic reactive molecule is peroxynitrite, ($ONOO^-$), the product of the interaction between superoxide ($O_2^-$) and NO. NO/ROS pathways seems to play a key role in the development of pain of several etiologies (Salvemini et al., 2011). However, there is lacking information regarding the implication of NO/ROS in the development of analgesic tolerance following chronic treatments with different opioid agonists.

The aim of this work was to explore *in vivo* the involvement of nNOS and ROS in the development of opioid analgesic tolerance. For that purpose, we examined by the tail-flick test the development of analgesic tolerance following chronic treatments with different opioids (morphine, methadone and fentanyl) and we evaluated its regulation by a selective nNOS inhibitor and antioxidant agents.

## 2. Materials and Methods

### *2.1 Animals and treatments*

The animals for this study were obtained from the animal house of the University of the Basque Country (Leioa, Spain). Male adult Sprague-Dawley rats (200-300 g) were housed under controlled environmental conditions (22ºC and 12-h light/dark cycle) with food and water *ad libitum*. Principles of laboratory animal care were followed in all experimental procedures reported in this manuscript. Experiments were carried out in accordance with the European Community Council Directive on "Protection of Animals Used in Experimental and Other Scientific Purposes" of 24 November 1986 (86/609/EEC). The use of animals for this study was also approved by the Animal Care and Use Committee of the University of the Basque Country. All the efforts were made to minimize animal suffering and to reduce the number of animals used.

For induction of morphine tolerance, rats were treated subcutaneously (s.c.) with a slow release emulsion containing free base morphine (200 mg/kg) for 72 h, as described by Santamarta et al. (2005). The emulsion was injected subcutaneously on the back of the rat under light anesthesia with chloral hydrate (200 mg/kg, intraperitoneally (i.p.)). Sham animals were implanted with the same vehicle emulsion without morphine. Behavioral or electrophysiological experiments were conducted 72h after administration of morphine or sham emulsions.

For chronic treatments with methadone or fentanyl, osmotic minipumps (Alzet 2ML1) were implanted subcutaneously, as described by Quillinan et al. (2011) and Trujillo et al. (2004), respectively. The minipumps have a 2 ml reservoir, which delivers the content continuously at the rate of 10 µl/h. Pumps were filled with the required concentration of methadone (60 mg/kg/day) or fentanyl (0.2 mg/kg/day), dissolved in

saline. Animals were first anaesthetized with isoflurane and an incision was made in the midscapular region to insert the minipump. Sham animals were implanted with saline-filled osmotic pumps under the same experimental conditions. For induction of methadone tolerance, rats were given methadone i.p injections before the implantation of the pump, as follows: the day before, they received 5 mg/kg at 9:00 h and 7 mg/kg at 18:00 h. Next day, they received 7 mg/kg at 9:00 h and the osmotic pump was implanted at 18:00 h. Once the minipump was inserted, sham and morphine-treated animals were daily injected with the antioxidant U-74389G (10 mg/kg, i.p.), Trolox (40 mg/kg, i.p.) or their vehichles (saline). Every time Trolox was administered, rats also received ascorbic acid (100 mg/kg, i.p.) (TX+AA) to prevent the oxidation of Trolox. Sham-, methadone- and fentanyl-receiving rats were intraperitoneally injected every day with U-74389G (10 mg/kg) or its vehicle (saline). In another set of experiments, sham- and opioid-treated animals were intraperitoneally injected every 12 h with the nNOS inhibitor 7-NI (30 mg/kg) or its vehicle (peanut oil). Experiments were carried out on day 7 in methadone-treated rats (6 days after minipump implantation) and on day 8 in fentanyl-treated rats (7 days after minipump implantation).

*2.2 Measurement of the antinociceptive response*

The analgesic effect of morphine was measured by the tail-flick test (Le Bars et al., 2001), which evaluates the response of the animal to a thermal nociceptive stimulus. Thus, the rat was placed in a Plexiglas trap and kept inside for 20 min to minimize the stress due to manipulation. Next, a beam of light was focused on the dorsal tail, approximately in the middle. When the animal removed the tail with an energetic movement the time (latency) was recorded. Three basal measures were taken from each animal at three different points of the tail, with a 15 s interval between measures. The mean of these three values was used as the result. The light intensity was initially adjusted

with naive animals so that the basal latency ($t_{basal}$) was close to 3 s. Next, the rat was injected with a challenge dose of morphine hydrocloride (10 mg/kg, i.p.) and the latency ($t_{reaction}$) was tested again 30 min later to measure the effect of the opioid. This dose of morphine was selected based on previous experiments that observed a near maximal effect. This strong effect of morphine was appropriate to achieve a measurable tolerance after chronic opioid treatments. To minimize tail skin damage, a cut-off latency time ($t_{max}$) was set at 10 s. Antinociception was expressed as a percentage of the maximal possible effect (M.P.E) according to the following formula:

$$\text{M. P. E (\%)} = \frac{t_{reaction} - t_{basal}}{t_{max} - t_{basal}} \cdot 100$$

*2.3 Drugs and reagents*

The following drugs were purchased from Sigma-Aldrich Química (Madrid, Spain): Fentanyl, L-ascorbic acid, methadone and 7-nitroindazole (7-NI). Morphine base was purchased from Alcaliber (Madrid, Spain). Trolox and U-74389G were obtained from Enzo Life Sciences (Lausen, Switzerland). For acute administrations during tail-flick tests, morphine hydrochloride (10 mg/kg) was dissolved in 0.9% NaCl. For morphine treatment, an oily emulsion of morphine free base (200 mg/ml) containing mannide monooleate, liquid parafine, and 0.9% NaCl (0.08: 0.42: 0.5, v/v/v) was made. All the drugs were dissolved in saline except 7-NI, which was dissolved in peanut oil.

*2.4 Data analysis and statistics*

Data are expressed as mean ± standard error of the mean (S.E.M). Latencies before and after the morphine challenge were compared by a paired Student's *t* test. In addition, to evaluate the differences between two groups, we compared latency values in the absence (control) or the presence of the drug by a two-sample Student's *t* test. When

values were compared between more than two groups, one-way analysis of variance (ANOVA) was performed followed by Tukey's post-hoc test using the computer program GraphPad Prism (version 5.0 for Windows). In some cases, when ANOVA showed that the basal values were significantly different between groups, analysis of covariance (ANCOVA) was performed with the basal data as covariate, followed by a Tukey's post-hoc test, using the software SPSS statistics (version 22.0 for Windows). A probability level of 0.05 was accepted as significantly different.

## 3. Results

### Development of tolerance for morphine-induced antinociception in morphine-, methadone- and fentanyl-treated animals

In nontreated animals, morphine challenge (10 mg/ kg, i.p.) increased by more than three times the tail-flick latency, which corresponded with an average antinociceptive effect of 97 ± 1% (M.P.E.; basal latency = 3.04 ± 0.05 s; $n$ = 124). To explore the development of opioid analgesic tolerance, the tail-flick test was performed in animals treated with different opioids (morphine, methadone and fentanyl). As expected, before opioid treatments the basal latencies and the antinociceptive effects induced by a challenge dose of morphine were not significantly different between groups.

After subchronic treatment, basal latencies were not different between sham (emulsion) and morphine-treated animals. Morphine challenge increased by four times the latency in sham animals when compared to the basal latency ($p < 0.005$). In contrast, it failed to change the latency in morphine-treated animals (Fig. 1A; Table 1). Thus, the analgesic effects induced by morphine challenge were statistically different between sham and morphine-treated animals, so that post-hoc analysis showed that morphine challenge induced a less pronounced analgesic effect in the morphine/vehicle group than it did in the sham/vehicle group ($p < 0.005$) (Fig. 1C; Table 1), which indicated the development of tolerance.

On the other hand, basal latencies were found to be significantly different between sham (minipump) and methadone-treated rats ($p < 0.005$) (Table 2; compare methadone/vehicle *vs* sham/vehicle group). In sham animals, morphine challenge increased by four times the latency ($p < 0.005$ *vs* basal latency) and in methadone-treated rats it increased the latency by two times ($p < 0.005$ *vs* basal latency) (Fig. 1B; Table 2).

The analgesic effects induced by a challenge dose of morphine were significantly different between sham and methadone-treated rats even when the basal latency values were used as a covariate by ANCOVA. Thus, morphine challenge caused a less antinociceptive effect in the methadone/vehicle group than in the sham/vehicle group, representative of tolerance ($p < 0.005$) (Fig. 1C; Table 2).

Finally, basal latencies were not significantly different between sham (minipump) and fentanyl-treated rats. The challenge dose of morphine in fentanyl-treated rats increased more than three times the latency when compared to the basal latency ($p < 0.005$). This increase was not different when compared to that in the sham group (Fig. 1B; Table 2). Hence, the antinociceptive effect of morphine challenge in the fentanyl/vehicle group did not differ from that in the sham/vehicle group (Fig. 1C; Table 2). Therefore, unlike morphine and methadone, this protocol of fentanyl infusion did not induce significant tolerance.

**Effect of the antioxidants Trolox + ascorbic acid and U-74389G on morphine-induced analgesic tolerance**

We have previously shown that the co-administration of the selective nNOS inhibitor 7-NI prevents the antinociceptive tolerance induced by a subchronic morphine treatment (3 days) in rats (Santamarta et al., 2005). To further explore the involvement of ROS, the product of reaction between NO and oxygen derivatives (Davis et al., 2001), we tested the effect of two structurally unrelated antioxidants, Trolox administered with ascorbic acid (TX+AA) and U-74389G. Basal latencies were found to be statistically different between sham/TX+AA and sham/vehicle groups (Table 1). Furthermore, the analgesic effects induced by a challenge dose of morphine treatment were significantly different between groups even when the basal latency values were used as a covariate by ANCOVA. Thus,

co-treatment with TX+AA (40 mg/kg and 100 mg/kg, respectively) in morphine-treated animals partially prevented the development of tolerance, since the analgesic effect of morphine challenge in the morphine/TX+AA group was significantly greater than that in the morphine-vehicle group ($p < 0.005$), but smaller than that in the corresponding sham group (Figure 2A; Table 1). Likewise, co-treatment with U-74389G (10 mg/kg/day) partially prevented the development of tolerance in morphine-treated rats. Hence, the antinociceptive response of the challenge dose of morphine in the morphine/U-74389G group was significantly greater than that in the morphine/vehicle group ($p < 0.005$) but smaller than that in the corresponding sham group (Fig. 2B; Table 1). On the other hand, subchronic administration of either TX+AA or U-74389G in sham-treated animals (sham/TX+AA and sham/U-74389G group) failed to affect the morphine-induced analgesic effect, as compared to the sham/vehicle group (Fig. 2A, 2B; Table 1).

**Effect of the neuronal nitric oxide synthase inhibitor 7-NI and the antioxidant U-74389G on methadone-induced analgesic tolerance**

To study the role of neuronal NOS in the antinociceptive tolerance induced by other opioid agonists, we tested the effect of 7-NI in the group of rats receiving methadone. As noted above, basal latencies were found to be significantly higher ($p < 0.05$) in methadone/vehicle than in sham/vehicle groups (Table 2). However, in animals co-treated with 7-NI, basal latencies were not different between methadone and sham groups. Co-administration of the nNOS inhibitor 7-NI (30 mg/kg/12 h) in rats treated chronically with methadone failed to modify the development of analgesic tolerance, even when the basal latency values were used as a covariate by ANCOVA. Thus, the analgesic effect induced by morphine challenge in the methadone/7-NI group did not differ from that in the methadone/7-NI vehicle group, but it was lower than that in sham/7-NI group (Fig.

3A; Table 2). Chronic treatment with 7-NI failed to change the morphine-induced effect, as compared the sham/7-NI group with the sham/7-NI vehicle group (Fig. 3A; Table 2).

To further explore the involvement of ROS, methadone-treated animals were co-treated with the antioxidant U-74389G (10 mg/kg/day). As mentioned, basal latencies were significantly higher in methadone/vehicle than in sham/vehicle groups, but this difference was not significant between methadone and sham animals after co-treatment with U-74389G. Co-treatment with U-74389G in methadone-treated rats failed to modify the development of analgesic tolerance, even when the basal latency values were used as a covariate by ANCOVA. Thus, the analgesic response after a challenge dose of morphine in the methadone/U-74389G group was not different from that in the methadone/U-74389G vehicle group, but it was lower than that in sham/ U-74389G group (Fig. 3B; Table 2). Chronic treatment with U-74389G failed to affect the morphine challenge-induced analgesic effect, as compared the sham/ U-74389G group with the sham/ U-74389G vehicle group (Fig. 3B; Table 2).

Taken together, these data indicate that NO/ROS pathways play a key role in the development of morphine-, but not methadone-induced analgesic tolerance and therefore, these pathways seem to be differentially involved in opioid-induced analgesic tolerance in vivo.

## 4. Discussion

In this study, we evaluated by the tail-flick technique the development of analgesic tolerance after chronic treatments with three different MOR agonists. We present behavioral evidence for a role of NO/ROS pathway in morphine-, but no other opioids-induced antinociceptive tolerance. Thus, morphine and methadone treatments induced tolerance to the antinociceptive effect of a challenge dose of morphine. In contrast, no tolerance to morphine effect was observed in fentanyl-treated animals. Co-administration of the antioxidants TX+AA or U-74389G partially prevented the development of antinociceptive tolerance in morphine-treated animals. On the contrary, co-treatment with neither the nNOS inhibitor 7-NI nor the antioxidant U-74389G affected the development of antinociceptive tolerance in methadone-treated rats.

Morphine tolerance was induced by subcutaneous implantation of an oily emulsion containing morphine base (200 mg/kg, a single administration, 72 h). Morphine base containing emulsions provide a slow drug release and prolonged exposure to the opioid (Salem and Hope, 1999). According to the time course described in treated mice, the oily emulsion promotes a rise in morphine concentration in serum 3–12 h after implantation and a gradual clearance of morphine over 4–5 days (Garzón and Sánchez-Blázquez, 2001). This morphine administration protocol has been reported to efficiently induce both analgesic and cellular tolerance in rats (Santamarta et al., 2005). The degree of tolerance was similar to that observed by Goodchild et al. (2009) who induced tolerance by a s.c. sustained release morphine emulsion (125 mg/kg/day, 2 days) in rats. Likewise, chronic administration of s.c. morphine (10 mg/kg, twice daily, 5 days) showed a similar degree of antinociceptive tolerance in thermal and mechanical test paradigms (Raghavendra et al., 2004).

Chronic treatment with methadone-filled osmotic pumps (60 mg/kg/day, 6 days) induced a less strong degree of tolerance. In agreement, chronic methadone treatment has been reported to cause substantially less antinociceptive tolerance than morphine when given at equianalgesic doses (Enquist et al., 2012). The dose was selected based on previous studies where cellular tolerance was observed in LC neurons (Quillinan et al., 2011). Methadone has been reported to produce antinociception in the tail flick and hot plate tests with a potency similar to that of morphine when given s.c. to rats (Giusti et al., 1997; He et al., 2009). The dose of methadone that is daily administered by the osmotic pump in the present study is similar to that estimated to be released by the morphine emulsion (~66 mg/kg/day), yet induces a less profound degree of tolerance. Methadone has been found to induce analgesic tolerance at higher doses, such as 96 mg/kg/day (s.c., 5 days) (Raehal and Bohn, 2011) and also at much lower doses, such as 3 mg/kg/day (s.c., 4 days) in mice (Enquist et al., 2012). However, no tolerance was observed with 4 mg/kg (s.c., twice daily, 5 days) (Kim et al., 2008). It has been proposed that the degree of tolerance that an agonist can induce is inversely related to its ability to induce receptor internalization (Whistler et al., 1999). It could be hypothesized that in the present study methadone causes a less strong degree of tolerance induces endocytosis and recycling of the MOR, whereas morphine is less effective (Alvarez et al., 2002; Celver et al., 2004; Keith et al., 1998; Koch et al., 2005). Indeed, in an animal model in which the MOR is genetically modified to enhance receptor degradation after endocytosis, mice show a stronger degree of antinociceptive tolerance after methadone treatment (Enquist et al., 2012). In agreement, transgenic mice with genetically modified MORs that have the ability to internalize and recycle develop a reduced tolerance to morphine (Kim et al., 2008).

On the other hand, chronic treatment with fentanyl pumps (0.2 mg/kg/day, 7 days) did not cause antinociceptive tolerance. Fentanyl has been reported to be up to 100 times more potent than morphine as an analgesic (Vardanyan and Hruby, 2014). The dose of fentanyl used in the present study is sufficient to activate the MOR and promote behavioral changes and neuronal adaptations, as it was found to produce locomotor sensitization (Trujillo et al., 2004) and cellular tolerance in LC neurons (Pablos et al., unpublished results). In another study, fentanyl (0.24 mg/kg/day) infused for 7 days by osmotic pumps also failed to induce significant analgesic tolerance in rats (Paronis and Holtzman, 1992). However, it was found to cause tolerance when given at a dose of 0.04 mg/kg (s.c., 4 times a day, 3 days) in mice (Popik et al., 2000) and also at much higher doses, such as 2.4 mg/kg/day (72 h) or 3.2 mg/kg/day (5 days) by subcutaneously implanted pumps in neonatal rats and mice (Raehal and Bohn, 2011; Thornton and Smith, 1997). Our results suggest that fentanyl, at doses expected to activate MOR and promote neuronal adaptations, is resistant to tolerance induction. Fentanyl induces endocytosis and recycling of the MOR (Celver et al., 2004), which was been associated with a less potential to induce tolerance. Furthermore, it could be hypothesized that the absence of antinociceptive tolerance may be the result of other adaptations in the whole animal caused by fentanyl that may counteract the development of cellular tolerance observed in LC neurons (Pablos et al., unpublished results).

Thus, we propose that the different magnitudes of tolerance among opioid agonists, may be explained, at least in part, by their different abilities to induce receptor internalization and recycling. However, β-arrestin2 knockout mice have been shown to develop attenuated analgesic tolerance to morphine but not to fentanyl or methadone (Bohn et al., 2000, 2002; Raehal and Bohn, 2011), which seems to contradict this hypothesis. Interistingly, Quillinan et al., (2011) showed that in morphine-treated rats

recovery from acute ME-induced desensitization and receptor recycling was diminished, an effect that was not present in mice lacking β-arrestin2. Thus, it can be hypothesized that β-arrestin2 may disrupt the ability of receptors to recycle after endocytosis, which would contribute to tolerance development.

Previous studies have implicated the NO system in the adaptations triggered by chronic morphine treatment. Thus, chronic treatment with morphine has been found to increase NOS activity and expression in the brain and spinal cord (Bhargava et al., 1998; Machelska et al., 1997; Cuéllar et al., 2000). Our previous studies show that *in vivo* administration of the nNOS inhibitor 7-NI attenuates the development of cellular and analgesic tolerance in morphine-treated rats (Santamarta et al., 2005). Likewise, at the cellular level, non-selective and selective NOS inhibitors block opioid-induced MOR desensitization *in vitro* (Santamarta et al., 2014; Torrecilla et al., 2001). 7-NI hardly distinguishes between nNOS and eNOS in brain homogenate preparations, but it exhibits a marked selectivity for neuronal NOS in intact cell models (Babbedge et al., 1993), which seems to be due to specific targets of 7-NI that are only present in neurons (Alderton et al., 2001; Handy and Moore, 1998). In agreement, following sustained morphine administration, nNOS-, but not eNOS-deficient mice, exhibit weak analgesic tolerance development when compared to wild type animals (Heinzen and Pollack, 2004). It is well known that NO reacts with oxygen derivatives to produce ROS, such as the powerful oxidant peroxynitrite (Davis, 2001). In electrophysiological experiments performed in the LC, Trolox and U-74389G separately attenuated the enhancement of MOR desensitization induced by NO donors (Llorente et al., 2012). In our study, both TX+AA and U-74389G blocked partially the development of analgesic tolerance induced by a subchronic treatment with morphine, whereas they did not alter the animal pain threshold. Trolox is a cell permeable derivative of vitamin E that has a relatively high

selectivity for scavenging peroxynitrite and hydroxyl radical (Balogh et al., 2005). Ascorbic acid is a potent antioxidant and ROS chelator by itself but in this study we used it as a Trolox recycler from oxidation (Guo and Packer, 2000). Delwing et al. (2005) reported that vitamin E (40 mg/kg) and ascorbic acid (100 mg/kg) prevent oxidative damage in the rat brain. The 21-aminosteroid U-74389G, whose molecular structure is unrelated to that of Trolox, potently inhibits ROS-mediated lipid peroxidation and has a strong antioxidant activity (Fabian et al., 1998; Villa and Gorini, 1997). Thus, we can assume that reduction of morphine tolerance by TX+AA and U-74389G is the consequence of prevention of ROS-induced effects. In agreement, targeting peroxynitrite by metalloporphyrins blocks the development of morphine-induced antinociceptive tolerance in mice (Batinić-Haberle et al., 2009; Muscoli et al., 2007). Likewise, antioxidant agents such as melatonin or alpha-lipoic acid have been reported to attenuate the development of morphine tolerance (Raghavendra and Kulkarni, 2000; Abdel-Zaher et al., 2013). Mice lacking NOX1, a major source of ROS formation, exhibited weaker analgesic tolerance induced by repeated administration of morphine than wild type animals (Ibi et al., 2011). NOX2 knockout mice developed antinociceptive tolerance similar to wild type mice after 3 days of continuous morphine, but showed restored morphine analgesia on day six, whereas wild type mice mice continued to develop tolerance (Doyle et al., 2013). In electrophysiological experiments, TX+AA and U-74389G separatedly blocked the development of cellular tolerance in morphine-treated rats (Pablos et al., unpublished results).

The mechanisms by which ROS modulate opioid tolerance remain unclear. The potent ROS peroxynitrite has emerged as a pivotal component of opioid antinociceptive tolerance and pain. (Little et al., 2012; Salvemini and Neumann, 2009). Thus, there are some mechanisms by which ROS formation might contribute to opioid tolerance.

Peroxynitrite has been shown to alter glutamate homeostasis within the dorsal horn of the spinal cord by the post-translational nitration of key proteins involved in maintaining a normal glutamate balance, such as NMDARs, glutamate transporters or glutamine synthase (Trotti et al., 1996; Zanelli et al., 2000, 2002). Nitration of these proteins by peroxynitrite would lead to a constant potentiation of the glutamatergic system. There is general agreement that dysfunction of the NMDAR/NO pathway is a key component of nociception. It has been described that morphine activation of MOR increases NO production via the Akt-nNOS pathway and activates PKC, which stimulates the activity of NMDARs (Sánchez-Blázquez et al., 2010). This increased NMDAR activity would induce the phosphorylation and uncoupling of MORs via nNOS/CaMKII pathway, which results in the development of morphine analgesic tolerance (Sánchez-Blázquez et al., 2013). In agreement, NMDAR antagonists and nNOS and CaMKII inhibitors attenuate opioid tolerance and dependence (Elliott et al., 1994; Herman et al., 1995). A second alternative would involve ROS-mediated activation of PKC (Knapp and Klann, 2000). Indeed, morphine tolerance is attenuated by administration of PKC inhibitors, or when PKC expression is reduced (Newton et al., 2007; Smith et al., 2003; Zeitz et al., 2001). A third potential ROS-dependent mechanism underlying tolerance might be glial activation and the consequent induction of proinflammatory processes. Chronic administration of morphine promotes neuroimmune activation as evidenced by activation of spinal cord glial cells and production of proinflammatory cytokines (Song and Zhao, 2001; Watkins et al., 2005, 2007; Zeng et al., 2014). The induction of those proinflammatory molecules would be relevant in the development of morphine tolerance, since the glial modulators propentofylline (Raghavendra et al., 2004), minocycline (Cui et al., 2008) or paeoniflorin (Jiang et al., 2014) attenuate morphine-induced antinociceptive tolerance. The possible mechanisms by which chronic morphine induces glial cell activation and cytokine

production are not known, but a role for peroxynitrite as a signaling molecule involved in this process has been reported (Little et al., 2013). Resveratrol, a potent anti-inflammatory and antioxidant molecule, has been reported to attenuate morphine analgesic tolerance by inhibiting microglial activation and down-regulating NMDAR expression in the spinal cord (Han et al., 2014; Tsai et al., 2012). A fourth ROS-related mechanism might involve neuronal cell death, which is present in morphine-induced antinociceptive tolerance (Mao et al., 2002; Sharifipour et al., 2014). Chronic morphine exposure causes apoptosis within the spinal cord dorsal horn (Mao et al., 2002) and increases supraspinal apoptosis in the cortex and amygdala in neonatal rats (Bajic et al., 2013). The mechanisms involved in morphine-induced apoptosis remain unclear, but ROS seem to take part in this process. Thus, low concentrations of peroxynitrite trigger apoptotic death, whereas higher concentrations induce necrosis (Bonfoco et al., 1995; Virág et al., 2003). The nuclear enzyme poly(ADP-ribose) polymerase (PARP) has been shown to contribute to peroxynitrite-induced neuronal cell death in the spinal cord *in vitro* (Scott et al., 2004). Inhibitors of PARP, which is involved in different paradigms of cell death (Aredia and Scovassi, 2014), prevent the development of morphine antinociceptive tolerance (Mayer et al., 1999).

On the other hand, we show that 7-NI and U-74389G did not affect the development of antinociceptive tolerance in methadone-treated rats. These findings are in agreement with electrophysiological experiments (Pablos et al., unpublished results), where 7-NI and U-74389G failed to alter the development of cellular tolerance in LC neurons from methadone-treated rats. These results suggest that the NO system is not involved in methadone-induced adaptations. Methadone has been described to behave as a weak noncompetitive NMDAR antagonist (Ebert et al., 1998). This ability of methadone to antagonize NMDA receptors and counteract maladaptive changes in glutamate

transmission might explain, at least in part, the reduced tolerance after methadone treatment and lack of effects of NO/ROS modulators on methadone-induced tolerance. Further studies are needed to unmask the mechanisms underlying methadone-induced adaptations.

In conclusion, our results show that morphine treatment induces a stronger degree of antinociceptive tolerance than methadone in rats, whereas fentanyl was resistant to tolerance induction. In addition, *in vivo* administration of antioxidant agents partially prevents the development of morphine-, but not methadone-induced analgesic tolerance, suggesting that the NO/ROS pathway is differentially involved in opioid antinociceptive tolerance. We provide pharmacological basis for the potential use of antioxidants as useful co-adjuvants in the management of chronic pain to prevent or, at least, attenuate the development of morphine analgesic tolerance.

## References


Abdel-Zaher AO, Mostafa MG, Farghaly HS, Hamdy MM, Abdel-Hady RH (2013) Role of oxidative stress and inducible nitric oxide synthase in morphine-induced tolerance and dependence in mice. Effect of alpha-lipoic acid. Behav Brain Res. 247:17–26.

Alderton WK, Cooper CE, Knowles RG (2001) Nitric oxide synthases: structure, function and inhibition. Biochem J 357:593–615.

Alvarez VA, Arttamangkul S, Dang V, Salem A, Whistler JL, Von Zastrow M, Grandy DK, Williams JT (2002) mu-Opioid receptors: Ligand-dependent activation of potassium conductance, desensitization, and internalization. J Neurosci 22:5769–5776.

Aredia F, Scovassi AI (2014) Poly(ADP-ribose): A signaling molecule in different paradigms of cell death. Biochem Pharmacol 92:157–163.

Babbedge RC, Bland-Ward PA, Hart SL, Moore PK (1993) Inhibition of rat cerebellar nitric oxide synthase by 7-nitro indazole and related substituted indazoles. Br J Pharmacol 110:225–228.

Bajic D, Commons KG, Soriano SG (2013) Morphine-enhanced apoptosis in selective brain regions of neonatal rats. Int J Dev Neurosci 31:258–266.

Balogh GT, Vukics K, Könczöl A, Kis-Varga A, Gere A, and Fischer J (2005) Nitrone derivatives of trolox as neuroprotective agents. Bioorg Med Chem Lett 15:3012–3015.

Batinić-Haberle I, Ndengele MM, Cuzzocrea S, Rebouças JS, Spasojević I, Salvemini D (2009) Lipophilicity is a critical parameter that dominates the efficacy of metalloporphyrins in blocking the development of morphine antinociceptive tolerance through peroxynitrite-mediated pathways. Free Radic Biol Med 46:212–219.

Bhargava HN, Kumar S, Barjavel MJ (1998) Kinetic properties of nitric oxide synthase in cerebral cortex and cerebellum of morphine tolerant mice. Pharmacology 56:252–256.

Bohn LM, Gainetdinov RR, Lin FT, Lefkowitz RJ, and Caron MG (2000) Mu-opioid receptor desensitization by beta-arrestin-2 determines morphine tolerance but not dependence. Nature 408:720–723.

Bohn LM, Lefkowitz RJ, and Caron MG (2002) Differential mechanisms of morphine antinociceptive tolerance revealed in (beta)arrestin-2 knock-out mice. J Neurosci. 22:10494–10500.

Bonfoco E, Krainc D, Ankarcrona M, Nicotera P, Lipton SA (1995) Apoptosis and necrosis: two distinct events induced, respectively, by mild and intense insults with N-methyl-D-aspartate or nitric oxide/superoxide in cortical cell cultures. Proc Natl Acad Sci USA 92:7162–7166.

Celver J, Xu M, Jin W, Lowe J, Chavkin C (2004) Distinct domains of the mu-opioid receptor control uncoupling and internalization. Mol Pharmacol 65:528–537.

Corbett AD, Henderson G, McKnight AT, Paterson SJ (2006) 75 years of opioid research: the exciting but vain quest for the Holy Grail. British Journal of Pharmacology 147:S153–S162.

Cuéllar B, Fernández AP, Lizasoain I, Moro MA, Lorenzo P, Bentura ML, Rodrigo J, Leza JC (2000) Up-regulation of neuronal NO synthase immunoreactivity in opiate dependence and withdrawal. Psychopharmacology (Berl). 148:66–73.

Cui Y, Liao XX, Liu W, Guo RX, Wu ZZ, Zhao CM, Chen PX, Feng JQ (2008) A novel role of minocycline: attenuating morphine antinociceptive tolerance by inhibition of p38 MAPK in the activated spinal microglia. Brain Behav Immun 22:114–123.

Davis KL, Martin E, Turko IV, Murad F (2001) Novel effects of nitric oxide. Annu Rev Pharmacol Toxicol 41:203–236.

Delwing D, Chiarani F, Bavaresco CS, Wannmacher CM, Wajner M, Dutra-Filho CS, Wyse AT (2005) Protective effect of antioxidants on brain oxidative damage caused by proline administration. Neurosci Res 52:69–74.

Doyle T, Esposito E, Bryant L, Cuzzocrea S, Salvemini D (2013) NADPH-oxidase 2 activation promotes opioid-induced antinociceptive tolerance in mice. Neuroscience 241:1–9.

Ebert B, Thorkildsen C, Andersen S, Christrup LL, Hjeds H (1998) Opioid analgesics as noncompetitive N-methyl-D-aspartate (NMDA) antagonists. Biochem Pharmacol. 56:553–559.

Elliott K, Minami N, Kolesnikov YA, Pasternak GW, Inturrisi CE (1994) The NMDA receptor antagonists, LY274614 and MK-801, and the nitric oxide synthase inhibitor, NG-nitro-L-arginine, attenuate analgesic tolerance to the mu-opioid morphine but not to kappa opioids. Pain 56:69–75.

Enquist J, Ferwerda M, Milan-Lobo L, Whistler JL (2012) Chronic methadone treatment shows a better cost/benefit ratio than chronic morphine in mice. J Pharmacol Exp Ther. 340:386–392.

Fabian RH, Dewitt DS, Kent TA (1998) The 21-aminosteroid U-74389G reduces cerebral superoxide anion concentration following fluid percussion injury of the brain. J Neurotrauma 15:433–440.

Garzón J, Sánchez-Blázquez P (2001) Administration of myr$^{+}$-$G_{i2}\alpha$ subunits prevents acute tolerance (tachyphylaxis) to mu-opioid effects in mice. Neuropharmacology. 40:560–569.

Giusti P, Buriani A, Cima L, Lipartiti M (1997) Effect of acute and chronic tramadol on [3H]-5-HT uptake in rat cortical synaptosomes. Br J Pharmacol. 122:302–306.

Goodchild CS, Kolosov A, Geng L, Winter LL, Nadeson R (2009) Prevention and reversal of morphine tolerance by the analgesic neuroactive steroid alphadolone. Pain Med. 10:890–901.

Guo Q, Packer L (2000) Ascorbate-dependent recycling of the vitamin E homologue trolox by dihydrolipoate and glutathione in murine skin homogenates. Free Radic Biol Med 29:368–374.

Haley JE, Dickenson AH, Schachter M (1992) Electrophysiological evidence for a role of nitric oxide in prolonged chemical nociception in the rat. Neuropharmacology 31:251–258.

Han Y, Jiang C, Tang J, Wang C, Wu P, Zhang G, Liu W, Jamangulova N, Wu X, Song X (2014) Resveratrol reduces morphine tolerance by inhibiting microglial activation via AMPK signalling. Eur J Pain 18:1458–1470.

Handy RL, Moore PK (1998) Handy and Moore reply: 7-nitroindazole (7-NI) fails to increase blood pressure in animals: The 7-NI 'conundrum'. Trends Pharmacol Sci. 19: 350.

He L, Kim J, Ou C, McFadden W, van Rijn RM, Whistler JL (2009) Methadone antinociception is dependent on peripheral opioid receptors. J Pain.10:369–79.

Heinzen EL, Pollack GM (2004) The development of morphine antinociceptive tolerance in nitric oxide synthase-deficient mice. Biochem Pharmacol 67:735–741.

Herman BH, Vocci F, Bridge P (1995) The effects of NMDA receptor antagonists and nitric oxide synthase inhibitors on opioid tolerance and withdrawal. Medication development issues for opiate addiction. Neuropsychopharmacology 13:269–293.

Ibi M, Matsuno K, Matsumoto M, Sasaki M, Nakagawa T, Katsuyama M, Iwata K, Zhang J, Kaneko S, Yabe-Nishimura C (2011) Involvement of NOX1/NADPH oxidase in morphine-induced analgesia and tolerance. J Neurosci 31:18094–18103.

Jiang C, Xu L, Chen L, Han Y, Tang J, Yang Y, Zhang G, Liu W (2014) Selective suppression of microglial activation by paeoniflorin attenuates morphine tolerance. Eur J Pain doi: 10.1002/ejp.617.

Keith DE, Anton B, Murray SR, Zaki PA, Chu PC, Lissin DV, Monteillet-Agius G, Stewart PL, Evans CJ, von Zastrow M (1998) μ-Opioid receptor internalization: opiate drugs have differential effects on a conserved endocytic mechanism in vitro and in the mammalian brain. Mol Pharmacol.53:377–384.

Kelly E (2013) Efficacy and ligand bias at the μ-opioid receptor. Br J Pharmacol 169:1430–1446.

Kim JA, Bartlett S, He L, Nielsen CK, Chang AM, Kharazia V, Waldhoer M, Ou CJ, Taylor S, Ferwerda M, Cado D, Whistler JL (2008) Morphine-induced receptor endocytosis in a novel knockin mouse reduces tolerance and dependence. Curr Biol. 18:129–135.

Koch T, Widera A, Bartzsch K, Schulz S, Brandenburg LO, Wundrack N, Beyer A, Grecksch G, Höllt V (2005) Receptor endocytosis counteracts the development of opioid tolerance. Mol Pharmacol. 67:280–287.

Knapp LT, Klann E (2000) Superoxide-induced stimulation of protein kinase C via thiol modification and modulation of zinc content. J Biol Chem 275:24136–24145.

Kornick CA, Santiago-Palma J, Moryl N, Payne R, Obbens EA (2003) Benefit-risk assessment of transdermal fentanyl for the treatment of chronic pain. Drug Saf. 26:951–973.

Le Bars D, Gozariu M, Cadden SW (2001) Animal models of nociception. Pharmacol Rev 53:597–652.

Little JW, Chen Z, Doyle T, Porreca F, Ghaffari M, Bryant L, Neumann WL, Salvemini D (2012) Supraspinal peroxynitrite modulates pain signaling by suppressing the endogenous opioid pathway. J Neurosci. 32:10797–10808.

Little JW, Cuzzocrea S, Bryant L, Esposito E, Doyle T, Rausaria S, Neumann WL, Salvemini D (2013) Spinal mitochondrial-derived peroxynitrite enhances neuroimmune activation during morphine hyperalgesia and antinociceptive tolerance. Pain 154:978–986.

Llorente J, Santamarta MT, Henderson G, Pineda J (2012) Enhancement of mu-opioid receptor desensitization by nitric oxide in rat locus coeruleus neurons: involvement of reactive oxygen species. J Pharmacol Exp Ther 342:552–560.

Machelska H, Ziolkowska B, Mika J, Przewlocka B, Przewlocki R (1997) Chronic morphine increases biosynthesis of nitric oxide synthase in the rat spinal cord. Neuroreport 8:2743–2747.

Mao J, Sung B, Ji RR, Lim G (2002) Neuronal apoptosis associated with morphine tolerance: evidence for an opioid-induced neurotoxic mechanism. J Neurosci 22:7650–7661.

Mayer DJ, Mao J, Holt J, Price DD (1999) Cellular mechanisms of neuropathic pain, morphine tolerance, and their interactions. Proc Natl Acad Sci U S A 96:7731–7736.

Muscoli C, Cuzzocrea S, Ndengele MM, Mollace V, Porreca F, Fabrizi F, Esposito E, Masini E, Matuschak GM, Salvemini D (2007) Therapeutic manipulation of peroxynitrite attenuates the development of opiate-induced antinociceptive tolerance in mice. J Clin Invest 117:3530–3539.

Newton PM, Kim JA, McGeehan AJ, Paredes JP, Chu K, Wallace MJ, Roberts AJ, Hodge CW, Messing RO (2007). Increased response to morphine in mice lacking protein kinase C epsilon. Genes Brain Behav 6:329–338.

Paronis CA, Holtzman SG (1992) Development of tolerance to the analgesic activity of mu agonists after continuous infusion of morphine, meperidine or fentanyl in rats. J Pharmacol Exp Ther 262:1–9.

Popik P, Kozela E, Pilc A (2000) Selective agonist of group II glutamate metabotropic receptors, LY354740, inhibits tolerance to analgesic effects of morphine in mice. Br J Pharmacol. 130:1425–1431.

Quillinan N, Lau EK, Virk M, von Zastrow M, Williams JT (2011) Recovery from mu-Opioid Receptor Desensitization after Chronic Treatment with Morphine and Methadone. J Neurosci 31:4434–4443.

Raehal KM, Bohn LM (2011) The role of β-arrestin2 in the severity of antinociceptive tolerance and physical dependence induced by different opioid pain therapeutics. Neuropharmacology 60:58–65.

Raghavendra V, Kulkarni SK (2000) Possible mechanisms of action in melatonin reversal of morphine tolerance and dependence in mice. Eur J Pharmacol. 409:279–289.

Raghavendra V, Tanga FY, DeLeo JA (2004) Attenuation of morphine tolerance, withdrawal-induced hyperalgesia, and associated spinal inflammatory immune responses by propentofylline in rats. Neuropsychopharmacology 29:327–334.

Salem A, Hope W (1999) Role of endogenous adenosine in the expression of opiate withdrawal in rats. Eur J Pharmacol.369:39–42.

Salvemini D, Little JW, Doyle T, Neumann WL (2011) Roles of reactive oxygen and nitrogen species in pain. Free Radic Biol Med 51:951–966.

Salvemini D, Neumann WL (2009) Peroxynitrite: a strategic linchpin of opioid analgesic tolerance. Trends Pharmacol Sci. 30:194-202.

Sánchez-Blázquez P, Rodríguez-Muñoz M, Garzón J (2010) Mu-opioid receptors transiently activate the Akt-nNOS pathway to produce sustained potentiation of PKC-mediated NMDAR-CaMKII signaling. PLoS One. 5:e11278.

Sánchez-Blázquez P, Rodríguez-Muñoz M, Berrocoso E, Garzón J (2013) The plasticity of the association between mu-opioid receptor and glutamate ionotropic receptor N in opioid analgesic tolerance and neuropathic pain. Eur J Pharmacol 716:94–105.

Santamarta MT, Llorente J, Mendiguren A, Pineda J (2014) Involvement of neuronal nitric oxide synthase in desensitisation of mu-opioid receptors in the rat locus coeruleus. J Psychopharmacol 28:903–914.

Santamarta MT, Ulibarri I, Pineda J (2005) Inhibition of neuronal nitric oxide synthase attenuates the development of morphine tolerance in rats. Synapse 57:38–46.

Scott GS, Szabó C, Hooper DC (2004) Poly(ADP-ribose) polymerase activity contributes to peroxynitrite-induced spinal cord neuronal cell death in vitro. J Neurotrauma 21:1255–1263.

Sharifipour M, Izadpanah E, Nikkhoo B, Zare S, Abdolmaleki A, Hassanzadeh K, Moradi F, Hassanzadeh K (2014) A new pharmacological role for donepezil: attenuation of morphine-induced tolerance and apoptosis in rat central nervous system. J Biomed Sci. 21:6.

Shelton BW, Deynes-Romero J, Tofani-Montalvo M, Ramírez-Rivera J, Jaumne-Anselmi F (2008) Methadone: an effective alternative to morphine for pain relief in cancer patients. Bol Asoc Med P R. 100:7–10.

Smith FL, Javed RR, Elzey MJ, Dewey WL (2003) The expression of a high level of morphine antinociceptive tolerance in mice involves both PKC and PKA. Brain Res 985:78–88.

Song P, Zhao ZQ (2001) The involvement of glial cells in the development of morphine tolerance. Neurosci Res 39:281–286.

Thornton SR, Smith FL (1997) Characterization of neonatal rat fentanyl tolerance and dependence. J Pharmacol Exp Ther 281:514–521.

Torrecilla M, Pineda J, Ugedo L (2001) NO synthase inhibitors reduce opioid desensitization in rat locus coeruleus neurons in vitro. Neuroreport. 12:1601–1604.

Trotti D, Rossi D, Gjesdal O, Levy LM, Racagni G, Danbolt NC, Volterra A (1996) Peroxynitrite inhibits glutamate transporter subtypes. J Biol Chem. 271:5976–5979.

Trujillo KA, Kubota KS, Warmoth KP (2004) Continuous administration of opioids produces locomotor sensitization. Pharmacol Biochem Behav 79:661–669.

Tsai RY, Chou KY, Shen CH, Chien CC, Tsai WY, Huang YN, Tao PL, Lin YS, Wong CS (2012) Resveratrol regulates N-methyl-D-aspartate receptor expression and suppresses neuroinflammation in morphine-tolerant rats. Anesth Analg 115:944–952.

Vardanyan RS, Hruby VJ (2014) Fentanyl-related compounds and derivatives: current status and future prospects for pharmaceutical applications. Future Med Chem. 6:385–412.

Villa RF, Gorini A (1997) Pharmacology of lazaroids and brain energy metabolism: a review. Pharmacol Rev 49:99–136.

Virág L, Szabo E, Gergely P, Szabo C (2003) Peroxynitrite-induced cytotoxicity: mechanism and opportunities for intervention. Toxicol Lett 140-141:113–124.

Von Zastrow M (2010) Regulation of opioid receptors by endocytic membrane traffic: Mechanisms and translational implications. Drug Alcohol Depend 108:166–171.

Watkins LR, Hutchinson MR, Johnston IN, Maier SF (2005) Glia:novel counter-regulators of opioid analgesia. Trends Neurosci 28:661–669.

Watkins LR, Hutchinson MR, Ledeboer A, Wieseler-Frank J, Milligan ED, Maier SF (2007) Norman Cousins Lecture. Glia as the "bad guys": implications for improving clinical pain control and the clinical utility of opioids. Brain Behav Immun. 21:131–46.

Whistler JL, Chuang HH, Chu P, Jan LY, von Zastrow M (1999) Functional dissociation of mu opioid receptor signaling and endocytosis: implications for the biology of opiate tolerance and addiction. Neuron 23:737–746.

Williams JT, Ingram SL, Henderson G, Chavkin C, von Zastrow M, Schulz S, Koch T, Evans CJ, Christie MJ (2013) Regulation of mu-opioid receptors: desensitization, phosphorylation, internalization, and tolerance. Pharmacol Rev 65:223–254.

Zanelli SA, Ashraf QM, Delivoria-Papadopoulos M, Mishra OP (2000) Peroxynitrite-induced modification of the N-methyl-D-aspartate receptor in the cerebral cortex of the guinea pig fetus at term. Neurosci Lett. 296:5–8.

Zanelli SA, Ashraf QM, Mishra OP (2002) Nitration is a mechanism of regulation of the NMDA receptor function during hypoxia. Neuroscience 112:869–877.

Zeitz KP, Malmberg AB, Gilbert H, Basbaum AI (2001) Reduced development of tolerance to the analgesic effects of morphine and clonidine in PKCγ mutant mice. Pain 94:245–253.

Zeng X, Lin MY, Wang D, Zhang Y, Hong Y (2014) Involvement of adrenomedullin in spinal glial activation following chronic administration of morphine in rats. Eur J Pain 18:1323–1332.

Zhou D, Chen ML, Zhang YQ, Zhao ZQ (2010) Involvement of spinal microglial P2X7 receptor in generation of tolerance to morphine analgesia in rats. J Neurosci 30:8042–8047.

**Figure legends**

**Figure 1.** Development of tolerance for morphine-induced antinociception in morphine-, methadone- and fentanyl-treated animals. **A, B.** Bar histograms show the mean ± S.E.M of the latency before (basal) and after a challenge dose of morphine in sham (emulsion) ($n$ = 10), sham (minipump) ($n$ = 10), morphine- ($n$ = 9), methadone- ($n$ = 9) and fentanyl-treated animals ($n$ = 6). Basal latencies were statistically different between methadone and sham groups $^{\&}p < 0.005$ when compared to the corresponding sham/vehicle group. Note that morphine challenge significantly increased the latency in sham-, methadone- and fentanyl-treated rats, but not in morphine-treated animals. $^{*}p < 0.005$ when compared to the corresponding basal latency by a paired Student's t test, and $^{\#}p < 0.005$, when compared to the corresponding sham group by two-sample Student's t test. **C.** Bar histograms represent the mean ± S.E.M of the maximum possible effect (M.P.E.) in sham (emulsion) ($n$ = 10), sham (minipump) ($n$ = 10) morphine- ($n$ = 9), methadone- ($n$ = 9) and fentanyl-treated animals ($n$ = 6). Note that morphine and methadone treatments reduce the analgesic effect of morphine challenge, indicative of tolerance. $^{\$}p < 0.005$ when compared to the corresponding sham group by two-sample Student's t test. $^{\dagger}p < 0.005$ when compared to the morphine group by two-sample Student's t test.

**Figure 2.** Effect of Trolox + ascorbic acid (TX+AA) and U-74389G on the on the antinociception induced by a challenge dose of morphine in sham-, and morphine-treated rats. **A.** Bar histograms show the mean ± S.E.M of the maximum possible effect (M.P.E.) in rats co-treated with the morphine emulsion and TX+AA (morphine/TX+AA group, $n$ = 10) or with their vehicles (sham-vehicle group, $n$ = 10; morphine-vehicle group, $n$ = 9; sham/TX+AA group, $n$ = 10). **B.** Bar histograms show the mean ± S.E.M of the maximum possible effect (M.P.E.) in rats co-treated with the morphine emulsion and U-74389G (morphine/U-74389G group, $n$ = 8) or with their vehicles (sham-vehicle group, $n$

= 10; morphine-vehicle group, $n$ = 9; sham/U-74389G group, $n$ = 7). Note that morphine treatment reduces the analgesic effect of morphine challenge and co-administration of TX+AA or U-74389G partially blocks this change. $^{\$}p < 0.05$ and $^{\$\$}p < 0.005$, as compared to the corresponding sham group (ANCOVA followed by a post-hoc Tukey's test); $^{\dagger}p < 0.005$, as compared to the corresponding vehicle group (ANCOVA followed by a post-hoc Tukey's test).

**Figure 3.** Effect of 7-NI and U-74389G on the on the antinociception induced by a challenge dose of morphine in sham-, and methadone-treated rats. **A**. Bar histograms show the mean ± S.E.M of the maximum possible effect (M.P.E.) in rats co-treated with methadone and 7-NI (methadone/7-NI group, $n$ = 8) or with their vehicles (sham/vehicle group, $n$ = 7; methadone/vehicle group, $n$ = 9; sham/7-NI group, $n$ = 7). **B.** Bar histograms show the mean ± S.E.M of the maximum possible effect (M.P.E.) in rats co-treated with methadone minipumps and U-74389G (methadone/U-74389G group, $n$ = 7) or with their vehicles (sham/vehicle group, $n$ = 10; methadone/vehicle group, $n$ = 9; sham/U-74389G group, $n$ = 7). Note that chronic methadone treatment reduces the analgesic effect of morphine challenge, but co-administration of either 7-NI or U-74389G fails to block this change. $^{\$}p < 0.005$, as compared to the corresponding sham group (ANCOVA followed by a post-hoc Tukey's test).

**Table 1. Effect of Trolox and ascorbic acid (TX+AA) and U-74389G on the tail-flick latencies and the analgesic response of sham- and morphine-treated rats.**

| Treatment groups[1] | Basal latency (s)[2] | Latency (s)[3] | M.P.E (%)[4] | n |
|---|---|---|---|---|
| Sham (emulsion) | | | | |
| Vehicle (saline) | 2.66 ± 0.14 | 9.41 ± 0.33* | 92.41 ± 4.23 | 10 |
| TX+AA | 3.43 ± 0.23$^{\#}$ | 9.10 ± 0.35* | 85.64 ± 5.69 | 10 |
| U-74389G | 2.57 ± 0.14 | 9.93 ± 0.06* | 99.08 ± 0.73 | 7 |
| Morphine | | | | |
| Vehicle (saline) | 3.19 ± 0.26 | 3.94 ± 0.30 | 13.77 ± 4.38$^{\$\$}$ | 9 |
| TX+AA | 2.92 ± 0.17 | 7.42 ± 0.51* | 62.04 ± 8.37$^{\$\dagger}$ | 10 |
| U-74389G | 2.80 ± 0.14 | 7.20 ± 0.65* | 61.74 ± 8.85$^{\$\$\dagger}$ | 8 |

[1]Animals were co-treated for 72 h with a morphine emulsion and TX+AA or U-74389G injections (morphine/TX+AA group and morphine/U-74389G group), or with their vehicles (sham/vehicle group, sham/TX+AA group, sham/U-74389G group and morphine/vehicle group).

[2]Basal latency values refer to the time until tail removal before administration of the morphine challenge. Data are shown as mean ± SEM of n experiments. After chronic treatments, basal latencies were statistically different between groups. $^{\#}p < 0.05$ when compared to the sham/vehicle group (one-way ANOVA followed by a post-hoc Tukey's test).

[3]Latency values refer to the time until tail removal after administration of the morphine challenge. Data are shown as mean ± SEM of n experiments. Latencies were statistically different when compared to basal latencies in all groups except in morphine/vehicle group. $^{*}p < 0.005$ (paired Student's t test).

[4]M.P.E is the percentage of the maximal possible effect (see Materials and Methods). Data are shown as mean ± SEM of n experiments. Note that morphine treatment attenuates the analgesic effect of morphine challenge and co-administration of TX+AA or U-74389G partially blocks this change. [$]$p < 0.05$ and [$$]$p < 0.005$, when compared to the corresponding sham group (ANCOVA followed by a post-hoc Tukey's test), [†]$p < 0.005$ when compared to the corresponding vehicle group (ANCOVA followed by a post-hoc Tukey's test).

**Table 2. Effect of 7-nitroindazole (7-NI) and U-74389G on the tail-flick latencies and the analgesic response of sham and methadone-treated rats.**

| Treatment groups[1] | Basal latency (s)[2] | Latency (s)[3] | M.P.E (%)[4] | n |
|---|---|---|---|---|
| Sham (minipump) | | | | |
| 7-NI vehicle (peanut oil) | 2.64 ± 0.14 | 9.87 ± 0.10* | 98.29 ± 1.29 | 7 |
| 7-NI | 2.93 ± 0.14 | 9.74 ± 0.14* | 96.43 ± 2.00 | 7 |
| U-74389G vehicle (saline) | 2.59 ± 0.14 | 9.79 ± 0.11* | 97.31 ± 1.43 | 10 |
| U-74389G | 2.66 ± 0.17 | 9.90 ± 0.06* | 98.75 ± 0.73 | 7 |
| Methadone | | | | |
| 7-NI vehicle (peanut oil) | 3.24 ± 0.07$^{\&}$ | 6.61 ± 0.41* | 49.48 ± 6.40$^{\$}$ | 9 |
| 7-NI | 2.86 ± 0.16 | 5.51 ± 0.61* | 37.77 ± 8.12$^{\$}$ | 8 |
| U-74389G vehicle (saline) | 3.32 ± 0.09$^{\&\&}$ | 6.51 ± 0.45* | 47.98 ± 6.40$^{\$}$ | 9 |
| U-74389G | 3.01 ± 0.07 | 5.99 ± 0.52* | 42.45 ± 7.41$^{\$}$ | 7 |
| Fentanyl | | | | |
| Vehicle (saline) | 2.90 ± 0.11 | 9.58 ± 0.18* | 94.14 ± 2.66 | 6 |

[1]Animals were co-treated for 6 days with methadone by an osmotic minipump and 7-NI or U-74389G injections (methadone/7-NI group, methadone/U-74389G group) or with their vehicles (sham/7-NI vehicle group, sham/U-74389G vehicle group, sham/7-NI group, sham/U-74389G group, methadone/7-NI vehicle group and methadone/U-74389G group). Another group of animals were co-treated for 7 days with fentanyl by an osmotic minipump.

[2]Basal latency values refer to the time until tail removal before administration of the morphine challenge. Data are shown as mean ± SEM of n experiments. After chronic treatments, basal latencies were statistically different between groups. $^{\&}p < 0.05$ and $^{\&\&}p < 0.005$ when compared to the corresponding sham/vehicle group (one-way ANOVA followed by a post-hoc Tukey's test).

[3]Latency values refer to the time until tail removal after administration of the morphine challenge. Data are shown as mean ± SEM of n experiments. Latencies were statistically different when compared to basal latencies in all groups. *$p < 0.005$ (paired Student's t test).

[4]M.P.E is the percentage of the maximal possible effect (see Materials and Methods). Data are shown as mean ± SEM of n experiments. Note that chronic methadone treatment attenuates the analgesic effect of morphine challenge, but co-administration of either 7-NI or U-74389G failed to block this effect, even when the basal latency values were used as a covariate. $^{\$}p < 0.005$ when compared to the corresponding sham group (ANCOVA followed by a post-hoc Tukey's test). Chronic treatment with fentanyl does not alter the analgesic effect of morphine challenge.

**FIGURE 1**

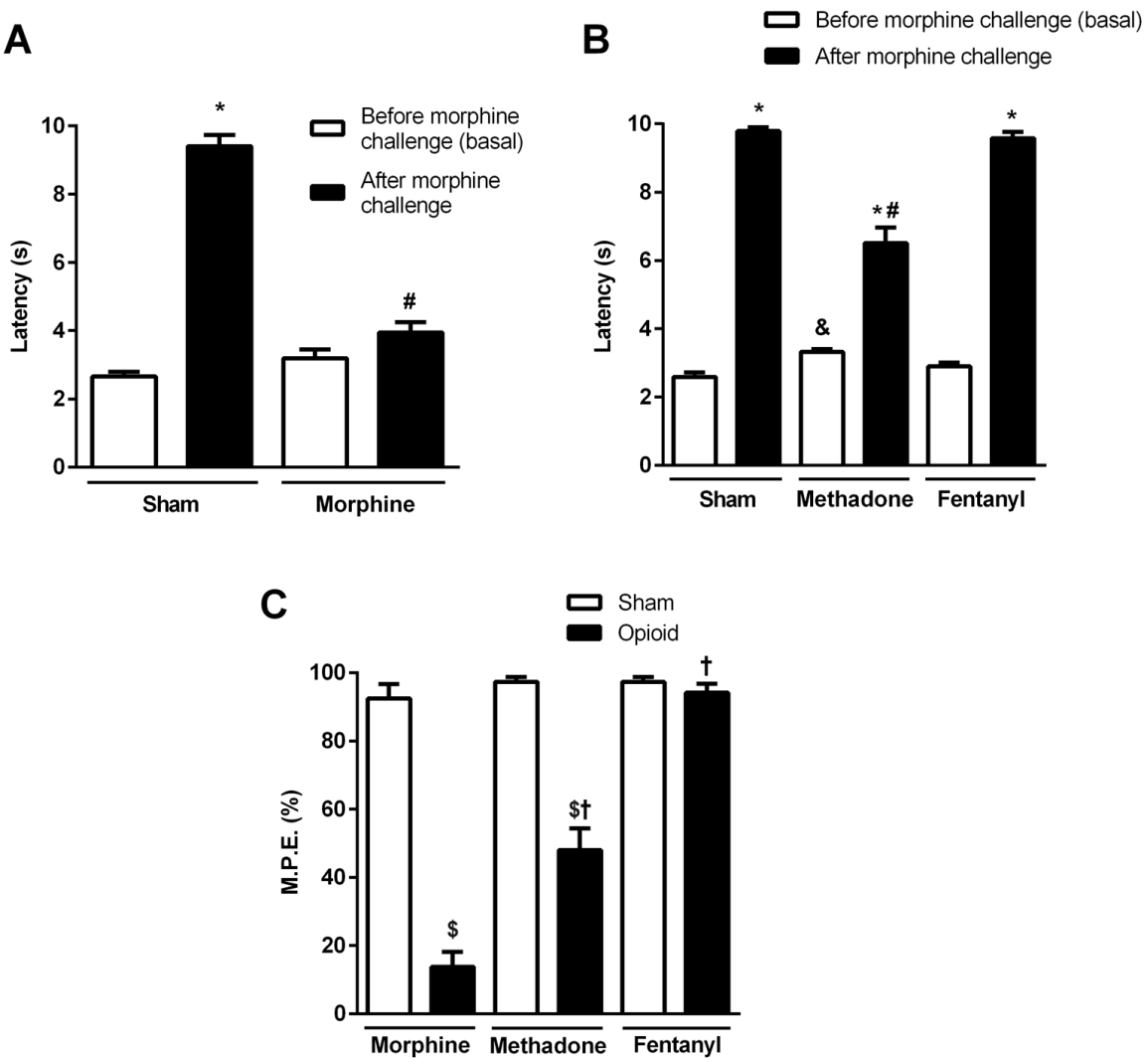
A
Before morphine challenge (basal)
After morphine challenge
Latency (s)
10
8
6
4
2
0
*
#
Sham
Morphine
B
Before morphine challenge (basal)
After morphine challenge
Latency (s)
*
*#
&
*
Sham
Methadone
Fentanyl
C
Sham
Opioid
M.P.E. (%)
100
80
60
40
20
0
$
$†
†
Morphine
Methadone
Fentanyl

**FIGURE 2**

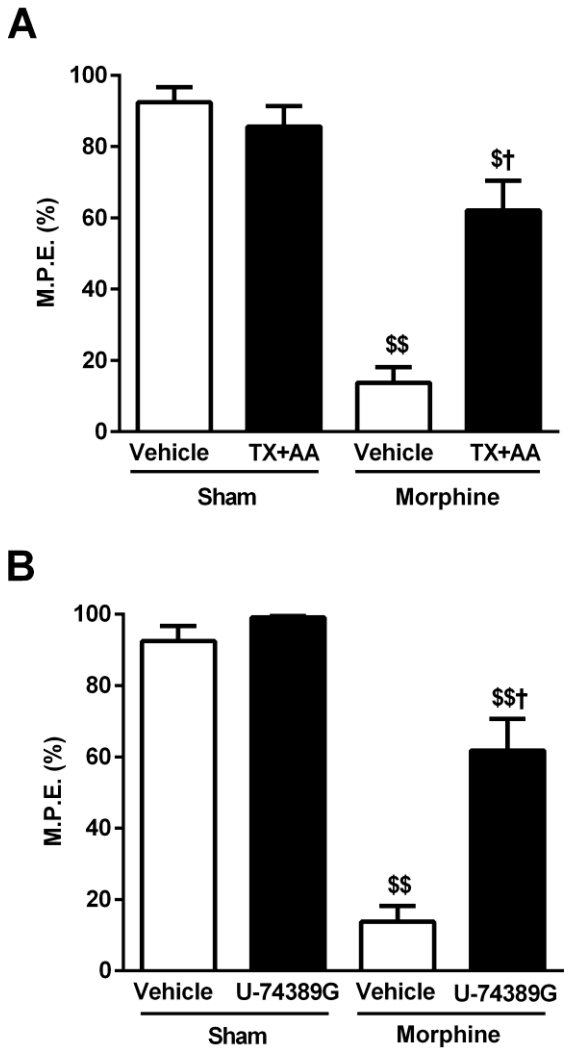
A
100
80
60
40
20
0
M.P.E. (%)
$†
$$
Vehicle
TX+AA
Vehicle
TX+AA
Sham
Morphine
B
100
80
60
40
20
0
M.P.E. (%)
$$†
$$
Vehicle
U-74389G
Vehicle
U-74389G
Sham
Morphine

**FIGURE 3**

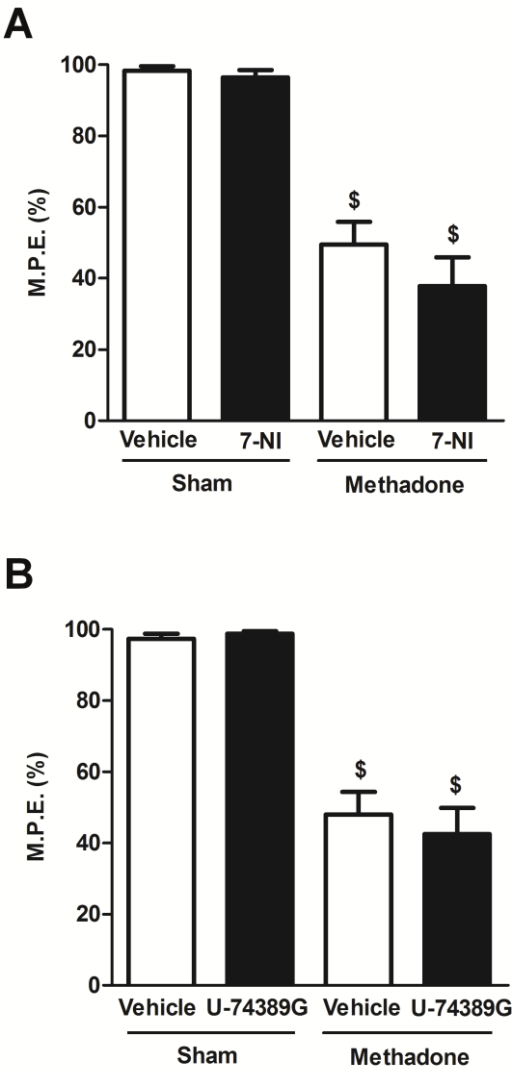
A
100
80
60
40
20
0
M.P.E. (%)
$
$
Vehicle
7-NI
Vehicle
7-NI
Sham
Methadone
B
100
80
60
40
20
0
M.P.E. (%)
$
$
Vehicle
U-74389G
Vehicle
U-74389G
Sham
Methadone